THE ACCEPTABILITY OF ALCOHOL FUELS FOR AUTOMOBILE ENGINES

JOTINDERPAL SINGH SIDHU

Doctor of Philosophy

THE UNIVERSITY OF ASTON IN BIRMINGHAM

April 1988

THE UNIVERSITY OF ASTON IN BIRMINGHAM
DEPARTMENT OF CHEMICAL ENGINEERING & APPLIED CHEMISTRY

THE ACCEPTABILITY OF ALCOHOL FUELS FOR AUTOMOBILE ENGINES

Jotinderpal Singh Sidhu
Doctor of Philosophy
April 1988

SUMMARY

The objective of this research was to carry out an investigation into suitable alternatives to gasoline for use in modern automobiles. It has been shown that methanol and ethanol can provide this alternative.

A Fiat 127 903 cm^3 four cylinder engine with a Weber fixed jet carburettor was used to carry out performance and exhaust emission comparisons. Manifold geometry studies were carried out on the Ricardo E6 single cylinder engine and alternative designs to the intake manifold to improve the efficiency have been suggested. A range of components from the carburettor were tested with the alcohols for material compatibility, results from which suggested that different materials to the ones presently used would be needed. Studies of distillation curve profiles showed that "start-up" and drivability would be a major drawback when using alcohol fuels. Additives to improve start-up and driveability have been suggested.

KEYWORDS:
Methanol
Ethanol
Gasohol
Gasoline-substitutes
Fuel additives
Corrosion
Automobiles

ACKNOWLEDGEMENTS

The author is indebted to the following:

Dr EL Smith and the Department of Chemical Engineering and Applied Chemistry for making available the facilities for research.

Dr RG Temple who supervised the work, for his help and guidance throughout this project.

For the provision of a scholarship by the Science and Engineering Research Council and ESSO Research for providing the equipment.

Dr D A Hasson for his guidance during the Ricardo E6 engine tests.

Mr N Roberts and the technical staff in the construction of the experimental equipment.

Finally, my family for their support throughout my PhD.

Dedication

To my family

CONTENTS

Tables 4.1.1 - 4.1.16
Figures 4.1.1 - 4.1.100
Figures 4.2.1 - 4.2.18
Tables 4.3.1 - 4.3.6
Figures 4.3.1 - 4.3.6
Figures 4.4.0 - 4.4.23
Plates 441 - 4417
Tables 5.1 - 5.4

CHAPTER ONE

CHAPTER 1

INTRODUCTION

The suitability of a fuel for use in high speed carburettor engines of modern design is usually determined by a range of physical and chemical properties. Chief among these are the following:

(a) ignition properties
(b) latent heat
(c) volatility
(d) calorific value

The range of volatile fuels available which satisfy the requirements are at present limited to the products of crude petroleum oil. Modern motor spirit, known generally in this country as petrol and in the United States as "gasoline", is a complex mixture of different hydrocarbons obtained from the crude petroleum by various systems of distillation and refining. The primary source of petrol is non-renewable fossil fuel and relying on this in future is short sighted at best. This however does not imply that they do not have a role to play, but as these fuels are being used, time should be spent to develop alternatives or finding ways of prolonging their use.

Alcohol fuels do provide this alternative. Methanol was an established cooling and heating fuel in Europe by the mid 19th century and was used for lighting until about 1820. Ethanol by then was being used as a motor vehicle fuel and was presumed by Henry Ford in the 1890's to be the fuel of choice for his automobiles during their earliest stages of development. Petroleum due to its relative abundance and lower costs quickly supplemented ethanol as a motor vehicle fuel. The World Wars I and II increased the use of methanol and ethanol as a motor vehicle fuel due to the attendant petroleum shortage. The 1973 oil embargo by OPEC (Organisation of Petroleum Exporting Countries) more recently reduced oil production and since then studies, symposia and experimental programmes concerning alcohol fuels have been initiated by the United States and other countries. Brazil, for example, has made a major commitment to convert to alcohol and alcohol-gasoline blends for use in motor vehicles. It was thus the aim of this project to carry out research in this field of motor vehicle development. Though enough work has been done using gasohol (up to 20% alcohol) little work has been done on blends higher than 20%. The more important areas of research have to be the development of carburettor, fuel systems and engine design parameters, performance, emission control and material compatibility.

A major part of the present work is concerned with altering the carburettor jet settings to allow for the various heating values of all the different fuels and testing the effects on performance of these on the Fiat 127 903 cc four cylinder engine. This engine was chosen because of its popularity in the European countries and more importantly its lower engine capacity. A Heenan Froude DPX1 water brake dynamometer provides the load to carry out the test bed experiments, the load on the dynamometer being measured using a load cell comprising of a series of strain guages wired in a Wheatstone bridge arrangement. Fuel and air flowrate measurements are used to evaluate the Fuel/Air (F/A) ratios.

The fuel flowrate is calculated from timing a measured quantity of fuel consumed, while the air flowrate is calculated by measuring the pressure drop in an Alcock Viscous Flow Canister.

Exhaust analysis using the Horiba Mexa 3211E and 301XE infra red analysers shows the effects of altering F/A ratios on exhaust emissions and on the efficiency of the engine.

By developing a technique to remove the wall film from the intake manifold of carburetted engines it is possible to determine the design specifications of intake manifolds for use with alcohol fuels and alcohol gasoline fuel blends. A carburetted single cylinder engine was available for a series of experiments. The single cylinder engine is preferred since fuel distribution in a multicylinder engine plays a major part in its performance and efficiency. The Ricardo E6 single cylinder, variable compression engine was used for this purpose.

The physical properties of a fuel can provide useful data as to how the fuel will behave during everyday operation of the motor vehicle. Distillation curves for the fuels were thus plotted. They provided information on "cold starting", "stalling", "warm-up" time, acceleration, high speed performance, "hot starting" and others, all of which are critically important in relation to satisfactory performance.

Material compatibility is of prime importance when considering the introduction of a new fuel. For this reason material compatibility tests were carried out using materials from the carburettor (the carburettor being the most vulnerable component in the engine as it meters the fuel into the cylinders and is always in contact with the fuel). The use of alcohols over several years has not yet revealed any major short-term effects. However vehicle components are often expected to have a useful life of 10-20 years and long-term studies may become more important during prolonged periods of use.

CHAPTER TWO

CHAPTER TWO

BACKGROUND AND LITERATURE REVIEW

2.1 Overview

The issues that need to be examined to evaluate alcohol fuel as an alternative to petroleum based liquid fuels include (1):

1. availability of feedstocks
2. viability of production processes
3. environmental impact of use of feedstock and production processes
4. performance in specified uses, such as motor vehicles
5. national priorities for feedstock and product use
6. economics

These features are now examined in respect of the two most likely substitute alcohols, methanol and ethanol.

2.2 Methanol

Most of the methanol production starts with a synthesis gas (syngas) (2,3,4) formed by gasification of fossil fuels.

Natural gas is currently the most common feedstock (5) although coal or wood are also used (2). From the resulting "syngas" methanol is produced by a catalytic process. This process produces purer methanol than most other processes because of the lower sulphur content.

Methanol can also be produced from biomass using (4):

1. anaerobic digestion of wet biomass producing methane which is then converted to methanol, and
2. partial combustion of dry biomass to produce syngas which in turn is used to produce methanol.

Rising prices and priority uses such as home heating make natural gas a poor choice of feedstock for methanol production. However, the methane and other tail gases that are burned off as waste in the petrol refinery processes may be utilised. This also means that the location of the synthysis plant has to be close to a refinery process.

Coal is a poor long-term feedstock as it is essentially used for power generation and is thus generally dearer than wood and other biomass.

Biomass particularly in the form of wood and agricultural waste (6,7) appear to be the best long-term feedstocks for methanol production. The principal advantage of using this process is that it saves money and results in less environmental degradation then using other feedstocks.

2.2.1 Investment and Operating Costs

Capital and operating costs depend on the feedstocks, site and production processes (8).

The present cost of methanol production is misleading when considering methanol as an alternative to motor fuel. The reason is that methanol through the years has been used primarily in industry where high grade methanol has been required, whereas impurities such as benzene and other organic compounds are acceptable in small percentages when used as an automotive fuel. The cost of producing low grade methanol is considerably less. In addition, if methanol became widely used as an automotive fuel, there would naturally be economies of scale.

2.2.2 Potential as a Motor Fuel

Methanol may be used in internal combustion (IC) engines, turbine engines etc. Its high octane ratings (109 MON, 112 RON) which are indicative of its high performance combustion capabilities make it an outstanding fuel for IC engines.

Straight methanol provides cleaner operation and lower pollutant emissions than gasoline (9,10,11). Due to its lower calorific value a higher fuel injection rate is required for smooth operation of the engine. Its lower vapour pressure creates problems when starting the engine below 5°C. The high polarity of the hydroxyl ion in methanol and its solvent like characteristics can cause corrosion of certain engine and carburettor components. These must be considered when using methanol as an automotive fuel. Other considerations such as adequate lubrication and cooling will also have to be resolved in the long term.

Methanol can be blended with gasoline. Blends of upto 20% v/v methanol require no engine or carburettor alterations (49). With slight modification, however, the efficiency of the engine can be improved(49). Phase separation is a major problem when using blended fuel.

These problems can be resolved, but government priorities will influence whether or not methanol is used on a large-scale in the transportation sector especially in countries where methanol can be readily available, for example, the USA.

2.3 Ethanol

Ethanol may be produced by:

1. fermentation of carbohydrates and sugars (14,15), and
2. chemical reaction produced by acid-catalysed hydration of ethylene.

The fermentation route is considered here, because if natural resources of petroleum run short the only feasible way to produce ethanol as an alternative fuel would be by the fermentation of carbohydrates and sugars.

Sugars and Carbohydrates from crops —> fermentation and distillation processes and dehydration —> Anhydrous alcohol —> Uses as a fuel

2.3.1 The Feedstocks

The following feedstocks are available for ethanol production:

1. sugar crops, eg. sugar cane, shorgam etc
2. starch crops, eg. corn
3. cellulose crops, eg. eucalyptus and pines and
4. agricultural product waste.

Feedstocks 1 and 2 are, of course, major food crops and as such are controlled by governments and it will be they who eventually decide whether to use these crops for food or transport-fuel. This will be the major issue in the developing and third world countries.

2.3.2 Potential as an Automotive Fuel

As an automotive fuel ethanol can be used in the following ways:

1. ethanol-gasoline blends,
2. hydrated (lower-proof) ethanol,*
3. straight anhydrous ethanol
4. dual carburetted diesel fuel supplement.

The market already exists for gasoline and other ethanol-gasoline blends. In 1979 fifty million gallons of ethanol were blended with gasoline for sale as a motor fuel (13) (no engine modifications were necessary).

The use of hydrated ethanol requires certain engine modifications. These include having a large volume fuel injection system and a special induction heating system to improve the vaporisation of the fuel especially during cold weather.

---

* The term "hydrated" alcohol is used in this work, as in some of the American literature, indicating alcohol/water mixture.

Stalling and hesitation during warm-up periods are the most common problems when using blends of greater than 15% v/v of ethanol with gasoline.

2.4 Production Cost, Methanol, Ethanol, Gasoline

The price of unleaded gasoline in the USA was quoted in 1976 as 0.74 dollars per gallon based on crude oil imported at 14.00 dollars per barrel, (12). Since then the oil market has remained fairly steady and the gasoline price has remained relatively unchanged.

2.4.1 Cost of Biomass-based Alcohol Fuels (13)

Assuming that imported crude oil in the USA is the most expensive, all prices will be compared to this.

The energy content (gross or higher heating values) of a gallon of gasoline is nearly twice that of methanol and one and a half times that of ethanol (12).

Fuel	Energy Content MJ/l
Gasoline	28,800
Methanol	15,050
Ethanol	19,649

Due to the energy differences in the fuels, the cost of production will be given on a constant energy basis i.e. \$ per 10^6 (J/m^3 kg) rather than constant volume i.e. \$ per litre.

2.4.2 Cost 1982 (12)

Fuel	Cost of Fuel $\$/J \times 10^3$	Range of Uncertainty $\$/J \times 10^3$
Gasoline	2.84	1.42
Methanol	7.1	1.42
Ethanol	12.32	3.79

2.4.3 Projected Costs in 1992 (12)

Fuel	Cost of Fuel $\$/J \times 10^3$	Range of Uncertainty $\$/J \times 10^3$
Gasoline	3.79	1.90
Methanol	5.69	1.42
Ethanol	10.43	2.84

Alcohol production costs are shown to decrease over time because new plants are assumed to become increasingly large, and therefore result in improved economies of scale.

The primary conclusion that can be drawn from these figures is that alcohol fuel will cost more then gasoline on an equivalent energy basis in the time period in question. Ethanol costs are about three to four times that of gasoline. However an abnormal increase in gasoline prices as occurred in the early 1970s could markedly disrupt this prediction.

2.5 Environmental and Safety Considerations

Since the alcohols can replace lead as an octane booster, their combustion in motor vehicles becomes inherently safer. As alcohols contain no impurities such as sulphur, no oxides of sulphur are released into the atmosphere.

Spillage of alcohols on a large scale both on land and sea is also less hazardous. The alcohols greater solubility in water means that the spill can be easily washed away on land and in the sea they pose no more hazardous problems then gasoline.

Alcohol fires can be easily put out by water spray, carbon dioxide and dry chemical or foam extinguishers, unlike gasoline fires which cannot be extinguished by water spray.

If ignited, methanol can naturally be quite dangerous. Since methanol is associated with grain alcohol, many cases of methanol poisoning have been documented.

The established threshold limit value (TLV) for methanol fumes is 200 ppm.

2.6 Fuels and Fuel Characteristics

2.6.1 General

The characteristics of good SI engine fuels are (1):

1. high standard heat of combustion;
2. high octane number;
3. high latent heat of vaporisation;
4. rapid rate of flame propagation;
5. phase stability throughout the range of ambient temperatures and conditions;
6. convenience of processing, storing, transporting and distributing; and
7. low level of harmful emissions.

2.6.2 Fuel Related Properties

Details of physical and chemical properties can be seen on Table 2.1.

2.6.3 Methanol

Methanol - also referred to as methyl alcohol or wood alcohol - is the simplest compound in the class of organic compounds called alcohols. It is a colourless and odourless liquid and is miscible in water in all proportions.

The oxygen in the molecule constitutes to 50% of its molecular weight. It forms a hydroxyl group in the molecule making it strongly polar as compared to non polar hydrocarbon fuels. This causes one of the major differences between the properties of methanol as a fuel and other conventional petroleum hydrocarbon-based fuels.

TABLE 2.1 Physical and Chemical Properties of Methanol and Ethanol.

	Units	Methanol	Ethanol	Ref
Colour		Colourless	Colourless	
Molecular wt.		32	46	50
Melting point	^{o}C	-97.8	-114.4	50
Boiling point	^{o}C	64.7	78.4	50
Specific gravity		0.796	0.794	50
Viscosity at 20^{o}C	kg $m^{-1}s^{-1}$	5.9×10^{-4}	1.22×10^{-3}	50
Explosion limits in air	lower vol%	6.7	3.9	35
	higher vol%	50.0	19.0	35
Flash point open cup	°C	18.1	13.7	16
Octane Rating				
MON		98	99	16
RON		112	110	16
HUCR		17:1	17:1	16
Autoignition temp.	^{o}C	470	392.2	50
Reid Vap. Pressure	psi	4.5	2.3	16
Heat of combustion	kJ/kg	23865	29773	16
Free energy of formation	kJ/mol (l)}	161.7	-174.8	50
Latent heat of vaporisation	kJ/kg	1100	856	50
Flame speed	m/s	0.49	0.43	50
Solubility in water		Total	Total	
Water in		Total	Total	
Solubility in gasoline		Total	Total	
gasoline in		Total	Total	

2.6.3.1 Combustion Characteristics

In all cases isooctane is used as a standard hydrocarbon to compare fuel proporties because it closely resembles gasoline in its C:H ratio.

The Stoichiometric equations for combustion or oxidation are:

Methanol: $CH_3OH + 1^1/_2 O_2 \longrightarrow CO_2 + 2H_2O$

Isooctane: $C_8H_{18} + 12^1/_2 O_2 \longrightarrow 8CO_2 + 9H_2O$

The heats of combustion (ΔHc^o) at 25°C (17,18,21) are as follows:

Methanol	Liquid kJ/kmol	Gas kJ/kmol
Higher: to H_2O (l)	-728.13	-764.08
Lower: to H_2O (g)	-638.11	-676.05
Isooctane		
Higher: to H_2O (l)	-5465.5	-5503.2
Lower: to H_2O (g)	-5069.3	-5107.0

The lower values of the heat combustion are usually used when comparing fuels since it is assumed that the water is exhausted from the engine as vapour.

2.6.3.2 Heat of Vapourisation (ΔHv^o 298):

There is a strong hydrogen bond between the molecules due to the hydroxyl (-OH) group present in methanol. This hydroxyl group also makes the molecule highly polar similar to water which has the H-OH molecule. Due to this the specific latent heat of vapourisation ΔHv^o 298 is 1167 kj/kmol (17) making it almost four times that of iosoctane (ΛHv^o 298 = 307.7 kj/kmol). This indicates a marked difference in their heats of combustion (19) and hence in the thermal efficiency of the engine.

2.6.3.3 Vapour pressure

Methanol has a relatively low vapour pressure and high boiling point due to its highly polar nature when compared with non polar hydrocarbons (eg. isooctane).

	M.wt	Boiling Point^{o}C	Vapour Pressure KPa
Methanol	32.04	64.5	37
Isooctane	114.23	99.3	15.5
*Gasoline	98	32-180	80 (average)

The vapour pressure exerted by methanol is considerably lower than that exerted by the lighter fractions of gasoline. Thus use of methanol as the sole fuel can lead to difficulty in starting the engine below temperatures of 10^{o}C. This problem can be overcome by blending methanol with the lighter fractions i.e. C_1-C_5 of petroleum compounds (see later).

2.6.3.4 Phase Stability

The polar nature of methanol makes it infinitely soluble in water. However, its hydrocarbon-like characteristics allow it to be completely soluble in dry gasoline. Very low temperatures and the presence of water (0.1%) will cause phase separation in methanol-gasoline blends making it difficult to transport such a fuel. The

---

*Gasoline has a large variety of light and heavy fractions depending on summer or winter conditions and thus one cannot specify a fixed molecular weight or boiling point, (see later).

problem can be overcome using additives thus enhancing the water tolerance (see later). Those under serious consideration are the higher molecular weight alcohols (20,33). Straight methanol however, can include some water.

2.6.3.5 Knock Resistance and Octane Rating:

Relationship between knock resistance and octane number rating is well known. It is common to define octane number rating as the motor octane number (MON) and research octane number (RON) (113).

The MON is the octane rating at 900 rpm, using a mixture that would give maximum knock; mixture temperature 149°C, ignition timing between 19° and 26° before tdc. These conditions of the test approximate to automobile engines at speeds of about 2500 rpm.

The RON is the octane rating obtained from laboratory test results and also results approximating to those of actual engines on their own, but at lower speeds, eg. 1000 rpm. The laboratory tests specify the following conditions; mixture strength that gives maximum knock; mixture temperature 51.6°C; and ignition timing 13° before tdc.

For methanol the motor octane number (MON) has been estimated as 98 and a research octane number (RON) ranging from 106 to 114 usually taken as 110. Isooctane is taken as a standard and has a RON and a MON of 100.

The high octane rating permits considerably higher compression ratio than with gasoline (16). The highest useful compression ratio (HUCR) that can be used with methanol is 17 to 1 (16). This means that one can achieve greater efficiency and power and is one of the main reasons why some racing cars use methanol as a fuel (22).

When blended with gasoline in small quantities, it increases the octane rating considerably more than in the proportion added (23,24).

2.6.3.6 Ignition and Flame Characteristics:

The lowest temperature at which a fuel-air mixture ignites spontaneously is the measure of the ignitability of the fuel. Depending on the operating conditions, ignitability of methanol has been reported to be between 400°C and 500°C. It is thus unsuitable in compression ignition engines. The addition of water increases the ignition temperature (25).

Methanol has a higher flame speed then petroleum based fuels (25) which allows rapid and complete combustion of the fuel in an IC engine. Thus better performance and higher efficiency can be attained. Exhaust emissions are correspondingly lower when compared with gasoline.

Methanol has a wider misfire limit than gasoline. The lean misfire limit is lower than gasoline (26) which allows engines to operate using leaner mixtures of methanol giving higher efficiency and lower exhaust emissions.

The flame temperatures of methanol in air has been estimated at 2194°K which is 250°K below that of isooctane (27). Since methanol contains no carbon-carbon bonds and does not therefore form any unoxidised carbon particles no thus soot is found when pure methanol is burned. It burns with a bluish flame with a very low luminosity rating. Researchers have found (28) that methanol flame will remove soot deposits left by previous petroleum based fuels from engine cylinders.

2.6.4 Ethanol

Ethanol, like methanol, has a hydroxyl group which is strongly polar but not as much as methanol and is thus more like petroleum based hydrocarbon fuels.

Details of physical and chemical properties can be seen in Table 2.1.

2.6.4.1 Combustion Characteristics

The heats of combustion (ΛHc^{o}) at 25°C (29).

Ethanol	Liquid kJ/kmol	Gas kJ/kmol
Higher: to H_2O (l)	-1365.4	-1407.7
Lower: to H_2O (g)	1230	1272.0

2.6.4.2 Latent Heat of Vapourisation:

The polarity exerted by the hydroxyl ion in ethanol is not as great as that in methanol, and thus the latent heat of vapourisation of 920 kJ/kmol is much lower and only three times that of isooctane. The volumetric efficiency of the engine therefore is not as high as that attained by methanol but still considerably higher than by gasoline (30).

2.6.4.3 Vapour Pressure:

Ethanol has a lower vapour pressure (31) than methanol in accordance with its higher molecular weight (46 compared to 32). In addition, alcohol/gasoline blends form azeotropes possibly causing a disproportionate increase in vapour pressure, particularly at lower concentrations. Being a single component liquid, ethanol has a fixed boiling point of 78.4°C as opposed to gasoline which has a wide boiling range (32°C - 180°C).

The lower vapour pressure creates difficulty when starting engines at temperatures below 10°C as with methanol.

2.6.4.4 Phase Stability

Though not as strongly polar as methanol, the presence of water particularly promotes phase separation in ethanol/gasoline blends. Low temperatures decrease water tolerance (12), and this creates serious problems in the fuel distribution system. The addition of benzole or other high molecular weight alcohols enhances water tolerance.

Researchers (32,33,34) suggest that the water tolerance increases with:

1 increase in temperature
2 increased content of alcohol (methanol or ethanol)
3 increased content of aromatics
4 addition of higher alcohols

Surfactants may also be a way of enhancing water tolerance (34).

When using straight ethanol for engine operation water content of up to 15% v/v can be tolerated (see later).

2.6.4.5 Knock Resistance and Octane Rating

Ethanol too, like methanol has a high octane number (MON - 99, RON - 115) and can thus permit the use of higher compression ratios than with gasoline. The HCUR for ethanol is 17 to 1 as it is with methanol and hence greater efficiency and power can be achieved. Ethanol can be used as an octane booster when blended with normal gasoline.

2.6.4.6 Ignition and Flame Characteristics

The autoignition temperature for ethanol is 392°C (35) which is lower than that of methanol (464°C). The addition of water will increase the autoignition temperature. It has a higher flame speed than petroleum based fuels (25) which allows rapid and complete combustion of the fuel in an IC engine thus giving lower exhaust emissions. Lean mixture engine operation is possible due to its lower misfire limit thus allowing higher efficiencies to be attained.

2.7 Exhaust Emissions

Exhaust pollutant emissions are lower than those obtained with gasoline but higher than those with methanol. Generally, one gets lower exhaust emissions with alcohols than with gasoline. This will be discussed more fully in the Experimental, Results and Discussion chapters.

2.8 Material Compatibility

The hydroxyl group in the alcohols make them strongly polar and thus reactive with and corrosive to many metals.

The major problem with methanol/gasoline blends in a conventional vehicle fuel tank is corrosion of the terneplate lining by methanol (36). The terneplate coating consists of 75-90% lead and 10-15% tin. Methanol attacks this thin (1/2 - 1 mm thick) coating forming lead hydroxide. The lead hydroxide subsequently plugs the fuel filter and clogs the carburettor jets or injector nozzles. In vehicles relying on such fuel tanks, corrosion inhibitors should be used (36) or use of alternative materials (37) should be considered. The use of magnesium and aluminium which are being increasingly used in engine blocks should be avoided (36) as both are severely attacked by methanol.

In a majority of cases ethanol is not as detrimental to metals as methanol. Ethanol for instance does not attack tin (38) as severely as methanol (39). This is because ethanol is less polar than methanol. Ethanol will however attack terneplate and other fuel tank coatings (40).

Plastics and elastomers are also attacked by methanol and ethanol. Their solvent properties and their affinity to hydrated materials only compound the problem.

Elaborate tests were carried out by Pinto (41) showing the effects of these alcohols on elastomers and plastics used in vehicles after which alternative materials were suggested. Results of these tests and those done by other researchers are listed in the table below.

Table 2.2 Materials Compatibility

Materials	Typical component use	Replacement in alcohol vehicles	Source of information
Zamak 4% Al, 1% Ca, 95% Zn	Diecast barb body	Elelholess nickel plated Zamak	47
Steel	Fuel line	Stainless steel tubing	47
Terne plate (90% Pb,) (10% Zn)	Fuel pump housing Fuel tank coating	Olive-crab chromate coated steel	47
	Fuel sander coating	Tin plating	47
Lead	Plugs for carburettor body	Brass	47
Aluminium	Some carburettor bodies		
Dual-layer neoprene hoses	Fuel lines	Teflon	87
PVC braided hose	Fuel lines	Teflon	87
Tygon tubing	Fuel lines	Teflon	87
Polyvinylolene chloride	Filter	Nylon carcass plus phosphor bronze screen	41.
Zn plated and chromated low carbon steel	Cap seal refiner	Tin plated low carbon steel	41
Nylon 11	Fuel line	Nylon 11 (OK)	41
Nylon 6	Filter body	Nylon 6 (OK)	41
Phenolic resin/ impregnated paper	Filter element	Same with extended cure time	41
Lead coated cam Carbon steel	Filter element heads	Tin coated low carbon steel	41
Low carbon steel	Fuel line tubes	Copper	41
Nitrilic rubber Materials	Fuel line connections	Nitrilic rubber	41
NBR	Fuel pump diaphram	NBR (OK)	41
Zn plated chromated low carbon steel	Fuel pump covers	Green chromated low carbon steel	41

Materials	Typical component use		Replacement in alcohol vehicles	Source of information
SA2 320 aluminium	Carburettor body		Same, chemical nickel plating, 15 to 20 µm thick	41
Black oxidised low carbon steel	Throttle shaft		Nickel plated low carbon steel	41
Brass	Idle mining needle		Brass (OK)	41
Leather	Acelerating pump piston		Brass	41
Zn plate chromated Low carbon steel	Accelerating pump stem		Cadmium plated double chromate coating	41
Aluminium	Power jet vacuum Control stem in carburettor		Brass	41
Zn plated chromated low carbon steel	Fuel return tube		Brass	41
Zn plated chromated high carbon steel	Accelerating pump springs		Stainless steel	41
Magnesium	Engine blocks coating material		eg. steels, nickel	36
Phosphatized steel	Fuel tank		Steel with copper coating	40
Cast iron	Valve seats of cylinder head		Sintered alloy	41
	Intake	Exhaust		
C	0,7-1,0	0.8-1.3		
Pb	2,5-3.5	0.5-1.0		
Ni	28.5-3.5	1.3-1.6		
Co	-	10.0-12.0		41
Mo	-	1.5-2.5		
	Hardness (Rb)	106-108	108-110	
Composition type} asbestos facing} low carbon steel Zn} plated} Clyinder Grommets}	Cylinder head gasket		Composition type, high resistance asbestos facing, stainless steel cylinder Grommets	41
SAE 5132	Intake valve		SAE 5135, aluminized head and face, flash chromed stems	41
21-4N	Exhaust valve		21-4N, aluminized head and face, flash chromed stems	41

2.8.1 Effects on the wear of alcohol-fueled engines

Tests carried out by various researchers (40,42-47) show that the combustion of alcohols and more importantly methanol in spark ignition engines can cause unusually high corrosive wear of the upper cylinder bore and ring areas. This wear of the cylinders is higher during conditions of warm-up and cold-weather operation. Corrosion is also observed in the exhaust valve guides, cam followers and lobes, and bearing surfaces but not as severe as the cylinder bore and rings. Ernst et al (44) compared the exhaust gas compositions of several test vehicles operating on neat methanol and gasoline. In accordance with higher NO_x emission concentration these researchers found that exhaust condensates from methanol-fueled vehicles contained significantly higher concentrations of nitric acid than those vehicles fueled with unleaded gasoline. This nitric acid contributes to the chemical attack of the cylinders as well as diluting the lubricating oil. Ernst et al (44) also suggested design improvements and also operating conditions to reduce engine wear. King and Chui (42) concluded in their tests that barrel faced chrome rings appeared to be the simplest and most cost effective improvement available for improved wear in a methanol fueled engine.

2.9 Lubrication

Alcohol influences the lubrication of an internal combustion engine different to gasoline because of unsimilar physical and chemical properties. Methanol and ethanol have a single boiling point and a high latent heat of vaporisation. Thus liquid methanol and ethanol are more likely to reach the cylinder wall than gasoline. The condensation of unburned methanol or ethanol (45) and water in the engine form an emulsion with oil. The emulsion when formed and distributed in the engine (48) may restrict the supply of oil for boundary lubrication. Methanol or ethanol and water droplets in the emulsion may flash to vapour upon contact with hot surface leaving insufficient oil on the lubricated area.

The blow-by gases of alcohol-fueled engines contain higher concentrations of corrosive components such as aldehydes and acids (formic and acetic) which are expected to contribute to more corrosion and wear than the blow-by gases of a gasoline fueled engine. These corrosive combustion products attack metals such as aluminium, copper and lead alloys (37).

Methanol and ethanol may decrease the effectiveness of oil additives by changing their chemical environment.

2.10 Design Modification Requirements

2.10.1 Introduction

It is of great importance that the whole process of carburation, fuel distribution and combustion in the cylinder is optimised for the fuel in use.

The following are some of the modifications required for vehicle operation on straight alcohols and alcohol gasoline blends.

2.10.2 The Carburettor

If the engine is intended to run on gasoline, the main jet - the fuel metering device, has a specific diameter. The idle jet allows the right proportion of fuel to enter the system during no load conditions. When using alcohol fuels, these jet settings have to be modified. The idling mixture is much easier to set as it is usually done by a turn of a screw which allows more or less fuel to enter the system. The correct jet setting can be found by monitoring exhaust gases . The fuel metering jet - the main jet with a larger diameter would be required to run the engine on straight alcohol or alcohol/gasoline blends with a high proportion of alcohol. The size of the jet required for a particular fuel is dependent on that fuel's calorific value. The lower the calorific value the larger the jet diameter required. Details of the calculation of the required jet sizes is in Appendix 2.

The carburettor float is another item that would require readjustment when using particular fuels. With fuels of higher density, the fuel level in the float chamber will be lower, and the flood mechanism will have to be adjusted to raise the level to the correct height.

2.10.3 The Manifold System

The fuel-air mixture is distributed to each cylinder of a multicylinder engine through a specially designed manifold which should keep the fuel and air thoroughly mixed. Hence manifold systems are designed for specific fuels. The manifold required for operation with alcohol and alcohol gasoline blended fuels should also therefore have the intake profile and cross section designed for greater efficiency (see later). In the case of straight alcohol, the diameter of the intake manifold would have to be increased to allow for the greater volumetric fuel charge. The shape of the manifold should give adequate distribution to all the cylinders as maldistribution of fuel charge can lower performance of the engine significantly. Pefely et al (51) defined the maldistribution index (MI) as:

$$MI = \frac{\emptyset \text{ richest cylinder} - \emptyset \text{ leanest cylinder}}{\emptyset \text{ average}}$$

$$\emptyset = \text{equivalence ratio} = \frac{\text{A/F ratio stoic}}{\text{A/F ratio}}$$

They suggested that poor nebulisation or atomisation of the fuel droplets combined with inadequate mixing with the air stream leads to the phenomena of maldistribution.

The above equation cannot represent all possible arrangements of ø values among four cylinders. However it does appear to be an adequate index to quantify changes resulting from maldistribution in engine power and thermal efficiency (19).

In summarising their results Pefley et al (51) concluded that the maldistribution of the fuel-air mixture among the cylinders of a four cylinder IC engine appeared to affect the power and thermal efficiency in a predictable manner except at very lean operating conditions. The exhaust emissions could not be accurately predicted using the maldistribution index.

Cold starting of the engine can also be improved by modifying the intake/exhaust manifolds. Neblon et al (57) suggested the following ideas:

1. Substitution of a copper gasket between the block and the intake manifold for the fibre gasket to improve conductivity.
2. Have the coolent flow around the intake manifold at an appreciable rate so as to increase the Reynolds number and thus improve the heat transfer between the coolant and incoming air and fuel.
3. Pre-heating of intake air over the exhaust manifold except at very high load, and
4. Electric heating of the air/fuel mixture.

2.10.4 Combustion Cylinders

The performance of conventional SI engines using straight alcohol fuel can generally be improved by modifications to increase the compression ratio (52, 53, 54, 55, 56, 57, 58, 59, 60). The HUCR for alcohols is appreciable higher than normal gasoline (see Table 2.1) owing to the higher octane rating (16). There are several methods - including the use of special pistons and designing the heads to reduce the cylinder volume - for making these modifications (1). Raising the compression ratio by milling the combustion chamber head (57) seems the most cost-effective way to take advantage of the alcohol's high octane rating. Milling the combustion chamber head costs one-fifth that of a piston exchange and returns most of the benefits (57). These include:

1. lower fuel consumption by leaner operation (56)
2. high mean effective pressure at full load (56)
3. greater thermal efficiency (16).

Disadvantages associated with the higher compression ratios include:

1. increase in hydrocarbon and nitrogen oxide emissions (56)
2. cold starting and warm-up are more difficult to control (56)
3. high-compression engines are prone to pre-ignition (56).

It is therefore important to optimise these when designing the vehicle for alcohol or alcohol-gasoline blended fuel operation.

2.10.5 Ignition and Valve Timing

With straight alcohols, the ignition timing is generally retarded (set so the spark occurs a few degrees before top dead center (tdc)). Alcohols burn at a faster rate than gasoline and therefore less time is required to completely combust all the mixture because its rate of flame propagation is more rapid. At slower engine speeds, the residence time of the fuel in the combustion chamber is longer than at faster engine speeds. Therefore, although the timing can be retarded at idle, the degree to which the ignition timing can be retarded must be progressively reduced back toward the normal setting as the engine speed increases (56, 61).

Spark plugs that fire at a cooler temperature and a reduced spark plug gap may be necessary (56, 62).

Generally no modifications of value timing are necessary to convert an SI engine to run on alcohol and alcohol-gasoline blended fuel, although larger intake values will increase volumetric efficiency.

2.11 Vehicle Operation and Driveability

2.11.1 General

Early studies of operation with alcohol fuels have steadily increased in the last decade. For example in August 1977 over 35 motor vehicles were converted to operate on straight ethanol (96%) by CTA (Brazillian Airforce) for the maintenance fleet of two Brazillian utility companies (63). The engines were developed such that the intake system was heated by hot exhaust gases in order to improve mixture distribution and increase the mixture temperature. Intake system modifications were also carried out to provide optimum distribution of the alcohol/air mixture to the individual cylinders. The carburettor was modified to give the correct stoichiometric air/fuel ratio and the air flow reduced for the same reason.

The above case study is typical of many companies and organisations which have tried to adapt their fleet of vehicles to operate on alcohols and alcohol-gasoline blends in the last ten years (64-82). All of these researchers and various others came up with similar conclusions. These can be summarised as follows:

2.11.2 Efficiency and Power

Alcohol blends provide increased torque and thermal efficiency compared to gasoline at all equivalence ratios investigated. The ethanol blend is less so than the methanol blend (80).

Bench tests using straight ethanol, straight methanol and a 15% methanol blend all with gasoline, have been compared with gasoline by Volkswagen AG (52). Results showed that when using low compression ratio engines neat methanol gave a 6% increased power output, neat ethanol a 4% increased power output and a 15% methanol blend a 2% increase in power output after carburettor adjustment. When the carburettor was not adjusted the power output decreased by 4% in the case of the 15% methanol blend and no engine operation in the case of neat methanol and ethanol. When using high compression ratio engines with neat methanol and ethanol, the power output compared to gasoline increased significantly. It was 26% greater in the case of neat methanol and 17% greater in the case of neat ethanol.

The indicated thermal efficiencies were greater for methanol and ethanol at all equivalence ratios (80).

The use of ethanol may also result in an increase of 20% of the maximum torque (63).

Neat methanol and ethanol give a greater volumetric efficiency than gasoline at all engine speeds (13, 58).

2.11.3 Fuel Economy

Fuel economy figures were presented (80) for alcohol blends of up to 20%. They show that as blend level increases to 20%, the leaning effect of the alcohol is slightly more important than its reduced energy content. Using a blend with a lower volatility such as gasoline provides a larger gain in fuel economy as blend level is increased. Volumetric fuel economy was not significantly different between base gasoline and the 10% ethanol blend. A slight (2%) decrease in volumetric fuel economy was noted for highway driving (83).

The theoretical effects of fuels energy differences on the distance a car would travel on each of the three fuels would result in the vehicle run on gasoline travelling twice the distance than on methanol and 1.5 times the distance than on ethanol (1).

Brinkmann (84) showed that the fuel consumption change is affected more by the equivalence ratio of the gasoline engine than by the compression ratio of the ethanol engine. When the engine is fueled with ethanol at the same equivalence ratio as the gasoline engine ($\varnothing = 0.8$), the fuel consumption increase ranges from 58% at CR = 7.5 to 36% at CR = 18. As equivalence ratio is increased ($\varnothing = 1.2$) the fuel consumption increase at CR = 7.5 is 20% and at CR = 18 is 15%. A similar trend is shown by other researchers when using methanol.

2.11.4 Exhaust Emission

When dealing with alternative fuels, the exhaust emissions are of prime importance. The combustion emission from the engine fuel system will fall into one of six major categories.

1. carbon monoxide (CO)
2. various hydrocarbon compounds (HC)
3. carbon dioxide (CO_2)
4. oxides of nitrogen (NO_x)
5. oxides of sulphur (SO_x)
6. particulates of smoke.

Of these only the first four are regulated and the last two are much less significant than the others. Oxides of sulphur are only present in petroleum derived fuels because of the sulphur content in the crude oil. Particulates are mainly of salts of lead or other metals used as antiknock additives. These are however not present in alcohol and alcohol/gasoline blended fuel as antiknock additives are not necessary (see Section 2.6.3.5).

The major exhaust emissions are now dealt with individually. In all cases the effect of fuel/air ratios on their concentration in the engine exhaust is of major significance.

2.11.4.1 Carbon monoxide

The F/A ratio almost entirely determines the CO in the exhaust. Mixtures richer than stoichiometric invariably lead to higher CO emissions in the exhaust (110). With excess fuel present relative to the amount of air available, combustion of the carbon in the fuel cannot be completed and significant proportions of CO will remain in the exhaust. With excess air present, the CO level in the exhaust will be reduced considerably but some will always be present in the exhaust because fuel and air are never perfectly mixed and apportioned in all cylinders.

Nearly all researchers have found that as the alcohol percentage in the gasoline is increased, the CO percentage in the exhaust decreased. This is to be expected on account of the increased percentage of oxygen in the fuel.

2.11.4.2 Hydrocarbon emissions

Hydrocarbon (HC) emissions from gasoline are mostly unburned fuel (UBF). When using alcohols, the UBF emissions are still present but they include some different chemical species from those found in gasoline combustion emissions because alcohols themselves are from a different organic series. Operated at the same equivalence ratio, an engine will produce very similar HC levels on straight gasoline and straight alcohols with a higher efficiency from straight alcohols. Since the alcohols have a lower learn misfire limit, engines can be operated reliably (without any lean misfire etc) on alcohols at equivalence ratios that are lower than gasoline. Reduced levels of UBF and CO in the exhaust can be achieved by lean operation of the engine operation rich fuel/air ratios, mixtures raise HC emissions.

The most important HC-producing mechanism is flame "quenching". As a flame front at very high temprature approaches a relatively cool combustion chamber wall, heat is extracted from it thus "quenching" the flame. Thus HC emissions can never reach a zero level in an engine where the fuel and air are premixed. This phenomena of "quenching", the effects of the HC emissions in the atmosphere and the use of a catalytic converter to reduce HC emission have been studied by numerous researchers. Some of these are mentioned in the bibliography (85-109).

2.11.4.3 Carbon dioxide

In virtually all cases as the levels of CO and HC fall, CO_2 levels increase when using hydrocarbon fuels. Alcohols are found to be no exception to this rule. Thus if complete combustion takes place, CO_2 levels are invariably higher.

2.11.4.4 Oxides of nitrogen

The oxides of nitrogen usually result when the normally inert atmospheric nitrogen (N_2), chemically unites with the oxygen. For this to occur, high temperatures are required, generally above 1100°C. Such temperatures are easily reached and exceeded in spark ignition engines. These high temperatures help reduce HC and CO levels in the exhaust to a minimum. Although the hottest temperatures are attained when there is a stoichiometric mixture, NO_x emissions are high at lean F/A ratios. This is usually because at lean combustion, free oxygen is readily available and exerts a strong influence on NO_x formation. When the mixture is too lean, the peak flame temperatues are not high enough to facilitate NO_x formation.

When operating vehicles with straight alcohol, substantially less NO_x is produced since the combustion temperatures are lower at a corresponding equivalence ratio to gasoline. However since the alcohols can be burned at lean mixtures without problems of lean misfire, the NO_x levels can be reduced further with increase in engine efficiency (110).

2.11.4.5 Start-up and Driveability

A common difficulty experienced with the use of pure alcohols or alcohol gasoline blends in engines is their poor cold-starting and warm-up driveability characteristics (111). Warm-up driveability is the term used to express how well the engine behaves when cold.

Alcohol fueled engines become progressively more difficult to start in winter temperatures (below 10^oC) due to their low front end volatility. Gasoline can be formulated to allow easier start-up at these lower temperature by special attention to the inclusion of low volatile components. Added volatile components such as butane can also be blended (see later) with the alcohols for cold starting enhancement. This is a slightly hazardous way of achieving cold startability as it lowers the explosive limits of the mixture.

Rajan in 1976 (111) suggested engine characteristics required for better cold start. They are:

1 Modification of the metering and induction system characteristics

2 Correct engine compression ratio

3 Improved ignition system.

Thus if the incoming fresh charge is preheated by direct heating of either the fuel or the air (112) and by using higher compression ratios, as they give better ignition and flame propagation and using higher ignition voltages and longer spark duration (52), start-up can be improved.

Warm up driveability can be greatly improved by using the exhaust gases (112) to heat the induction gases. Various other researchers at Volkswagen AG (52) have researched into this.

CHAPTER THREE

CHAPTER 3

EXPERIMENTAL

3.1 Introduction

This chapter outlines the various experimental procedures adopted to achieve the objectives of the research programme. These included:

1 Performance testing using alcohol and alcohol gasoline blends on an existing engine on a test bed,

2 Methods of enhancing performance by design changes, eg. design alterations to the intake manifold.

3 Methods of improving cold starting and warm-up driveability by using additives to the alcohols were suggested.

4 Testing for material compatibility by carrying out a series of corrosion tests.

3.2 Performance

3.2.1 Introduction

Past research into the use of alcohol blends and neat alcohols as gasoline substitutes have shown that for alcohol gasoline blends of up to 20% v/v alcohol, no design alterations are required (1,13,19). However, for blends ranging from 20% v/v alcohol content to neat alcohol operation, modifications to the carburettor and intake manifold become necessary (13,19). In this section performance evaluation of alcohol gasoline blends and straight alcohols is carried out after such modifications to the carburettor jets was made. The intake manifold was left unaltered.

3.2.2 Experimental Equipment (Plate 311)

The engine is a Fiat 127, 903cc standard model, the most widely used engine in Europe. All problems that were initially encountered [24] have now been solved and the engine now provides good low and high speed operation similar to those found in a production car. Stripping of the engine revealed some piston crown damage, but no ring damage or valve damage was observed. The cylinder and head volumes were checked to assess the compression ratio in each cylinder and this was found to be very close to the manufacturer's specifications. (A high compression ratio in one cylinder may lead to knock in that cylinder not representative of a standard engine). Engine configuration can be seen in Appendix 4.

The load on the engine is provided with a small Froude DPX1 water brake/dynamometer, (Plate 312) a machine smaller than the car engine. A load can be exerted on the engine by the operation of sluice gates which direct water onto a rotor. The power absorbed is converted into heat which is carried away by the water flow. Water is supplied from a large tank on the roof of the building and recirculated to it. The proportionally small flow rate to tank capacity ensures a relatively constant inlet water temperature. The load on the dynamometer in conventional use is measured by a load cell. However, to reduce expenditure a system was developed using a radial arm and a ball bearing having point contact on a cantilever which has four strain gauges in a bridge circuit mounted on it. The output from the bridge was measured on a digital multiroll meter and engine torque was obtained from a calibration chart.

The propellor shaft connecting the engine to the dynamometer is of a Hardy Spicer design. Universal joints at both ends reduce the need for perfect alignment as small flexings of the shaft can be absorbed without damage to the bearings. The speed of the shaft was measured using an optical tachometer directed at a reflective mark on the rotor of the dynamometer. Digital readout facilitated accurate setting of speed and the ability to repeat experiments very well.

Thermocouples were inserted into the cylinder head water passages and into the oil sump. Readings obtained from these suggest that the cooling water temperature was satisfactory at between 88 and 93°C after warm up. The oil temperature however rises above the optimum of about 60°C to a temperature of up to 100°C after forty minutes. This was because there was no air cooling which is normal when driving on roads. A blower was used initially with little improvement to the cooling effect. Fins were then welded onto the sump and subsequent runs proved satisfactory. Cooling of the engine cooling water is not carried out using a radiator and electric fan, as in a production car, but by a heat exchanger using water. This proved itself under all conditions.

Knock in the cylinders was detected by two methods. The first of these was achieved by using a "knock washer", a piezo electric device which fitted onto a spark-plug instead of the compression washer. Abnormal pressure variations accompanied by knock on that cylinder were detected as spikes on the normally smooth, pressure curves displayed on a storage oscilloscope.

The second method involved another piezo electric device mounted on a screen thread tapped into a cylinder head bolt. The signal from this device could monitor all four cylinders at once. To use this accelerometer as it is known to its full potential, a preamplifier and dual storage oscilloscope were required to enable 20 or 30 seconds worth of information to be built up on the screen. In this way the spikes associated with knock were easily distinguishable.

The inlet air flow-rate to the engine was measured through a Ricardo in-line flow meter. Fuel flow-rate was measured by measuring consumption of a fixed volume with time. The air fuel ratio, excess air etc could also be monitored continuously using infrared gas analysing equipment which sampled the exhaust gases.

3.2.3 Experimental procedure

The measurement of performance from an engine requires a carefully planned test procedure since ambient conditions and varying test techniques affect the engine performance.

Before and after the test the following test conditions were noted.

1. Ambient temperature,
2. Relative humidity,
3. Atmospheric pressure.

The above parameters alter engine performance in different ways. The following steps were undertaken to ensure repeatability of tests.

1. Engine warm up time was at least 20 minutes before any fuel was tested. This was done so that oil and water temperatures were reasonably constant (± $5^{o}C$) before the fuels were tested.

2. Water pressure for the dynamometer supply was greater than 40 psi. At lower pressure than this it was difficult to steady the engine revolutions. This also ensured that the flowrate through the dynamometer was large enough to cool it sufficient for better operation.

3 The exhaust analysing equipment was recalibrated (according to the manufacturers recommendations) and all filters used in the analysers were changed to ensure accurate measurement, and to avoid an unncessary replenishment of filters during a test run in case they were blocked.

4 Water flowrate to the external heat exchanger used to cool the engine, was set at a level high enough to provide adequate cooling. This valve was found during the initial trial runs carried out prior to any performance evaluation tests.

5 The blower to cool the sump oil was switched on. This was done to avoid overheating of the sump oil.

6 The spark timing was checked to be at top dead center (TDC) using the static timing method.

Trial runs were carried out to familarise oneself with the system. During the trial runs, standard carburettor jet settings were used for economical reasons and the fuel used was four star petrol obtained from a local petrol station. All subsequent petrol used for blending purposes was also bought from the same service station.

Tests carried out at wide open throttle (WOT) during the trial runs showed that the engine performance, ie. maximum horsepower, maximum torque values at specified engine speeds were in accordance with values specified by the engine manufacturers (Fiat). Hydrocarbon and carbon dioxide levels in the exhaust were close to those specified by Fiat, but the carbon monoxide levels were higher.

Having familiarised oneself with the system completely, the following tests were carried out.

1 Effect of fuel type on torque, horsepower (brake and indicated), thermal and mechanical efficiency, carbon monoxide and hydrocarbon levels in the exhaust.

2 Effect of fuel/air ratio on torque, horsepower (brake and indicated),thermal and mechanical efficiency, carbon monoxide and hydrocarbon levels in the exhaust.

The procedure adopted for each test was as follows:

1 The fuel to be tested was prepared one hour before the test began. All fuel blending was done at room temperature (15-18^{O}C) at all times.

2 Ambient conditions were noted 15 minutes before the test began and 30 minutes after the end of the test.

3 All electrical instrumentation was switched on 30 minutes before the test began.

4 The exhaust analysers were checked, recalibrated if necessary, and all filters changed.

5 The ignition timing was checked to be at TDC using the static timing method.

6 Water to the dynamometer and heat exchanger were switched on.

7 The required carburettor jets (both the main jet and the idle jet) were fitted to the carburettor - usually predetermined.

8 The engine was started using the choke and allowed to run for five minutes. The choke was then removed.

9 The idle and the mixture strength screws were adjusted such that an engine idle speed of 800 rpm is maintained. The engine was then allowed to idle as such for 10 minutes.

10 After a 10 minute warm up time, if it was thought necessary (ie. if engine speed rose above 1000 rpm), the idle and mixture strength screws are readjusted to maintain 800 rpm engine speed at idle. This was maintained for a further 10 minutes.

11 The throttle was opened wide and the sluice gates on the dynamometer were opened such that a full load condition was reached and a speed of 1500 rpm maintained. This was maintained for a further 10 minutes.

12 After a total of half an hour warm up time, the test was started.

The test was done in the following manner:

1 The required engine speed was established.

2 The data from instrumentation relating to performance was recorded.

3 The time taken to consume 100 cc of fuel was recorded in order to measure the fuel flowrate.

4 The exhaust gases were analysed.

5 The overall engine behaviour was noted especially for smooth running, misfire etc.

3.2.4 Analysis of Results

The average air flowrate was calculated from a multiplication factor provided by Ricardo to convert the water pressure gauge reading to mass flow rate (g/s). The fuel flowrate was calculated from step (3) in the previous section. From these two the fuel/air (F/A) ratio was calculated.

Equations (113) are then used to evaluate the following to determine the performance of the engine for each fuel (Appendix 3).

(i) Torque
(ii) Indicated mean effective pressure
(iii) Break power
(iv) Indicated power
(v) Mechanical efficiency
(vi) Thermal efficiency

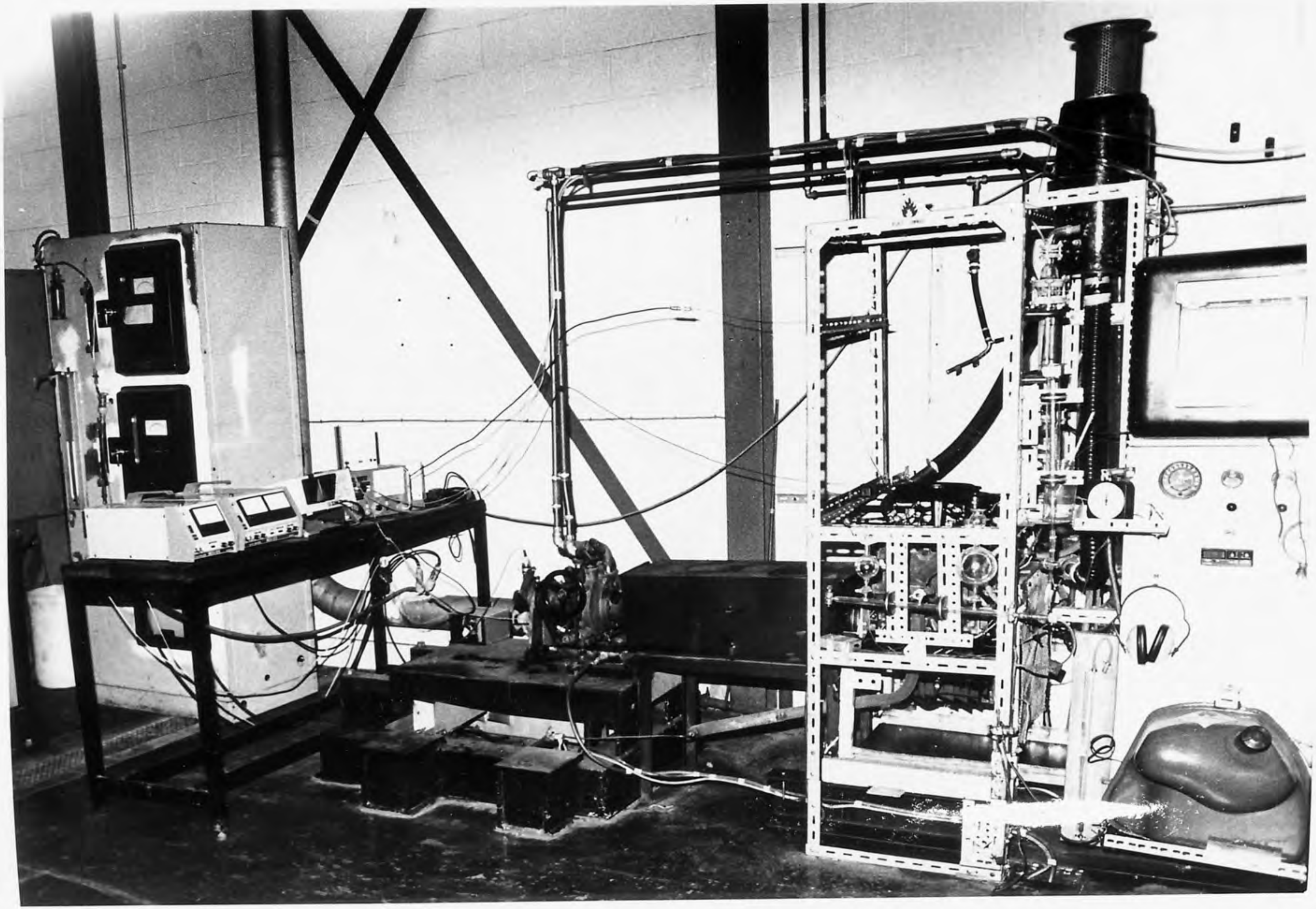

A - Load cell
B - Optical tachometer

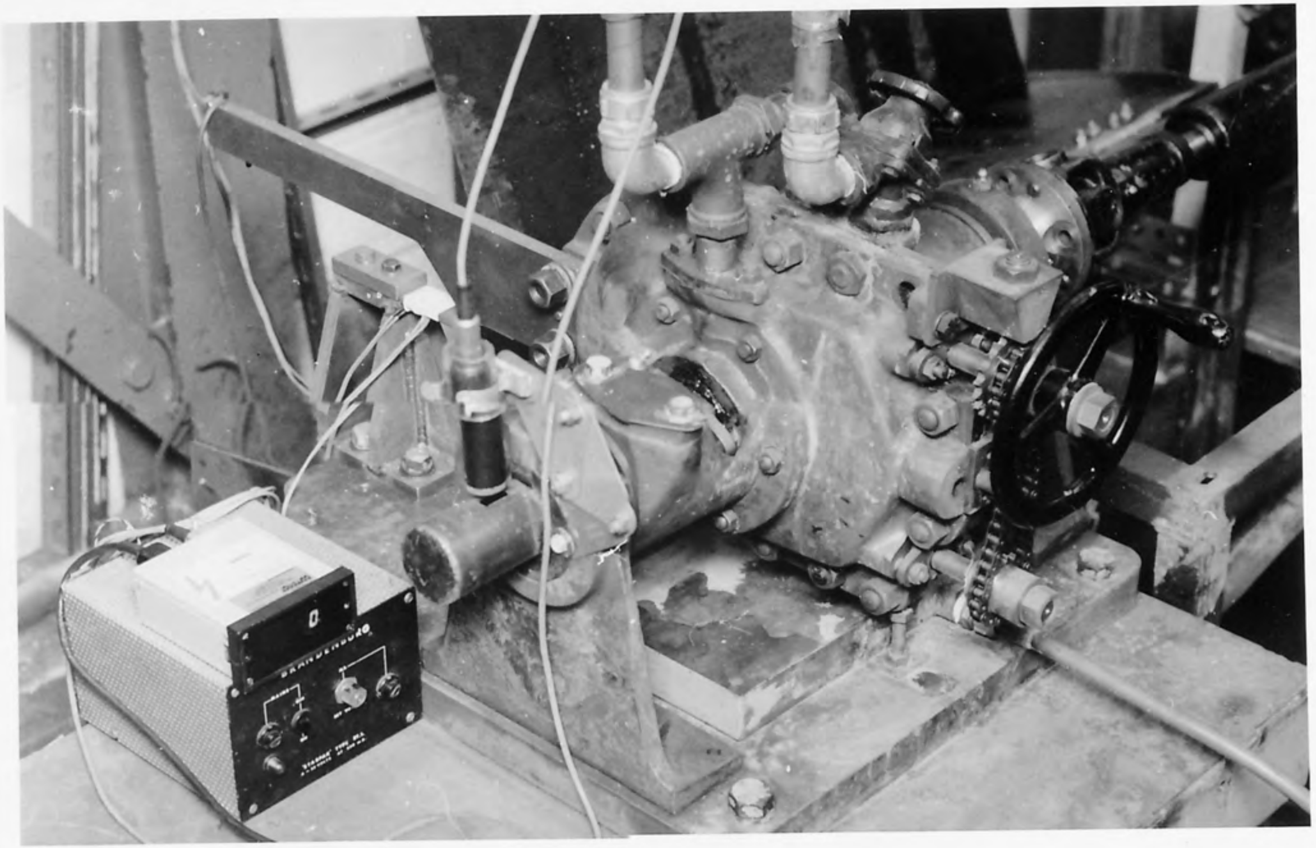

Plate 312: Froude DPX1 meter brake dynamometer

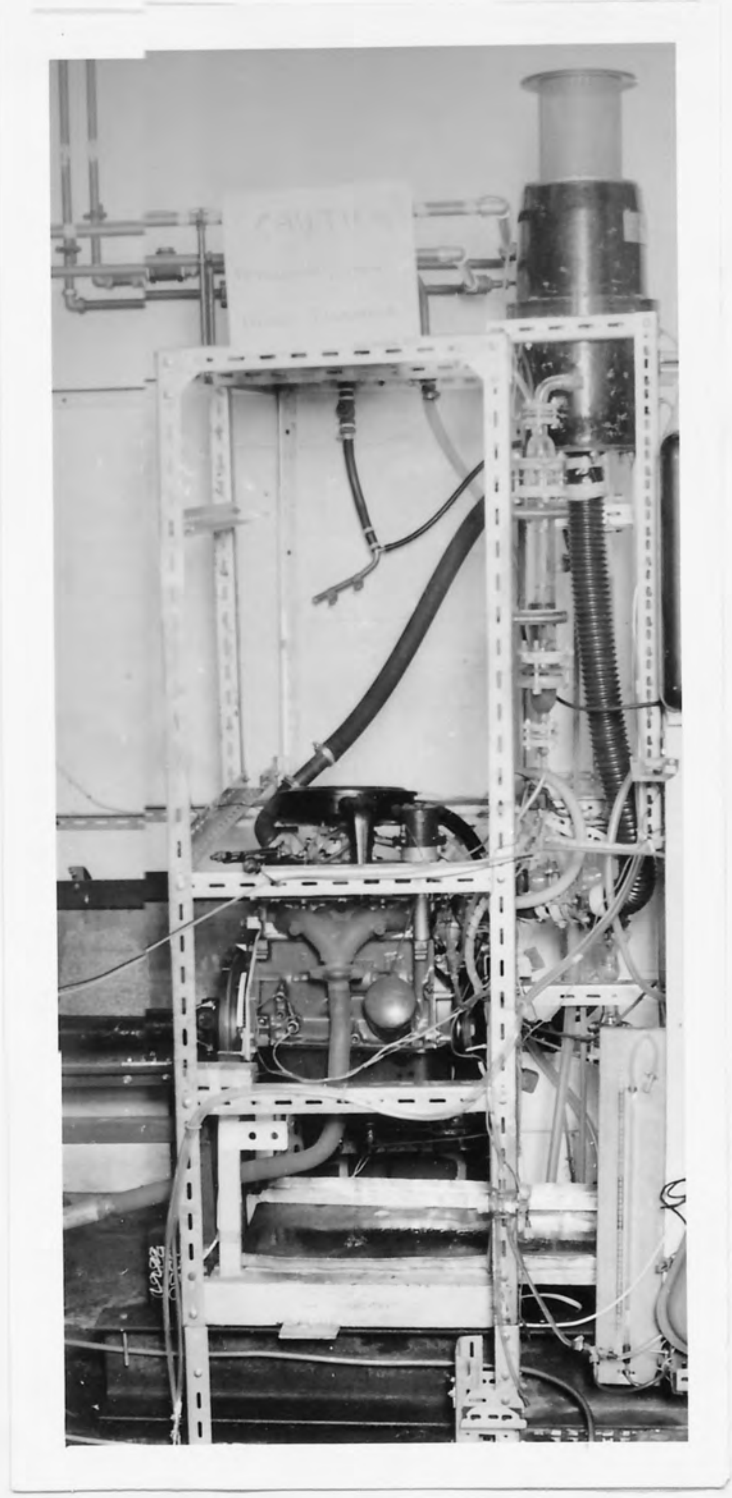

Plate 313: The Fiat 127 engine

A - Ricardo airflow meter
B - Calibrated glass tube to measure fuel flowrate

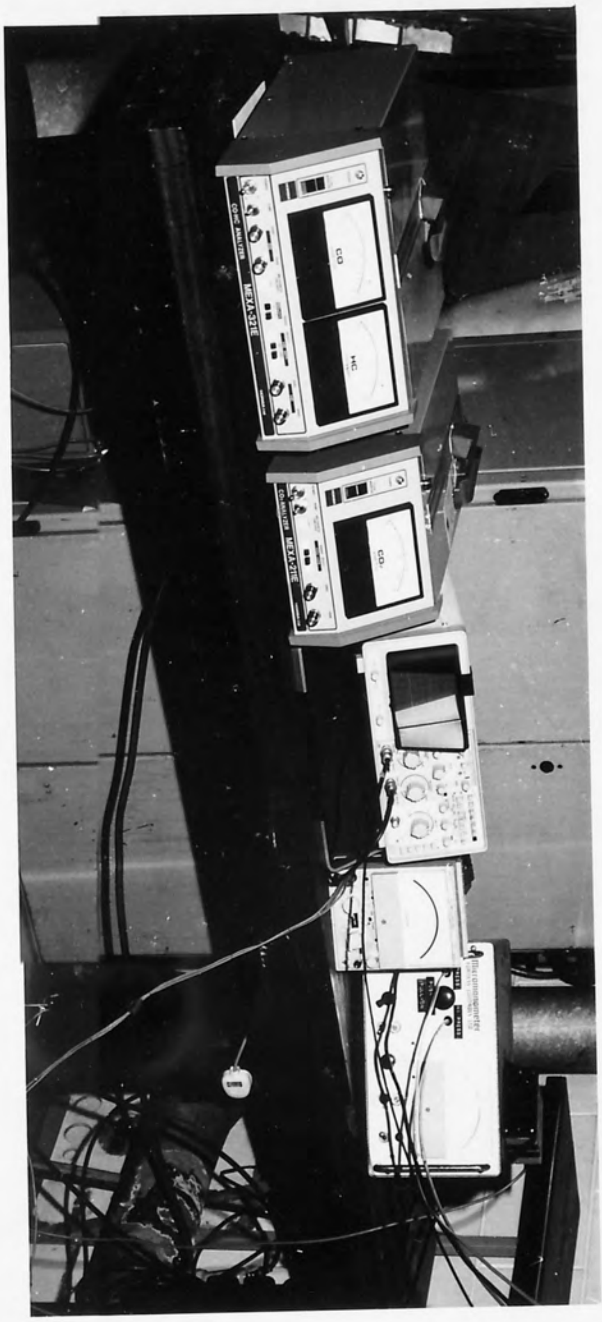

Plate 314: Instrumentation used

A - MEXA-321E and 211E gas analysers
B - Storage oscillioscope
C - Milivoltmeter, to measure engine torque
D - Micromanometer, to measure airflow rate

3.3 Manifold Design

3.3.1 Introduction

Nearly all investigations into enhancing engine performance and lowering exhaust emissions using alcohols and alcohol/gasoline blends suggest changes to the combustion cylinder (57,58,61,63). These changes include increasing the compression ratio, change in ignition timing etc. Some have even suggested operating the engine on lean mixtures (10,13,19).

It is well known that operating the engine on a homogenous mixture of fuel and air will result in smoother running of the engine and lower levels of carbon monoxide and unburnt fuel (19). Homogeneity of the fuel air mixture in a carburetted spark ignition engine is only possible if all the liquid fuel is completely evaporated and is present in vapour form only. In conventional engines this can only be achieved if the fuel is preheated to a temperature close to its boiling point or the intake manifold is long enough to allow complete evaporation of the fuel in the cold stream of air the liquid fuel droplets are caught up in.

When using alcohol fuels or alcohol/gasoline blends where the alcohol concentration is greater than 20% v/v, the greater volumetric charge that is required by the engine cannot be accommodated by the intake manifolds of existing engines. It is therefore necessary to alter the geometry of the intake manifold according to the percentage of the alcohol in the blended fuel. To establish how to alter the manifold geometry specific experimental work is necessary. The induction manifold efficiency can be ascertained by a measurement of the thermal efficiency based on the quantity of air consumed by the engine, provided that the design of the combustion chamber etc are such as to prohibit loss of efficiency in that direction.

The absolute values found for the thermal efficiency by this method are, in all cases, somewhat higher than those obtained from the fuel consumption readings, the differences being due to:

1. The larger increase in specific volume when an over-rich mixture is used.
2. The slight loss due to condensation of liquid fuel on the cylinder walls, which escapes combustion and ultimately finds its way past the piston onto the crank case.
3. The loss due to deposition of liquid fuel droplets on the walls of the induction pipe which causes fuel to enter the cylinder in gulps of liquid. This deposition forms the "wall film".
4. The small loss of liquid or vapour due to "blow-back" or reverse flow in the induction pipe, due to sudden closing of the inlet valve.

It is generally accepted that the loss due to deposition of liquid fuel droplets on the wall of the induction manifold (3 above) is the greatest of the losses.

An experimental programme was thus set up with the following objectives in mind.

1. To devise a technique to remove the liquid wall film from the intake manifold and to measure its flowrate.
2. To determine the effects of various parameters such as air/fuel ratio, throttle plate opening, engine speed and manifold geometry on the wall film.
3. To use the information obtained in (2) to determine the manifold geometry for alcohol and alcohol-gasoline blended fuel.

3.3.2 Wall film development

During carburation it is impossible to complete the evaporation of the liquid fuel in the infinitesimal amount of residence time available in the intake manifold. Thus the liquid fuel droplets that are formed during the atomisation of the fuel during carburation precipitate themselves on the wall of the intake manifold. In this two phase flow system, the liquid phase is more commonly termed as the wall film.

The wall film begins to develop at the point of carburation. In the case of petrol which consists of light and heavy fraction the lighter fractions evaporate at a rapid rate leaving the heavier components to deposit themselves on the manifold wall.

3.3.3 The Wall Film and its Separation Techniques

Many techniques to measure the mean film flowrate have been reported in literature which include:

1. measurement of liquid film mean thickness and velocity
2. liquid film sampling
3. liquid film separation.

Mazarov (1952-1961) (114,115) used the salt tracer technique to measure the thickness and velocity of the wall film in a horizontal pipe. Quandt (116) on the other hand injected a dye to the liquid film at a given injection point and by sampling the liquid film at successive downstream locations estimated the entrainment of the liqiud film. The film flowrate was measured using a simple mass and dye concentration balance.

Other investigators (117,118,119) have used the extraction method as a means of measuring wall film flowrate. The slit method as used by Trayser et al (120) extracted the wall film by sucking the liquid through a series of fine holes around the tube periphery. Finlay et al (121) on the other hand used a knife edge probe for the same purpose. These two techniques are useful when film distribution is of interest.

In the current investigation a slit method technique was used to measure the wall film flowrate. The device used can be seen in Figure 3.2.1. It was designed such that the film was allowed to flow out through the gap (of no more than 2mm), the vaporised fuel and small fuel droplets passed straight into the combustion cylinder. The pressure between the manifold and measuring cylinder (which was kept air tight) was equalised since pressure in the manifold is subatmospheric which would stop the liquid film flowing out under gravity.

The intake manifold was divided into two parts separated by a small axial gap. The internal diameter between the carburettor exit port and the separating device was kept at 40 mm for all manifold geometries tested. The internal diameter after the separating device was kept at 36mm corresponding to the diameter of the inlet port of the Ricardo engine. This length was kept as short as possible to reduce further development of wall film.

The liquid film separated was collected in a glass tube which was designed such that the liquid collected was prevented from being sucked back into the manifold especially at high engine speeds and small throttle openings.

The entire arrangement can be seen on Plate 322. The technique allowed measurement of the wall film flowrate above 0.2 gm/s.

3.3.4 Test Equipment and Procedure

3.3.4.1 Equipment - Plate 321

The Ricardo E6 single cylinder variable compression engine was used equipped with a SU constant depression carburettor. The load was provided by a d.c. swinging field starter dynamometer.

A compression ratio of 8.5:1 was chosen. All other engine specifications can be seen in Appendix 5.

The instrumentation used measured fuel and air flowrates, engine speed and brake load. Exhaust analyses were carried out using infra-red gas analysing equipment. The proble for the analysers was positioned such that enough gas was sucked in through the sample inlet holes of the probe to give a good analysis.

Cylinder pressure was measured using a water cooled Piezo-electric AVL transducer coupled to a Kistler charge amplifier. The signals from the transducer were recorded on a RACAL multi-channel tape recorder.

Wall film flowrate measurements were carried out by timing the collection of a fixed volume of liquid. The density of the wall film was also measured using a density bottle.

Manifold wall temperatures were measured at three positions along the length of the manifold in order to calculate the heat input through the manifold wall. The average of the three temperature measurements was used in conjunction with the room temperature to estimate the heat transferred from the room to the intake manifold. This was found to be in the region of 2 watts. This figure is too small to cause serious error in experimentation.

3.3.4.2 Test Procedure

A carefully planned test procedure was required since film flowrate is strongly dependent on ambient conditions. Consequently the following steps were undertaken to ensure repeatability of test.

1. The test fuel temperature was maintained at room temperature.
2. Engine warm up time was allowed to be 45 minutes for all tests.

3 Engine cell temperature was kept constant (± $2^{o}C$) during the duration of the test.

A previous study of secondary variables such as ignition timing, compression ratio, showed that these had no effect on wall film flowrates.

A further study of fuel type on film flowrate showed that the most significant variable was the Air-Fuel ratio (see Section 4.2.2). Therefore all subsequent tests were carried out using four star petrol because of its availability and relative ease of handling.

The principle tests carried out examined the following:

1 A series of manifold shapes and sizes (see Plate 323).

2 Four throttle plate settings namely, $^{1}/4$, $^{1}/2$, $^{3}/4$ and full.

3 Variation in engine speed.

4 Variation in air/fuel ratio.

A constant ignition timing was used. The test procedure adopted was as follows.

1 The throttle plate was set at the required position.

2 Initial values of atmospheric pressure were recorded.

3 The engine was warmed up at the required test speed.

4 Tests were carried out going over a range of F/A ratios from rich to lean misfire limits.

5 All required data was recorded. This included:

i Load on the dynamometer.

ii Manifold pressure.

iii Manifold wall temperature.

iv Air, fuel, and exhaust temperature.

v Exhaust emissions.

vi Cylinder pressure.

vii Air and fuel flowrates.

6 The wall film was collected and the time taken for the collection of a specific volume was recorded. This data provided the wall film flowrate.

7 Steps 5 and 6 were repeated at varying air fuel ratios until the misfire limit was reached.

The data obtained was used to calculate the power output, air/fuel ratio at the carburettor, air/fuel ratio in the cylinder, film mass flowrate, % film flowrate and heat input through manifold.

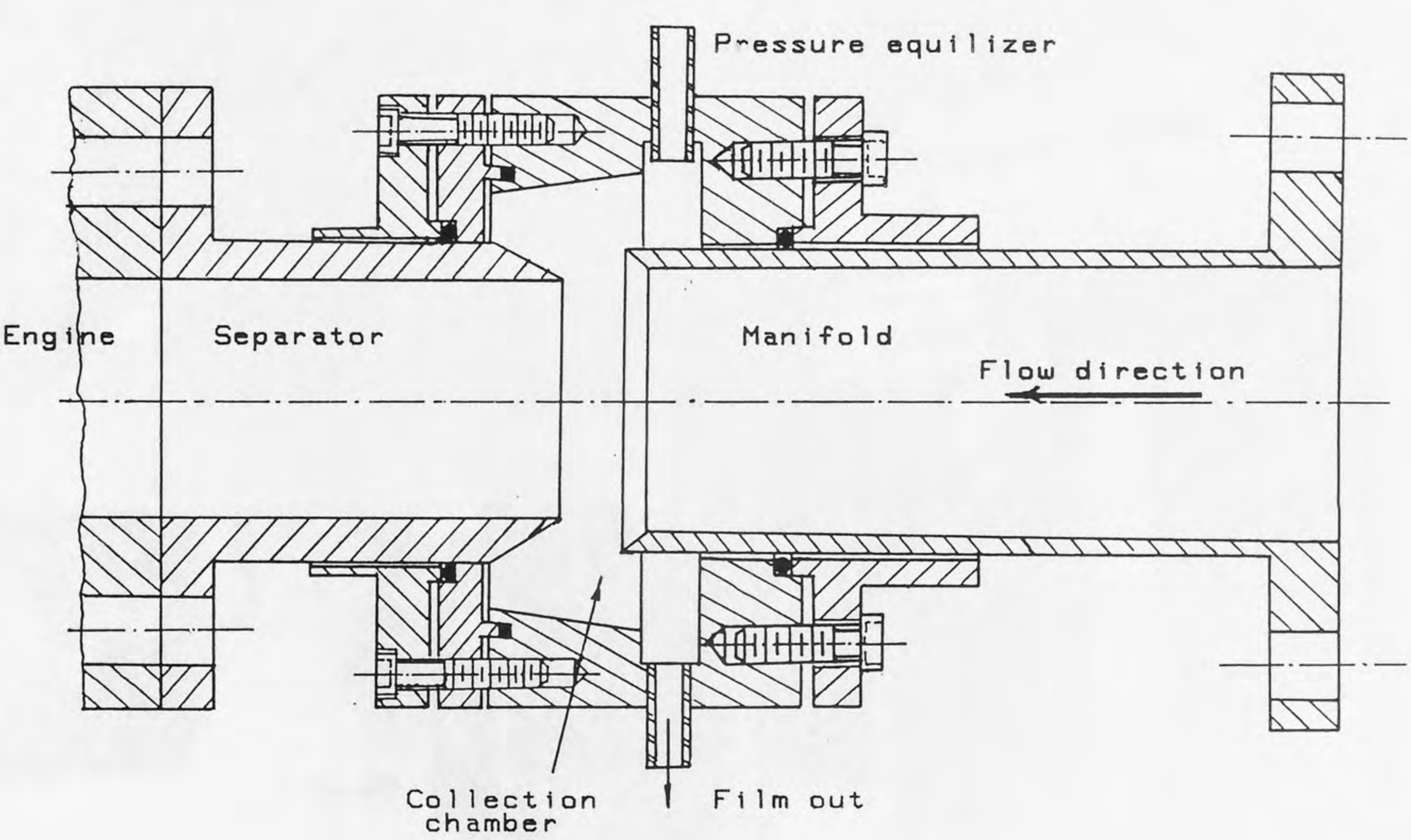

FIG. 3.2.1 Inlet Manifold With Film Separation Slit

Plate 311: Experimental Rig; Ricardo E6

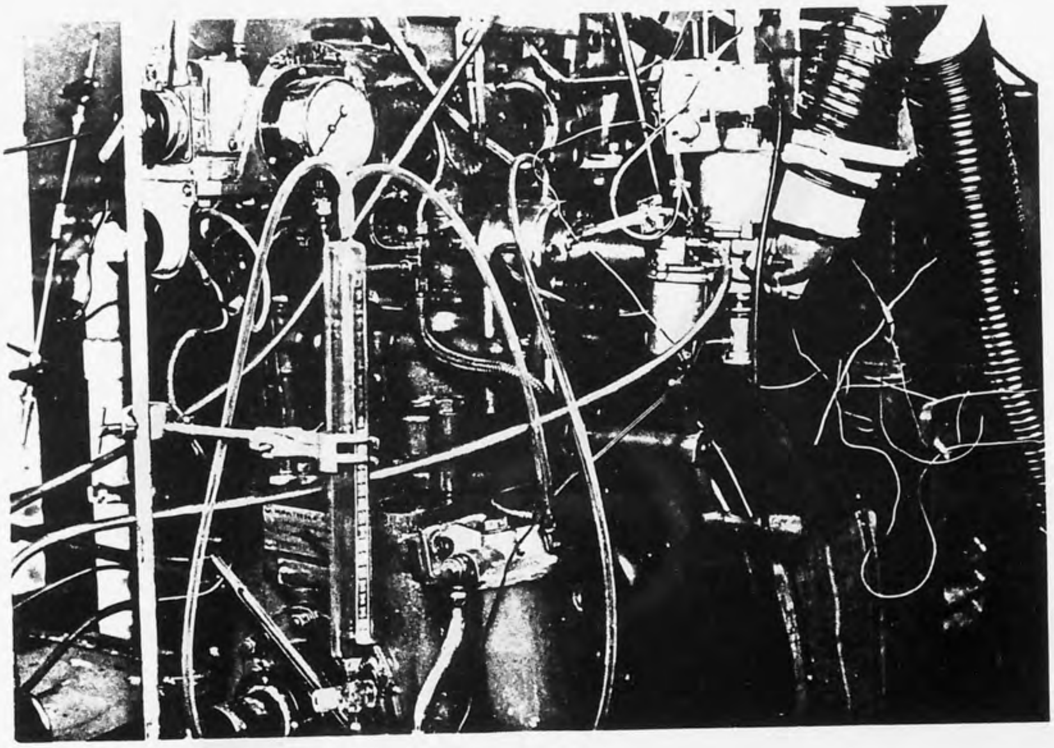

Plate 322: Close up of separator (A) and collection tube (B)

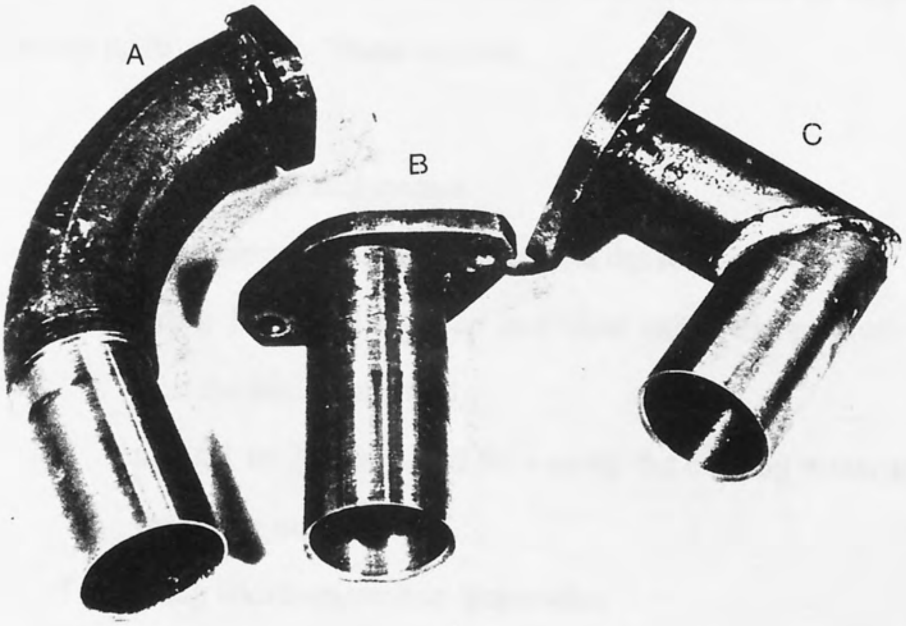

Plate 323: Manifold shapes

A - 200 mm smooth bend manifold
B - 100 mm straight manifold
C - 200 mm sharp bend manifold

3.4 Volatility

3.4.1 Introduction

Alcohol fuels, more specifically methanol and ethanol, either blended or by themselves can be used to operate automobile engines satisfactorily. The most frequently encountered difficulty associated with the use of these fuels is the poor cold starting and warm up driveability performance. This problem is particularly severe at or below 10°C.

The fuel properties that strongly influence cold start and warm up driveability are volatility and heat release.

Various methods over the past years have been used to improve cold starting and warm up driveability. These include:

1. using a dual fuel system
2. using electrical systems to preheat the fuel
3. using 1 or 2 to start up and then using the exhaust gases to heat the intake manifold
4. using 1 or 2 as in 3 and then using the cooling water to heat up the intake manifold
5. using additives such as isopentane.

Of all of these the use of additives appears to be the most cost effective way of improving cold start and warm up driveability.

An experimental programme was thus set up firstly to obtain all the necessary distillation curves as specified by the IP standards and then to use additives to see how they affect the distillation curve.

3.4.2 Experimental

The experimental procedure adopted was in accordance with the Standard of the American Society of Testing and Materials (ASTM) (122) issued under the fixed designation D86. The method was adopted as a joint ASTM-IP (Institute of Petroleum) standard in 1964.

The method of test covers the distillation of all fuels including commercial vehicle petrol.

3.4.2.1 Experimental Apparatus

Unlike the apparatus suggested in the ASTM-IP standard, Quick-fit apparatus was used which is specifically designed for distillation of petroleum products.

The apparatus was set up as shown (Plate 331).

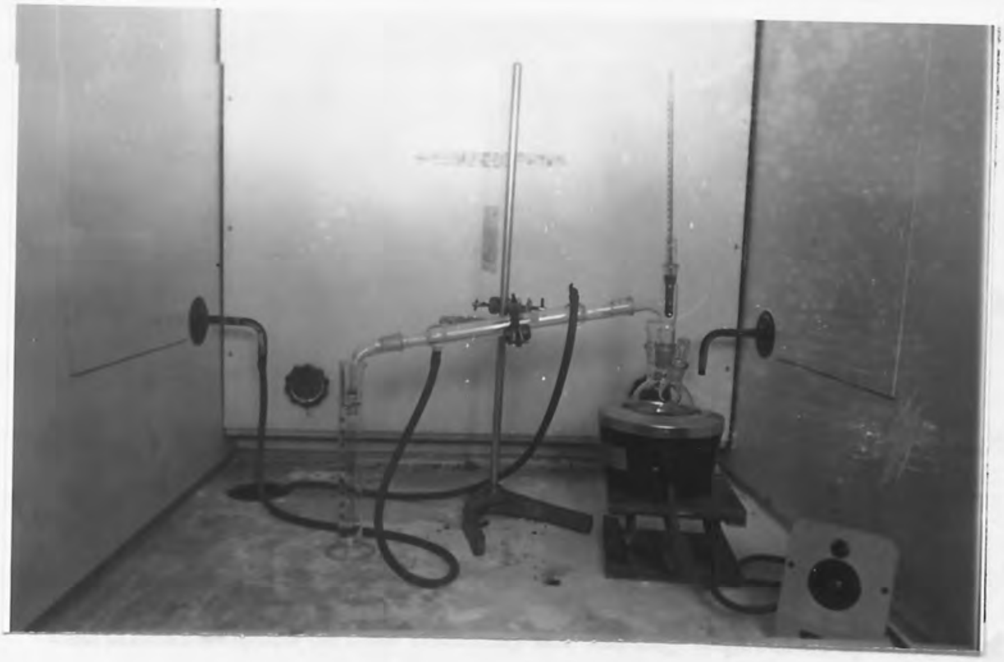

Plate 331

3.4.2.2 Experimental Procedure

A 100 ml sample is distilled under the ASTM-IP standards prescribed conditions for group 1 type fuels. Periodic observations of thermometer readings and volumes of condensate are made. Special significance is given to the following temperature points.

1. The initial boiling point - the thermometer reading which is obtained at the instant that the first drop of condensate falls from the lower end of the condenser tube.
2. End point or Final boiling point - the maximum thermometer reading obtained during the test. This usually occurs after the evaporation of all liquid from the bottom of the flask. The term "maximum temperature" is a frequently used synonym.
3. Dry point - the thermometer reading which is obtained at the instant the last drop of liquid evaporates from the lowest point in the flask. Any drops of film of liquid on the side of the flask or on the thermometer are disregarded.

In this investigation points 1 and 2 were of great interest and point 3 for most test fuels was ignored.

3.4.3 Theory

3.4.3.1 Introduction

The characteristics of fuel volatility are usually expressed by means of the ASTM process of distillation.

Modern petroleum spirit starts to distill at about 25°C, the curve rising steeply until about 10% is recovered, after which it climbs again until its end point usually at temperatures greater than 150°C.

The diagram below (Figure 3.3.1) shows in graphic form the relation of engine performance features and problems to any particular portion of the fuel distillation curve.

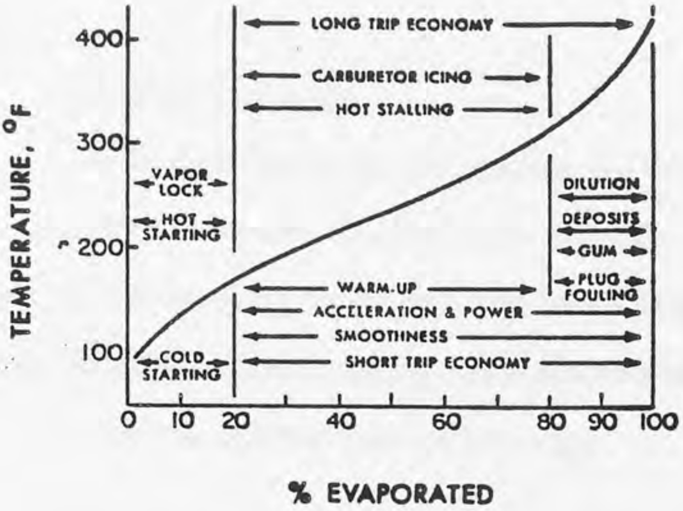

Figure 3.3.1 Effects of Volatility Characteristics on Engine Performance

From this it can be noted that the 0-20% range is most significant when considering cold start. However the same fuel characteristics that contribute to the severe cold starting difficulties are also responsible for the overall problems associated with the engine's running behaviour during warm up and driveability tests. Vapour locking is the most severe of these problems.

The warm up and driveability characteristic are related to the temperature at which a further 50% of the fuel is vaporised. The hydrocarbons associated in this region are those which may be responsible for carburettor icing and hot stalling.

Fuel economy is related to the temperature at which 90% of the fuel is distilled. The heavy ends in this region have high heating values which in turn give a high thermal efficiency and hence better fuel economy. The very same heavy fractions form deposits on combustion chamber, piston heads etc and also cause spark plug fouling. This pattern however does not apply to alcohol fuels since they have a single boiling point. Their high initial boiling point makes it difficult for engines operating on them to start up in the cold. However, once started, the engine will warm-up satisfactorily since all the fuel can be evaporated at a relatively low temperatures thus providing the extra fuel required for warm-up.

3.4.4 Analysis of Results

In all cases the initial boiling point, and thermometer readings at 5% and greater than 95% recovered distillate were recorded. The readings were taken at intervals of 5% recovery up to and including 95% recovery. The record of thermometric and volumetric readings was in accordance with the ASTM-IP standard.

The data collected gave the following:

1. Percent recovered - the volume in mililitres of condensate observed in the receiving cylinder, in connection with a simultaneous thermometer reading.
2. Percent recovery - the maximum percent recovered until two successive observation agree, made after a 2 minute time interval.
3. Percent total recovery - the combined percent recovery and residue in the flask.
4. Percent loss - 100 minus the total percent recovery.
5. Percent residue - the percent total recovery minus the percent recovery - or the volume of residue in ml if measured directly.
6. Percent evaporated - the sum of percent recovered and the percent loss.

3.4.4.2 Effect of Volatility on Engine Performance

(i) Effect on Cold Starting

For ignition of the charge the fuel-vapour air mixture delivered by the carburettor of a spark ignition engine must be within the limits of flammability. The percentage of fuel evaporated during cold start is low because of the low fuel and air temperatures. This necessitates the use of a choke valve which reduces the air flow and increases the fuel flow. If, for example, conditions were such that only 5% of the fuel were to vaporise than for stoichiometric mixtures to burn we would require for:

1. Methanol - fuel-air ratio of 10:3
2. Ethanol - fuel-air ratio of 10:4
3. Petrol - fuel-air ratio of 10:7

(see Section 5.1.2) for a combustible mixture to form.

Therefore if we need to bring the F/A ratios for a combustible mixture for methanol and ethanol closer to that of petrol, a volatile additive is necessary.

The effect of volatility on starting time is essentially independent of front-end volatility at temperatures higher than $5^{o}C$ for alcohols since at this temperature enough fuel is evaporated for start-up. However, at temperatures below this, starting time increases considerably.

(ii) Effect on warm up and acceleration

Warm up characteristics may be expressd in several ways:

1. By starting the engine and driving as soon as the engine will fire sufficiently strongly. The time and distance travelled until the engine is sufficiently warm to pull away without the need of a choke are measured. The greater the time and shorter the distance

indicate an undesirable warm-up period.

2 By measuring the full throttle acceleration from 0 to 50 mph at fixed 1 or 2 minute intervals during the warm up cycle (101).

From a user's point of view the fuel consumption during warm-up is poor and hence it is beneficial to use fuels which have a good mid-range boiling point such that up to 80% of the fuel is vaporised. For this reason, alcohol fuels are fairly good during warm-up periods.

(iii) Effect on Carburettor Icing

High fuel volatility may result in an increased tendency toward carburettor icing. Carburettor icing occurs when there is a severe drop in air temperature due to the refrigerant action caused by the latent heat of the evaporating fuel. The ice formed causes the engine to run slower and often to stall, especially at idle.

When using petroleum based fuels, carburettor icing is usually prevented by either using a heat source to warm the carburettor or using anti-icing additives to the fuels. No such problems should occur when using alcohol fuels. Their freezing point is low (ethanol -112°C, methanol -97°C) and in fact they are often used as additives to prevent carburettor icing.

(iv) Effect on Vapour Lock

An increase in fuel volatility usually results in vapour lock. Vapour lock of a fuel system occurs when fuel vapour forms in a quantity large enough to reduce the liquid fuel flow to less than that required for engine operation. This may be due to extreme atmospheric conditions of high ambient temperature or very high under-bonnet temperature resulting after a long operating period of the engine.

The alcohols when used as automotive fuels are prone to vapour locking.

This is because of their relatively low boiling point (68°C for Methanol and 78°C for ethanol) which causes them to vapourise when under-bonnet temperatures are high during long operating periods.

(v) Effect on Evaporation Loss

Evaporation losses from the fuel tank and carburettor are directly related to fuel volatility. The ligher fractions make up the bulk of the evaporative losses from both the carburettor and fuel tank when using gasoline. Evaporation losses when using alcohols on the other hand are less likely. This is because the front end volatility of the alcohols is fairly low, appreciably lower than those of the lighter fractions of gasoline. Evaporation losses will however occur when the engine run is terminated resulting in very high under-bonnet temperatures while standing, thereby evaporating the fuels which escape into the atmosphere.

(vi) Effect on Crankcase Dilution

Dilution of the crankcase oil with any fuel is the result of the incomplete evaporation of the fuel in the cylinder. With gasoline this is usually due to the heavier ends present. Crankcase oil dilution is at its greatest during starting and warm-up periods and is a minimum under normal operating conditions.

Due to the increased throughout of the fuel when using alcohols a greater percentage of the fuel is present in a liquid state. The alcohols with their solvent-like properties may cause greater crankcase dilution than gasoline.

3.5 Material Compatibility

3.5.1 Introduction

In an experimental programme which looks into the acceptability of alcohol fuels as gasoline substitutes it was considered necessary for the materials that would most come into contact with the fuels to be tested for corrosion and oxidation.

The use of alcohol fuels is specialised applications, such as in racing cars, is well known. However, these vehicles are subject to frequent attention and much less is known about the longer term effects of alcohols on the usual materials of construction of car engines and components. The materials currently in use for carburettor, inlet manifold, fuel tank and feed lines have been selected according to the ambient conditions, material cost and resistance to hydrocarbons in the gasoline range. Any departure from existing materials may give rise to significant extra costs and therefore the materials in current use for these components were studied with regard to their resistance to alcohols.

3.5.2 Materials and Methods

Investigations in the past have shown that the most vulnerable components are those found in the carburettor and fuel system.

In this study the effects of alcohols on components from various carburettors and fuel feed systems were studied. The carburettor materials tested were brass, zinc, copper, aluminium and stainless steel, all of which were obtained from various component manufacturers. These were tested in turn with alcohols and alcohol/gasoline blends. In some cases the alcohols were doped with formic acid to accelerate the corrosion/oxidation process.

3.5.3 Experimental

3.5.3.1 Introduction

The test procedures were adopted such that they stimulated actual conditions during automobile operation. These included aerating the fuel using air at room temperatures and using high test temperature to accelerate the corrosion/oxidation process. In some cases two different components made up of different metals were tested in the same test fuel to note if there were any electrochemical effects that would increase or decrease the corrosion/oxidation rates.

3.5.3.2 Aeration Experiments

The sample was suspended in the test fuel and was totally immersed. The aeration of the test fuel was carried out using a small pump similar to those used in domestic fish tanks. This pump was operated periodically at four hour intervals for a 15 minute duration. The system was kept at room temperature (usually between 15-18°C). The reaction flasks were "topped up" whenever necessary with fresh test fuel. This test was to simulate conditions inside the carburettor as when the air and fuel mix, considerable aeration of the fuel takes place.

3.5.3.3 Temperature Experiments

Three different temperatures were chosen: 50°C, 65°C and 90°C.

For the tests carried out at 50°C, the apparatus was set up similar to that for the ambient aeration tests. The flasks containing the test sample were placed in a hot water bath. The flasks were "topped up" with fresh test fuel whenever required with fresh test fuel such that the liquid level was not allowed to fall below a particular mark.

For those tests carried out at 65°C, the samples were placed in 100cc quickfit test tubes connected to a condenser such that any fuel evaporation was refluxed back into the test tube. The test tubes were placed in an oil bath kept at this temperature.

For the tests carried out at 90°C, the samples were placed in Quickfit glassware and placed inside an oven kept constant at the required temperature.

The temperature experiments are carried out to simulate under-bonnet temperatures which usually exceed 50°C.

Prior to the tests, all test specimens were ultrasonically cleaned. This was also done before weighing each specimen when removed from the test fuel medium.

Duration of the tests were 300 days each for the aeration test and for those samples at 50°C. At 65°C, the test duration was 30 days and at 95°C, the test duration was 3 days.

At periodic intervals, the samples were removed from the test solution, cleaned ultrasonically using acetone, weighed. They were then subject to visual examination by naked eye and microscope.

3.5.4 Theory: Corrosion

3.5.4.1 Introduction

Most metallic components eventually deteriorate in use, due to the chemical nature of the process applications. This may be termed as corrosion.

By definition corrosion is the deterioration that occurs when a metal or alloy reacts with its environment. This corrosion may take many forms whose classification is usually based on one of three factors:

1. Nature of the corrodent.
2. Mechanism of corrosion - this involves either electrochemical or direct chemical reactions.

3 Surface factors - corrosion is either uniform and the metal corrodes at the same rate over its entire surface; or it is localised, in which case only small areas are affected.

The various types of corrosion are listed in the table below (124).

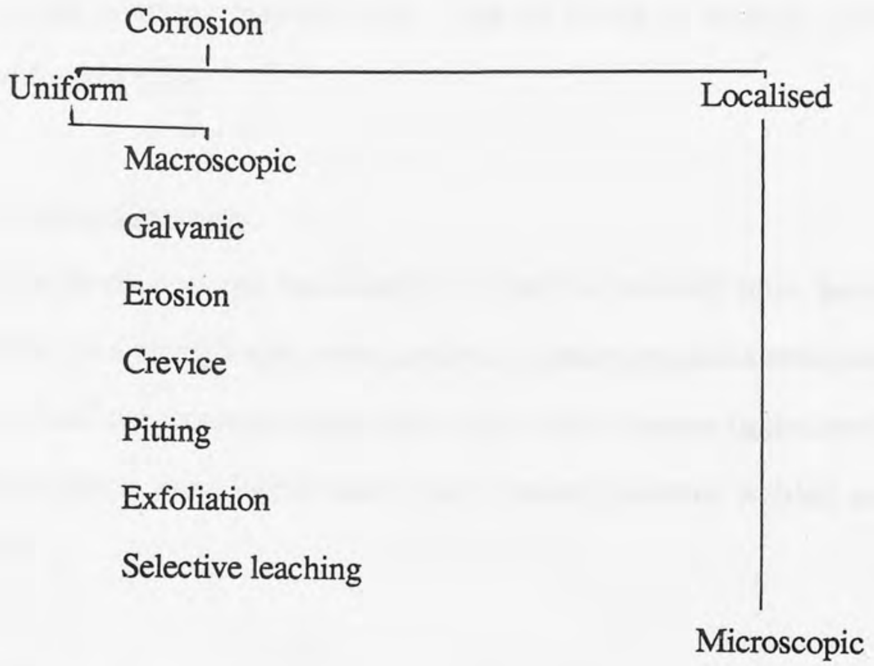

3.5.4.2 Uniform Corrosion

Uniform attack over large areas of a metal surface is the most common form of corrosion. It can be electrochemical or chemical (124).

3.5.4.3 Galvanic Corrosion

Galvanic corrosion may occur when two different metals in contact (as in the carburettor) are exposed to a conductive solution. A difference in electrical potential exists between different metals and serves as the driving force to pass current through the corrodent. This current then results in corrosion of one of the metals in the couple (124).

3.5.4.4 Erosion Corrosion

When movement of a corrodent over a metal surface increases the rate of attack due to mechanical wear and corrosion, the attack is called erosion corrosion. Such corrosion is highly likely in carburettors since the flow of liquids through nozzles and jets is quite rapid. This form of corrosion will invariably effect any protective surface coatings that are used. Special forms of erosion corrosion are cavitation and fretting (124).

3.5.4.5 Crevice Corrosion

The environmental conditions in a crevice can with time, become quite different to those on a nearly clean, open surface. A more aggresive environment may develop due to local concentrations and thus cause local corrosion in the crevice. Such a form of corrosion is most likely at lap joints, bolts, rivets or welded and brazed sections (124).

3.5.5 Theory: Oxidation

A common form of corrosion is oxidation (123). Test on materials for oxidation reaction is similar to that for aqueous corrosion. In these cases, the surface finish of the test sample is important, just as it is in aqueous corrosion tests.

It is common in laboratory oxidation tests to measure the weight gain due to the oxide scale.

The rate of deterioration during an oxidation attack is slow and in most cases it takes a long time to reach a constant rate of attack.

Oxide layers that spall or flake off tend to expose a fresh surface that will re-oxidise. This usually leads to a weight loss followed by a further progressive weight gain.

3.5.5.1 General

General oxidation follows three courses. Most of the equations put forward to explain the transient growth at relatively low temperatures involve logarithmic or exponential terms. They are grouped together as the log laws. At higher temperatures the oxide thickening obeys a parabolic law. This involves a greater risk of cracking or flaking.

Figure 3.4.1 Main Types of Growth Laws (123)

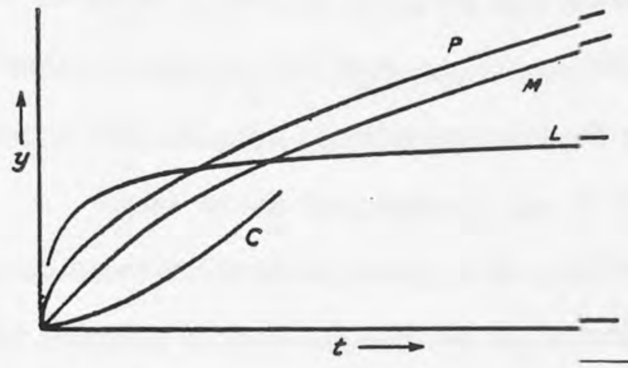

P - simple parabolic
M - mixed paraboilc
L - log laws
C - concave upwards

Depending on the temperature and time it is possible for a system to follow any one of the above curves. It is however generally considered that a material which thickens by the parabolic law is often accepted to be reasonably resistant. In this case there is a higher risk of cracking and flaking and obviously if flaking occurs, the oxidation process will start again, thus eventually causing material loss. If in contrast the oxidation process follows the log laws, the oxidation will almost reach a stand-still at small oxidation thicknesses. It is thus important to use a material which thickens according to a favourable growth law. This can be achieved by using certain alloying materials.

The alloying materials will not alter the growth law (ie. if it was parabolic initially it will still remain parabolic), but will vary the rate of growth accordingly. In some cases the alloying constituent introduces a new phase at the base of the oxide layer and here for instance the effect of the alloy may give rise to a log law. This may be more desirable from the designer's point of view.

At somewhat lower temperatures as in the case of this experimental study, the mechanical breakdown may be avoided, at least for a considerable time until a critical thickness is reached. Here we may obtain a parabolic thickening over an intermediate temperature and approximately rectilinear growth at higher temperatures. This can be seen when the oxidation rate suddenly speeds up at a certain thickness.

Cases where the parabolic law is replaced by a log law arise with particular metals (material) depending on the conditions in which the material is placed. Several graphical methods are available for deciding the law which is being obeyed. Here in these experiments a simple test is to plot the square of the weight increase (w) against time (t), ie. w^2, vs t. A straight line indicates parabolic thickening. A simple plot of w vs t will then show the rectilinear law if a straight line is obtained.

Figure 3.4.2 Features of parabolic growth (123)

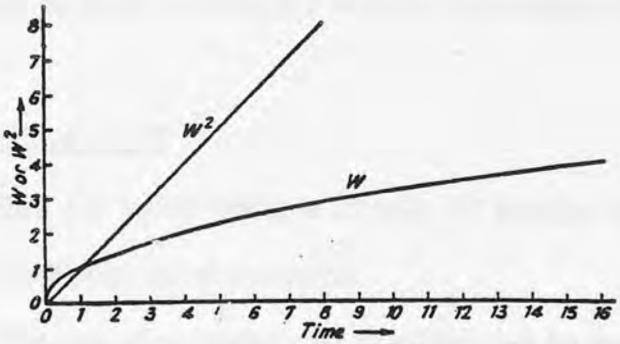

3.5.6 Effect of process variables on corrosion and oxidation

The process variables that most affect corrosion and oxidation rates are (124):

1. Concentration of major constituents.
2. Temperature.
3. pH.
4. Degree of aeration.
5. Velocity.
6. Additives.

We shall now look at each one in turn.

3.5.6.1 Concentration of Major Constituents

The rate of corrosion or oxidation of a given material usually increases as the concentration of the corrodant or oxidant increases. In the petrol-alcohol system it can be said that as the alcohol concentration increases, the rate of corrosion or oxidation should increase (124).

3.5.6.2 Effect of Temperature

An increase in temperature will usually increase the rate of corrosion or oxidation. There are a few exceptions and these are usually due to a decrease in oxygen content of the solution as the temperature is raised (124).

3.5.6.3 Effect of pH

The pH value being a criteria of acidity is of critical importance in determining the likelihood of corrosion.

The rate of corrosion due to acidity can be determined using a flow band diagram (124).

3.5.6.4 The influence of aeration on metals

Ready access to oxygen can increase, decrease or have no effect on the corrosion or oxidation of metals.

In most cases the metals that show passivity and that are corroding will generally do so at a faster rate if the oxygen content of the solution is increased.

Materials in a passive state will generally be uninfluenced by an increase in oxygen.

3.5.6.5 Flow velocity effects

When the corrosion or oxidation is diffusion-controlled, fluid media velocity can have large effects. An increase in velocity ensures a plentiful supply of fresh ions and removes more swiftly any products of corrosion or oxidation.

3.5.7 Analysis of Results

Weight loss or gain which is the most common of corrosion and oxidation measurement techniques was used.

For this investigation the rate of corrosion or oxidation is not of as much importance as the ultimate effect of corrosion and oxidation. Thus the behaviour of the samples during corrosion tests was noted.

CHAPTER FOUR

CHAPTER 4

RESULTS AND OBSERVATIONS

4.1 Performance Evaluation

4.1.1 Introduction

The objective of the comparative mappings of performance and emissions is to draw contrasts between all the various blends of alcohols used. These contrasts are drawn in terms of engine power, thermal efficiency, mechanical efficiency, lean burn capability, and the pollutant exhaust emissions of carbon dioxide (CO_2), carbon monoxide (CO) and hydrocarbons (HC).

The motive behind such an experimental objective was to examine the question of whether conventional gasoline engines can yield equivalent or better operation while using alco[illegible]oline blends having carried out only the minimum of design modifications. Results obtained in this experimental study were compared with those from other researches both experimental and theoretical.

4.1.2 Power

Figures 4.1.1-4.1.24 display, for wide open throttle (WOT), indicated and brake horsepower for methanol and ethanol blends with two star petrol. The power curves are shown as a function of F/A ratio. Figures also show varying engine speeds.

The indicated horsepower (Ihp) curves show that as the engine speed increases, the Ihp also increases. The same effect is noted as the F/A ratio increases. This is because the Ihp is a function of engine cylinder dimensions, the calorific value of the fuel and also the weight of fuel used.

The brake horsepower (Bhp) of an engine however is that which is measured by the dynamometer with no other load on the engine. In this research this

CHAPTER 4

RESULTS AND OBSERVATIONS

4.1 Performance Evaluation

4.1.1 Introduction

The objective of the comparative mappings of performance and emissions is to draw contrasts between all the various blends of alcohols used. These contrasts are drawn in terms of engine power, thermal efficiency, mechanical efficiency, lean burn capability, and the pollutant exhaust emissions of carbon dioxide (CO_2), carbon monoxide (CO) and hydrocarbons (HC).

The motive behind such an experimental objective was to examine the question of whether conventional gasoline engines can yield equivalent or better operation while using alcohol fuels or alcohol/gasoline blends having carried out only the minimum of design modifications. Results obtained in this experimental study were compared with those from other researchers both experimental and theoretical.

4.1.2 Power

Figures 4.1.1-4.1.24 display, for wide open throttle (WOT), indicated and brake horsepower for methanol and ethanol blends with two star petrol. The power curves are shown as a function of F/A ratio. Figures also show varying engine speeds.

The indicated horsepower (Ihp) curves show that as the engine speed increases, the Ihp also increases. The same effect is noted as the F/A ratio increases. This is because the Ihp is a function of engine cylinder dimensions, the calorific value of the fuel and also the weignt of fuel used.

The brake horsepower (Bhp) of an engine however is that which is measured by the dynamometer with no other load on the engine. In this research this was done using a set of strain gauge (see experimental section) wired to a Wheatstone bridge circuit. The output from the bridge was measured on a digital multiroll meter from which torque was obtained using a calibration chart. The gross bhp was calculated by multiplying the torque with the engine speed, ie. gross Bhp = torque x rpm.

From this analysis (Figs 4.1.7-4.1.12 and 4.1.19-4.1.25) it was found that the bhp of an engine is little affected by the F/A ratio especially for alcohol blends greater than 40%. This is because alcohols have a wider lean misfire limit than petrol which provides a greater F/A region where maximum power can be obtained.

When considering stoichiometric operation we find that there is an increase in the power when going from a low to a high blend of alcohol. This can be explained simply in terms of the combustion product characteristics and the ratio of moles of product to moles of reactant in the following manner:

When the fuel and air react in an engine cylinder to produce products of combustion, the number of moles of product is different from the number of moles of reactant.

Let us first consider the reaction between octane and air at stoichiometric proportions. (Octane is chosen as it closely resembles petrol in its carbon to hydrogen ratio). The reaction is thus:

$$C_8H_{18} + 12.5\ O_2 + 47.ON_2 \longrightarrow 8CO_2 + 9H_2O + 47.ON_2$$

assuming the reaction goes to completion.

This reaction shows that 60.5 moles of reactant result in 64.0 moles of product. This shows that the product to reactant ratio, P:R is 1.058.

Similarly for methanol:

$$CH_3OH + 1.50_2 + 5.65N_2 \longrightarrow CO_2 + 2H_2O + 5.65N_2$$

indicates that for 8.15 moles of reactant we get 8.65 moles of product at a P:R ratio of 1.061.

Finally for ethanol:

$$C_2H_5OH + 3O_2 + 11.3N_2 \longrightarrow 2CO_2 + 3H_2O + 11.3N_2$$

gives us 16.3 moles of product from 15.3 moles of reactant at a P:R of 1.065.

Furthermore dissociation alters the P:R ratio and the P:A ratio as elaborated in Chapter 5, paragraph 5.1.3.

4.1.3 Mechanical Efficiency

It is evident from Figures 4.1.31-4.1.42 that as the F/A ratio increases, the mechanical efficiency decreases. This is not totally unexpected as the Ihp increases with increase in F/A ratio. Since mechanical efficiency is inversely related to Ihp, the Ihp increase would decrease the mechanical efficiency. For stoichiometric composition Figures 4.1.43-4.1.44 and Tables 4.1.7 & 4.1.8 show that as the alcohol content in the blend increases, the mechanical efficiency decreases. This again can be explained by looking at the equation for the Ihp. It can be seen that the Ihp is a function of calorific value of the fuel. As the calorific value decreases, the Ihp increases and hence the mechanical efficiency decreases. Tables 4.1.7 and 4.1.8 also show that as the engine speed increases the mechanical efficiency also increases. For ethanol, it can be seen that the optimum point is between 3500 rpm and 4000 rpm. After 4000 rpm the mechanical efficiency would fall. With methanol however, the trend continues upwards but it is believed that this would level off possibly at around 4500 rpm.

4.1.4 Thermal Efficiency

The internal combustion engine is essentially a heat machine and as such its efficiency may be expressed in terms of the ratio:

$$\frac{\text{Useful work obtained}}{\text{Heat contained in the fuel}}$$

Thermal efficiency may be expressed in terms of brake thermal efficiency or indicated thermal efficiency. Brake thermal efficiency is the ratio of actual power obtained at the crankshaft to the heat supplied by the fuel consumed while the indicated thermal efficiency is calculated from the ratio of the useful work obtained to the energy in the fuel:

$$\text{Thermal efficiency} = \frac{\text{Ihp}}{w_f \times C_v}$$

where:

Ihp = Indicated horse power

w_f = Weight of fuel used

C_v = Nett calorific value of fuel.

The brake thermal efficiency is represented by the indicated thermal efficiency multiplied by the figure of the mechanical efficiency of the engine under consideration.

The thermal efficiency results obtained for the Fiat 127 903cc engine can be seen in Figures 4.1.46 to 4.1.57. In these diagrams thermal efficiency is plotted against F/A ratio for the various fuels and fuel blends.

The results show that the brake thermal efficiency is greatest in all cases at F/A ratios just below stoichiometric for that fuel. Results for alcohols at stoichiometric proportions (Table 4.1.9-4.1.10 and Figure 4.1.58) show that the trend for thermal efficiency with engine speed has a wave pattern with the highest thermal efficiency usually being at 1500, 2500 and 3500 rpm. This may not be all that unexpected as engines for road use are usually designed to operate at optimal efficiency at certain specific engine revolutions.

4.1.5 Misfire Limits

The misfire limits shown for example in the brake horsepower curves (Figs 4.1.7-4.1.12 and 4.1.19-4.1.25) are generally typical of results found by most workers in this field. As the F/A ratio decreases, ie. at lean operation, there is a loss of power. However at high F/A ratios, alcohols have a tendency to sustain the power output attained during stoichiometric operation. This is no doubt related to higher flame speed compared with gasoline.

It must be noted however that peak thermal efficiency occurs in the lean region. This however is greatly affected by the distribution of the fuel from cylinder to cylinder. In cases where the fuel is unevenly distributed, due to the design of the intake manifold, the lean limit occurs at higher equivalence ratios (Ø). For this particular system there was no way to measure fuel distribution and hence this study was not carried out.

4.1.6 Comparative Exhaust Emissions

As with performance, in a four-cylinder engine, exhaust emissions are highly influenced by the variations of F/A ratio. The distribution of fuel from cylinder to cylinder can play an important part, but since the exhaust analyses were taken from a point at which the exhaust from all cylinders is fairly well mixed, the analyses are a mean of the four cylinders.

The measured emissions included the principle combustion product CO_2 together with the pollutants CO and HC (from unburned fuel). The measurements were carried out using infrared gas analysers as specified in the experimental chapter.

Comparative results for CO_2 (Figures 4.1.59-4.1.70) show that as the alcohol content in the blend increases, the CO_2 level in the exhaust also increases. This is true for all engine speeds and equivalence ratios (Ø). At Ø = 1, ie. stoichiometric compositions (Figures 4.1.70-4.1.71 and Tables 4.1.11 and 4.1.12) the CO_2 content increased from 10% to 12.5% in the exhaust going from 20% v/v methanol in the blend to straight methanol and from 8.7% to 12.1% in the exhaust going from 20% v/v ethanol in the blend to straight ethanol at 1500 rpm. A similar trend is obtained for all the other engine speeds tested.

There is however a peaking effect whereby maximum CO_2 in the exhaust is obtained at F/A ratios close to stoichiometric and falling off in both directions when moving away from stoichiometric compositions.

When considering CO emissions the reverse pattern emerges (Figures 4.1.73-4.1.84). The CO levels in the exhaust decrease with an increase in alcohol content for all F/A ratios and engine speeds. As the engine speed increases, the CO level in the exhaust decreases,especially when considering higher alcohol blends in the fuel (> 60% v/v alcohol). With an increase in F/A ratio, the CO level in the exhaust increases for all engine speeds. This is more significant at lower alcohol blends (< 40% v/v alcohol).

At $\emptyset = 1$, the CO in the exhaust falls drastically when going from 20% v/v alcohol in the blend to neat alcohol. This is more significant with methanol than with ethanol (Tables 4.1.13 & 4.1.14 and Figures 4.1.85 & 4.1.86). Ethanol and ethanol blends give higher CO emissions than methanol and methanol blends at the same equivalence ratio.

HC emissions follow a similar pattern to CO emissions (Figures 4.1.87-4.1.98). The HC levels increase with an increase in F/A ratio and decrease with an increase in alcohol blend content. At $\emptyset = 1$, the HC content in the exhaust falls drastically as the alcohol blend level increases. This is true for all engine speeds tested (Tables 4.1.15-4.1.16 and Figures 4.1.99-4.1.100).

The effect of engine speed on HC content in the exhaust is however different when considering any one particular fuel. Here the usual trend is a high HC level at 1500 and 4000 rpm with a dipping effect between 2000 and 3000 rpm.

4.2.0 Manifold Design

4.2.1 Introduction

At present lean mixture operation seems to be an attractive proposition as it gives lower pollutants in the exhaust (see comparative study of exhaust analysis) and better fuel economy. However lean mixture running of a carburetted Spark Ignition Engine (SIE) can be critically dependent on air-fuel mixture distribution to the individual cylinders (assuming multicylinder engines) and hence the homogeneity of the mixture is important.

To influence homogeneity of the mixture, fuel properties both physical and chemical have to be studied. Investigations have shown that the physical properties of the fuel have a significant effect on the exhaust emissions but the magnitude of the effect is dependent on the design of the intake manifold.

In the intake system of a carburetted SIE the fuel is exposed to the air in the carburettor and the manifold. In the carburettor the fuel is atomised at the main jet in the carburettor venturi, evaporating some of the fuel and producing fuel droplets with the rest. In the case of multicomponent fuels such as petrol, the lower fractions are evaporated first and the heavy fractions go on to produce the fuel droplets. In the case of alcohols and alcohol blends with gasoline, the greater volume of fuel that is required increases the formation of droplets in current carburetted engines.

A percentage of the droplets formed will fall on the surface of the intake manifold and form the wall film (see Chapter 3). By removing the wall film a study of manifold design requirements was carried out.

4.2.2 Analysis of Results

Figure 4.2.1 shows the effect of fuel type on the wall film mass flowrate. This shows that the amount of wall film produced is dependent more on the A/F ratio than the fuel properties. It was for this reason that all subsequent tests were carried out using four star petrol.

4.2.3 Results of film flowrate measurements

The effect of throttle setting on fuel distribution and hence wall film quantity is clearly distinguished (Figures 4.2.2- 4.2.8). Film flowrate is maximum at 1/2 throttle setting due to the effect of the throttle plate deflecting flow towards the manifold wall. 1/4 throttle setting gave the least film flowrate which is believed to be due to the high air velocities that are created at this throttle setting. This causes rapid entrainment of the film back into the main stream of flow. Flow deflection for the full throttle setting is less than for the 3/4 setting which in turn is less than for the 1/2 setting which explains the order of wall film flowrates going from
1/2 —> 3/4 —> full —> 1/4.

This however is not entirely the case where there are bends in the manifold whereby the throttle setting effect is less than the effect of the bends where the fuel is re-distributed. In this case the large fuel droplets hit the wall at such speeds so as to break up the droplets and force them back into the main stream or creating more wall film.

This effect of manifold shape can be seen in Figures 4.2.9-4.2.12 which show that for all throttle settings, the straight manifold gives the least film flowrate and the sharp bend the maximum film flowrate. This indicates that the fuel droplets formed cannot negotiate the geometry of the bend thereby increasing the rate of impact of droplets on the wall and thus giving a larger wall film. However, the fact that the smooth bend gives a larger wall film flowrate then the sharp bend is significant since it is well known that the bends should be sharp so as to throw the wall film back into the main stream.

As engine speed increases, the total fuel flowrate increases and hence the wall film quantity (Figures 4.2.13 and 4.2.14 show the effect of engine speed on film flowrate at 1/2 throttle setting). The 1/2 throttle setting was chosen as it gives the maximum wall film flowrate as does the sharp bend. The engine speeds chosen were 1000, 1500 and 2000 rpm. It must be noted that the film mass flowrate at 1500 rpm is intersecting those of 1000 and 2000 rpm at the lean and rich regions respectively. No simple explanation can be found for this phenomena.

Figures 4.2.15-4.2.18 show the effect of manifold length on film flowrate. These show that as manifold length increases the film flowrate decreases. This is presumably a feature of evaporation within the intake manifold.

In all cases the separated wall film liquid had a higher density than the fresh fuel which supports the theory that it is the heavy less volatile fractions that form the droplets and eventually the wall film.

4.3.0 Volatility Tests/Distillation Curves

4.3.1 Introduction

The distillation curve of a fuel can be used to determine engine behaviour. The shape of the curve can be used to predict factors such as "cold starting", "hot starting", "warm-up" time, stalling etc which are indicative of the properties of a good fuel.

The results below show distillation curves for some of the fuels tested on the Fiat 127 903cc engine. Distillation curves for the blends not tested can be interpolated using these curves.

4.3.2 Results

Figures 4.3.1-4.3.6 show the distillation curves for some of the fuels and additives tested.

The results show that for cold starting purposes a 10% point on the distillation curve is important as this signifies the temperature at which a reasonable quantity of combustible fuel air mixture will be available for start-up. To improve the percentage take-off for the alcohols, certain readily available specific hydrocarbons such as n- and iso-pentane were found to be valuable ingredients (Figure 4.3.3 and Figure 4.3.6). Up to 30% gasoline added to either of the two alcohols would also give a reasonably good startup (Figure 4.3.1 and Figure 4.3.4).

No signficant problems with warm-up driveability should occur with alcohols. The use of n-pentane (GPR) and iso-pentane (GRP) in the neat alcohols also results in a slightly lower temperature for 10% v/v take off but this is not sufficient to improve startibility. However the pentanes can be used in alcohol/gasoline blends when the alcohol content is greater than 70%. In this case a slight reduction to the percentage of gasoline should be compensated by either of the two pentanes.

If the pentanes alone are to be used then the minimum quantity required would be 20% v/v in the alcohol. This may well be too large a quantity for economic viability. This however is another issue which will not be discussed here.

The pentane however cannot be used when using hydrated alcohols because phase separation occurs. It is thus suggested that when using hydrated alcohols another system of cold start be used. These include dual fuelling, electrically heated carburettor and intake system etc.

The warm-up and acceleration characteristics of the fuel are determined by the mid-range which can be grouped at 20% v/v to 70% v/v take off. This, when using gasoline, is between the temperature ranges of 55°C to 122°C. As can be seen from all the distillation curves of alcohol and alcohol gasoline blends, this is a temperature range which is high enough to allow good warm-up and acceleration for all the fuels tested.

In general it was found that alcohols have a good warm-up and acceleration qualities provided they are used in stoichiometric proportions.

The 80% to 100% range of the petrol distillation curve is usually where all the heavy ends are. These usually control such items as the Btu content, oil dilution and cleanliness. These however are not present when using large percentages of alcohols in the alcohol/gasoline blends. It is therefore suggested that some additives be found that will perhaps provide these qualities. These additives should be comparatively easy to find as heavy hydrocarbon compounds are numerous and most of them would mix with alcohols in all proportions.

4.4.0 Material Compatibility

Compatibility of engine material with gasoline constituents has been well established by trial and improvement over twenty or more years. In contrast, while alcohols have been well proved for racing car engines their long term use is only recently becoming established. Research to study corrosion propensities between alcohols and engine metals or polymers must therefore be carried out with special attention to accelerated tests to enable early predictions to be made on compatibility.

4.4.1 Electrical conductivity measurement

Corrosion propensities are known to be directly related to electrical potential and thus conductivity of the liquid media is of prime importance in any potentially corrosive system.

The electrical conductivity of methanol and ethanol and blends of methanol and ethanol with gasoline showed that methanol and its blends were more conductive than ethanol and its blends (Figure 4.4.0). This would indicate that methanol is perhaps more corrosive than ethanol.

Furthermore both of the alcohols show much higher electrical conductivity than gasoline suggesting a greater corrosion propensity.

4.4.2 Aeration Tests

(i) Brass in ethanol

After a period of 25 days the sample had lost most of its shine. The sample was beginning to turn a shade of black. This black "coat" was easily removed if the sample was scratched revealing the metal beneath (Plate 4.4.1).

The initial gain in weight (Figure 4.4.1) suggests that the sample had developed an oxide layer which would explain both the sample weight and colour.

Further observation showed that the sample condition deteriorated with time. The loss in weight is possibly due to flaking of the oxide. A test for (Cu^+) ions was carried out using the colour method but the results showed that no such ions were present in solution. This supports the theory that corrosion proceeds via oxidation and flaking of an insoluble oxide layer.

The final condition of the sample is as in Plate 4.4.1. The absence of any localised corrosion on the sample suggests that brass of such copper/zinc compositions could be used in metering the fuel, ie. as a needle valve or as a metering jet.

(ii) Brass in methanol

Though the general behaviour of the sample regarding weight analysis is very similar to the brass in ethanol (Figure 4.4.1), the condition of the sample was however in a slightly better condition. The final condition of the sample can be seen in Plate 441. The localised corrosion on the end of the sample suggests the methanol attacks brass causing pitting. This would therefore be unacceptable for using as a needle valve or metering jet since the localised corrosion would cause "sticking" of the needle valve. This would in turn lead to stalling or hesitation in the engine. Any flaking of the material would cause blockage of other secondary jets in the carburettor.

(iii) Brass in gasoline

The sample condition at the termination of the experiment was the worst of the three brass samples (Plate 441). The sample initially lost considerable weight, gained weight after approximately 65 days and then again lost weight to its final low at nearly 1.5% w/w of the original sample (Figure 4.4.1). Although the sample looks the worse of the three, the absence of localised corrosion means that the brass would be adequate as a fuel metering jet but not as a needle valve. This was the case in the Weber carburettor used on the Fiat 127 engine. Here this brass sample was used as an emulsion tube leading to the carburettor jet. The needle valve used was of a different brass composition, rich in zinc which is more resistant to gasoline.

(iv) Zinc in ethanol

Though appearing slightly dull in appearance after 25 days, the sample overall condition was extremely good. Weighing analysis shows that the sample gained weight for a considerable period (nearly 250 days) before eventually losing weight by nearly 1.5% w/w. The sample at the termination of the experiment did show signs of minor pitting (Plate 442). Since the main carburettor body is made up of zinc, the pitting would cause severe problems in the long term, especially since the secondary jets are usually orifices in the carubrettor body. This would cause hesitation during engine operations. Plate 4414 shows that this would occur during normal operation with ethanol.

(v) Zinc in methanol

The sample condition was worse than in the previous case, ie. zinc in ethanol. The sample appeared to be darker in some areas than others. This suggests some kind of localised activity. The pitting of the sample was more severe than in ethanol. The sample gained weight initially (first 65 days) from which point onwards the sample lost weight, then gained weight and at the end of the experiment had lost almost 1.0% w/w of its original weight (Figure 4.4.2). The condition of the sample can be seen in Plate 442. Here too the pitting in the zinc sample suggests that the secondary jets in the carburettor body would be enlarged causing improper metering of the fuel. The result of improper metering would be a higher fuel composition and loss in efficiency.

(vi) Zinc in gasoline

The sample condition was the worst of the three zinc samples. The sample had a rough texture and had lost all of its shine (Plate 442). The rough texture does not however cause any major problems. Since the metal showed no signs of localised corrosion it suggests that in the long term the metal condition would deteriorate without causing any irregularities in the fuel metering. This would be acceptable to the automobile user.

The weight analysis shows that the sample continually gained weight suggesting a high degree of oxidation (Figure 4.4.2).

4.4.3 Effect of Temperature

All samples and solutions were at a temperature of 50°C at all times during the course of the experiment.

(i) Brass in Ethanol at 50°C

The condition of the sample was largely unchanged for the first 65 days. The sample from then on began to develop a blackish tint as in the earlier brass sample (brass in aerated ethanol) (Plate 443). However, there are signs of localised corrosion on the top end of the sample. This as in the previous case 4.4.2 (i) would cause problems with regard to fuel metering and secondary jet blockage if flaking occurs. This metal would therefore be unacceptable for use as a metering jet or needle valve.

Weighing analysis shows that the sample gained considerable weight in the first 65 days and subsequently lost weight until the sample weight was below its original weight (Figure 4.4.3).

(ii) Brass in Methanol at 50°C

The sample condition was apparently worse than that in the ethanol (ie. brass in ethanol at 50°C). However after initially gaining weight the sample showed few signs of losing any weight. Figure 4.4.3 shows that the sample weight remained fairly constant for much of the period. The methanol in this instance did not attack the brass sample as before 4.4.2 (iv) (Plate 443). The overall condition suggests that this sample is resistant to methanol at 50°C. However when using the metal in the carburettor, the metal is subjected to both aeration and temperature. Thus taking the result from 4.4.2 (ii) the metal would be unacceptable for use with methanol fuels.

(iii) Brass in Gasoline at 50°C

The sample condition again was not as good as the brass samples in ethanol and methanol (Plate 443). The weight measurement pattern was however very similar to the brass in methanol (Figure 4.4.3). The fairly constant weight after the initial rise suggests that the oxidation of the metal reaches a steady state from which point onwards the metal remains unchanged for long periods. The absence of localised corrosion in this test and in 4.4.2 (iii) suggests that the metal is acceptable for use in gasoline fueled vehicles.

(iv) Zinc in Ethanol at 50°C

The sample condition was fairly good during the course of the experiment (Plate 4.4.4). The sample did however lose considerable weight in the first 100 days after which it slowly regained weight apparently primarily by oxidation. The weight loss and gain may be harmful to the carburettor. The loss in weight suggests flaking or spalling of an oxide layer from the metal. This may lead to blockage of the fuel metering jets. There were no signs of localised corrosion on the metal surface (Plate 444).

At the end of the experiment the sample weight was still lower than that at the start of the test (Figure 4.4.4).

(v) Zinc in Methanol

Here too the sample appeared in fairly good condition at the end of the test (Plate 4.4.4). The weight analysis pattern too was very similar to the above (zinc in ethanol at 50°C). The only difference was that having initially lost weight the oxidation process resulted in increasing the weight of the sample to that greater than at the start of the experiment (Figure 4.4.4).

Under close examination however (Plate 444) the edges of the metal sample appeared to have pin holes. This as before would be unacceptable since the entire carburettor body is made up of zinc.

(vi) Zinc in Gasoline at 50°C

The sample condition was the worst of the three zinc samples at this temperature, (Plate 444) showing extensive discolouration and pitting. This would cause improper metering of the fuel.

Weight analysis showed (Figure 4.4.4) that the sample gained considerable weight after the initial loss.

4.4.4 Effect of metallic contact on the oxidation and corrosion of brass and zinc in ethanol and methanol

4.4.4.1 The aerated solutions

(i) Brass/Zinc in ethanol

The metal the brass was in contact with at all times was zinc and the weight and condition of both metals were being monitored.

The brass sample had lost most of its shine and had a blackish tint to it (Plate 4.4.5). There were signs of localised corrosion on the brass sample in ethanol. The extent of the localised corrosion was greater than in case 4.4.2 (i). The zinc sample too (Plate 445 (A)) showed greater pitting and was generally worse than in case 4.4.2 (ii). This suggests that the metallic contact creates an electrolytic cell which is harmful to the brass and zinc sample.

The sample gained considerable weight initially, remained fairly constant for a further 50 days after which point the weight loss was as dramatic as the weight gain (Figure 4.4.5).

The zinc sample on the other hand had severe pitting and had deposits of oxide on most of its surface (Plate 455). The weight analysis shows a gain in weight over the entire period of the tests (Figure 4.4.6). This is due to the severe oxidation of the sample.

(ii) Brass/Zinc in methanol

The pattern of weight loss and gain can be seen in Figures 4.4.5 and 4.4.6 respectively for both the samples.

The brass in methanol gained and lost weight at almost every weigh in. The sample condition was similar to that of the brass in ethanol under similar conditions. Ethanol under similar conditions had less localised corrosion.

The zinc sample however showed little change in weight for the first 250 days. From this point onwards the sample gained some weight. The sample did suffer from severe pitting and had deposits of oxide over much of the surface (Plate 445). Here too the results sugest that contact of two metals in a solution of methanol is harmful to both metals. This in turn would cause severe problems during fuel metering and overall engine operation.

4.4.4.2 Reaction at 50°C

(i) Brass/Zinc in Ethanol at 50°C

The sample conditions can be seen on Plate 446. Weighing analysis shows that the brass sample gained considerable weight during the test period (Figure 4.4.7). The zinc sample too gained weight at first and then eventually lost considerable weight (Figure 4.4.8). The high temperature caused severe damage to the zinc and brass metals. The zinc sample was severely pitted at the edges (Plate 446) which would cause fuel metering problems. The condition of the sample was worse than in case 4.4.2 (iv) which suggests that metallic content increases the rate of corrosion. The brass sample too showed greater localised corrosion when compared with case 4.4.3 (i).

(ii) Brass/Zinc in Methanol at 50°C

The sample condition can be seen on Plate 446. The weight analysis as can be seen on Figures 4.4.7 and 4.4.8 shows that the brass initially gained weight and then lost weight until eventually the weight of the sample was below its original weight.

The zinc sample in methanol gave a wave pattern to the weight analysis showing weight gain and loss periodically. Here too both samples show greater localised corrosion (Plate 446) than with the metals in methanol (cases 4.4.3 (iv) and 4.4.3 (v)). The severity of the pitting in the zinc sample suggests that methanol would cause severe damage to the zinc carburettor body.

4.4.5 Blended Fuels

(i) Brass in methanol and ethanol blends

The sample condition in all the test fuels was very good, showing little change (Plate 4.4.7). This suggests that blended fuels are less damaging than pure methanol and ethanol.

The weight analysis for all the brass samples was very similar showing weight gain and loss periodically. The weight gain or loss, however was fairly slight being no greater than ±0.15% w/w. Details of the changes can be seen in Figures 4.4.9-4.4.12.

(ii) Zinc in methanol and ethanol blends

Here too as in the case of the brass samples, the zinc sample showed little change in sample condition over the entire test period (Plate 448). However there were signs of some pitting (Plate 448). These were not as severe as the metal in pure methanol and ethanol.

Weight analysis too showed that the gain and loss of weight was at periodic intervals showing a weight variation no greater than 0.15% w/w. Details of this can be seen on Figure 4.4.13-4.4.16.

4.4.6 Effect of Higher Temperture

Brass in methanol and ethanol at 90°C

The liquid phases (methanol and ethanol) became straw coloured after a period of 12 hours (Plate 449). This suggests the possible oxidation of the alcohols to formic and acetic acid respectively at the higher temperature. If this is true then the oxidation and corrosion rates of the sample should increase. This was found to be true since after a period of only 80 hours, the brass in ethanol had gained more weight than the brass in ethanol in the lower temperature tests (see previous sections). The weight loss and gain were at a much higher rate than the previous cases (Figure 4.4.18).

The brass in methanol lost some weight initially (Figure 4.4.17) but later gained weight.

The sample condition however in both cases was fairly good. The samples had practically all their initial shine.

4.4.7 Effect of doping with acid on corrosion and oxidation rates

(i) Aluminium in Methanol +5% formic acid at 65°C

After 125 hours there seemed to be no change in sample condition however the weight had increased by nearly 1.5%. After 175 hours of test time the sample had not increased in weight any further since the weighing after 125 hours but the sample condition had deteriorated. After 270 hours it was noted that the edges were beginning to corrode and there was also a decrease in weight. The sample after a further 75 hours had not lost or gained any weight but had developed a yellowish tint. At this point the aluminium ion concentration was measured and found to be approximately 40 ppm. After 490 hours the sample had increased in weight but the condition was rapidly deteriorating (Figure 4.4.19). The sample after 634 hours had pinholes on its surface suggesting that pitting corrosion had taken place (Plate 4410).

(ii) Aluminium in methanol at 65°C

After 125 hours of immersion, the sample surface had a very rough texture and the edges were beginning to corrode. This continued until the test terminated over 500 hours later. At the end of the test the sample conditions were worse than the aluminium sample in methanol +5% formic acid. In this case it can be said that the formic acid retarded the corrosion process. It is well known that aluminium with certain strong acids develops a passive protective layer.

Weighing analysis showed an oscillating pattern whereby the sample increases and then decreases in weight. This pattern may reflect the build up of the passive layer and its subsequent removal (Figure 4420).

The [Al^{3+}] ion concentration in solution was higher than that of the solution with formic acid (55 ppm as compared to 40 ppm after 345 hours). The results show that the corrosion of aluminium in hot methanol is more severe than its corrosion in methanol and 5% formic acid (Plate 4410).

(iii) Copper in methanol and formic acid at 65°C

After a period of 125 hours a black layer of oxide was formed over the whole surface. Under the microscope it was observed that the layer had a granular structure. After 175 hours however the sample colour had changed to dark orange which came off easily when cleaned ultrasonically using acetone. Weight analysis showed little change in weight before and after the orange layer was removed suggesting that its weight was too low for measurement. The sample appeared coarse and had lost most of its shine. After 270 hours the sample had blue deposits on its edges. This is most likely to be copper formate.

After 345 hours the sample had reverted back to its black colour, originally seen after 125 hours. This suggests a recycle of the whole process. At this point there was a also a loss in weight (Figure 4.4.21). The original colour reappeared after 490 hours thus confirming the recycling process. There was also a gain in weight. The blue deposits were again seen after a period of 634 hours at which point the test was terminated (Plate 4411).

The test indicated that copper goes through the following stages:

Metal ——> black layer (of oxide) on metal ——> orange colour of sample ——> blue deposits ——> black layer of oxide

The test solution was examined for copper ions [Cu^+] and after 345 hours the concentration of these was found to be 150 ppm rising to 250 ppm after 490 hours and 375 ppm after 630 hours respectively. This shows that the [Cu^+] ion concentration in solution is slowly increasing suggesting that significant corrosion is taking place.

(iv) Copper and methanol at 65°C

After a period of 125 hours the sample had become a shade darker than before, (ie. original sample), the edges darker than the main section of the sample. The sample condition after 175 hours was similar to that of the copper sample in methanol and formic acid, suggesting that the formic acid does accelerate the process of oxidation and presumably the corrosion. The sample was almost totally black in colour after 270 hours and under the microscope it appeared to have a granular structure. The appearance of blue spots was noted after 345 hours of test time which also showed a gain in weight after a previous loss in weight. The sample had an orange appearance after 490 hours which suggests once again that the previous test with formic acid did accelerate the process of oxidation and corrosion. After 634 hours the sample returned back to its black colour (Plate 4411) indicating the cyclic sequence of corrosion.

The weight analysis shows that the changes in weight were not as dramatic as the copper in methanol +5% formic acid. However, the same overall trend is present (Figure 4.4.21).

The [Cu^+] ion concentration was lower than the previous test going from 10ppm after 345 hours to 50 ppm after 490 hours and to 80 ppm after 630 hours of test time.

(v) Stainless steel in methanol and formic acid at 65°C

The condition of the sample remained unchanged throughout the test (Plate 4412). After an initial gain in weight the sample weight remained near constant at about 1.1% above its original weight (Figure 4.4.23).

4.4.8 Condition of the Carburettor

Further indications of corrosion and metal deterioration were obtained by examination of the carburettor of the Fiat engine used in the performance tests described earlier (Chapter 3).

The condition of this carburettor can be seen on Plate 4413 to 4417). The plates show severe damage to the inside of the carburettor bowl with large deposits of oxide on surface. Large areas of the bowl are pitted and the primary jets seemed to be blocked with deposits of oxide. Such a condition is likely ultimately to cause improper metering of the fuel leading to lower performance.

CHAPTER FIVE

CHAPTER FIVE

DISCUSSION OF RESULTS

Introduction

The purpose of this chapter is to provide a more detailed explanation of the results and observations made in the earlier chapter (Chapter 4).

5.1 Performance Comparisons

Performance comparisons are carried out in terms of engine power, thermal efficiency, lean burn capability and exhaust emissions. The results described in the previous chapter are also compared with those obtained by other researchers.

5.1.1 Power and Effectiveness of Alcohol Fuels

As outlined by several authors including for example, Starkman, Newhall and Sutton (177), methanol and ethanol are quite satisfactory as engine fuels. Their performance relative to gasoline can be predicted by reference to the product reactant (P:R) ratio in combustion, the state of the inlet mixture (proportion unevaporated) and their respective enthalpies.

A simple examination of the stoichiometric combustion equations (ignoring dissociation) reveals the differences in product:reactant ratio:

For octane $C_8H_{18} + 12.5\ O_2 + 47\ N_2 \longrightarrow 8\ CO_2 + 9H_2O + 47\ N_2$

For methanol $CH_3OH + 1.5\ O_2 + 5.65\ N_2 \longrightarrow CO_2 + 2H_2O + 5.65\ N_2$

For ethanol $C_2H_5\ OH + 3\ O_2 + 11.3\ N_2 \longrightarrow 2\ CO_2 + 3H_2O + 11.3\ N_2$

Product:Reactant ratios (PR) are as in column 1 below assuming the fuels entering the engine cylinder are completely evaporated.

	1 P:R Ratio (Evaporated fuel)	2 P:A Ratio
Octane	1.058	1.075
Methanol	1.061	1.210
Ethanol	1.065	1.140

However, in the carburetted engine the fuel is not completely evaporated and may even be largely unevaporated. For comparison the most extreme condition is in the direct injection engine with the fuel entirely unevaporated. In this case a more significant comparison may be with the product:combustion air ratio (P:A) since the fuel will occupy a negligible volume. As shown above (again ignoring dissociation) P:A ratios show a greater advantage to the alcohols and especially to methanol. In a carburetted engine the extent of evaporation of the inlet fuel will vary according to ambient conditions, inlet manifold pressure and driving mode etc, and thus the comparative performance would be expected to be somewhere in between the extremes represented by the P:R & P:A ratios.

The effects of dissociation are naturally highly significant at the temperatures reached in engine combustion processes. The product to reactant or product to combustion air ratios will be significantly affected by the extent of such dissociation. Starkman et al (127) have calculated the extent of such effects. They show that, allowing for dissociation, P:R ratios for ethanol are 2% greater than for octane, and for methanol 1% greater. P:A ratios show the alcohols changing rank, with values for methanol 13% greater than octane, and for ethanol 7% greater. This greater product to reactant ratio or product to combustion air above should result in ethanol and/or methanol providing the greatest power output as it would give the greatest cylinder pressure.

5.1.2 Energy in the Fuel

Energies of combustion of the alcohols also greatly affect their potential performance although a simple comparison is misleading. The extent to which combustion energy is developed as power output naturally varies according to dissociation, and the equilibrium combustion products . Any comparison depends on the energy density of the charge and the equilibrium temperature and pressure of combustion. Intake condition of the fuel:air mixture and compression ratio are thus vitally significant and comparison of results with other workers can only be soundly made if conditions are closely similar. However the rank of the three fuels does not change if account is taken of specific combustion energy. The greater product to reactant ratio above should result in ethanol providing the greatest power output as it would give the greatest cylinder pressure. This however is not so as we note in Figure 4.1.26 and 4.1.29 (graphs of brake power vs blend content for methanol and ethanol respectively) which show that the brake power at stoichiometric composition is almost equal for all blends. Other researchers (52-60) have usually worked on higher compression ratios and have thus obtained greater brake power output and thermal efficiency. Since in the present study the compression ratio was not altered when using the various alternative fuels, it was not possible to take advantage of the greater HUCR (highest useful compression ratio) that can be obtained from the alcohols (Table 2.1). The almost equal power output obtained from the alcohols and alcohol gasoline blends is probably due to the differing thermodynamic properties of the fuels (such as heat of combustion and heat of vaporisation). In this instance the gain one fuel has in terms of P:R ratio is counter-balanced by the dissociation reactions which lower the power and efficiency of the system (Benson & Whitehouse, 126). During combustion the peak temperatures that are attained by the alcohols and alcohol gasoline blends are different, methanol and ethanol giving a lower peak temperature than iso-octane (Starkman et al, 127). The dissociation reactions that follow give varying CO, CO_2 and H_2O concentrations in the exhaust depending on the temperature of the combustion products[50]. The CO_2 and H_2O that are produced during a stoichiometric reaction dissociate to form carbon monoxide (CO), oxygen (O_2) and hydrogen (H_2). The nitrogen and oxygen react to produce nitrogen oxides. The following dissociation and equilibrium reactions occur for CO_2 and H_2O.

(i) $CO_2 = CO + 1/2\ O_2$

(ii) $H_2O = H_2 + 1/2\ O_2$

(iii) $CO + H_2O = H_2 + CO_2$

the equilibrium constant for (i) is represented as:

$$K_{p_1} = \frac{P_{CO_2}}{P_{CO}\sqrt{P_{O_2}}}$$

where

K_{p_1} = equilibrium constant for the reaction,

P_{CO_2}, P_{CO} and P_{O_2} are partial pressures respectively.

$$K_{p_2} = \frac{P_{H_2O}}{P_{H_2}\sqrt{PO_2}}$$

For equation (iii) we have

$$K_{p_3} = \frac{P_{H_2} P_{CO_2}}{P_{CO} P_{H_2O}}$$

where K_{p_3} = equilibrium constant for the reaction P_{H_2}, P_{CO_2}, P_{CO} & P_{H_2O} are partial pressures respectively.

The dissociation reactions are the main reason we have CO in the exhaust for combustion at stoichiometric composition. Values for K_{p1}, K_{p2}, and K_{p3} are listed in literature (50).

The nitrogen and oxygen in the combustion products dissociate and react in the following manner:

$$O_2 \rightleftharpoons 2O$$

$$O + N_2 \rightleftharpoons NO + N$$

$$N + O_2 \rightleftharpoons NO + O$$

The reactions are referred to by Newhall and Starkman (136) and are known as the Zeldovich chain reaction. The reactions suggest that at elevated temperatures (> 2500°C) in the cylinder, molecular oxygen dissociates to atomic oxygen and reacts with molecular nitrogen. Further extensions of the Zeldovich reaction have been outlined by Lavoie (128) (showing dissociation of OH) and Annand (129)(N+OH). Bonson et al (130, 131])used Annand's method and predicted NO emissions for a single cylinder gas engine. Results using a propane/air mixture were comparable with those of experimental results.

These dissociation reactions suggest that consideration of product to reactant ratio is not an accurate method of comparing power outputs or thermal efficiency since dissociation of the combustion products changes the P:R ratio of the fuels used.

This effect of dissociation was studied by Starkman et al (127) who showed that at stoichiometric compositions, the combustion temperature and pressure altered the P:R ratio. The P:R ratio increased with increase in temperature.

To compare all the fuels tested in this experimental programme using a theoretical approach would result in an extremely complex representation since the engine is not ideal and due to the number of cylinders, fuel distribution would also have to be considered (a computer study of this type has been done by Gravestock (137) using computer simulation techniques). The computer predicted results were compared with those obtained experimentally by other researchers (Peffley et al (51), Bernhardt (53)) who used a Ford Pinto 2.3 l engine and a Volkswagen 1.5 l engine. These results compared well and showed similar trends to this work. For instance Figure 4.1 shows a gradual rise in CO concentration as the F/A mixture is made richer. Figure 4.1 also shows that maximum CO_2 in the exhaust is obtained at F/A ratios just below stoichiometric.

5.1.3 Thermal Efficiency

The indicated thermal efficiency is the ratio of work done to the net calorific value of the fuels supplied. For an ideal Otto cycle, it may be expressed as follows (126):

$$\eta_{TH} = \frac{\oint_{A}^{A} pdv\ N}{-\ w_f\, Q_{vs}}$$

where η_{TH} = thermal efficiency

$\oint_{A}^{A} pdv$ = the area of the pressure: volume diagram

N = No of cycles

Qvs = heat of reaction

w_f = weight of fuel used

The mean effective pressure

$$P_m = \int_{A}^{A} \frac{P\,dv}{V_s}$$

where

V_s = swept volume

If the above equations are used to model an ideal Otto engine (Benson and Whitehouse (126) we note that the maximum temperature varies with F/A ratio. If it is assumed that dissociation does not occur, the reaction would go to completion and the peak temperature would be at stoichiometric condition. In a non-ideal system as in the present experimental study, dissociation does occur and the specific heats of the combustion products CO_2 and CO shift the peak temperature to the rich side due to the loss in dissociation energy (Benson and Whitehouse, 126). This variation in peak temperature alters the concentration of CO and CO_2 in the exhaust and hence the specific heats of the combustion products. However, if we compare the thermal efficiency curves obtained in this work (Figure 4.1.46 is typical) with those of the theoretical model (Benson and Whitehouse, 126) of an ideal Otto cycle and experimental results by Pefley et al (51) (using a Ford Pinto 2.4 l engine), we note that the trends (shape of curves) are very similar. Exact comparison with experimental data obtained by Pefley et al (51) cannot be made due to the difference in engine types and size. The theoretical model (for iso octane, using a single cylinder), shows that the thermal efficiency is high at lean mixtures and rapidly falls as the mixture strength is increased. The same is true of the typical curves obtained (Figure 4.1.46) for the Fiat 127 multicylinder engine. Other curves obtained in this work (Figure 4.1.47-4.1.67) show similar trends for both methanol and ethanol. It can be noted that engine speed does not alter the trend nor the overall thermal efficiency greatly. At stoichiometric composition however the magnitude of thermal efficiency (Figure 4.1.58) does alter showing peaks at 1500, 2000 and 3500 rpm. This is to be expected as engines for road use are usually designed to operate efficiently at certain specific engine revolutions. For this engine max torque was obtained at 3500 rpm (Table 4.1.1 and Table 4.1.4 for methanol and ethanol respectively) which is probably why thermal efficiency is high at this engine speed. The other speeds 1500 and 2500 rpm showing efficiency peaks are probably optimum engine speeds for specific gears.

If we consider the reciprocating engine as a machine which regardless of fuel would induct one volume of reactant per unit of time, and assuming that all the fuels noted above would enter the engine completely evaporated and burn to completion then it follows that there are some differences in the fuels themselves that may generate extra power. The fuel that gives the largest number of moles of product per mole of reactant should produce the greatest cylinder pressure after the combustion which would in turn result in greater engine power. However if we look at the curves of Ihp, Bhp, and torque Vs alcohol content at stoichiometric compositions (Figures 4.1.25-4.1.30) we note that the increase in power is only slight and at times equal to that produced using gasoline. This is because a modern engine is not an ideal reciprocating engine and at times the mixture of fuel supplied to the engine is not totally evaporated which leads to incomplete combustion and hence results in loss of power. This is especially so when using straight alcohols where the F/A ratio is so great that not enough time is available for the fuel to completely evaporate in the intake manifold of the system (see manifold design) leading to large droplets of fuel going into the cylinder which do not completely burn and are exhausted as unburned fuel.

5.1.4 Comparison of Exhaust Emissions

In addition to the work referred to above, various other mathematical techniques (Benson et al (130), Annand (129), Phllipis (135) & Benson (131)) have been used to model the reaction. These models have made comparisons of the cycle predictions based on the ideal Otto cycle and the real cycle. The main difference between the two cycles is in the thermal efficiency and power. These differences are due to the combustion processes.

The chemical reactions during the combustion process are complex but a simple general expression for the combustion of hydrocarbon fuels may be developed:

$$C_n\,H_m + \left(n + \frac{m}{4}\right) O_2 + 3.75\left(n + \frac{m}{4}\right) N_2 \longrightarrow n\,CO_2 + \frac{m}{2}\,H_2O + 3.76\left(n + \frac{m}{4}\right) N_2$$

When using alcohols, the oxygen within the molecule facilitates combustion. The combustion reactions for iso-octane (which closely resembles gasoline in its carbon to hydrogen ratio), methanol and ethanol are as follows:

$C_8\,H_{18} + 12.5\,O_2 + 47\,N_2 \longrightarrow 8\,CO_2 + 9\,H_2O + 47\,N_2$ (iso-octane)

$CH_3OH + 1.5\,O_2 + 5.65\,N_2 \longrightarrow 6\,CO_2 + 2\,H_2O + 5.65\,N_2$ (methanol)

$C_2H_5OH + 3\,O_2 + 11.3\,N_2 \longrightarrow 2\,CO_2 + 3\,H_2O + 11.3\,N_2$ (ethanol)

At elevated temperatures however, the carbon dioxide and water dissociate to form carbon monoxide, oxygen and hydrogen. Furthermore the molecular oxygen, hydrogen and nitrogen dissociate to form atomic oxygen, hydrogen and nitrogen. Thus in the exhaust gases, the following species are usually found:

CO_2, CO, H_2O, OH, H_2, O_2, N_2, NO, H, O, N

These molecular and atomic species give rise to various compounds some of which are oxides of nitrogen (NO_x) and aldehydes in the exhaust which are environmentally unacceptable. These were not recorded in this test programme. In the present study, the exhaust emissions measured were CO_2, CO and hydrocarbons (as hexane) HC.

If we take a typical graph, say 4.1.59, for CO_2 emission in the exhaust, we note that as the alcohol content in the blend increases, the CO_2 in the exhaust increases due to alcohol/gasoline replacement. This suggests that as the alcohol content in the blend increases, the temperature in the combustion chamber falls (since alcohols burn at a lower temperature than gasoline), and less dissociation of the CO_2 and H_2O takes place. The rise to an optimum of the CO_2 curve takes place at a point which is on the lean side of stoichiometric composition, CO_2 levels in exhaust falling off on either side of stoichiometric (a result also noted in the theoretical approach for methanol using Harker's method, (150). This is due to CO_2 dissociation on the lean side and combustion of rich mixtures on the rich side not going to completion. On the rich side the fuel content is high and the combustion is incomplete. This gives a greater CO concentration in the exhaust, ie.

$$C + 1/2\, O_2 = CO$$

this reaction has a high equilibrium constant (1.06 x 10^6 at 1600°C). This trend has also been found by Pefley et al (151) using methanol and indolene at all fuel air ratios within the misfire limit using a Ford Pinto 2.3 l engine. At stoichiometric composition the presence of CO is due to incomplete combustion and the dissociation reactions (section 4.1.2). Figure 4.1.73 which is typical of CO emissions in the exhaust using the alcohols and alcohol-gasoline blends shows that there is an increase in CO concentration in the exhaust as fuel air ratio is increased. These CO emission values compare well with typical computed mathematical modelling results (Benson and Whitehouse, 176) and those found experimentally by other researchers (132, 60, 51, 134, 55).

As the alcohol content in the blend is increased, the CO concentration in the exhaust decreases. This is due to the lower carbon content in the fuel as we note that methanol and methanol blends give lesser CO emissions than ethanol and ethanol blends (Figures 4.1.75 - 4.1.84). At stoichiometric compositions (Tables 4.1.13 and 4.1.14 for methanol and ethanol respectively) we note that when going from low to high engine speeds, ie. from 1500 to 4000 rpm, the CO % in the exhaust begins to fall, (up to speeds of 3500 rpm) and then increases at 4000 rpm. This is due to the erratic behaviour of the engine at low speeds where there are cycle to cycle variations leading to unsteady inlet manifold pressure and thus inconsistent fuel metering. This causes at times excess fuel to enter the combustion chamber which does not burn and is exhausted as unburned fuel and at other times causing less fuel to enter the combustion chamber, increasing the combustion temperature and increasing dissociation of CO_2 to CO. At higher engine speeds the residence time of the fuel air mixture in the combustion chamber is low which causes incomplete combustion and hence greater CO levels in the exhaust.

Hydrocarbons present in the exhaust gas appear for a number of reasons. Unstable ignition (misfire), poor operation (ie. excess lubricating oil pressure) and combustion chamber design are all factors which affect the production of hydrocarbons. The two main combustion generated sources are the intermediate products and wall quenching. (Benson & Whitehouse (126), Woshcni G (138)). Intermediate products for alcohol fueled cars are mainly the aldehydes some of which are stable and pass into the exhaust. In the present study, Figure 4.1.87, which is typical of the HC vs F/A ratio curves, shows that the trends for hydrocarbon emission of all the fuels (methanol, methanol-gasoline blends, ethanol and ethanol-gasoline blends) are very similar. A similar result was found by Ninomiya (139) using a Ford engine. Our results (Figure 4.1.87) show that at lean operation the HC emissions are all comparatively low and for high alcohol blends almost equal; at rich mixture operation HC levels are high; high for the lean alcohol blends. For the low alcohol-gasoline blends (< 40%) at rich mixture operation, incomplete combustion of the gasoline leads to high HC in the exhaust. For high alcohol-gasoline blends however (> 50% v/v) the greater HC levels are due to the formation of the aldehydes brought about from the incomplete combustion of the alcohols. The aldehydes inhibit the combustion of hydrocarbons.

It was not possible to consider the NO_x's and aldehydes in the current programme. A theoretical approach was however carried out which used the method proposed by JH Harker (150) for calculating equilibrium compositions of any mixture of flame gases. Flame compositions and temperature have also been calculated by Gaydon and Wolfhard (151) but these latter were for fuel in oxygen and thus the methanol was not used. The method, assuming that the combustion products obey the ideal gas laws, are homogeneous and of constant composition throughout the flame, uses the simultaneous equations set up by linear (mass balance) and non-linear (equilibrium) equations of the molecular and atomic species. These are outlined as follows. When hydrocarbon fuels are burnt with air, the combustion products contain carbon, hydrogen, oxygen and nitrogen. The following dissociation reactions will then have to be considered.

$CO_2 \rightleftharpoons CO + 1/2\,O_2$

$H_2O \rightleftharpoons H_2 + 1/2\,O_2$

$H_2O \rightleftharpoons 1/2\,H_2 + OH$

$1/2\,H_2 \rightleftharpoons H$

$1/2\,O_2 \rightleftharpoons O$

$1/2\,O_2 + 1/2\,N_2 \rightleftharpoons NO$

At equilibrium the following relationships must be satisfied:

$$K_1 = \frac{P_{CO}\sqrt{P_{O_2}}}{P_{CO_2}} \qquad K_2 = \frac{P_{H_2}\sqrt{P_{O_2}}}{P_{H_2O}} \qquad K_3 = \frac{P_{OH}\sqrt{P_{H_2}}}{P_{H_2O}}$$

$$K_4 = \frac{P_H}{\sqrt{P_{H_2}}} \qquad K_5 = \frac{P_O}{\sqrt{P_{O_2}}} \qquad K_6 = \frac{P_{NO}}{\sqrt{P_{O_2}}\sqrt{P_{N_2}}}$$

where P_{CO}, P_{O_2} etc are the partial pressures of CO and O_2 and K_1 to K_6 are the equilibrium constants which are dependent on gas temperature.

Let $a = P_{CO}$, $b = P_{CO_2}$ etc

then, $a + b + c + d + e + f + g + h + i + j = 1$ (1)

and the six equilibrium equations become:

$$K_1 = \frac{a\sqrt{c}}{b} \quad (2) \qquad K_2 = \frac{a\sqrt{c}}{e} \quad (3) \qquad K_3 = \frac{f\sqrt{d}}{e} \quad (4)$$

$$K_4 = \frac{g}{\sqrt{d}} \quad (5) \qquad K_5 = \frac{h}{\sqrt{c}} \quad (6) \qquad K_6 = \frac{i}{\sqrt{j}\sqrt{c}} \quad (7)$$

the mass balance equations become:

no of carbon atoms $n_c = P_{CO} + P_{CO_2} = a + b$

no of hydrogen atoms $n = 2d + 2e + f + g$

no of oxygen atoms $n_o = a + 2b + 2c + e + f + h + i$

no of nitrogen atoms $n_n = i + 2j$

If k, l and m are the ratio of carbon, oxygen and nitrogen atoms to hydrogen, ie.

$k = \frac{n_c}{n}$ $\quad l = \frac{n_o}{n}$ $\quad$ and $\quad m = \frac{n_n}{n}$ $\quad$ then

$k_n = a + b$ (8)

$d_n = a + 2b + 2c + e + f + h + i$ (9)

and $m_n = i + 2j$ (10)

when $n = 2d + 2e \;\; f + g$ (11)

Thus there are 11 equations and 11 unknowns. The computer program developed by Harker[150] was rewritten for the IBM PC micro computer (Appendix 6) to evaluate combustion products for methanol and ethanol. Tables 5.1 and 5.2 show the values of l, m and k for methanol and ethanol used in the computer program. The summary of the results is given in Tables 5.3 and 5.4.

Comparing carbon monoxide and carbon dioxide emissions, the results of this work on the Fiat engine compared well with predicted values obtained from the theoretical approach following Harker's model. For instance Table 5.3 shows carbon monoxide in the exhaust as the fuel/air mixture becomes leaner. This trend is also seen in Figure 4.1.59 - 4.1.84, (exhaust emission curves) at all engine speeds. Comparing absolute carbon monoxide values from Table 5.3 and those from Figure 4.1.73, the curve for 100% methanol at engine speed 1500 rpm, shows that the values are almost identical. For instance, the carbon monoxide in the gaseous product from the flame at a fuel air ratio of 1:6 is 4.9% which is almost identical to that of the carbon monoxide percentage in the exhaust products from the Fiat engine at 1500 rpm. This is true also for fuel air ratios of 1:7, 1:8 and 1:9. If the curve in Figure 4.1.73 were extended it would be closely similar for fuel/air ratios of 1:10 and 1:11. At higher engine speeds exact comparisons cannot be made since conditions are widely different. However, similar trends do occur. Similar comparisons to the above were made between Table 5.4 and Figure 4.1.74 for ethanol. Here although similar trends were observed, exact comparisons showed that the model gives carbon monoxide values far higher than those obtained from experimental results. One likely explanation for this could be that the methanol with its higher percentage of oxygen within the fuel (51% for the methanol molecule is oxygen compared with 35% for the ethanol molecule) assists in the combustion of the fuel. Furthermore during experimentation, the sampling point for the exhaust products is some distance away from the exhaust port and hence further oxidation of carbon monoxide would result in the exhaust pipe thus leading to a lesser overall CO value.

Carbon dioxide values taken from Harker's model (Table 5.3) for methanol are also very similar to those obtained experimentally shown in Figure 4.1.59. This is to be expected since predicted and actual values of carbon monoxide percentage are also closely related. Table 5.3 shows that the maximum value for CO_2 is reached at a methanol fuel/air ratio of $\simeq$ 1:7 (0.1429) which is comparable to that in Figure 4.1.59, the CO_2 curve for combustion of 100% methanol in the Fiat engine. The magnitude of the values obtained from the model are lower because further oxidation of CO in the exhaust systems would lead to a higher value of CO_2 at the sampling point whereas the model predicts CO_2 values at the flame. The difference between values from the model and experimental results is even greater when comparing CO_2 values in Table 5.4 and Figure 4.1.65. The trend however, going from lean to rich combustion, remains the same.

5.2 Manifold Design

The condition of the fuel/air mixture on arrival at the inlet valve will be determined by evaporation and entrainment of the fuel followed by deposition of fuel droplets on the manifold wall and some re-entrainment. The design of the inlet manifold will have a significant effect on the state of the inlet mixture (proportion of liquid, vapour, and size of fuel droplets, etc).

5.2.1 Inlet Mixture Conditions

In theory the fuel evaporation and transportation in the intake system is considered downstream of the throttle plate.

If we consider a straight horizontal manifold and at any given point the mass flowrate is mf_1, and at any other point, donwstream of the first, the mass flowrate is mf_2, then,

$$mf_2 = mf_1 + m_d - m_e - m_n$$

where,

m_d = increased mass flow due to further droplet deposition,

m_e = liquid mass evaporation of the wall film

m_n = liquid mass entrainment of the wall film.

Hence the net change in film flow between the two points can be represented by:

$$mf_2 - mf_1 = m_d - m_e - m_n$$

ie. the change in mass flow is a function of droplet deposition rate, entrainment and evaporation of the wall film.

The rate of change of the film flow can be expressed in the following manner:

$$m_f = \frac{mf_1 - mf_2}{A_{12}}$$

where,

m_f = rate of change of film flow
A_{12} = the surface area between the two points.

thus,

$$m_f = \frac{m_e + m_n - m_d}{A_{12}} = Q_e + Q_n - Q_d$$

where,

$$Q_e = \frac{m_e}{A_{12}} = \text{specific evaporation rate}$$

$$Q_n = \frac{m_n}{A_{12}} = \text{specific entrainment rate}$$

$$Q_d = \frac{m_d}{A_{12}} = \text{specific deposition rate}$$

While evaporation, entrainment and deposition have been studied in other systems such as spray dryers, heat exchangers, steam condensers etc their values have not yet been reported for flow conditions in the intake manifold of carburetted engines.

As the intake manifolds of conventional vehicles are not straight as described in the above equations is it necessary to have a "bend factor" which allows for the different kinds of bends. It is well known that bend geometry has a significant effect on inlet mixture condition.

5.2.2 Evaporation, Entrainment and Deposition Rates

The rate of film evaporation may be affected by many flow parameters such as fuel temperature, air temperature, manifold pressure, air velocity, manifold wall temperature and liquid film composition. Alcohol fuels have a higher constant boiling temperature, lower vapour pressure and higher evaporation enthalpies than gasoline and it is therefore advantageous if the intake manifold is heated or the fuel preheated to a temperature close to its boiling point to increase the evaporation of the liquid film thereby increasing the homogenity of the fuel/air mixture that is being carried through into the cylinders. Homogenity is only possible if all the liquid fuel is completely evaporated and is present in vapour form only.

When there is no heating system in use, ie. the intake manifold is not heated and the fuel is not preheated prior to carburation, then the two most important variables are throttle setting and length of intake manifold. The throttle setting will vary wall film flowrate in numerous ways. Chief among these is the throttle position. The smaller the throttle opening, the higher the manifold vacuum and the higher the air velocity in the manifold. The air velocity tends to increase turbulence and evaporation rate and hence lower the total film flowrate.

The rate of entrainment is such that the sharp bend manifold entrainment rate is higher than that for the smooth bend which in turn is higher than that for the straight manifold. This can be explained simply by considering the geometries of the three manifold shapes.

There is no simple quantifiable way of determining the deposition rate but the simple correlation suggested by Alexander and Coldren (125) may be assumed:

$$Q_d = k\,(V_a)^x\,C$$

where,

Q_d = deposition rate; V_a = air velocity, and; C = droplet concentration

k,x = constant

5.2.3 Significance of Wall Film Comparison

Section 4.2.3 gives the general results which show the effects of differing engine operating conditions on the measured wall film mass flowrate. Absolute values of film flowrate gave a better representation of the system than when using percentage film flowrate (quantity of film removed as a percentage of the amount of fuel injected). This is better demonstrated when observing Figure 4.2.13 and 4.2.14. Figure 4.2.13 indicates that as engine speed is increased at given air fuel ratio, the film mass flowrate (g/min) increases with increase in engine speed. On the other hand Figure 4.2.14 suggests that as the engine speed increased, at a given air fuel ratio, the percentage film flowrate (%) decreases with increase in engine speed. Nevertheless the percentage film flowrate figures show that in some cases (Figure 4.2.14) up to 45% of the fuel is "wasted" forming the wall film.

At a constant engine speed (1500 rpm), the variation of film mass flowrate with total air fuel ratio is seen in Figure 4.2.3 - Figure 4.2.5 with varying manifold types. We can summarise these in the following manner:

1 The wall film mass flowrate follows approximately an exponential curve with air/fuel ratio (Figure 4.2.5). Film flowrate increases with increase in air fuel ratio. This is not unexpected since the greater air fuel ratio will increase droplet concentration entering the manifold. It must be noted however that it is not possible to completely eliminate the wall film, the minimum being dependent on manifold geometry and engine speed. The lowest percentage film flowrate that was obtained was 7% (Figure 4.2.5).

2 The effect of the throttle plate position on fuel distribution and hence wall film flowrate is clearly distinguished as shown in Figure 4.2.2 - 4.2.4. In all cases the 1/2 throttle setting gave the maximum film flowrate. The 1/4 throttle setting, should

give the maximum but measured values suggested otherwise (Figure 4.2.2-4.2.4). This is due to the high air velocities and greater manifold depression that is achieved at 1/4 throttle setting which enhances the rate of re-entrainment of the film back into the main flow stream. Figure 4.2.6 and 4.2.7 support this theory which show that for a smooth bend, the film rate both actual and percentage are nearly the same for full and 1/4 throttle setting even though Figure 4.2.8 suggests that the effect of throttle setting is not as great as the effect of a sharp bend. Comparisons of Figures 4.2.6, 4.2.7 and 4.2.8 also suggest that the relatively large fuel droplets cannot negotiate the geometry of the sharp bend and thus go on to produce the greater amount of wall film. This can also be seen in Figure 4.2.12 which shows that the sharp bend produces the greatest wall film.

3 Increasing engine speed merely increased the fuel throughput and hence wall film flowrate. Figure 4.2.13 shows the effect of film flowrate. Figures 4.2.15 - 4.2.18 also show that as total fuel mass flowrate is increased, the film mass flowrate is also increased. These figures also show the greater the manifold length, the less the wall film flowrate. The rate at which the film flowrate decreases is not constant however since the rate of wall film development is dependent on deposition rate - a function of droplet concentration, reentrainment rate - function of film thickness and film flowrate and evaporation rate - function of temperature and fuel composition.

These comparisons and analyses of results can clearly be used to propose optimum manifold geometry, angles and other features (such as heating etc) which should be incorporated in the intake manifold for use with alcohols and alcohol gasoline blends.

5.2.4 Proposed intake manifold design for use with alcohol and alcohol/gasoline blends

From the experimental data obtained it was evident that the alcohol would require a larger and predominantly different intake manifold (Figure 4.2.1 shows that alcohol fuels would give a greater wall film flowrate). The required design must allow more of the alcohol to vapourise in the intake manifold. This would provide lower exhaust emissions (19) and greater efficiency as it would reduce maldistribution of the fuel from cylinder to cylinder (19).

In order to achieve greater vapourisation of the fuel the evaporation and entrainment rates would have to be improved. Thus the intake manifold would have to be designed in such a way that the evaporation of the liquid wall film is improved either by heating system or by reentrainment with the geometry altered so that the liquid wall film is "thrown" back into the air stream.

To improve the evaporation simply by increasing the manifold length and diameter would be impractical as the length and diameters required would need to be too large. This is due to the low vapour pressure of methanol and ethanol at low temperatures. Therefore the only practical method of improving the evaporation is by some form of heating system connected to the intake manifold. Numerous systems have been proposed by researchers (142, 143, 144 and others). A heating system using heating rods connecting the hot engine block to the intake manifold have been suggested. Bond (140) suggested a system of using self-regulating solid state ceramic circuit element heaters placed inside the manifold. This system would require a power supply in excess of 2 KW which is difficult to supply especially during cold start. The Shell-NEL (142) heat pipe vapouriser technique (Vapipe) which uses a small compact heat exchanger unit consisting of a sealed vertical metal tube containing a specific liquid provides better vapourisation of the liquid wall film. Here the exhaust gases are used to heat the lower part of the heat pipe, causing the liquid within to evaporate and recondense in the upper cooler part of the pipe. The upper part of the pipe is connected to or inserted in the intake manifold and here the condensing vapour gives up latent heat to evaporate the fuel, the condensing liquid falling back under gravity. This cycle is continuously repeated until steady state; this system of intake manifold heating using a 1.5 l Volkswagen engine running at full throttle would provide nearly

2.5 kW energy, enough to give a mixture temperature rise of 40°C in the intake manifold. This system was found to be adequate for gasoline fuel but when using alcohols the energy required would need to be about 3.5 kW to give the same temperature rise (141, 146). However the increased heating would provide a greater amount of fuel vapourisation in the intake manifold leading to better distribution of the fuel to the cylinders and hence higher efficiency of the engine. The heating system suggested by Menrad (142) uses the exhaust gases directly instead of a cooler specified in the Shell-NEL system. This would be better during the warm-up phase of vehicle operation. Menrad (143) also suggested using a sufficient surface area to avoid hot spots during heating of the intake manifold.

The entrainment rate, ie. the rate at which the liquid wall film is thrown back into the air stream can be improved by having sharp bends in the intake manifold, especially leading to the distribution function. The sharp bends would be difficult for the wall film to negotiate and thus the liquid wall film would be thrown back into the air stream. These can be seen from the wall film experimental results (Figure 4.2.9) which show that the manifold with sharp bends gives less wall film flowrate than a smooth bend at the same air fuel ratio. A rough surface inside the intake manifold would serve in a similar way.

The recommended design of manifold could thus be as shown in Figure 5.1. The baffles on the inside surface of the manifold will throw the liquid wall film back into the air stream. Since the quantity of liquid film is greatest just after carburation, baffles in this part of the manifold should be of greater depth. As the liquid film is reduced in quantity along the length of the manifold so the baffle plates are reduced in size. The vapipe is similar to the shell-vapipes (142) connecting the exhaust manifold and the intake manifold at points corresponding to the baffle plate should improve the evaporation of the liquid wall film. To improve heat transfer the lower baffles connected with the vapipe may be made hollow so that the condensation which is fundamental to the operation of the vapipe will take place on the inner surface of that baffle.

An alternative design for re-entrainment of the wall film is indicated in Figure 5.2. A continuous helical baffle is shown and this could be angled so that wall film liquid would be projected back to the inner edge and returned to the stream of inlet air. Again in this design the baffle could be hollow and connected to a vapipe so that heat transfer would be increased, more of the wall film liquid being evaporated.

It is important to avoid great increase in pressure drop in the baffled manifold compared with the clearway provided in conventional designs. However the baffles have two effects - to return the wall film liquid to the central flow of inlet air and fuel vapour and to increase turbulence to assist and maintain entrainment. This increased turbulence should be achieved with baffles of height approximately 1/10 or 1/15 of the manifold diameter, without unduly increasing pressure drop. Investigation of various manifold designs and baffle configurations would be a fruitful subject for further work in this field.

Using the various heating systems can increase the mixture temperature in the intake manifold by up to 50% (143). Thus the above methods, ie. heating the manifold and altering the size and geometry can improve evaporation considerably. The improved evaporation of the fuel would also improve the distribution of the fuel to the various cylinders and thus reduce cylinder to cylinder variations.

If the methods of improving evaporation of the fuel in the intake manifold are incorporated in an alcohol or alcohol-gasoline fueled vehicle greater efficiency will be obtained by the improved combustion and also by the heat recovery involved in the designs discussed.

Figure 5.1: Proposed manifold design: radial baffles

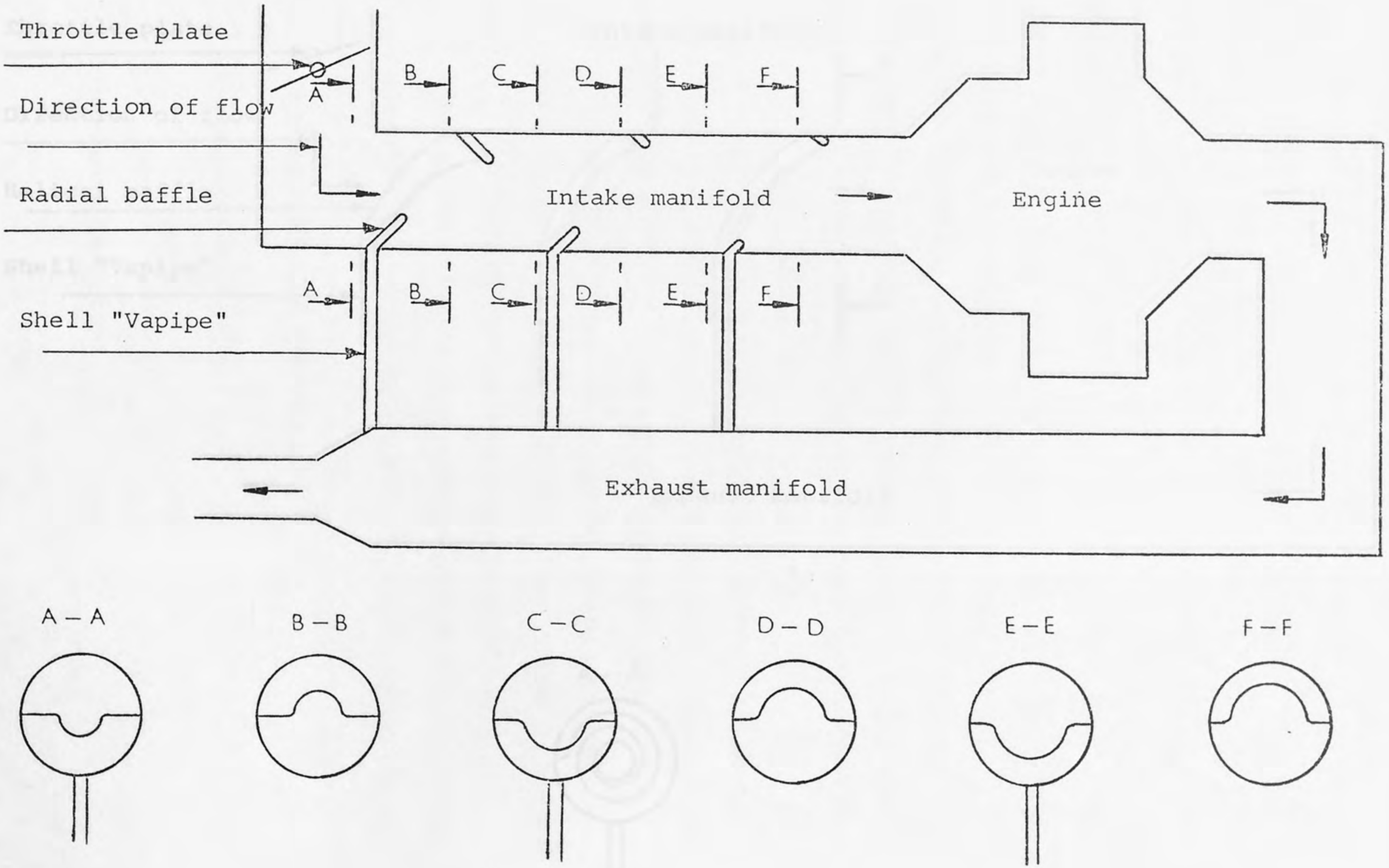

Figure 5.2: Proposed manifold design: Helical baffle

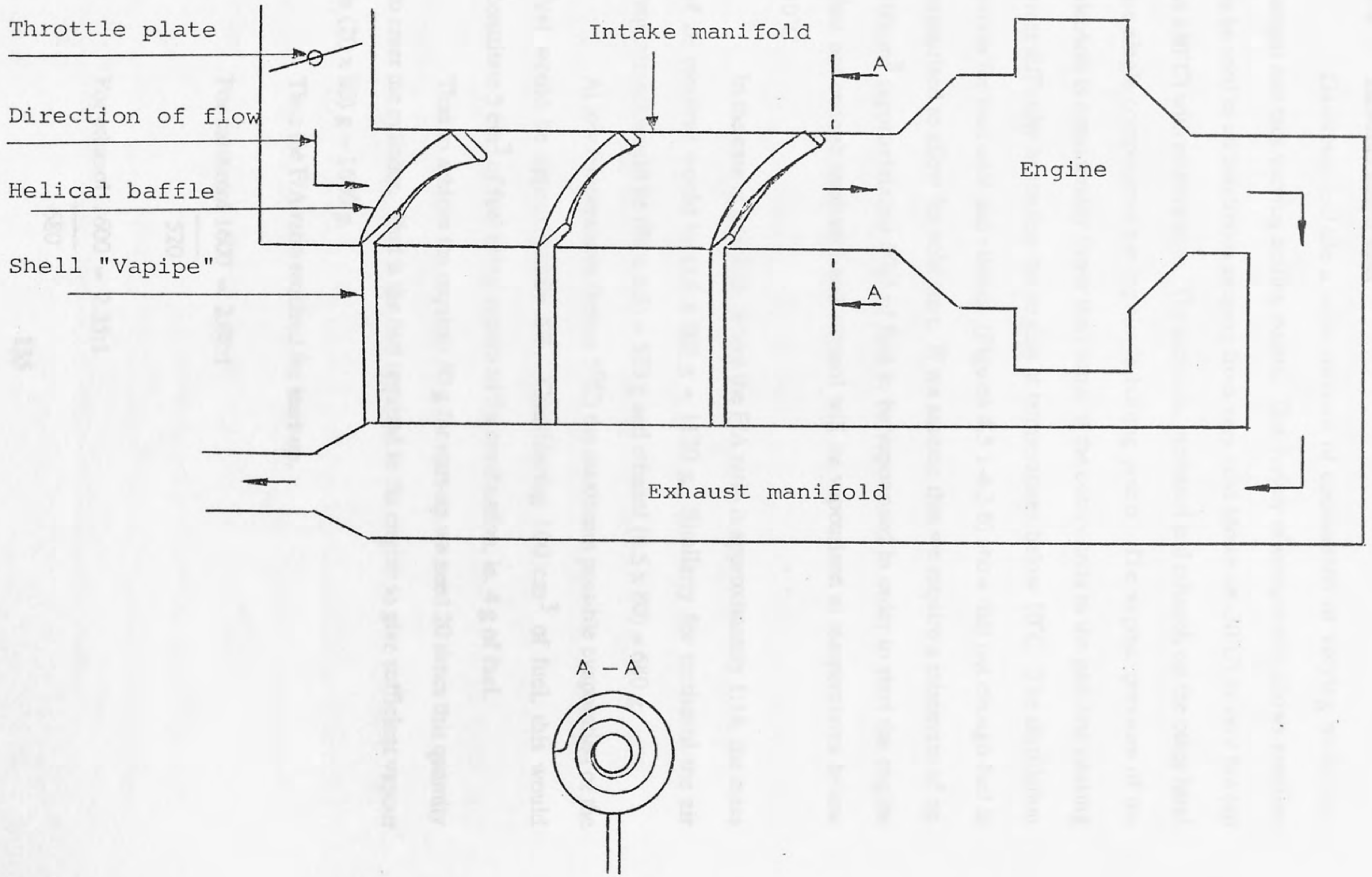

5.3 Volatility Constraints

Gasolines include a wide mixture of compounds of varying molecular weight and thus varying boiling points. This variety of compounds allows gasoline to be used in all conditions ranging from very cold (down to -30°C) to very hot (up to +30°C) with relative ease. The alcohols, methanol and ethanol, on the other hand are single components having single boiling points. The vapour pressure of the alcohols is considerably lower than some of the compounds in the gasoline causing great difficulty in starting the engine at temperatures below 10°C. The distillation curves for methanol and ethanol (Figures 4.3.1-4.3.6) show that not enough fuel is vapourised to allow for cold start. If we assume that we require a minimum of eg. 100cm^3 (approximately 80g) of fuel to be vapourised in order to start the engine then not enough methanol and ethanol will be vapourised at temperatures below 10°C.

In the case of gasoline, where the F/A ratio is approximately 1:14, the mass of air required would be (14 x 80) g = 1120 g. Similarly for methanol the air requirement would be (80 x 6.5) = 520 g and ethanol (8.5 x 80) = 680 g.

At low temperatures (below 5^{o}C) the maximum possible evaporation of the fuel would be approximately 5%. Considering 100 cm^3 of fuel, this would constitute 5 cm^3 of fuel being vaporised for combustion, ie. 4 g of fuel.

Thus to achieve the required 80 g for start-up we need 20 times this quantity to enter the cylinder. That is the fuel required in the engine to give sufficient vapour is (20 x 80) g = 1600 g.

Thus the F/A ratio required for start-up,

For methanol $\frac{1600}{520} = 2.08:1$

For ethanol $\frac{1600}{680} = 2.35:1$

$$\text{For gasoline } \frac{1600}{1120} = 1.42:1$$

Alternatively, by using a low vapour pressure compound such as n-pentane, blended with the alcohols the required amount of fuel can be vapourised at lower temperatures. This is shown in Figures 4.3.1-4.3.6 which show that the volume take off at lower temperatures is increased when n-pentane and gasoline are added to the alcohols. The greater the volume of additive, the greater the volume distilled at lower temperature. This increase of volume evaporated however does not solve all the problems since the higher vapour pressure of the components in gasoline and of n-pentane may give rise to vapour locking, which does not occur when using pure alcohols, in hot climatic conditions. This is because polar and non-polar liquids such as gasoline and methanol, do not mix well with the result that excessively high vapour pressures are observed (152). High underbonnet temperatures when stationary after a long running period of an automobile can also give rise to vapour locking. In order to overcome this problem some of the light fractions in gasoline would need to be removed but this would be counter productive since it is these that help cold start problems. A compromise between the two opposing requirements is thus essential in selecting an optimum blend of alcohols with gasoline.

As shown above the distillation curve of a fuel can thus be used to predict engine behaviour. The shape of the curve will give a good indication of how the engine will behave with regard to factors such as "cold starting", "hot starting", "warm-up" time, stalling etc and can be used to predict such behaviour.

Figs 4.3.1-4.3.6 show distillation curves obtained for some of the fuels and fuel blends tested on the Fiat 127 903cc engine. Distillation curves for other fuels and blends referred to but not tested can be interpolated using these curves.

The distillation curve for two star petrol for example shows that 10% of the fuel vapourised at temperatures below 45°C. Using such fuel the engine will start from cold at ambient temperature of -25°C using a choke mechanism. It is well understood that in the case of alcohols (when only 10% is vapourised at temperatures in the region of 65°C for methanol and 78°C for ethanol) the minimum ambient temperature required for cold start is between 5-10°C. The temperatures are very significant in the sense that it is possible to determine the additive quantity (% v/v) required to mix with the fuel in order to have a cold starting ability at temperatures between -5°C and 15°C.

Figures 4.3.1 and 4.3.4 suggest that when using alcohol blends the minimum petrol content that is required to have a reasonably good start up is 30% v/v of gasoline in either of the two alcohols. This quantity of gasoline enables up to 10% v/v of fuel to vaporise at temperatures below 45°C thus making start-up easier.

The use of n-pentane and iso-pentane in the neat alcohols also results in a slightly lower temperature for 10% v/v take off but this is not sufficient to improve startibility. However the pentanes can be used in alcohol/gasoline blends when the alcohol content is greater than 70%. In this case a slight reduction to the percentage of gasoline should be compensated by either of the two pentanes.

If the pentanes alone are to be used then the minimum quantity required would be 20% v/v in the alcohol. This may well be too large a quantity for economic viability at current price levels.

The pentane however cannot be used when using hydrated alcohols because phase separation occurs. It is thus suggested that when using hydrated alcohols another system of cold start be used. These include dual fuelling, electrically heated carburettor and intake system etc.

The warm-up and acceleration characteristics of the fuel are determined by the mid-range which can be grouped at 20% v/v to 70% v/v take off. This, when using gasoline, is between the temperature ranges of 55°C to 122°C. As can be seen from all the distillation curves of alcohol and alcohol gasoline blends, this is a temperature range which is high enough to allow good warm-up and acceleration for all the fuels tested.

In general it was found that alcohols have good warm-up and acceleration qualities provided they are used in stoichiometric proportions.

The 80% to 100% range of the petrol distillation curve is usually where all the heavy ends are. These are higher boiling point hydrocarbons and have significant influence on such items as calorific value of the fuel and on lubricating oil dilution and cleanliness. These heavy ends are relatively ineffective when using large percentages of alcohols in the alcohol/gasoline blends. It is therefore suggested that for these blends additional similarly "heavy" hydrocarbons be added back to replace the desirable features. These additives should be comparatively easy to find as heavy hydrocarbon compounds are numerous and most of them would mix with alcohols in all proportions.

Analysis of these various volatility considerations indicates that an optimum volatility profile would be achieved by a composition close to a 50% alcohol/50% gasoline mixture (Figure 4.3.1).

5.4 Material Compatibility

5.4.1 Significance of corrosion comparison

The purpose of carrying out corrosion tests was to evaluate and select materials for use in carburettors and other critical items of the fuel feed system in automobiles using alcohol fuels, both for economic reasons and engine efficiency. The loss of material from say the metering needle of the carburettor will lead to inefficient engine running giving rise to greater fuel cost. Other deterioration eg. in float chamber etc may obstruct smooth operation.

The individual tests, aeration or temperature tests, do not themselves separately provide conclusive information. In a carburetted engine in operation however, all the various test conditions are experienced. The fuel passing through the metering jet is aerated by the incoming air and the operating engine gives rise to high temperature (up to 50°C). When the automobile stops, underbonnet temperatures can be as high as 90°C. Thus the materials used in the carburettor will need to withstand all these conditions simultaneously.

Among the non-ferrous metals found in engine fuel systems, the yellow brasses, as used for example in the Weber Carburettor consist of approximately 30% zinc and 70% copper. The most common form of corrosion of brasses is dezincification (152, 153). This is the selective removal of zinc in brass alloys. There are two general types of dezincification, one is uniform or larger type and the other is localised, or plug-type. The overall dimensions do not change appreciably when dezincification occurs.

There was visible evidence of both types of dezincification of the brass samples in both the aeration and temperature tests. The dezincification mechanism as outlined by Fontana and Green (154) is a simple consecutive sequence in which the brass dissolves, zinc ions remain in solution and the copper plates back on the metal. This replated copper will be in a form readily accessible. The presence of oxygen increases the rate of the dezincification process as it enters the cathodic reaction for zinc.

The loss and gain in weight will then be related to the loss of brass into solution, followed by the copper plating back on to the sample and eventually oxidising and flaking off again. The final oxidising of the copper would give rise to the dark grey film observed on our brass samples in tests 4.4.2 (i)-(iii) and 4.4.3 (i)-(iii). The better resistance to attack as the tests progressed may be attributed to the greater stability of the dark grey (CuO) film.

At higher temperatures as in test 4.4.6, the rate of corrosion is increased greatly as the process is enhanced by the formation of formic and acetic acids which attack brass (60-90% copper) (155).

Zinc is not particularly a corrosion-resistant metal and is utilised in the chemical industry for cathodic protection. Tests 4.4.2 (iv)-(vi) and 4.4.3 (iv)-(vi), show that the zinc sample had pitted in some areas. Zinc reacts vigorously in hydrochloric acid and it is suspected that there is similar reaction between the zinc and the weak acids which are produced by oxidation of methanol and ethanol namely formic and acetic acid. The electrochemical reaction that would take place between zinc and formic acid would be similar to that of zinc in hydrochloric acid, ie.

$$Zn + 2H^+ \longrightarrow Zn^{++} + H_2$$

Hence zinc reacts with the hydrogen ions of the acid solution to yield zinc ions and hydrogen gas. The presence of oxygen enhances the rate of attack and test 4.4.2 (iv)-(vi) as expected showed greater pitting of the samples than test 4.4.3 (iv)-(vi). The condition of the carburettor body section 4.4.8 also shows evidence of this oxygen enhanced attack as the fuel in the carburettor is continually aerated. Test 4.4.2 (iv)-(vi) also indicates that methanol is more corrosive to zinc than ethanol. This may be expected due to its polar nature. Gasoline (test 4.4.2 (vi)) is the least corrosive medium of the three.

During test 4.4.4 with two metals in contact, pitting of the zinc sample was more severe indicating that the electrochemical reactions that were set up were such that zinc acted as a sacrificial anode. Again methanol proved to be a more corrosive medium than ethanol. The brass sample during these tests showed small but significant signs of localised corrosion, ie. plug-type dezincification.

Aluminium (as can be seen from tests 4.4.7) was severely attacked by the methanol leaving large pitted areas. Pitting usually develops as a result of differential aeration cells (153) which convert into passive-active cells. The crevice that was present between the aluminium rivet and the teflon (Plate 4410) is where the pitting was initiated. The deficiency of oxygen in the crevice leads to the formation of an anodic area. Loss of passivity in the region followed, giving rise to a larger pitted area around the edges of the rivet. A similar action to this is to be seen with iron in sodium chloride solution (153).

The colour changes that occurred in the copper rivet in tests 4.4.7 and 4.4.8 suggest a high degree of oxidation of copper.

However this attack is likely to be a secondary effect since copper, like aluminium, is not resistant to organic acids such as formic and acetic which are formed in methanol and ethanol when they are oxidised. Copper is highly susceptible to attack by acetic and formic acid when copper ions are in solution (154).

$$Cu^{++} + Cu \longrightarrow 2Cu^{+}$$

In an aerated solution, the rate of corrosion is thus significantly increased (154). Formic acid is one of the strongest organic acids and is known to be the most corrosive. Aluminium is particularly unsuitable for parts in contact with formic acid.

5.4.2 Prospects for extended use of alcohol fuels

If alcohols are to be used with materials such as brass, zinc, aluminium and copper then the problems associated with these materials such as dezincification of brass, pitting of zinc and aluminium and serious oxidation of copper will have to be overcome.

In other situations one way of minimising dezincification is by reducing the aggressiveness of the environment (ie. oxygen removal) (154). This however is impractical in the carburetted engine since continuous air/fuel contact is an essential feature of the induction system. It might however be possible to coat the brass components with vitreous enamels (153). This is essentially a glass-type coating which is bonded onto the metal surface by sintering glass powder over the whole of the contact surfaces. This however would be an uneconomic process for inlet manifold and carburettor parts. Another method of minimising dezincification is by using a less susceptible alloy such as red brass (15% Zn) which is known to be almost immune from such attack.

In reducing the corrosion of aluminium, copper and zinc in alcohol environments, it is quite possible to coat the metals with vitreous enamels, organic coatings (eg. Teflon) and metal coatings (eg. nickel).

Metallic coatings such as nickel are easily applied on metals such as copper by electroplating (153). Coatings of 0.025-0.25mm are quite common which give sufficient protection. It is difficult to get organic coatings such as teflon to bond well on any metal surface due to its extreme inertness (153). Other types of organic coatings such as rubber, neoprene and vinylidene chloride would be useless in alcohol environments because of their solvent properties which would readily dissolve these materials.

One of the methods used at present by the petroleum industry is the use of additives to act as corrosion inhibitors. A study of such inhibitors has been carried out by Robinson (156). Over thirty references have been cited on the use of various compounds such as anhydrides, esters, amines, carboxylic acids, aldehydes, epoxides etc which act as corrosion inhibitors, lubricants, detergents, antifrosting agents etc. These compounds can be formulated for use with alcohols and alcohol gasoline blends to give prolonged engine life with these fuels.

CHAPTER SIX

CHAPTER SIX

CONCLUSIONS

General and Experimental

The Fiat engine rig with water brake dynamometer proved satisfactory for the studies of engine performance using alcohol and alcohol/gasoline blended fuels. The engine did however require regular servicing as would be expected with any other engine. The engine condition at the end of the experimental programme was as good as that at initial inspection. This indicated that, over the period of this work, the alcohols were generally no more detrimental to the engine than conventionally used fuel such as gasoline.

All other instrumentation, such as temperature measurement, air-flow metering etc proved to be adequate for the accuracies required in this experimental programme. The fuel-metering method was as used at Esso Research, Abingdon, being a simple method of measuring volumetric fuel consumption in a given time to measure fuel flowrate. Perhaps a more sophisticated electronic method could have provided more flexible fuel flowrate measurements. This however did not affect the overall experimental results.

The Ricardo E6 single cylinder engine which was used to investigate intake manifold geometries required no modifications and most of the instrumentation was already set up. However special manifolds were made for wall film studies. The "slit" method used to measure wall film flowrate was very successful, and results from these tests were easily reproduced.

The materials and equipment used to carry out the material compatibility tests were easily available. The experimental procedure adopted provided a good method for selecting materials for use with alcohol fuels. Results over an initial sample period of 24 days showed good reproducibility compared with a similar period of actual test.

Performance and Emissions

The comparative mappings of performance and emissions provided some valuable results. The power output of the engine both brake horsepower and indicated horsepower were higher when using alcohols and alcohol-gasoline blends than for gasoline alone. The magnitude of the rise was not as high as was expected from the induced charge to exhaust product ratio calculations (Product: Reactant Ratio (P:R)). These ratio comparisons showed that P:R & P:A for the alcohols were greater than for octane and one might conclude that the fuel which gave the highest P:R or P:A ratio would provide the greatest engine power output. This however was not so, as we note from the graphs (power vs F/A ratio) that the increase in power output is only slightly in favour of ethanol and methanol. At times the brake power output achieved from the alcohols and their blends was only equal to that when using gasoline. This however can be improved by increasing the compression ratio of the engine.

This method of comparing P:R and/or P:A with power output does however suggest that the fuel ingested by the engine is not totally combusted since, if it had been, a greater mean effective pressure would be obtained and hence a greater power output.

There are many reasons why the fuel was not totally combusted, including:

1 The engine: The fact that the Fiat 127 903cc engine is not an ideal engine and therefore some fuel will remain unburned.

2 The fuels concerned: When using alcohols there is a need for a greater fuel charge. This means that when using the alcohols, residence time of the fuel in the engine prior to combustion is not great enough for all the fuel to be evaporated. This results in a greater number of fuel droplets in the fuel charge that enters the cylinder leading to incomplete combustion as the fuel droplets themselves are not in the combustion cylinder

long enough to evaporate and combust.

3 The design of the intake manifold: The intake manifold, because it has been designed for use with gasoline, is not so effective with alcohols and their blends with gasoline especially at high alcohol compositions in the fuel. The manifold length is not great enough to provide a long enough residence time in the manifold to completely evaporate the greater quantity of fuel. This would result in fuel droplets entering the combustion cylinder and eventually being exhausted as unburned fuel. The diameter too is not large enough to provide an adequate surface area to allow for a greater evaporation of the fuel charge. The geometry of the manifold suggests that when using alcohols and alcohol gasoline blends, there will be a greater wall film present in the manifold. This would also result in the film finding its way into the combustion cylinder also leading to presence of unburned fuel in the exhaust.

From the above three reasons, it can be concluded that:

1 The Fiat 127 903cc engine as it stands, is not highly suitable for use with alcohols and alcohol gasoline blends with a high percentage of alcohols in the blend.

2 The intake manifold is not ideal for handling the greater quantity of fuel required with alcohols compared with gasoline.

At this point it is appropriate to consider other properties of the alcohols which may have a bearing on the results. Chief among these are the calorific values and the latent heat of vapourisation of methanol and ethanol. Since the calorific value of the fuel determines its energy content and hence the amount of energy that can be drawn from it, it was thought best to use these values to determine the jet diameter requirements for all the fuels used. Appendix 1 shows the results. It can be concluded that this method of determining the jet diameter requirement for each individual fuel was very successful and no problems were encountered during experimentation.

To add further to the conclusions on performance evaluation, it is best if reference to the comparative mappings is made. It can be concluded that:

1 The calorific value of the fuel, amount of fuel used and engine speed all affect the indicated power. The indicated power is higher for methanol and methanol blends than ethanol and ethanol blends at the same speed.

2 The brake power is not greatly affected by fuel type. It is at most times in the same order of magnitude. However, maximum brake power for any one particular fuel is usually attained at F/A ratios just below or at stoichiometric depending on the alcohol content in the fuel. When alcohol content is high the maximum brake power is at a point below stoichiometric and this moves towards stoichiometric as the alcohol content in the blend decreases. It is at this point that we must note that when a fuel of a higher alcohol content (> 60%) is used, the range or width of F/A ratio at which the brake power is close to or at its maximum point is greater than when the alcohol content is low (≤ 40% v/v). It is beneficial to the automobile user to have this information as it is then possible to operate the engine efficiently at lesser alcohol content.

3 The brake thermal efficiency when using ethanol and ethanol/gasoline blends was greater than when using methanol and methanol/gasoline blends at stoichiometric composition, in line with calorific values. However when using lean mixtures methanol and methanol/gasoline blends provide a greater thermal efficiency than ethanol and ethanol/gasoline blends. This advantage is due to the fact that methanol and methanol

gasoline blends show a better lean misfire limit. Engine speed did not affect this trend.

4 The mechanical efficiency decreased as the F/A ratio increased suggesting that the engine is less efficient when it is running on a fuel-rich mixture. An increase in the alcohol content in the fuel also results in a decrease in mechanical efficiency. This suggests that a lower volumetric throughput results in a higher mechanical efficiency. This is also encouraging information for the automobile user as it means that the engine when operating on higher blends of alcohols can run on lean mixtures (as it has a better lean misfire limit) with a higher degree of mechanical efficiency.

5 A greater lean misfire limit is attained when using fuels with a high alcohol content in the blended fuel. Lean mixture operation is naturally better at higher engine speeds.

6 The carbon monoxide content in the exhaust decreases as the alcohol content (for both methanol and ethanol blends) increases. Also levels of carbon monoxide in the exhaust are lower when using methanol than when using ethanol. This is due to the lower carbon content in the methanol molecule. An increase in engine speed reduces the carbon monoxide level in the exhaust for all alcohol/gasoline blended fuel.

7 The carbon dioxide content in the exhaust increases as the alcohol content in the blend increases. This is true for all engine speeds and equivalence ratios (Ø).

8 Hydrocarbon emissions follow a similar pattern to the carbon dioxide emissions. Hydrocarbon levels increase with an increase in F/A ratio. Hydrocarbon emissions at stoichiometric compositions are lower at high alcohol content in the blended

fuels. This is no doubt due to the lower "hydrocarbon" content in the fuel composition. Engine speed has a variable affect on the hydrocarbon emissions when considering any one particular fuel. Here it shows that hydrocarbon content in the exhaust is higher at very high and very low engine speeds having a somewhat "dipping" effect. This is due to the effect of changed residence time in relation to the combustion characteristics of the fuel.

Manifold Wall Film Studies

The method of determining the jet diameter requirement (mentioned earlier) provided useful information on the quantity of charge that entered the combustion chamber. It showed that the A/F ratios when using methanol (unblended) and ethanol (dehydrated, unblended) were typically 6:1 and 8:1 respectively. This provided the basis for carrying out the tests on the Ricardo E6 single cylinder engine which provided valuable information on optimum manifold design. From the results obtained from these tests we can conclude that in general and for alcohol fuels as well as gasolines:-

1 The amount of wall film produced is dependent on the A/F ratio. The richer the mixture the greater the wall film produced.

2 Maximum wall film is produced at 1/2 throttle setting and the minimum at 1/4 throttle setting.

3 The geometry of the manifold plays a significant part in wall film production. A straight manifold produces less wall film than a sharp bend manifold which in turn produces less wall film than a smooth bend manifold. It is therefore best to use a straight manifold. Since this is not possible on conventional engines it is best to use as

long a manifold as possible where the bends are as sharp as possible. Alternatively a baffled manifold designed to return wall film liquid to the inlet mixture stream would enhance uniform distribution between cylinders and efficiency. Proposed designs are shown in Figures 5.1 and 5.2.

4 An increase in engine speed usually results in a decrease in wall film flowrate indicating better fuel distribution and vapourisation within the inlet manifold.

5 The specific gravity of the wall film is greater than that of the fuel used. As might be expected the fractions concentrating in the wall film will include heavier condensate fractions.

Volatility

Cold starting tests were not carried out since the engine was situated in a laboratory where ambient temperatures were at least 10°C. This temperature was usually high enough to start up using most of the fuels. Some difficulty was observed when using hydrated alcohols, the degree of difficulty being dependent on the amount of water present in the alcohol fuel.

The results of the volatility test show that the difficulty to start the engine at low temperature was due to the fact that not enough vapour was formed to initiate and sustain combustion. The results show that for the dehydrated alcohols without any blending with other hydrocarbons, the temperature for an initial 10% v/v take off (the amount of vapour required for ignition and then sustaining the combustion) was 64.5°C for methanol and 78°C for ethanol. These temperatures are far too high to achieve in cold weather conditions where ambient temperatures are perhaps only as high as 5°C. Blending with volatile hydrocarbons is a way of overcoming this problem but this, as we note from the results, indicates that the minimum blending volume required would be about 40% v/v when using gasoline and >15% v/v of iso- or n-pentanes with either of the two alcohols. These would provide a large enough vapour content in the combustion chamber to ease start-up. No such solution is practicable with hydrated alcohols since phase separation occurs when blending hydrated alcohol with any organic solvent. A water miscible ingredient would be required in this case and such liquids are likely to be much more expensive.

In conclusion we can therefore state that not enough vapour is formed to facilitate start up at low temperature when using neat alcohols or alcohol gasoline blends with a high percentage of alcohol. Using volatile hydrocarbons such as iso- and n-pentane could solve the problem when using dehydrated alcohols but other methods, such as heated manifold etc, should be investigated when using hydrated alcohols. The greatest allowable water content in the hydrated alcohol is 15% v/v water in the fuel for ethanol and 10% v/v water in the fuel for methanol.

Material Compatibility

Oxidation and corrosion tests on the carburettor materials provided useful information as to the type of materials required for prolonged operation when utilising alcohol fuels in carburetted engines. The electrical conductivity measurements of methanol and ethanol and blends of the two alcohols with gasoline showed that methanol and its blends with gasoline were more electrically conductive. This explained why in many instances the sample in methanol was more severely affected than the sample in ethanol. The brasses for instance showed greater surface damage in methanol than in ethanol. The brasses were in general however fairly resistant to the alcohols in aerated environments and high temperatures. The high temperature accelerates the acid formation in the alcohols which does give rise to more severe attack on some metal surfaces. On copper surfaces for instance the presence of formic acid in methanol encourages pin-holing and pitting. Aluminium metal on the other hand is severely attacked by methanol, the presence of formic acid making little difference to the overall result. Stainless steel in methanol with or without the acid is not affected at all. Copper and aluminium ion concentrations in the test solution were found to increase when carrying out tests with methanol and methanol/formic acid test solutions at 65°C. Metal ion concentration tests were also carried out on other test solutions but those that were aerated registered little or no metallic ion concentration. The results were not reproducible and this method of registering sample condition was abandoned. The zinc carburettor samples showed greater surface damage in methanol than in ethanol as judged by the dulling in appearance. This can be related back to the fact that methanol is more electrically conductive than ethanol. It is therefore difficult to conclude simply which materials should or should not be used. It is however best to state that use of aluminium when using methanol should be avoided as much as possible, especially in the carburettor. Zinc or zinc plating is obviously a better material to use in this case. Copper can be used in the carburettor but care must be taken as this material produces large amounts of the oxide in presence of methanol which may cause problems by blocking needle valves and hence give rise to inefficient fuel metering. The condition of the carburettor on the Fiat 127 903 cc engine showed that some pitting of the carburettor had occurred when used with the alcohol based fuels. It is difficult to determine the time period which could be allowed before damage to the carburettor had reached a point when it was no longer useful, but this could be reasonably estimated to be a few years (>3 years). This is perhaps not as long as one would like it to be but it must be noted that this carburettor was not designed for use with alcohol fuels. An inexpensive purpose-designed carburettor would no doubt be more resistant to attack.

As a final note on this point of material compatibility and selection, it can be said that present material can be used if the metals are treated with some form of protective coating so that they are more resistant to the alcohols. This may include polymeric or metallic coatings on entire surfaces, such as the carburettor bend, or specific areas, such as the point of a needle valve.

0

To sum up we can say that this study of the use of alcohol fuels in automotive engines has given valuable insights into the limitations and possibilities of alcohol motor fuels. It was seen as a project which would most benefit the third world countries in many of which the fuels can be produced with relative ease from crops that are readily available. The technology to produce the alcohols from crops does exist and the vehicles to use these fuels require no greatly unusual techniques for manufacturing. The study has indicated those areas of engine design and operation which merit further more detailed research as the use of alcohol fuels progressively increases.

0

REFERENCES

1 DOANN HOUGHTON-ALICO, "Alcohol fuels, policies, production and potential", Westview Press Inc, 1982.

2 HAYES W, "American chemical industry - a history", Vol I, 1923-1929, D Van Nostrand Co Inc, 1948.

3 WOODWARD HFJ, "Methanol" Kirk Otmer Inc, Chem Tech, 2nd Ed, Vol 13, 1967, pp 370-378.

4 HAYES DL, "Methanol: its synthesis, use as a fuel, economics and hazards". December 1976. Available from: National Technical Information Service, US Department of Commerce, 5285 Port Royal Road, Springfield, Virginia, 22151. NP-21727

5 Chemical Engineering Progress Symposium Series No 98, Vol 66, GA Danner (Ed) Am Inst Chem Eng, New York, 1970.

6 Brookhena Nat Labs, Woodwell GM, Pecon EV (Ed), "Carbon and the biosphere, Proc 24th Brookhena Symp in Biology, Upton, NY, May 16-18, 1972.

7 Scientific American "The Biosphere", September 1970.

8 REUBEN BG & BURSTALL ML "The chemical economy a guide to the technology and economics of the chemical industry". Longman, 1973

9 CASSADY PE, "The use of methanol as a motor fuel", 169th Am Soc National Meeting, Philadelphia, April 6-11, 1974 (43 refs).

10 PEFLEY et al, "Study of decomposed methanol as a low emission fuel - final report" - Office of programmes and environmental protection agency, NTIS No PB 202 732, April 1871

11 PEFLEY et al, "Performance and emission characteristics using blends of methanol and dissociated methanol as an automotive fuel", 6th Intersoc Energy Con SAE Paper 719008.

12 DOE HCP/T4 101-03, "Biomass based alcohol fuels: the near term potential for use with gasoline", prepared by W Park, G Price and D Salo of the Mitre Corporation, Metrek Division, for the US Department of Energy, August 1978.

13 PAUL JK, "Ethyl alcohol production and use as a motor fuel", Noyes Data Corporation, Park Ridge, NJ, 1980.

14 LIPINSKEY ES et al, "Fuels from sugar crops", Battelle - Columbus Laboratories, Columbus, OH, 1976.

15 McELROY AD "Utilisation of lead with limited capabilities", Midwest Research Institute, paper presented at Biomass - A Cash Crop for the Future Conference, Kansas City, MO, March 1977.

16 EH FISHER, "Carburation Vol 1", Chapman & Hall Ltd, London, 1963.

17 WILHOIST RC & ZWOLINSKI BJ "Physical and thermodynamic properties of aliphatic alcohols", J Phys Chem Ref Data Vol 2, 1973, Suppl No 1, pp 1-40 & 1-54.

18 ROSSINI FD et al, "Selected values of physical and thermodynamic properties of hydrocarbons and related compounds". Am Petroleum Inst Carnegie Press, 1953.

19 PAUL JK, "Methanol technology and application in motor fuels", Noyes Data Corporation, Park Ridge, NJ, USA, 1978.

20 ALLSUP JR, "Methanol/water/fuel composition, temp phase diagrams", Bartesville Energy Research Centre, ERDA, Battesville, 1976.

21 HAGAN DL, "Methanol as a fuel: a review with bibliography: in Alcohols as motor fuels, Warrendale PA SAE, 1980.

22 POWELL T, "Racing experiences with methanol and ethanol based motor-fuel blends", SAE No 750124, Feb 24-28, 1975, Detroit.

23 REED TB, "Advantages of neat and blended operation of methanol in vehicles", 1974 Eng Foundation Conf, "Methanol as an alternative fuel", Henniker NH, July 7-12, 1976.

24 GRIBBLE NR, Internal report, Department of Chemical Engineering, University of Aston, 1984.

25 Federal Ministry of Research and Technology, Bonn, 1974, on the trial of new fuels - Alternative fuels for motor vehicles", Translation from German, Gersbach & John Verlag, Munich, UCRL-Trans 10879, 2974.

26 EBERSOLE GD & MANNING FS "Engine performance and exhaust emissions: MeOh vs Isoctene", SAE Paper 720692, August, 1972.

27 PETLEY RK, "Methanol/gasoline blends - university viewpoint", Paper at 1974 Eng Foundation Conf, "Methanol as an alternative fuel", Henniker NH, July 7-12, 1974.

28 DAHL RW, "Methyl fuel from remote gas sources", Am Inst Chem Eng, South California, 11th Annual Tech meeting, LA, April 16, 1974.

29 Technical Data on Fuel, 5th Ed, 1955. World power conference, British National Committee.

30 PLEETH SJW, 1949, "Alcohol a fuel for internal combustion engines", Chapman & Hall, London.

31 STULL DR, "Vapour pressure of pure substances - organic compounds" Ind & Eng Chem, 39 (1947), 517-40.

32 SVAHN LG GOERAN "Specifications of alcohol motor fuels", Symp Alcohols Fuel Tech, 4th, 1980

33 TERZONI G, PEA R, & ANCILOTTI F, "Improvement of water tolerability of methanol/basoline blends", 3rd Int Symp Alcohols Fuels Tech, California, May 1979.

34 COX F, "The physical properties of gasoline/alchols automotive fuels", 3rd Int Symp Alcohols Fuels Tech, California, May 1979.

35 ROTHMAN H, GREENSHIELDS R & CALLE FR, "The alcohol economy: Fuel Ethanol and the Brazillian Experience", Frances Pinter Publishers London, 1983.

36 INGAMELLS JC, & LINDQUIST RH "Methanol as a motor fuel or a gasoline blending component", SAE paper 750123, Automotive Eng Congress, Michigan, Feb, 1975.

37 GRANGER K, & ROBERTA J, "Development of experimental vehicles for methanol fuels", Symposium on chemistry of oxygenates in fuels. American Chemical Soc, Kansas City meeting, 12-17 Sept, 1982.

38 WANDERLEY VG, BASTIN SM, WEALER S, & ULLER L, "Corrosivity of some metallic materials in fuel alcohol and type C1 gasoline", Corrosion Lab, INT/FTI, 1981.

39 MARINO L, CHINKOVIC OR, & SPINELLI D, "Corrosion in alcohol medium of materials used in automotive vehicle fuel tanks", EESC/USP.

40 TANAKA DK, & WOLYNEX S, "Analysis of corrosion in engines and in fuel of exhaust systems in alcohol fuel powered vehicles", IPT.

41 PINTO FBP, "Aspects of the design, development and production of ethanol powered passenger cars", IV International Symp, Alcohol Fuels Technology, Guarja, Brazil, 1980.

42 KING ET & CHUI GK "Hardware effects on the wear of methanol fueled engines", SAE Paper 84/377 SAE

43 NAEGELI DW, YOST DM, & OWENS EC, "Engine wear with methanol fuel in a nitrogen-free environment", SAE Paper 841374, Fuels and Lubricants, Maryland, 1984.

44 ERNST RJ, PEFLEY RK, & WIENS F, "Methanol engine durability", SAE paper 831704, Fuels and Lubricants, California, 1983.

45 HURN RW, ALLSUP JR & ECCLESTON BH, "Characteristics of methanol as internal combustion engine fuel", 10th Intersoc Energy Conversion Eng Conf Newmark, 1975

46 DAVIS GC & DOUTHIT WH "The use of alcohol mixtures as gasoline additives", 1980 NPRA Annual meeting, 1980 New Orleans

47 CHUI GK & NICHOLAS RJ "Development of experimental vehicles for methanol fuels", Symposium on Chemistry of Oxygenates and Fuels, American Chemical Soc, Kansas City meeting, Sept 12-17, 1982.

48 CHUI GK & MILLARD DHT, SAE Paper 811203 (1981).

49 NAKAZUCHI NK, KELLER JL, "Methanol fuel modification for highway vehicle use", Report No ALO-EY-76-C-04-363-31, US Dept of Energy, 1979.

50 PERRY & CHILTON "The Chemical Engineers Handbook" 5th Ed, McGraw-Hill, Kogakusha Ltd, Tokyo, 1973.

51 PEFLEY RK et al "Characteristics and research investigations of methanol and methyl fuels" Final Report, Uni of Santa Clara, Aug 1977

52 BERNHARDT WE et al, "Recent progress in automotive alcohol fuel application", Volkswagen AG, Wolfsburg, FRG. 4th Int Symp on Automotive Fuel Systems (NATO/CCMS) Washington DC, April 1977.

53 BERNHARDT WE "Methanol fuels in automobiles", Experience at Volkswagen, IVA Energy Symp, June 1980, Stockholm

54 Engine Manufacturers Association, SAE Publication 820261, SAE Trans, 1982, Section 1, Vol 91.

55 BERNHARDT WE, "The use of methanol and ethanol for motive power", Volkswagen Wolfburg, Bioenergy 84, Vol 1, Proc Int Conf on bioenergy, Swedish Fair Centre, June, 1984.

56 MENRAD H, DECKER G, WEIDMANN K, "Alcohol fuel vehicles of Volkswagen, SAE 820968, 1983.

57 NEBLON J, O'MEARA R, PEFLEY R, & DIVACHY R, "The development and application of kits to convert a vehicle fleet to neat alcohol", 5th Int Symp, May 1982, Auckland, New Zealand, C4-10, pp 3-59 - 3-65.

58 MENRAD H, LEE W & BERNHARDT WE, "Development of a pure methanol fuel car", SAE Paper 770790, "Passenger car meeting", Detroit, Michigan, Sept 1977.

59 BRINKMAN ND, "Ethanol fuel - a single-cylinder engine study of efficiency and exhaust emissions", SAE Paper 810345.

60 MENRAD AK, & LOECH H, "Results from basic research on alcohol powered vehicles", Int Symp on Alcohol Fuels Tech, 4th 1980, Vol 2, Guarja, Brazil, 1980.

61 STOCKWEL, "Auto mechanics fundamentals", South Holland IL: The Good Heart Wilcox Company Ltd, USA, 1969.

62 NAKAZUCHI NK, & KELLER JL, "Methanol fuel modification for highway vehicle use", Report No ALO-EY-76-C-04-363-31, US Dept of Energy, 1979.

63 NTIS/CONF/771175. Proceedings: Int Symp on Alcohol Fuel Technology - Methanol and Ethanol, Nov 21-23, 1977, Germany.

64 BRINKMAN ND, GALLAPOULOUS NE & JACKSON, MW. General Motors Corporation; Research Laboratory, SAE Tech Paper 75 0420, 1975

65 OWENS EE, Southwest Research Institute, Army Fuels Lubricants, Research Laboratory, Proc Int Symp Alcohol Fuel Tech Methanol Ethanol Conf, 771175 (1978).

66 PEFLEY RK, NEBOLON J & ALDEMAN H, University of Santa Clare (California) Mech Eng Dept, SAE Spec Publ SP471, 1980

67 BYKOWSKI BB, Southwest Research Institute, San Antonia Ind Eng Chem Prod Rec Dev, 1981, 20(4), 726-34 (Eng)

68 MARTIN GB, US Environmental Protection Agency, Ind Environmental Research Lab, Energy Assessment and Control Division, Combustion Research Branch, 1983 - continuing ...

69 WIGG EE, Exxon Research and Development Co, Science 1974, 186 (4166), 785-305 (Eng)

70 REED TB, LERNER RM, HINKLEY E & FAHEY RE, Lincoln Laboratory Massachusettes Inst of Tech, Science, 1973, 182 (4119) 1299-305 (Eng).

71 MOST WJ & LONGWELL JP, Exxon Corp Research Laboratories, SAE Tech Paper 750119, 1975.

72 ALLSUP J, US Dept of Energy, Energy Tech Center, Bartlesville, OH, SAE Tech Paper 750763, 1975

73 HARRIS W & DAVISON RR, Texas A&M University, Dept of Chem Eng, Encycl Chem Processes Des 1977, 2, 340-56.

74 KEMPEN WH "Engines run well on alcohols", Hydrocarbon Processing, Feb 1980, pp72-75

75 KELLER JL "Alcohols as motor fuels", Hydrocarbon Processing, Vol 58, No 5, May 1979, pp127-138

76 SCHELLER W, Dept Chem Eng, Univ of Nebraska, US, Arg Res Survey West Reg, 1974, ARS-W-19, 36-42 (Eng)

77 BERNHARDT WE "Engine performance and exhaust emission characteristics for methanol fueled automobile", Symposium "Future Auto Fuels Prospects", General Motors Technical Centre, Mitchigan, Oct 6-7 1975

78 BRINKMAN ND "Effect of compression ratio on exhaust emission and performance of a methanol fueled single cylinder engine". Submitted to SAE passenger car meeting, Detroit September 26, 1977

79 ALLSUP JR "Experimental results using methanol and methanol gasoline blends as automotive engine fuel", BERC/RJ-76/15 January 1977

80 DOE HCP/M2923-01. "Status of alcohol fuels utilisation technology for highway transportation". Muller Associates Inc, US DOE, June 1978.

81 NIERHAUVE B, "Driveability testing of cars adapted to methanol fuels in Germany", Aral Research Centre, Bochum, W Germany, 1982.

82 QUADFLIEG H, "M-100 Research and fleet tests in the German Federal alcohol fuels project".

83 "Gasoline test vehicles", Interim report prepared by Bartlesville, Energy Research Centre, MS, DOE, Aug, 1977.

84 BRINKMAN ND, "Ethanol fuel - a single-cylinder engine study of efficiency and exhaust emissions", SAE Paper 810345.

85 HAEGAN-SMIT AJ & FOX M M, "Automobile exhaust and ozone formation", Paper No 421, presented January 1955 at SAE Annual Meeting.

86 LARSON GP, CHIPMAN JC & KAUPER EK, "Prohibition and effects of automotive gases in Los Angeles", Paper No 420 presented January 1955 at the SAE Annual Meeting.

87 WENTWORTH JT & DANIEL WA, "Flame photographs of light load combustion point the way to reduction of HC in exhaust gas", Paper No 425 presented January 1955 at SAE Annual Meeting.

88 SHINN JA & OLSON DR, "Some factors affecting unburned HC in engine combustion products", Paper No 146, presented June 1957 at SAE Summer Meeting.

89 ROUNDS FG, BENNET PA & NEBEL GJ, "Some effects of engine-fuel variables on exhaust-gas HC content", SAE Trans Vol 63 (1955), 602-619.

90 WENTWORTH JT, "Carburettor evaporation losses", Paper No 12B presented January 1958 at the SAE Annual Meeting.

91 JACKSON MW, WIESE WM & WENTWORTH JT, "The influence of A/F ratio, spark timing, and combustion chamber deposits in exhaust HC emission", Paper No 486A presented March 1962 at the SAE National Automobile meeting.

92 DANIEL WA & WENTWORTH JT, "Exhaust gas hydrocarbons - Genesis & Exodus", Paper No 486B presented March 1962 at the SAE National Automobile meeting.

93 HAGEN DF & HOLIDAY GW, "The effects of engine operating and design variables on exhaust emissions", Paper No 486C presented March 1962 at the SAE National Automobile meeting.

94 NEBEL GJ, "Automobile exhaust gas treatment - an industry report", Paper No 173 presented August 1957 at the SAE National West Coast meeting.

95 CHANDLER JM, SMITH AM & STRUCK JH, "Development of the concept of non-flame exhaust gas reactors", Paper No 486M presented March 1962 at the SAE National Automobile meeting.

96 FAITH WL, "Methods and devices for controlling the HC content of automobile exhaust gases", Paper presented at SAE Seminar on Fuels and Laboratories, April 1955.

97 CANNON WA, HILL EF & WELLING CE, "Single cylinder engine tests of oxidation catalysts", Paper No 174 presented at the SAE National West Coast meeting August 1957.

98 NEBEL GJ & BISHOP RW, "Catalytic oxidation of automobile exhaust bases", Paper No 29R presented at the SAE Annual Meeting, January 1959.

99 VANDERVEER RT & CHANDLER JM, "The development of a catalytic converter for the oxidation of exhaust hydrocarbons", Paper No 295 presented at the SAE Annual Meeting, January 1959.

100 CANNON WA &WELLING CE, "The application of Vanada-Alumina catalyst for the oxidation of exhaust hydrocarbons", Paper No 29T presented at the SAE Annual Meeting, January 1959.

101 RIDGWAY SL, "Homogenous reaction kinetics and the afterburner problems", Paper No 29U presented at the SAE Annual Meeting, January 1959.

102 FAGLEY WS, SINK MV, & HEINEN CU, "Maintenance & automobile exhaust", Paper No 29V presented at the SAE Annual Meeting, January 1959.

103 CORNELIUS GW, "Approaches to the direct flame afterburner", Paper No 210B Nat West Coast Meeting August, 1960.

104 HOMFIELD MF et al, "The GM catalytic converter", Paper No 486D presented at the SAE National Auto Meeting, March 1962.

105 DAVIS DL & ONISHI GE, "Catalytic converter development problems", Paper No 486F, SAE National Auto meeting, March 1962.

106 YINGST JE et al, "Development of flame type afterburner", Paper No 486G presented at the SAE National Automobile Meeting, March 1962.

107 HULLS TA, MYERS PS & UYENHARA OA, "SI engine operation and design for minimum exhaust emission", Pub SAE Trans Vol 75, 1967.

108 BARTHOLMEW E, "Potentialities of emission reduction by design of induction systems", Paper 661009 presented at the SAE Automobile Eng Congress, Detroit, January 1966.

109 KOPA RD, "Control of Automobile exhaust emission by modifications of the carburation system", Paper No 660114 SAE Automobile Eng Congress, Detroit, January 1966.

110 DOE/HCP/W1737-01. "Comparative automotive engine operation when fueled with ethanol and methanol", Prepared by the University of Santa Clara, University of Miami and EE ECKLAND of the US DOE, May 1978

111 RAJAN S, "Factors influencing cold starting of engines operating on alcohol fuels", 3rd Int Symp Alcohols Tech, California, May 1979.

112 BRINKMAN ND, "Vehicle evaluation of neat methanol compromises among exhaust emissions, fuel economy and driveability", GM Research Laboratory, 4th Int Symp on Automotive fuel Systems (NATO/CCMS), Washington DC, April 1977.

113 JUDGE AW "Modern petrol engines", 3rd Ed, Chapman Hall, 1965

114 MORZAROV, MA. 1959. An investigation on the critical rate of stripping of a film of moisture from the wall of a steam pipe line. Teploenergition No 2, 1950

115 MORZAROV, MA. 1961. On the maximum permissible rate of steam flow through separator. Teploenergition NO 11, pg 60

116 QUANT, FR. 1965. Measurement of some basic parameters in two phase annular flow. AIChemE J 11, 311

117 HEWITT & WALKER, 1963. Flooding an accurated phenomena in falling film flow in a tube AIRE-R 4022

118 HEWITT et al, 1965. Transition in film flow in a vertical tube. Sym on two-phase flow, Exeter, 21-23 June 1965

119 COUSINS et al, 1965. Liquid mass transfer in annular two-phase flow. (Proceedings; Symposium on Two-phase Flow, Exeter, 1965, Vol 2 Paper B4).

120 TRAYSER et al, 1969. Influence on fuel automisation, vaporisation and mixing processes on pollutant emission on motor-vehicle power plant. US Clearing house Fed Sci Tech, Inform PB rep 1969.

121 FINLAY IC, 1967. Heat transfer enhancement by addition of liquid film. Nat Eng Lab, Nature 214(5086), 430 (1967), England.

122 IP Standards for Petroleum and its products, part 1, Methods for Analysis and Testing, 35th Ed, 1976, Applied Science Publishers

123 EVANS UR "The corrosion and oxidation of metals: scientific principles and practical applications", Edward Arnold Publishers Ltd, London, 1976

124 Corrosion causes and control, basic course for Chemical Egnineers, McGraw-Hill Book Inc, 330 West 42nd Street, New York, NY10036

125 ALEXANDER LG and COLDREN CL "Droplet transfer from suspending air to duct walls", Ind & Eng, Vol 43, No 6, pp1325-31, 1951

126 BENSON RS & WHITEHOUSE ND "Internal combustion engines", A detailed introduction to the thermodynamics", Pergamon Press, London, 1979

127 STARKMAN ES, NEWHALL HK & SUTTON RD "Comparative performance of alcohol and hydrocarbon fuels", SAE/PT-80/19, 1980

128 LAVOIE GA , HEYWOOD JB & KECK JC "Experimental and theoretical study of nitric oxide formation in IC engines", Combustion Sci & Tech, 1, 313, 1970

129 ANNAND WJD "Effects of simplifying kinetic assumptions in calculating nitric oxide formation in SI engines", Proc Inst Mech Eng, 188, 431, 1974

130 BENSON RS, ANNAND WJD & BARNAK PC "A simulation model including intake and exhaust systems for a single cylinder four-stroke cycle SI engine", Int J MEch Sci 17 (2), 97, 1975

131 BENSON RS & BRONISH PC "A generalised calculation for an ideal otto cycle with hydrocarbon-air mixture allowing for dissociation and variable specific heats", Int J Mech Eng Ed 4 (1), 49-81, 1976

132 BERNHARDT W & LEE W "Combustion of methyl alcohol in SI engines", 15th Symp on Combustion. The Combustion Inst, 1974

133 ALLSUP JR "Experimental results using methanol and methanol/gasoline blends as automotive engine fuel", Bartleville Energy Research Centre, Jan 1977

134 BRINKMAN ND, GALLOPANLOUS NE & JACKSON M "Exhaust emission, fuel economy and driveability of vehicles fueled with alcohol gasoline blends", SAE 750120, 1975

135 PHILLIPS RA & ORMAN PL "Simulation and combustion in gasoline engine using a digital computer", Advances in Auto Engines, Vol 4, Pergamon Press, Oxford, 1966

136 NEWHALL HK & STARKMAN ES "Direct spectroscopic determination of NO in reciprocating engine cylinders", SAE 670122, 1967

137 GRAVESTOCK RE "Studies in engine simulation", 3rd Int Symp on Auto Engine Testing, London, 1974

138 WOSCHNI G, SAE 670931, 1967

139 NINOMIYA, JAPACA, 20, 314, 1970

140 BOND WD "Quinch-heat intake manifolds for reducing cold engine emissions", SAE 720935, 1972

141 HUGES DW & GANLBURN JR "Economy with reduced exhaust emissions - a simple technique", SAE 760140, 1976

142 "Vapipe" - a simple method of car exhaust emission control", NEL Publication, Scotland, 1976, SAE 760 564

143 MENRAD H "SAP", VW Research Report F2/75-16, Wolfsburg, Germany, 1975

144 LINDSAY R & WILSON JL "Heat pipe vaporisation of gasoline-vapipe", 1st Symp on low pollutant power system development, Michigan, 1973

145 LINDSAY et al "Carburettor heating and heat pipe for vaporising fuel", US Patent 3, 763838, 1973

146 HERNETT JL "Heat pipe early fuel evaporation", SAE 760565, 1976

147 GACKENBACK RE "Materials selection for process plants", Reinhold New York, 1960

148 THRING RH "Another look at alternative fuels", SAE Vol 92, 1 Jan 1984, pp60-64

149 HENTHORNE M "Fundamentals of corrosion", Chem Eng, May 17, 1971

150 HARKER JH "The calculation of equilibrium flame gas compositions". J Inst Fuel, May 1967

151 GAYDON & WOLFHARD "Flames their structure radiation and temperature", Chapman & Gall, 1979, 3rd Ed, 1970

152 INGAMELLIS JC, LINDQUIST RH "Methanol as a motor fuel or a gasoline blending component", SAE Paper No 750123. 1975

153 URLIG HH "Corrosion and corrosion control an introduction to corrosion science and engineering", John Wiley & Sons, New York, 1963

154 FONTANA MG & GREEN ND "Corrosion Engineering", McGraw-Hill, USA, 1978

155 RABALD E "Corrosion Guide", 2nd Revised Edition, Elsevier Publishing Co, New York, 1968

156 ROBBINS JS "Corrosion Inhibitors - Recent Developments", Noyes Data Corporation, New Jersey, 1979

APPENDICES

Table 4.1.1 - Data for Torque for Methanol and Methanol/Gasoline Blends at Stoichiometric Compositions

Alcohol content in blend	Torque kN at RPM					
	1500	2000	2500	3000	3500	4000
10	66.6	69.5	72.8	74.7	76.3	75.7
20	66.6	69.5	72.8	74.7	76.3	75.7
30	65.3	70.0	73.6	75.0	76.8	76.2
40	66.6	69.5	75.2	75.0	77.1	76.2
50	66.6	70.0	75.6	76.6	77.7	77.0
60	66.6	67.0	72.8	74.7	77.1	77.2
70	65.3	69.0	72.0	74.7	75.7	75.7
80	65.4	69.0	72.8	74.7	76.8	76.0
90	65.3	69.5	74.0	74.0	77.1	75.7
100	66.0	69.5	75.2	74.0	78.6	75.5

Table 4.1.2 Data for Brake Power for Methanol and Methanol/Gasoline Blends at Stoichiometric Compositions

	Brake power in kW at RPM					
Alcohol content in blend	1500	2000	2500	3000	3500	4000
10	10.0	13.9	18.2	22.4	26.7	30.3
20	10.0	13.9	18.2	22.4	26.7	30.3
30	9.8	14.0	18.4	22.5	26.9	30.5
40	10.0	13.9	18.8	22.5	27.0	30.5
50	10.0	14.0	18.9	23.0	27.2	30.8
60	10.0	13.8	18.2	22.4	27.0	30.9
70	9.8	13.8	18.0	22.4	26.5	30.3
80	9.5	13.8	18.2	22.4	26.9	30.4
90	9.8	13.9	18.5	22.2	27.0	30.3
100	9.9	13.4	18.8	22.0	27.5	30.2

Table 4.1.3 Data for Indicated Power for Methanol and Methanol/Gasoline Blends at Stoichiometric Compositions

Alcohol content in blend	Indicated power in kW at RPM					
	1500	2000	2500	3000	3500	4000
10	15.2	20.0	25.0	30.0	34.9	39.0
20	15.2	20.0	25.0	30.0	34.9	39.0
30	15.2	20.2	25.5	30.0	35.2	40.0
40	15.5	20.5	25.5	31.0	35.5	44.5
50	17.0	22.5	27.0	33.5	37.5	44.5
60	19.0	24.5	30.0	35.5	41.0	46.5
70	18.9	25.5	31.5	37.0	43.0	49.0
80	18.9	26.1	32.0	39.0	46.0	50.0
90	19.2	25.2	32.5	38.0	45.6	51.0
100	19.5	24.2	32.5	25.6	45.6	47.0

Table 4.1.4 Data for Torque Power for Ethanol and Ethanol/Gasoline Blends at Stoichiometric Compositions

	Torque kN at RPM					
Alcohol content in blend	1500	2000	2500	3000	3500	4000
10	65.3	69.5	72.4	75.0	75.7	75
20	65.3	69.5	72.4	75.0	75.7	75
30	65.3	69.0	72.8	75.3	75.7	75.25
40	66.6	69.0	72.0	75.0	77.1	75.5
50	67.3	70.0	72.0	76.3	75.7	75.7
60	68.6	70.5	73.6	76.0	78.5	75.7
70	69.3	70.0	73.2	76.0	77.1	75.5
80	65.3	70.0	74.0	76.6	77.1	75.5
90	65.3	70.0	73.6	76.0	78.5	75.5
100	65.3	69.0	74.0	76.0	75.7	75.5

Table 4.1.5 Data for Brake Power for Ethanol Fuel Blends at Stoichiometric Compositions

Alcohol content in blend	Brake power in kW at RPM					
	1500	2000	2500	3000	3500	4000
10	9.8	13.9	18.1	22.5	26.5	30.0
20	9.8	13.9	18.1	22.5	26.5	30.0
30	9.8	13.8	18.2	22.6	26.5	30.1
40	10.0	13.8	18.0	22.5	27.0	30.2
50	10.1	14.0	18.0	22.9	26.5	30.3
60	10.2	14.1	18.4	22.8	27.5	30.3
70	10.4	14.0	18.3	22.8	27.0	30.2
80	9.8	14.0	18.5	23.0	27.0	30.2
90	9.5	14.0	18.4	22.8	27.5	30.2
100	9.5	13.8	18.5	22.8	26.5	30.2

Table 4.1.6 Data for Indicated Power for Ethanol Fuel Blends at Stoichiometric Compositions

Alcohol content in blend	Indicated power in kW at RPM					
	1500	2000	2500	3000	3500	4000
10	15.1	19.2	23.9	28.2	33.5	38.5
20	15.1	19.2	23.9	28.2	33.5	38.5
30	15.1	19.2	23.9	28.1	33.2	38.0
40	15.1	19.2	23.6	28.4	33.0	38.2
50	15.4	19.2	23.5	28.4	33.6	38.4
60	15.5	19.2	23.3	28.7	33.5	38.4
70	15.5	19.2	29.5	28.9	33.5	38.8
80	15.0	19.5	24.0	29.1	33.5	38.6
90	14.9	19.5	24.2	29.3	34.5	39.2
100	14.9	19.5	24.9	29.6	34.5	39.2

Table 4.1.7 Data for Mechanical Efficiency for Methanol and Methanol/Gasoline Blends at Stoichiometric Compositions

Alcohol content in blend	Mechanical Efficiency % at RPM					
	1500	2000	2500	3000	3500	4000
10	65.7	69.5	72.8	74.7	74.4	77.7
20	65.7	69.5	72.3	74.7	74.0	77.7
30	64.5	69.3	72.1	75.0	76.4	75.0
40	64.5	67.8	73.7	72.6	76.0	74.7
50	58.8	62.2	70.0	68.7	72.0	75.3
60	52.6	56.3	60.7	63.1	65.8	76.3
70	51.3	54.1	57.1	60.5	61.6	75.5
80	50.1	52.8	56.9	57.4	58.5	78.0
90	51.0	55.2	56.9	58.4	59.2	74.5
100	50.8	55.4	57.8	61.8	60.3	75.7

Table 4.1.8 Data for Mechanical Efficiency for Ethanol and Ethanol/Gasoline Blends at Stoichiometric Compositions

Alcohol content in blend	Mechanical Efficiency % at RPM					
	1500	2000	2500	3000	3500	4000
10	64.9	72.4	75.7	79.8	78.8	77.9
20	64.9	72.4	75.7	79.8	78.8	77.9
30	64.9	71.9	76.2	80.4	79.8	79.2
40	65.8	71.9	76.3	79.2	81.8	79.1
50	65.6	72.9	76.6	80.6	78.8	78.9
60	65.8	73.4	72.9	79.4	80.6	78.9
70	67.1	72.9	77.9	78.9	80.6	77.9
80	65.3	71.8	77.1	79.0	80.6	78.2
90	63.8	71.8	76.0	77.8	79.7	77.0
100	63.8	70.8	74.3	77.0	76.8	77.0

Table 4.1.9 Data for Brake Thermal Efficiency for Methanol and Methanol/Gasoline Blends at Stoichiometric Composition

Alcohol content in blend	Brake thermal efficiency % at RPM					
	1500	2000	2500	3000	3500	4000
10	25.6	26.8	28.0	27.0	29.1	27.5
20	25.6	25.8	28.0	27.0	29.1	27.5
30	22.5	24.2	24.2	25.2	29.1	24.9
40	24.4	26.0	26.2	26.8	28.0	26.8
50	24.2	25.0	25.4	26.5	26.6	27.2
60	23.4	24.2	25.0	27.0	25.1	27.0
70	23.8	23.5	24.5	25.6	25.1	25.8
80	24.0	25.0	26.5	26.9	27.1	28.0
90	24.5	25.5	26.5	26.9	27.1	28.2
100	24.5	26.0	27.9	27.5	28.7	28.8

Table 4.1.10 Data for Thermal Efficiency for Ethanol and Ethanol Gasoline Blends at Stoichiometric Compositions

Alcohol content in blend	Brake thermal efficiency % at rpm					
	1500	2000	2500	3000	3500	4000
10	30.0	28.4	32	29.6	30.0	27.8
20	30.0	28.4	32	29.6	30.0	27.8
30	29.4	28.5	30.5	29.6	28.0	27.8
40	27.8	28.3	28.5	29.5	31.0	27.3
50	27.8	28.2	2.4	29.2	31.6	28.2
60	28.0	28.5	27.9	28.9	31.5	28.5
70	27.0	28.1	27.8	29.2	31.0	29.0
80	26.0	28.1	27.5	29.1	29.8	29.5
90	26.0	27.9	27.4	29.3	30	30.0
100	26.4	27.8	27.4	29.5	29.4	30.5

Table 4.1.11 Data for CO_2 emissions for methanol and methanol/gasoline blends at stoichiometric composition

Alcohol content in blend	CO_2 % in exhaust at RPM					
	1500	2000	2500	3000	3500	4000
10	10.1	10.2	10.2	10.7	11.2	11.0
20	10.2	10.2	10.4	10.7	11.2	11.0
30	10.2	10.2	10.9	10.9	11.2	11.4
40	10.7	10.2	11.6	11.3	11.8	12.2
50	11.2	11.2	11.7	12.2	12.8	12.7
60	11.7	11.3	12.3	12.3	12.9	12.8
70	11.6	11.3	12.1	12.2	12.8	12.6
80	12.1	11.8	12.3	12.6	12.9	13.4
90	12.2	12.7	12.9	13.4	13.8	13.6
100	12.5	12.7	14.2	14.4	15.0	14.8

Table 4.1.12 Data for CO_2 emissions for ethanol and ethanol/gasoline blends at stoichiometric compositions

Alcohol content in blend	% CO_2 in Exhaust at RPM					
	1500	2000	2500	3000	3500	4000
10	8.7	9.4	9.7	9.7	9.8	10.2
20	8.7	9.5	9.8	9.8	9.9	10.3
30	8.8	9.8	10.1	10.6	10.6	11.1
40	10.4	11.5	11.2	11.5	11.4	11.6
50	11.8	12.4	12.0	12.4	12.4	12.5
60	11.8	12.2	11.8	12.4	12.2	12.6
70	11.8	12.7	12.1	13.2	12.1	13.5
80	12.2	12.3	12.5	13.0	12.5	13.1
90	12.1	12.5	12.3	12.8	12.7	12.6
100	12.1	12.4	12.5	12.9	12.7	13.0

Table 4.1.13 Data for CO emissions for methanol and methanol/gasoline blends at stoichiometric compositions

Methanol content in blend	CO % in exhaust at RPM					
	1000	2000	2500	3000	3500	4000
10	7.7	7.2	7.0	6.8	6.5	6.5
20	7.5	6.7	6.9	6.6	6.2	6.4
30	7.4	7.6	6.8	6.7	5.9	6.5
40	7.3	6.8	6.8	6.0	5.6	6.3
50	6.7	6.7	6.1	5.5	5.1	5.7
60	6.3	6.4	5.7	5.4	4.9	5.4
70	6.1	6.2	5.6	5.8	4.7	5.6
80	5.4	5.1	5.2	4.5	4.1	3.8
90	4.4	3.8	3.6	2.9	3.0	2.7
100	3.2	2.1	2.1	1.6	1.7	1.0

Table 4.1.14 Data for CO emissions for ethanol and ethanol/gasoline blends at stoichiometric compositions

Alcohol content in blend	CO % in exhaust at RPM					
	1500	2000	2500	3000	3500	4000
10	7.0	6.0	5.7	5.2	5.0	5.5
20	6.8	6.1	5.5	5.3	4.9	5.2
30	6.7	6.2	5.4	5.4	4.7	5.5
40	6.2	6.0	5.8	5.4	4.6	5.2
50	6.5	6.6	5.7	5.3	5.1	5.0
60	6.2	6.2	5.6	5.6	4.9	4.7
70	5.3	5.0	5.1	5.3	4.6	4.5
80	4.8	4.6	4.4	4.5	3.8	3.8
90	4.2	4.4	4.2	4.0	3.8	3.5
100	3.8	4.0	3.6	3.3	3.1	3.0

Table 4.1.15 Data for HC emission for methanol and methanol/gasoline blends as stiochiometric compositions

Alcohol content in blend	HC (ppm) in exhaust at RPM					
	1500	2000	2500	3000	3500	4000
10	420	370	350	310	320	260
20	400	360	340	300	300	250
30	400	320	310	270	260	250
40	390	310	300	260	250	210
50	370	320	270	250	230	220
60	360	310	280	240	230	220
70	420	300	285	260	270	270
80	420	310	260	270	245	260
90	450	260	230	260	240	280
100	470	250	240	120	180	180

4.1.16 Data for HC emissions for ethanol and ethanol/gasoline blends at stoichiometric compositions

Alcohol content in blend	HC (ppm) in exhaust at RPM					
	1500	2000	2500	3000	3500	4000
10	360	320	280	250	240	250
20	340	300	270	235	230	230
30	330	280	260	230	220	220
40	290	250	220	225	180	180
50	285	240	220	200	160	175
60	280	240	190	175	150	160
70	240	200	170	165	160	150
80	225	185	160	160	140	145
90	220	180	150	165	110	140
100	200	160	130	145	100	110

EFFECT OF F/A RATIO ON Ihp.
ENGINE SPEED:1500 RPM

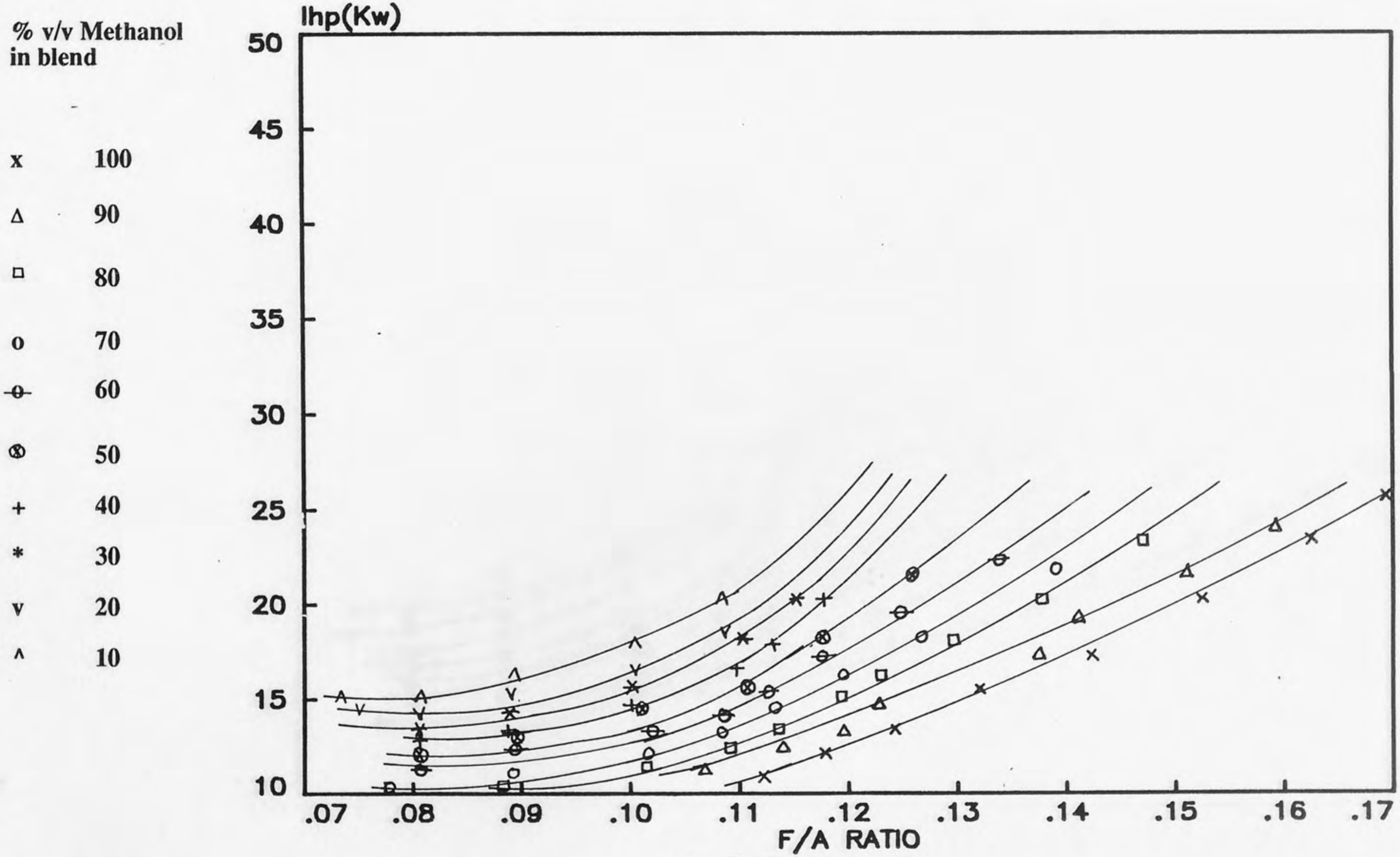

FIG: 4.1.1

EFFECT OF F/A RATIO ON Ihp.
ENGINE SPEED:2000 RPM

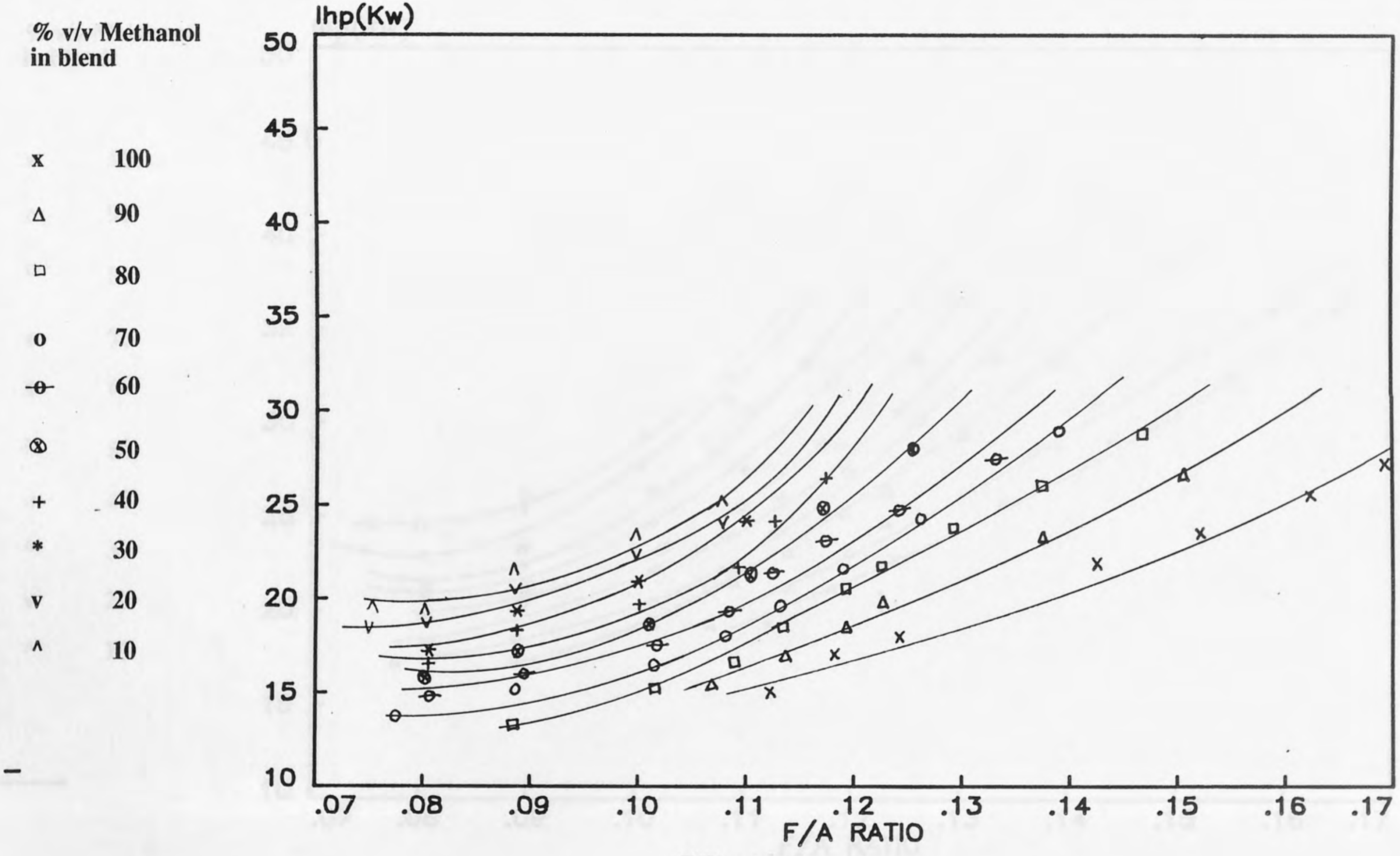

FIG: 4.1.2

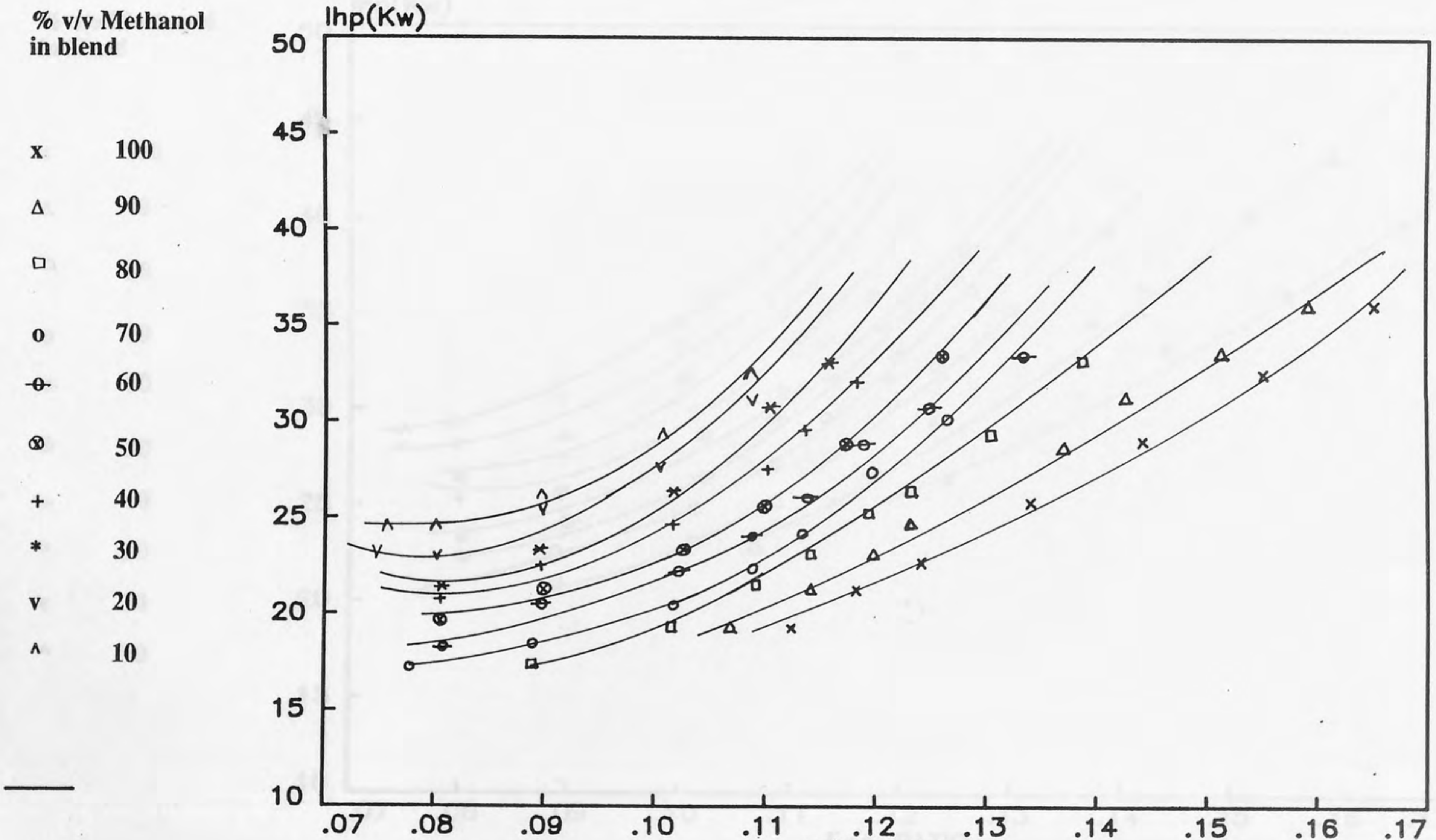
EFFECT OF F/A RATIO ON Ihp.
ENGINE SPEED:2500 RPM

FIG: 4.1.3

EFFECT OF F/A RATIO ON Ihp.
ENGINE SPEED:3000 RPM

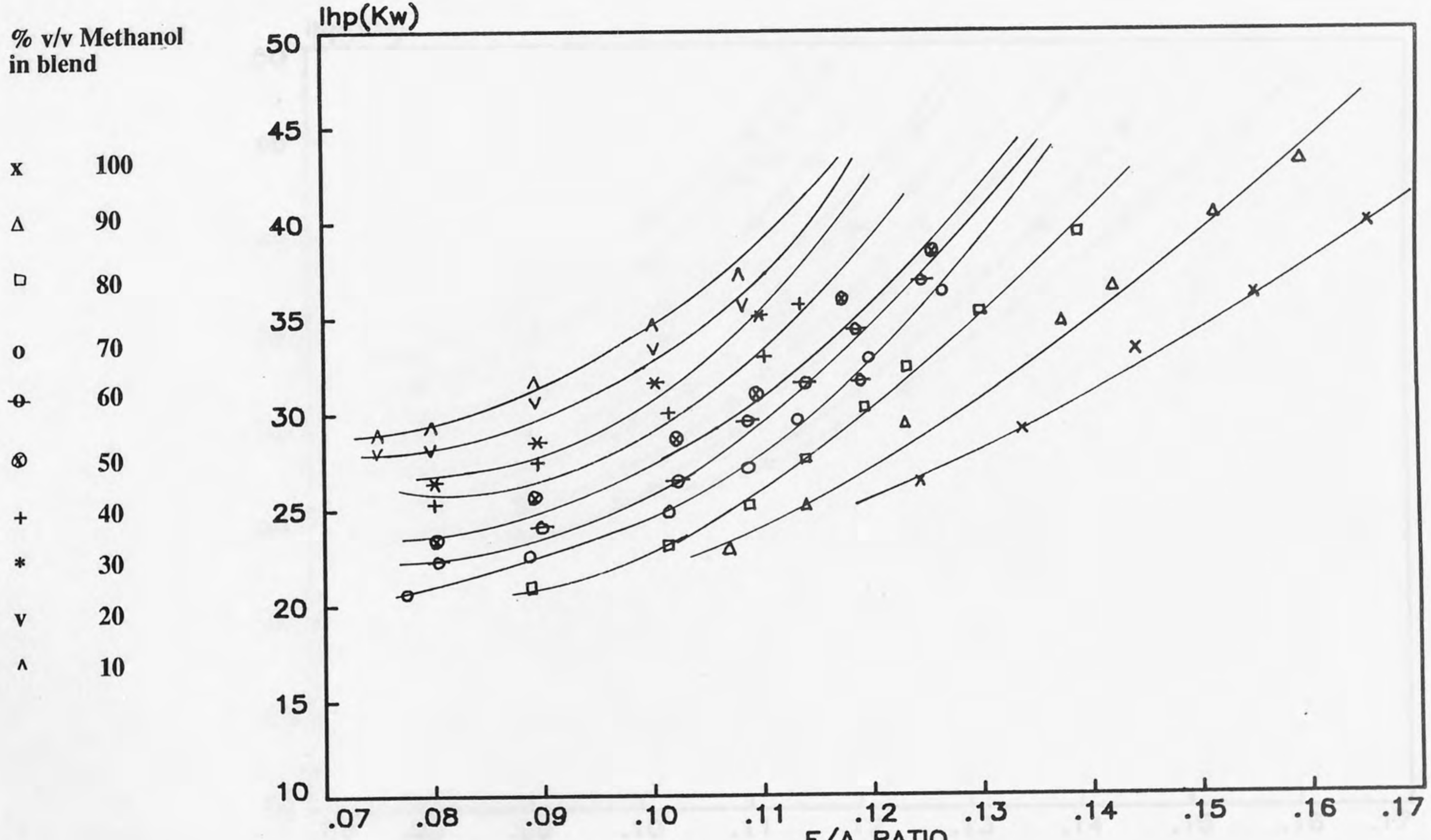

FIG: 4.1.4

EFFECT OF F/A RATIO ON Ihp.
ENGINE SPEED: 500 RPM

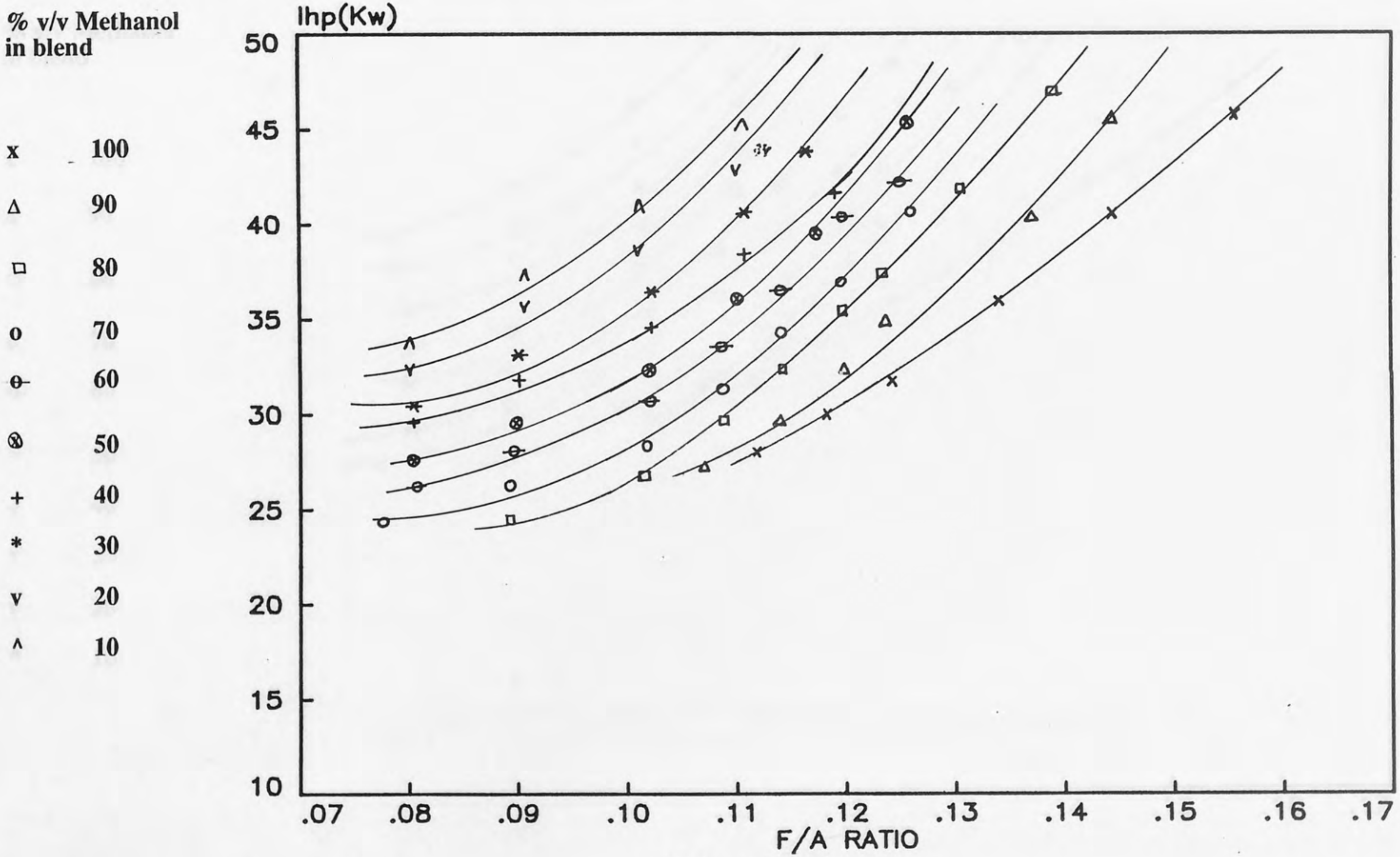

FIG: 4.1.5

EFFECT OF F/A RATIO ON Ihp.
ENGINE SPEED:4000 RPM

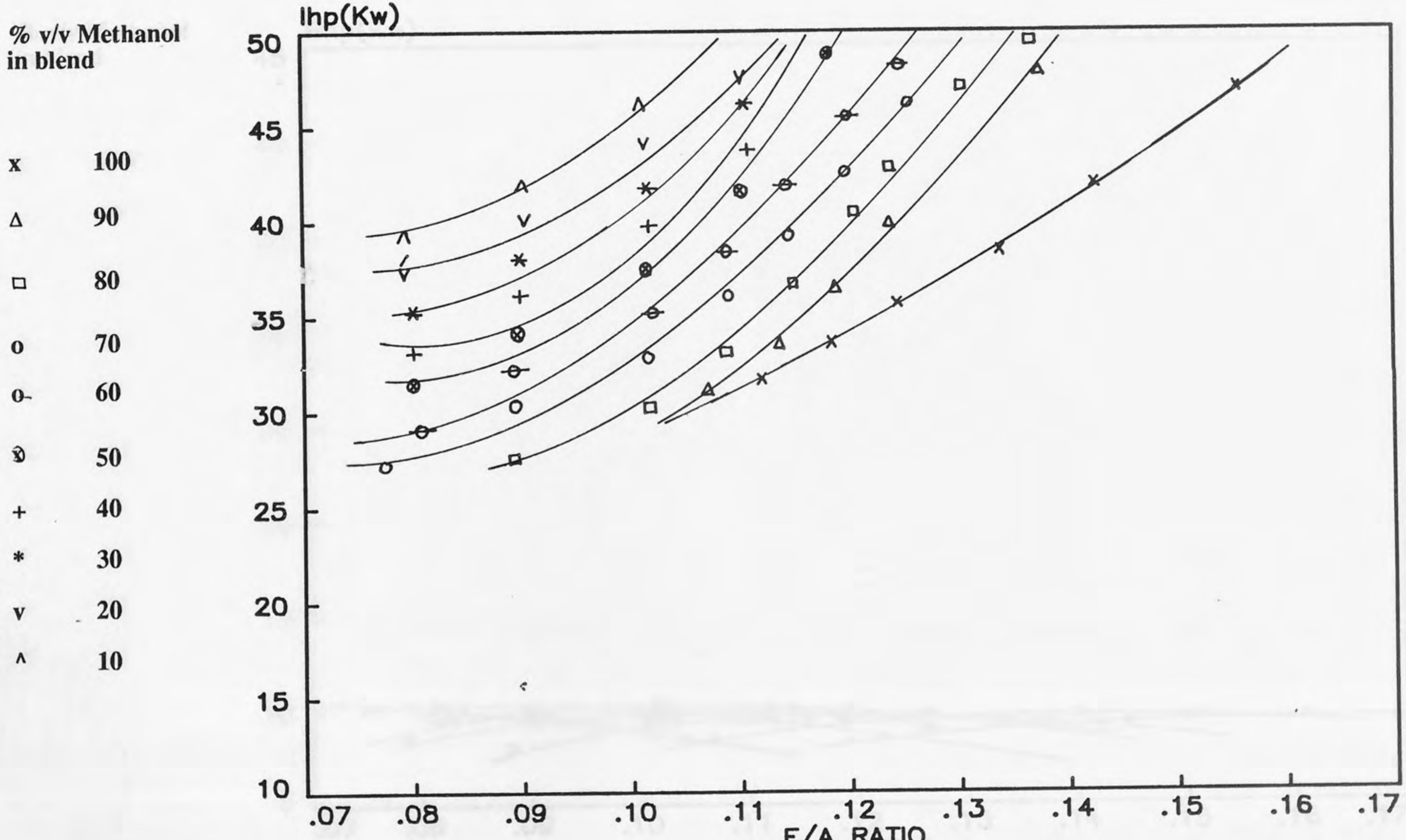

FIG: 4.1.6

EFFECT OF F/A RATIO ON Bhp.
ENGINE SPEED:1500 RPM

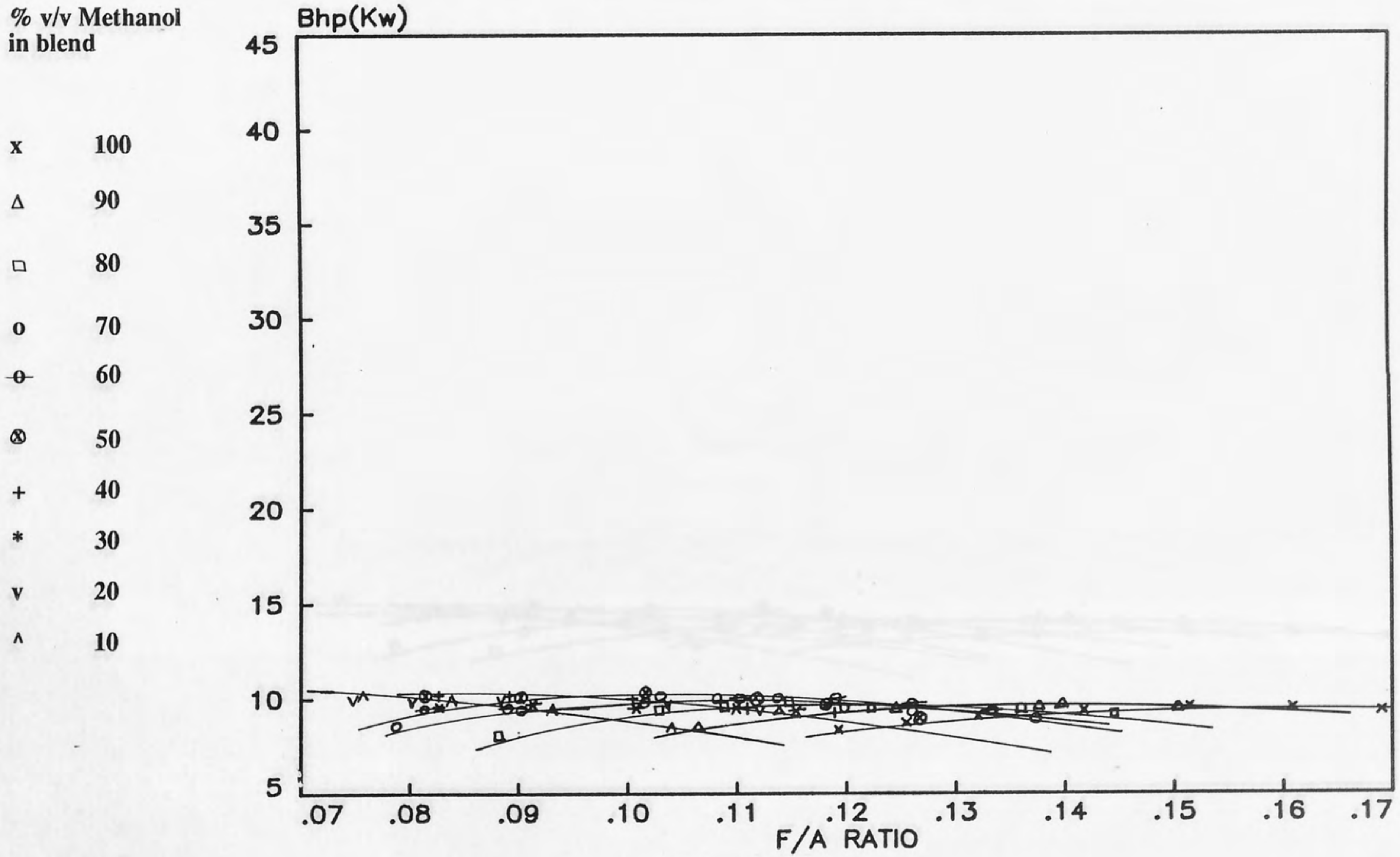

FIG: 4.1.7

EFFECT OF F/A RATIO ON Bhp.
ENGINE SPEED:2000 RPM

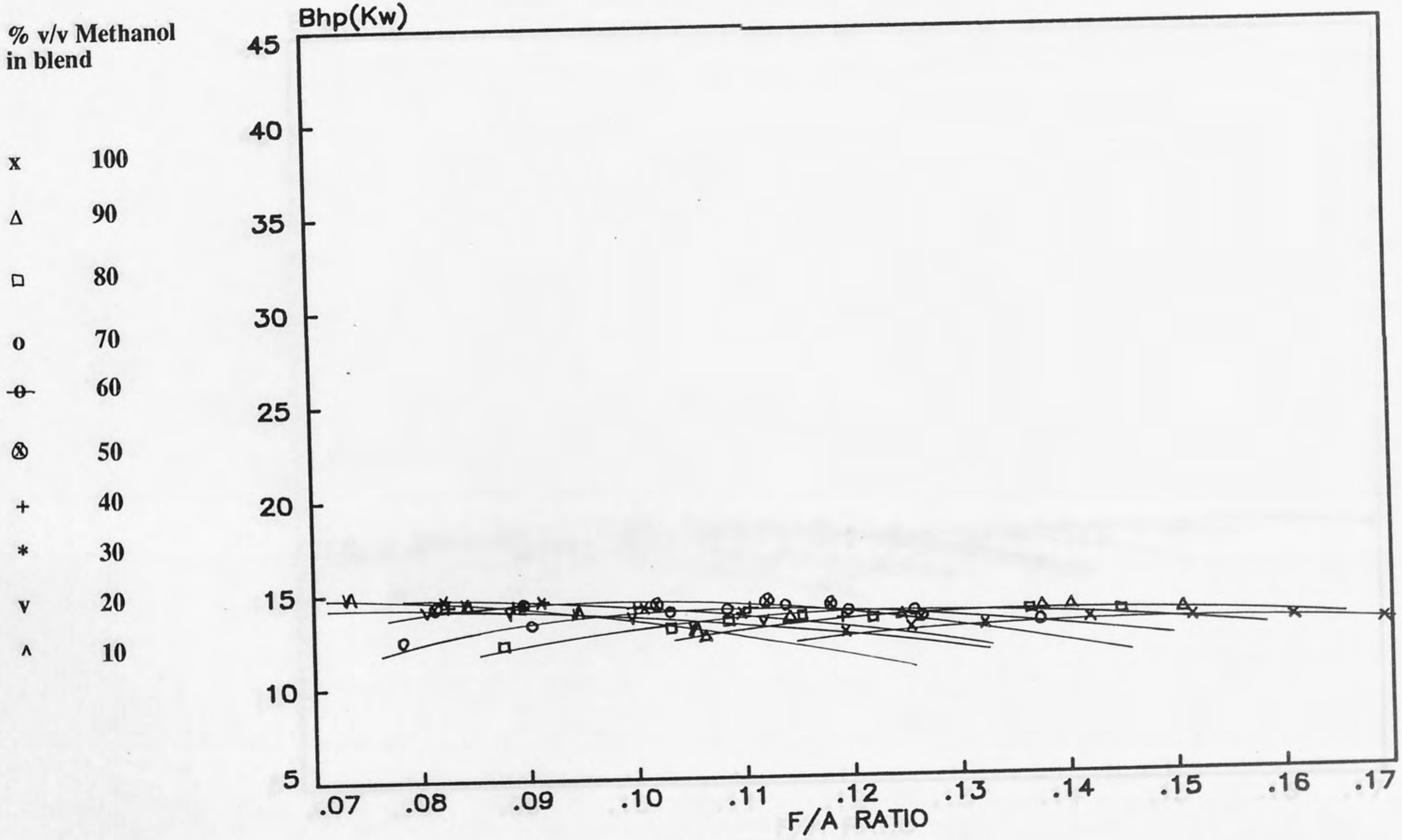

FIG: 4.1.8

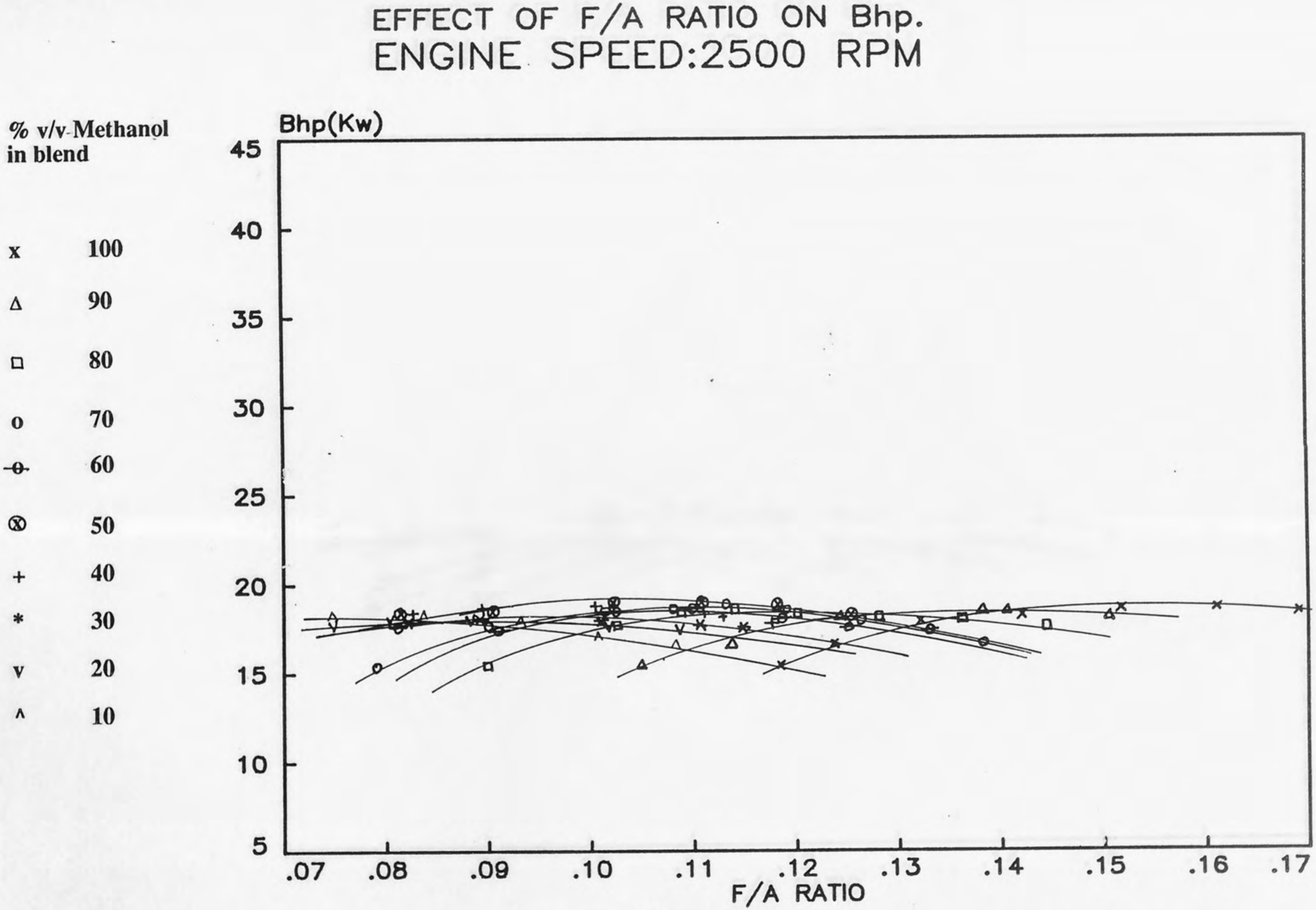
EFFECT OF F/A RATIO ON Bhp.
ENGINE SPEED:2500 RPM
% v/v-Methanol in blend
x 100
Δ 90
□ 80
o 70
-θ- 60
⊗ 50
+ 40
* 30
v 20
^ 10
Bhp(Kw)
45
40
35
30
25
20
15
10
5
.07
.08
.09
.10
.11
.12
.13
.14
.15
.16
.17
F/A RATIO

FIG: 4.1.9

EFFECT OF F/A RATIO ON Bhp.
ENGINE SPEED:3000 RPM

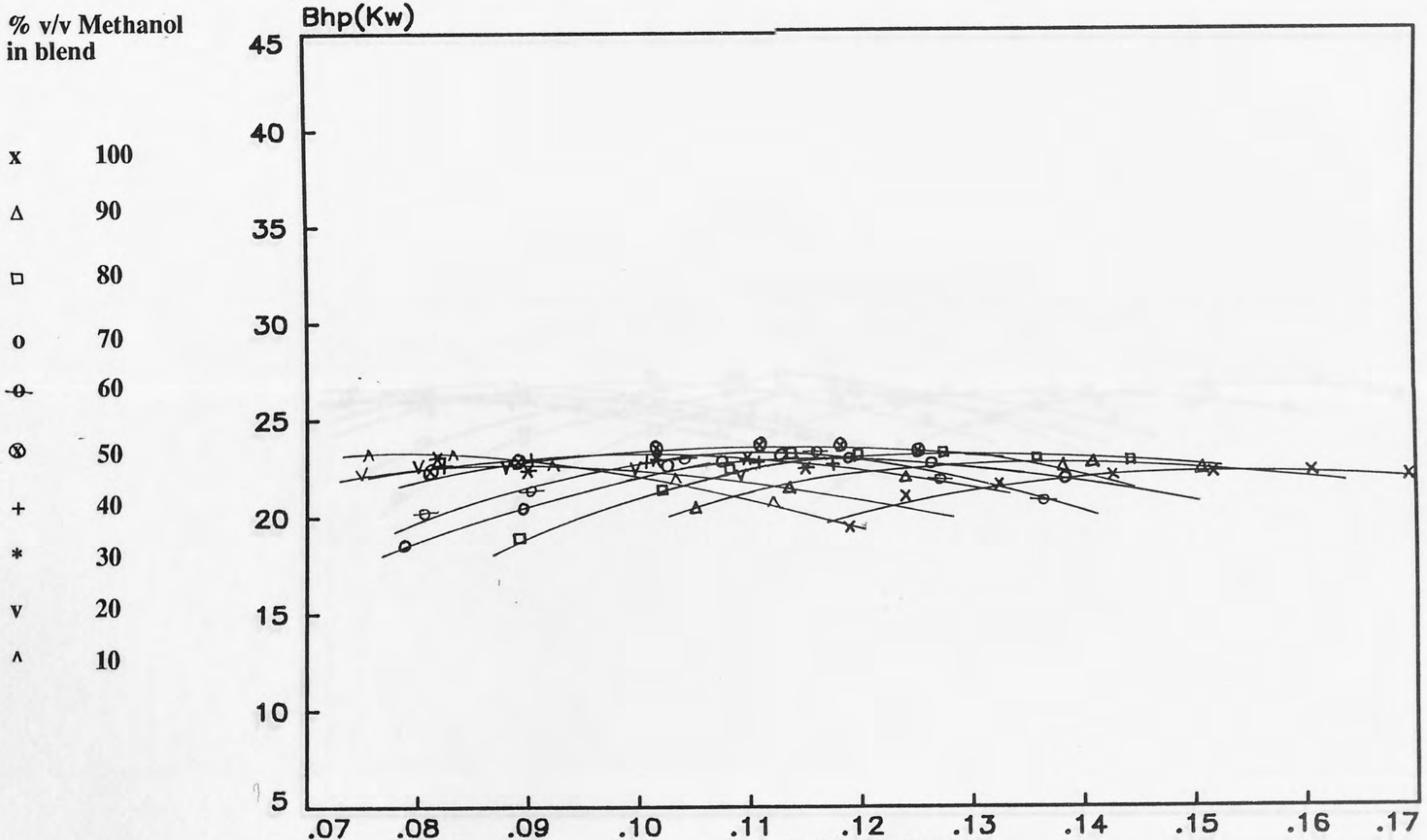

FIG: 4.1.10

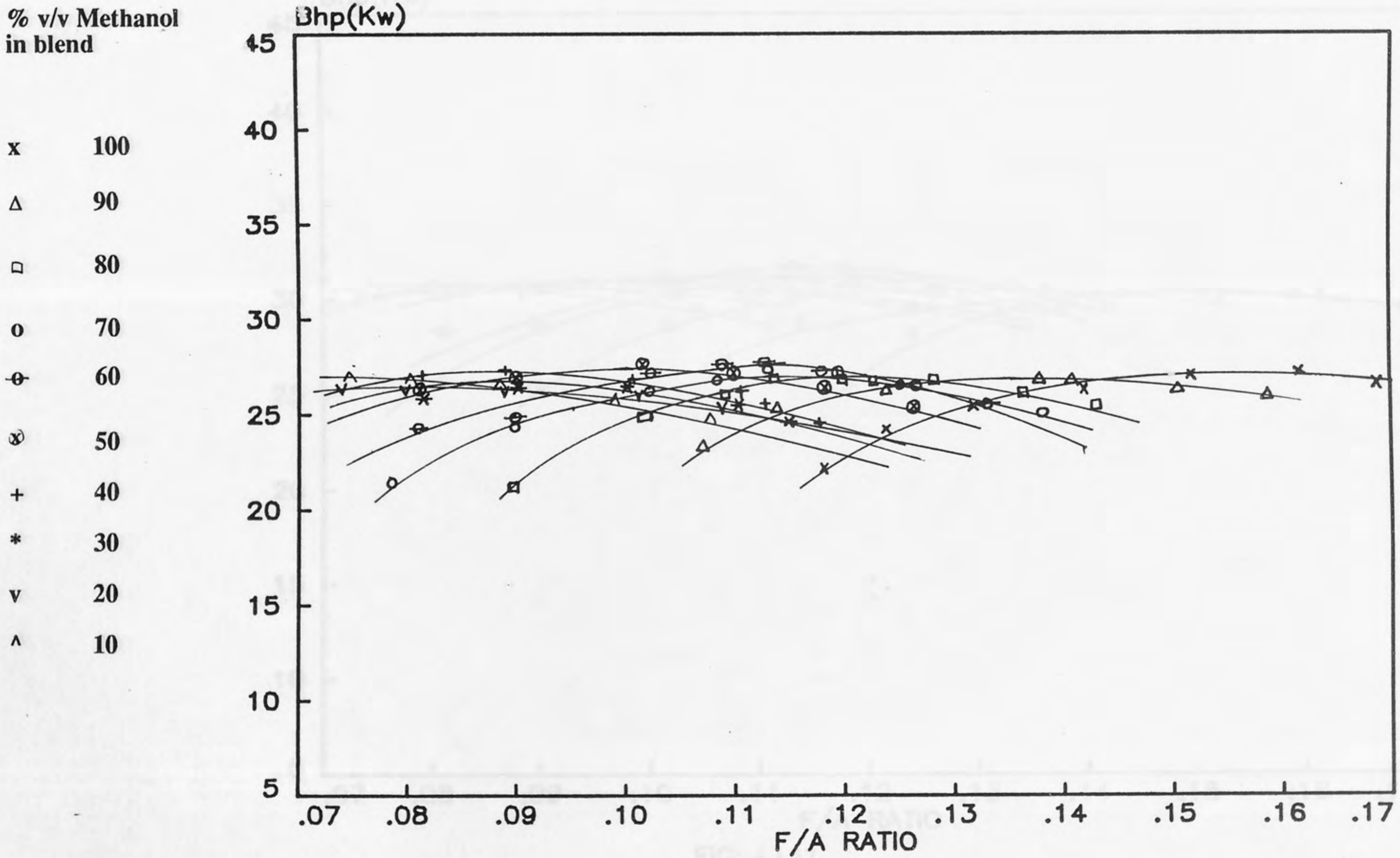

EFFECT OF F/A RATIO ON Bhp.
ENGINE SPEED:3500 RPM

FIG: 4.1.11

EFFECT OF F/A RATIO ON Bhp.
ENGINE SPEED:4000 RPM

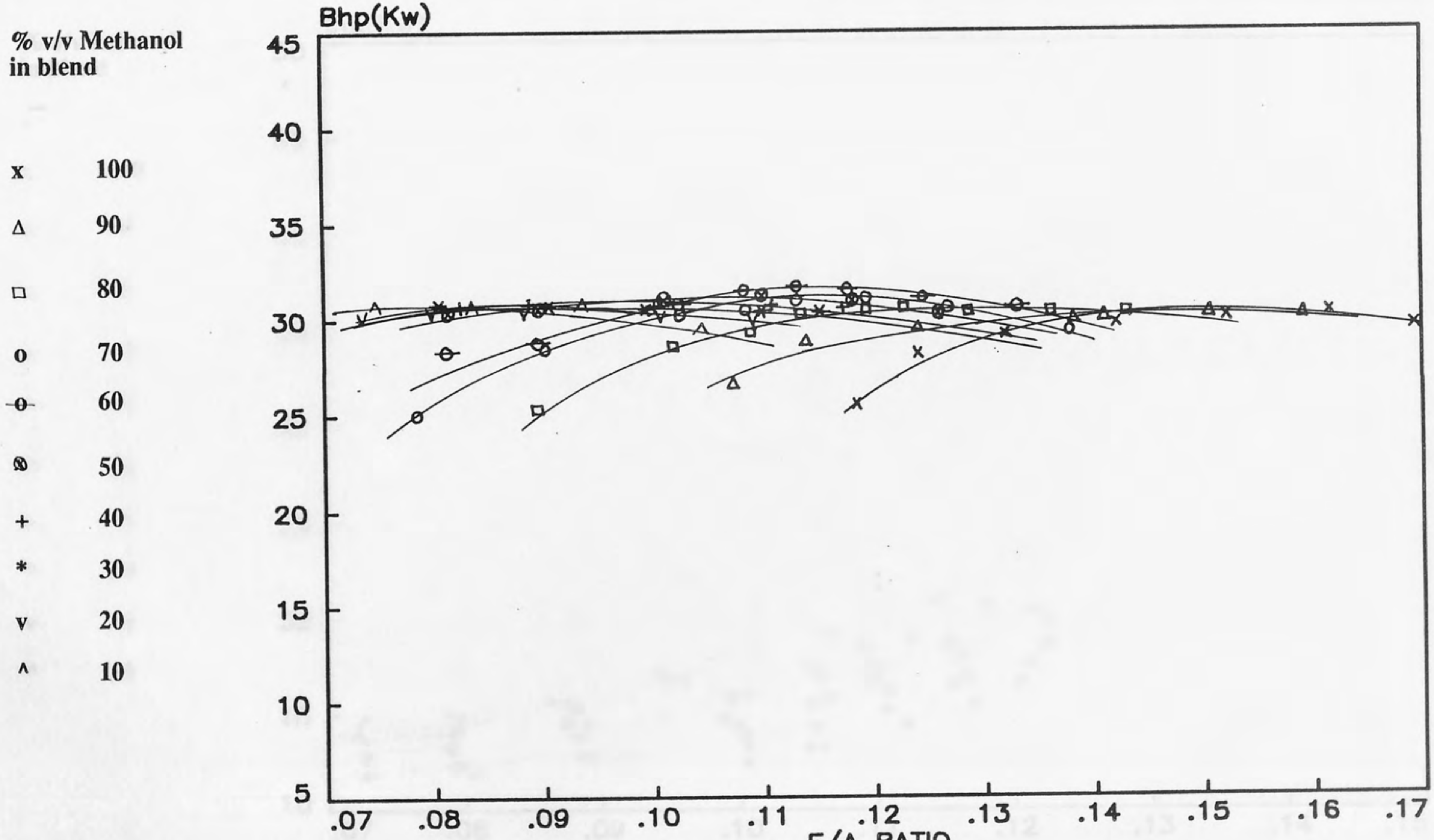

FIG: 4.1.12

EFFECT OF F/A RATIO ON Ihp.
ENGINE SPEED:1500 RPM

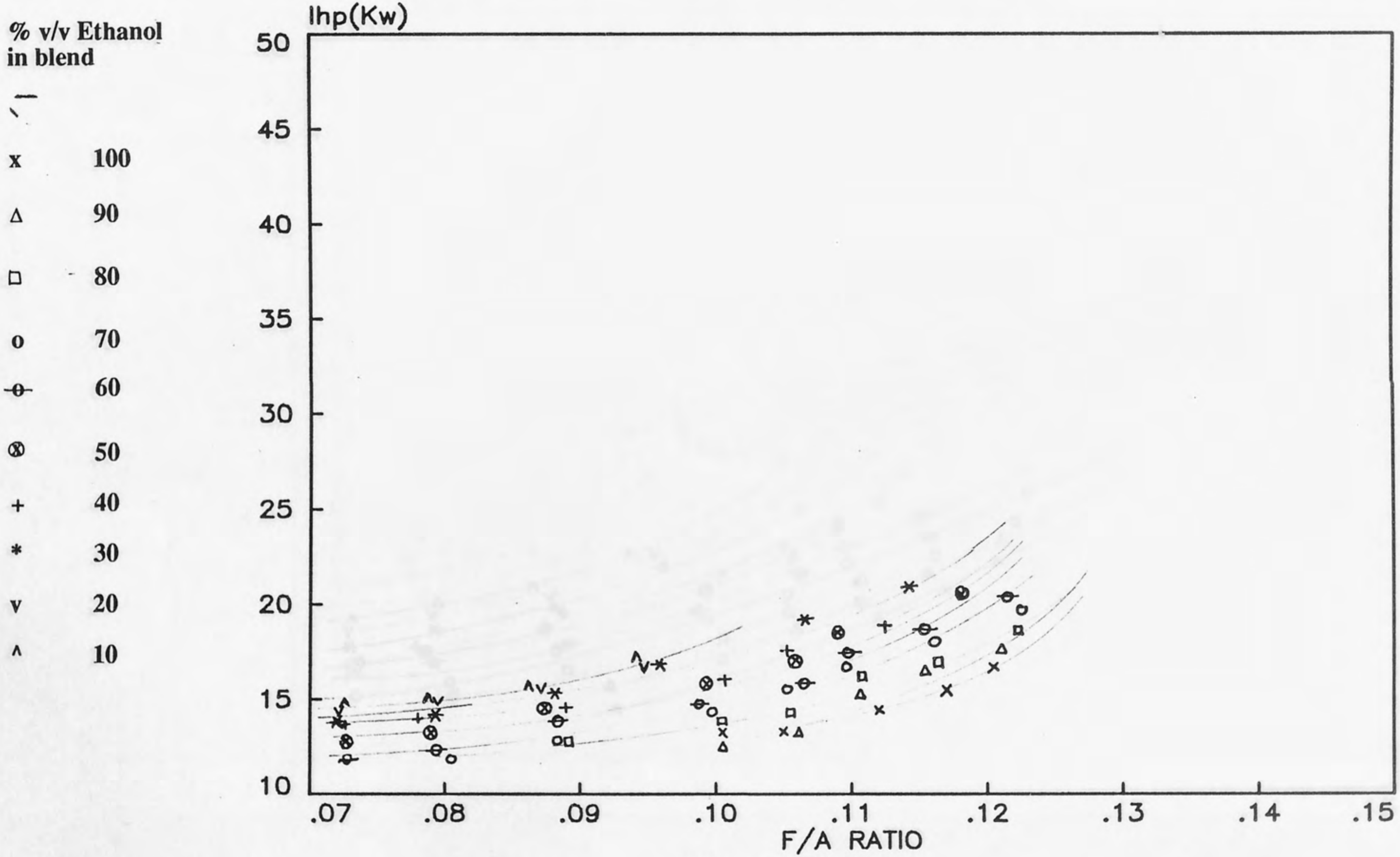

FIG: 4.1.13

EFFECT OF F/A RATIO ON Ihp.
ENGINE SPEED:2000 RPM

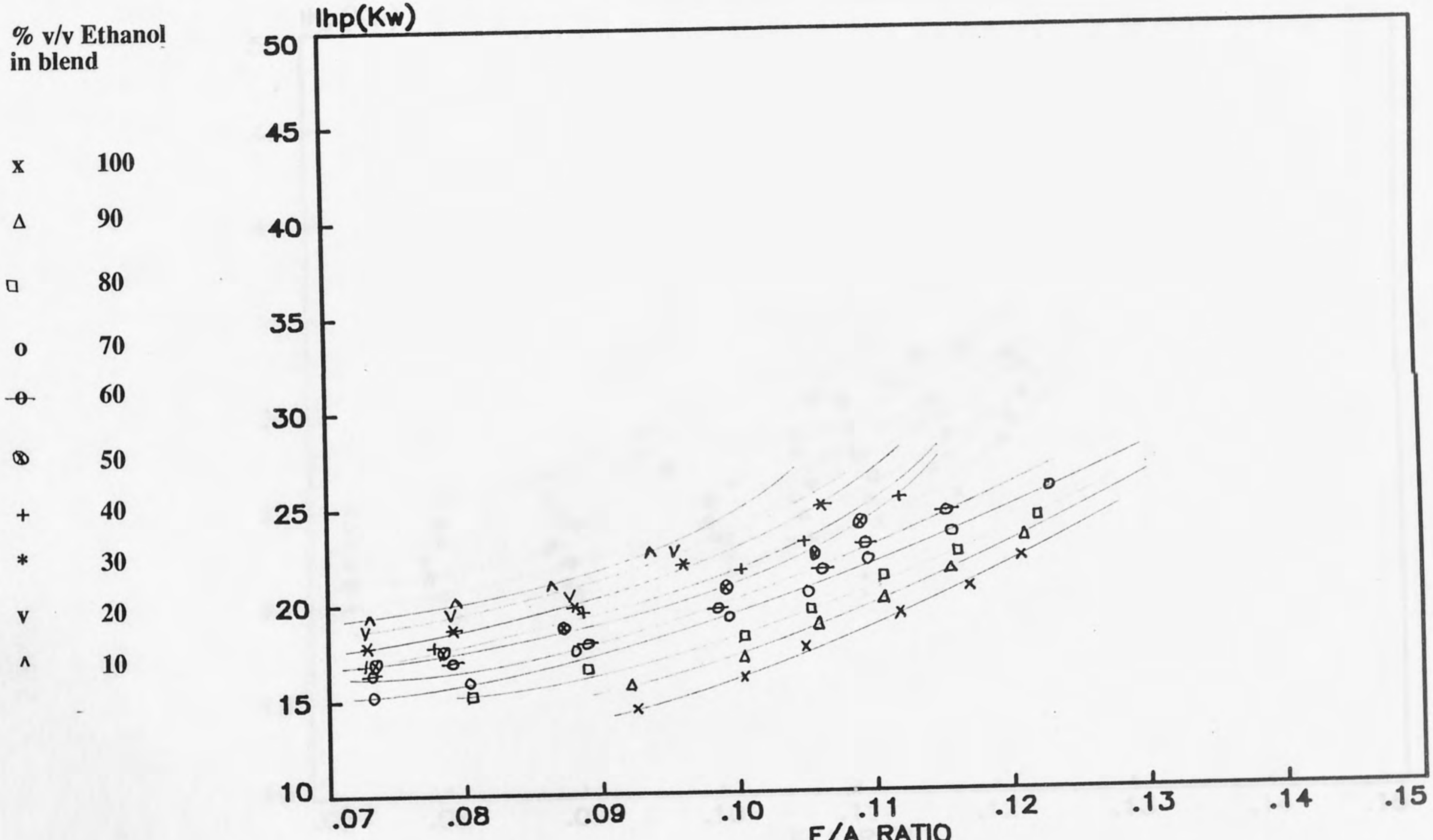

FIG: 4.4.14

EFFECT OF F/A RATIO ON Ihp.
ENGINE SPEED:2500 RPM

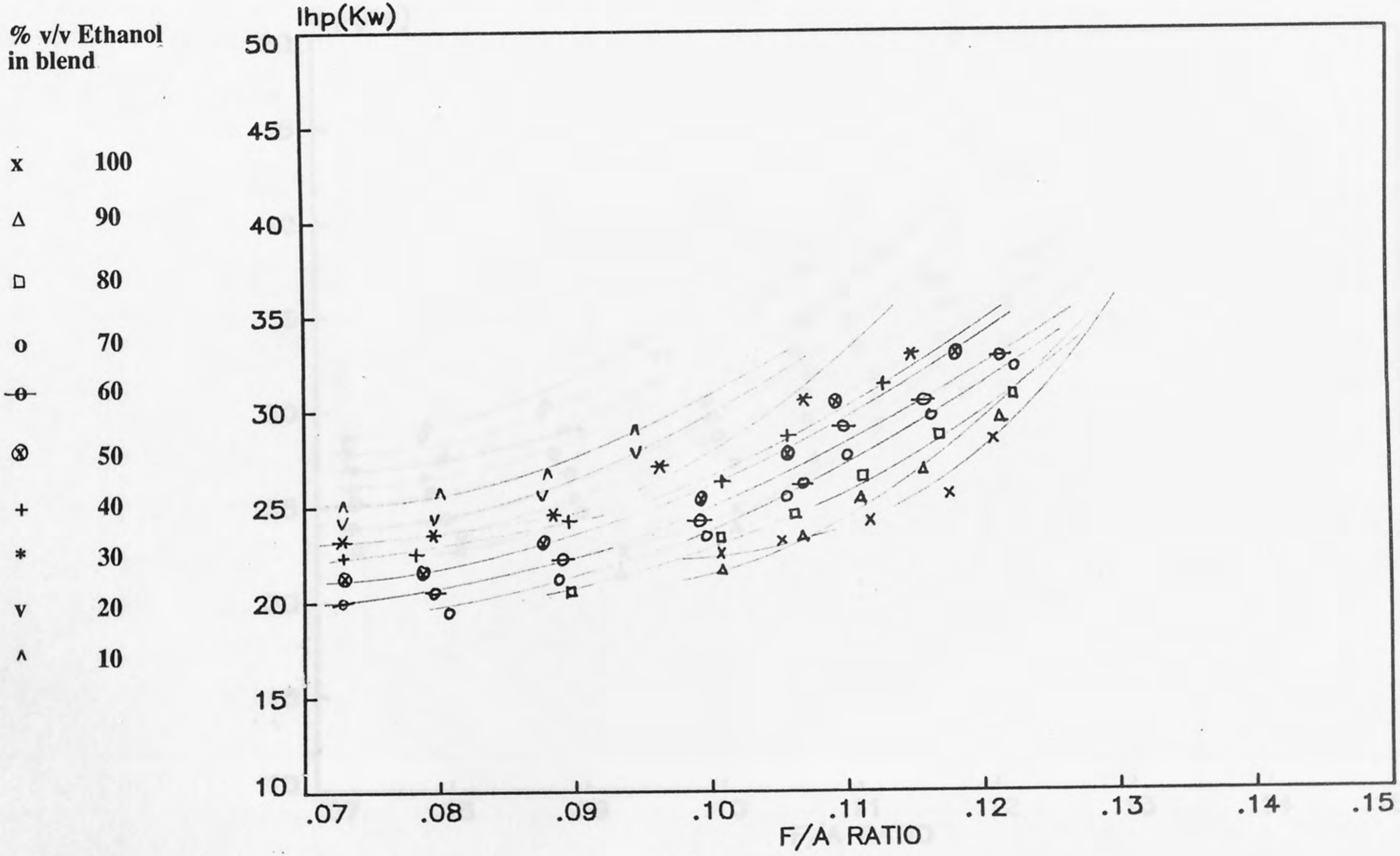

FIG: 4.1.15

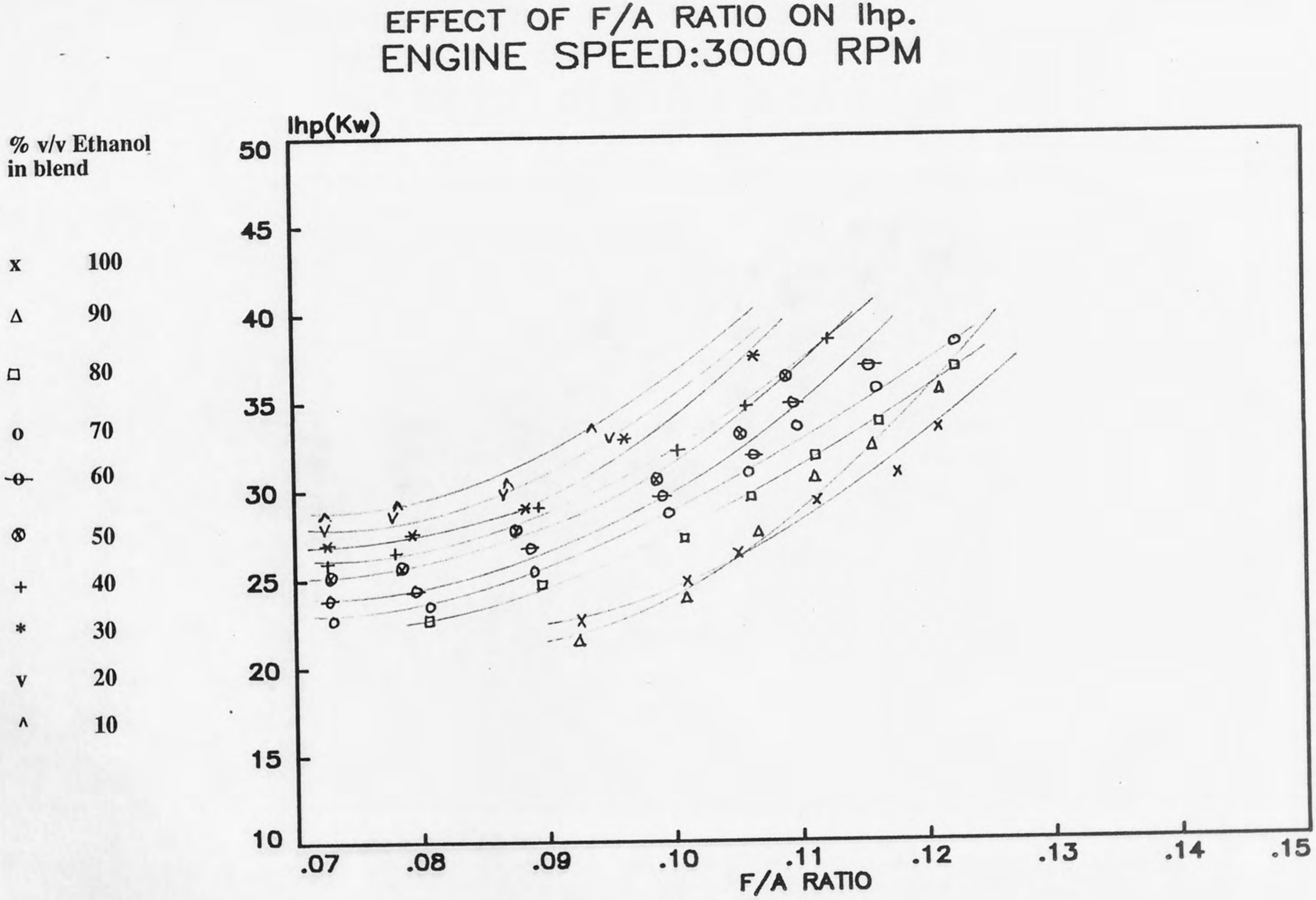
EFFECT OF F/A RATIO ON Ihp.
ENGINE SPEED:3000 RPM
% v/v Ethanol in blend
x 100
Δ 90
□ 80
o 70
-φ- 60
⊗ 50
+ 40
* 30
v 20
^ 10
Ihp(Kw)
50
45
40
35
30
25
20
15
10
.07
.08
.09
.10
.11
.12
.13
.14
.15
F/A RATIO

FIG: 4.1.16

EFFECT OF F/A RATIO ON Ihp.
ENGINE SPEED:3500 RPM

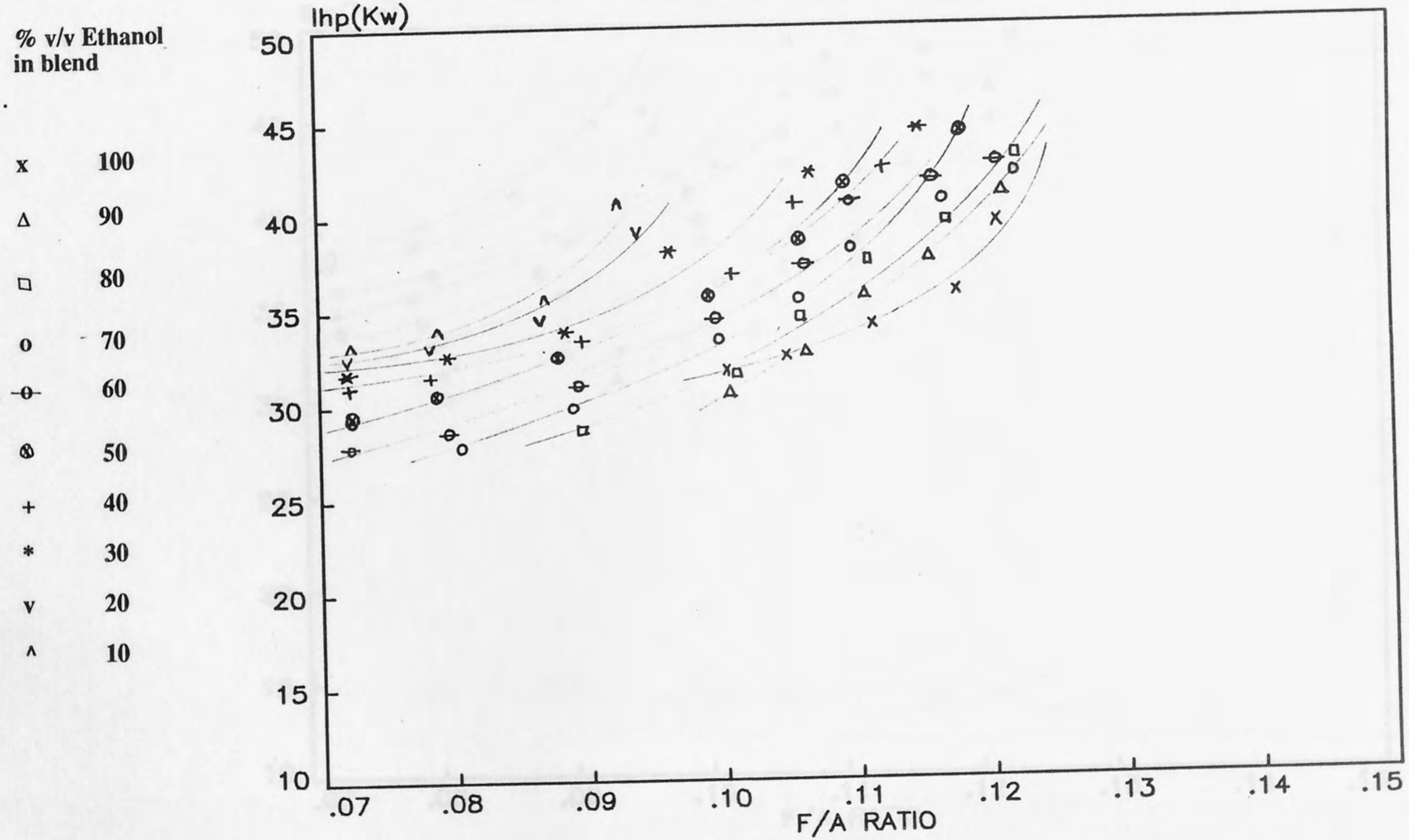

FIG: 4.1.17

EFFECT OF F/A RATIO ON Ihp.
ENGINE SPEED:4000 RPM

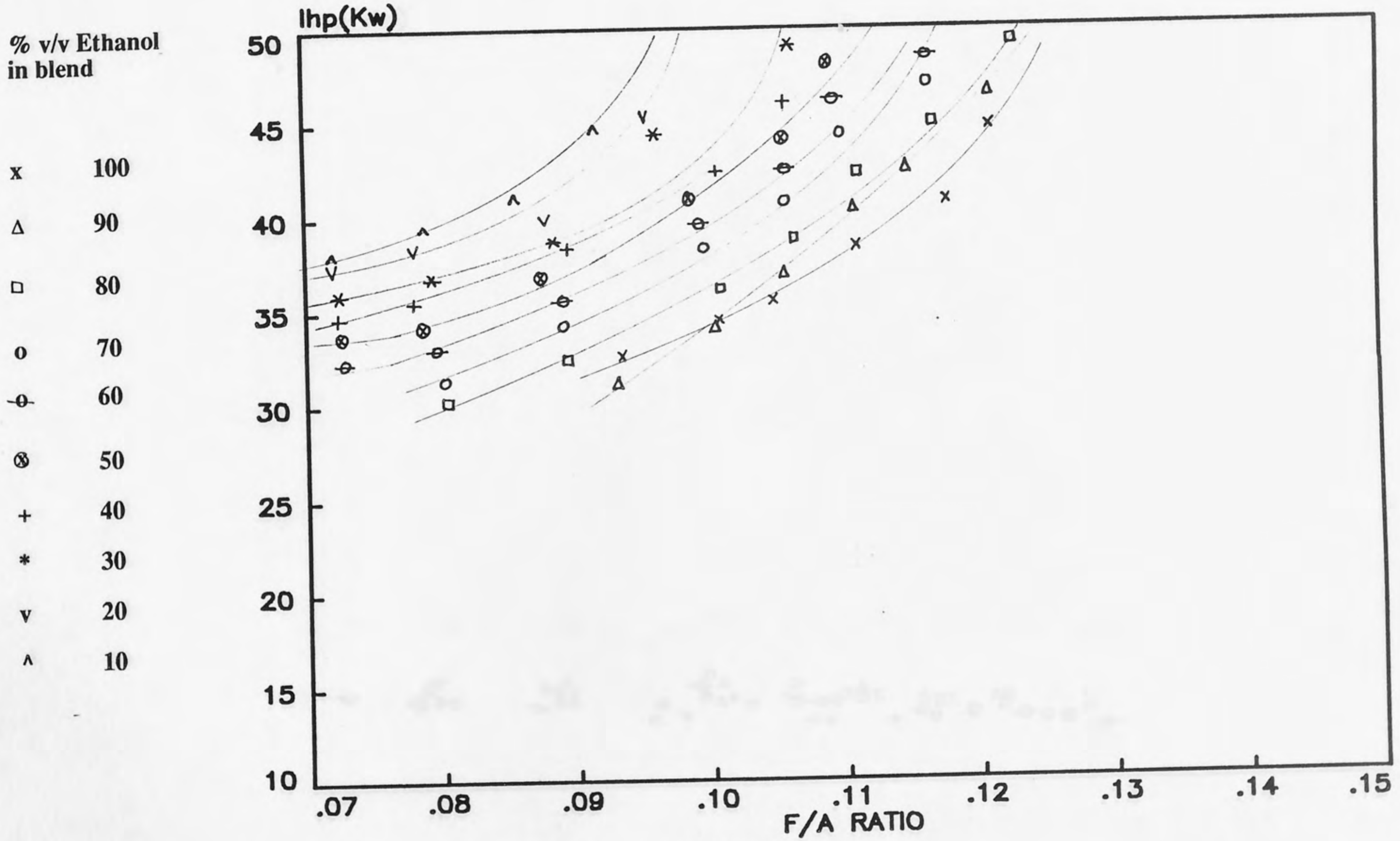

FIG: 4.1.18

EFFECT OF F/A RATIO ON Bhp.
ENGINE SPEED:1500 RPM

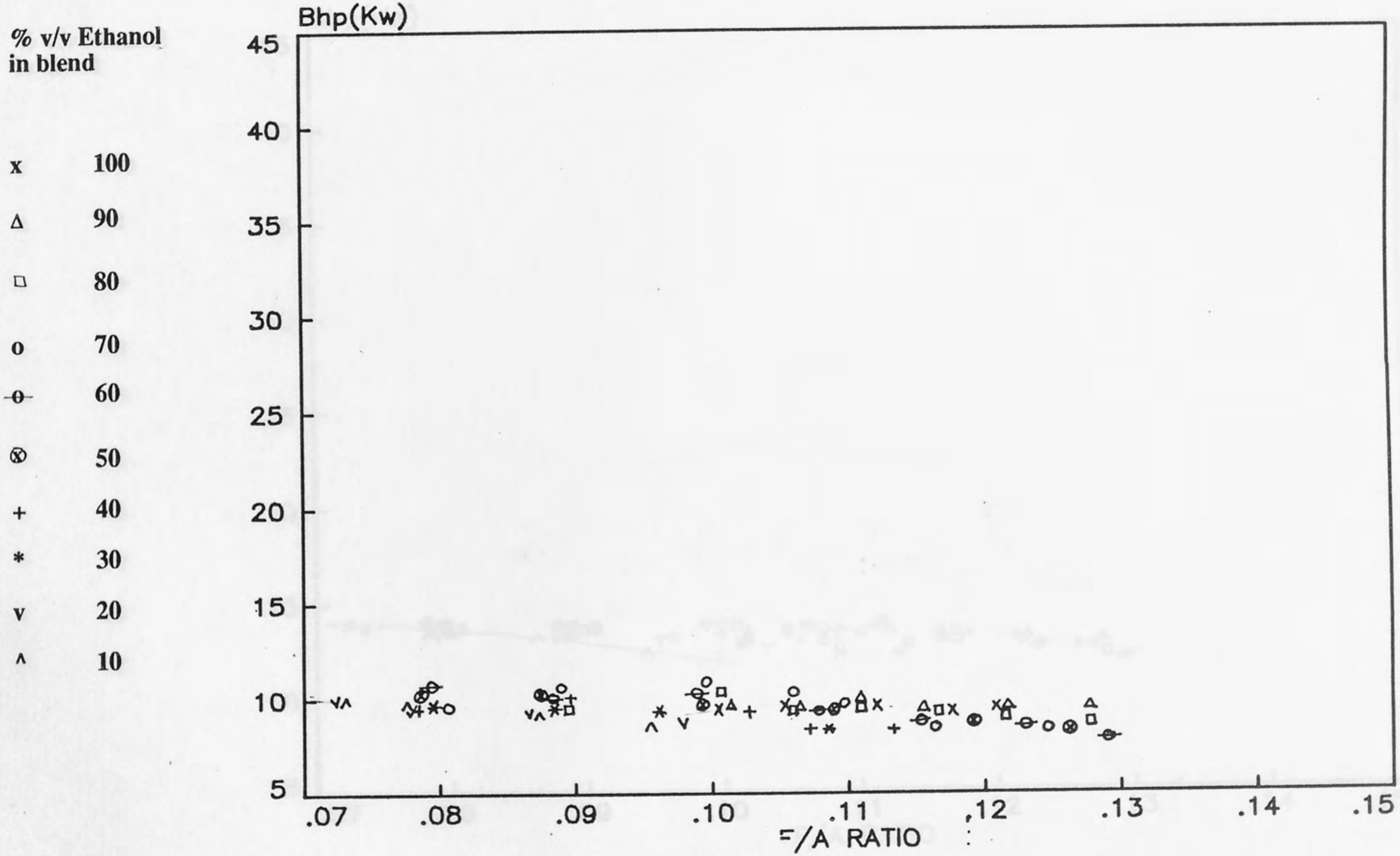

FIG: 4.1.19

EFFECT OF F/A RATIO ON Bhp.
ENGINE SPEED:2000 RPM

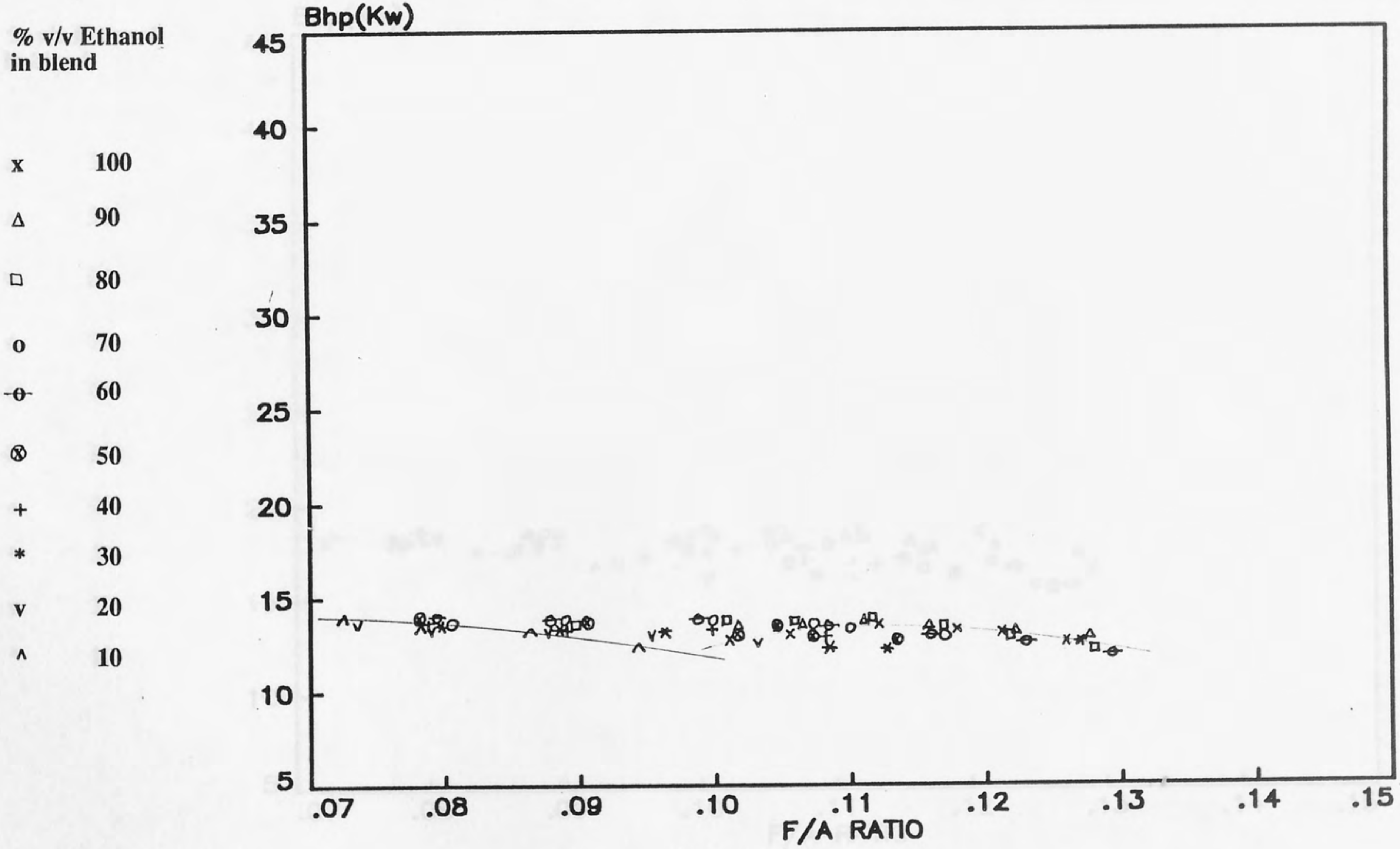

FIG: 4.1.20

EFFECT OF F/A RATIO ON Bhp.
ENGINE SPEED:2500 RPM

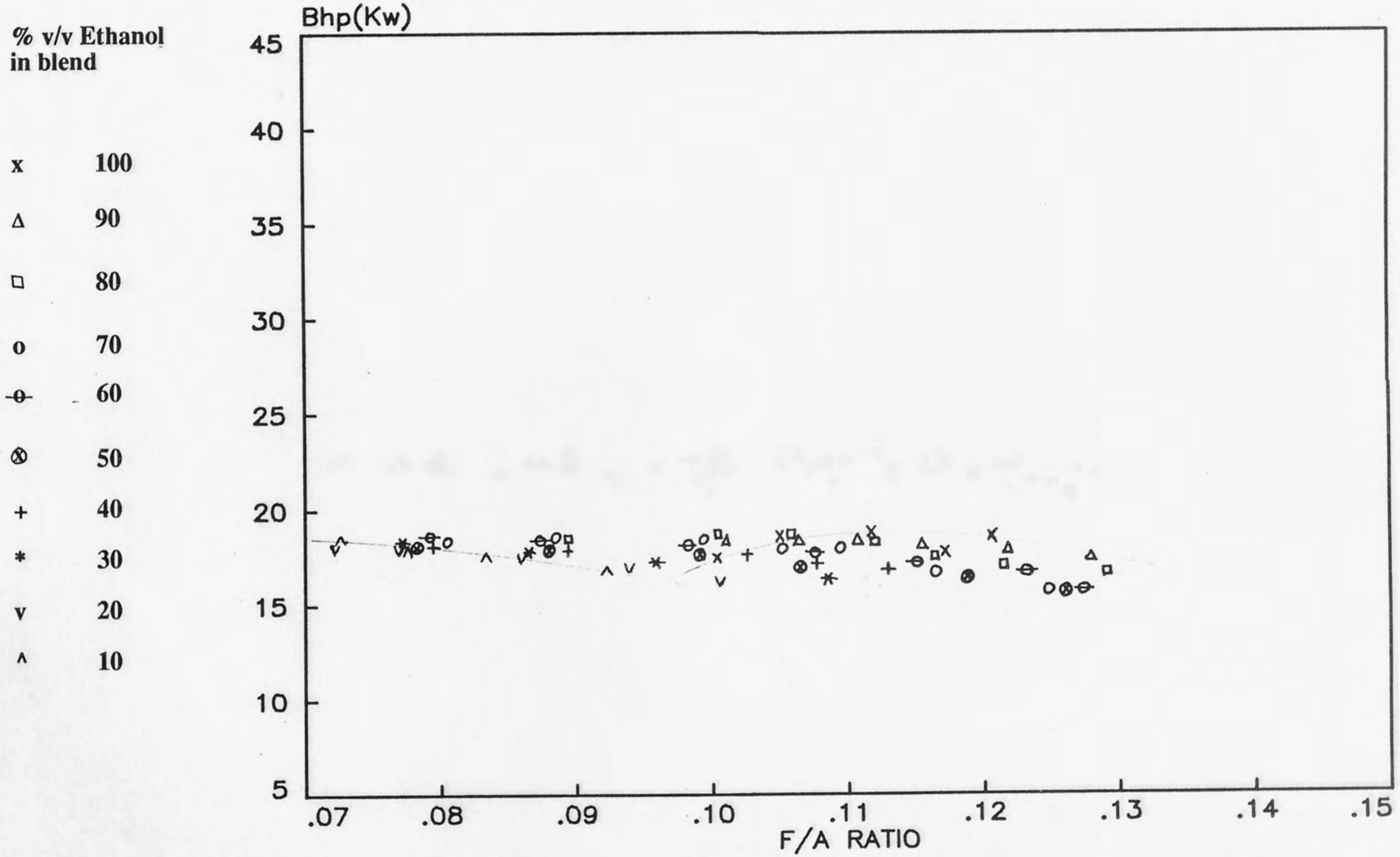

FIG: 4.1.21

EFFECT OF F/A RATIO ON Bhp.
ENGINE SPEED:3000 RPM

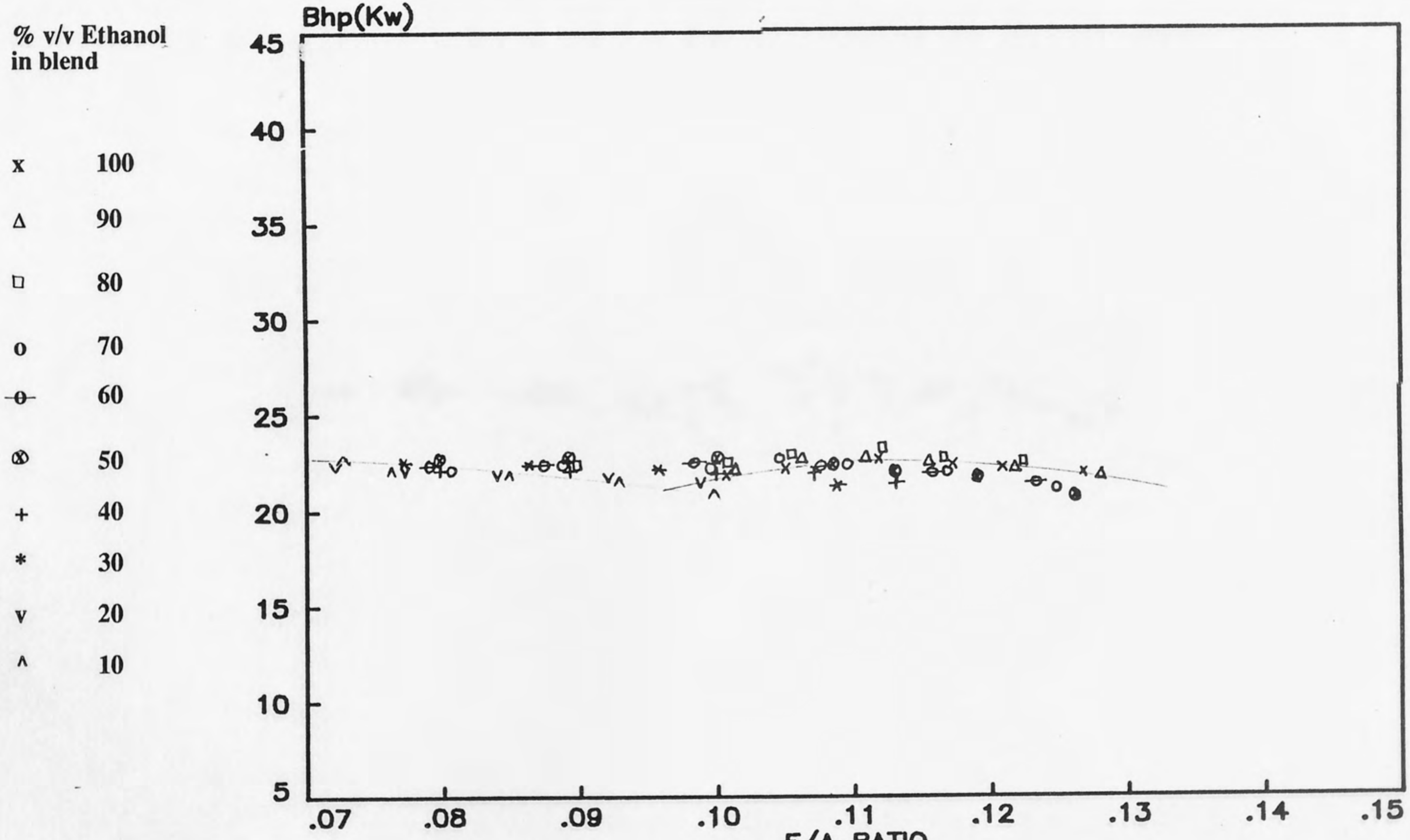

FIG: 4.1.22

EFFECT OF F/A RATIO ON Bhp.
ENGINE SPEED:3500 RPM

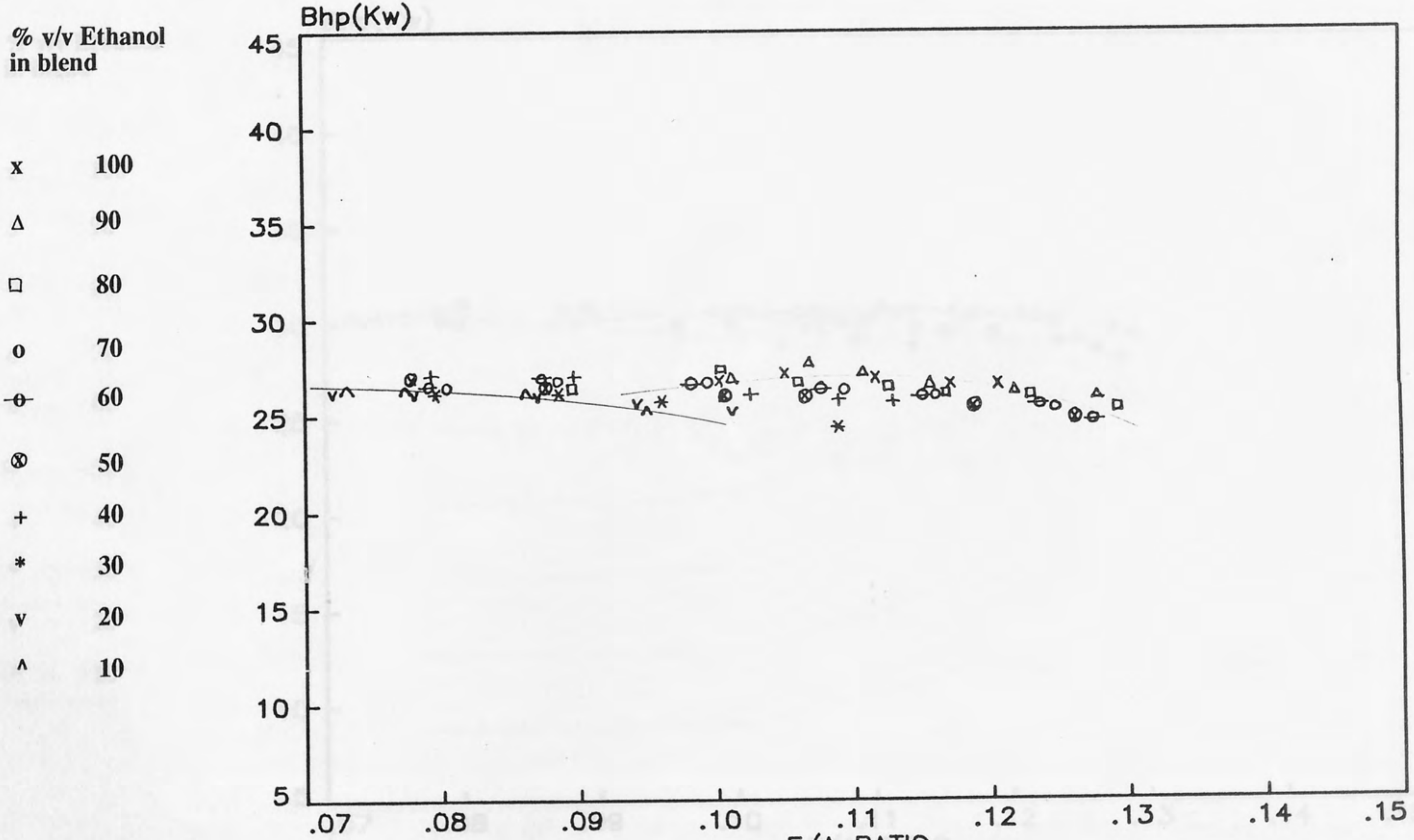

FIG: 4.1.23

EFFECT OF F/A RATIO ON Bhp.
ENGINE SPEED:4000 RPM

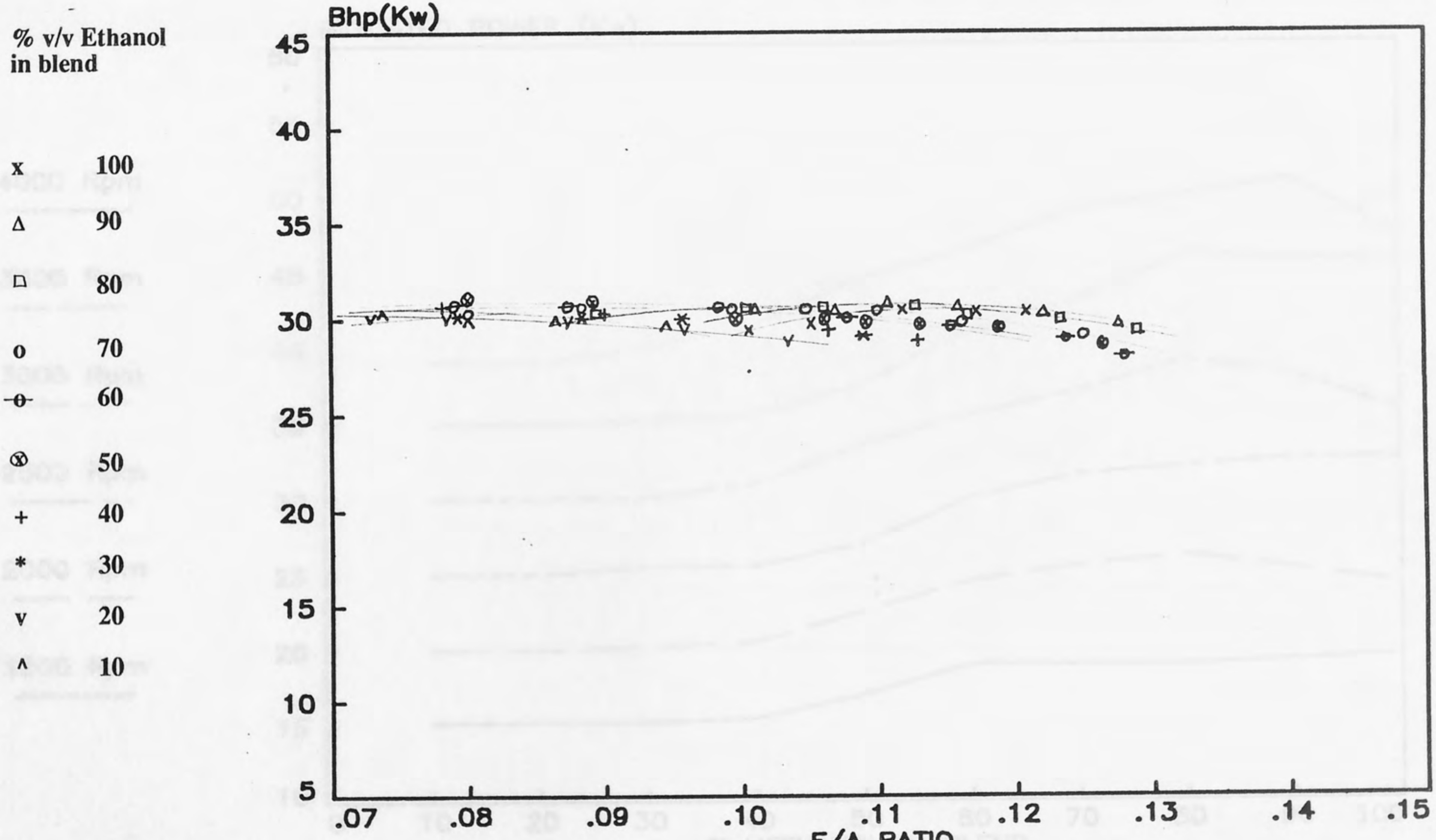

FIG: 4.1.24

EFFECT OF ALCOHOL CONTENT ON INDICATED POWER
AT STOICHIOMETRIC F/A RATIO

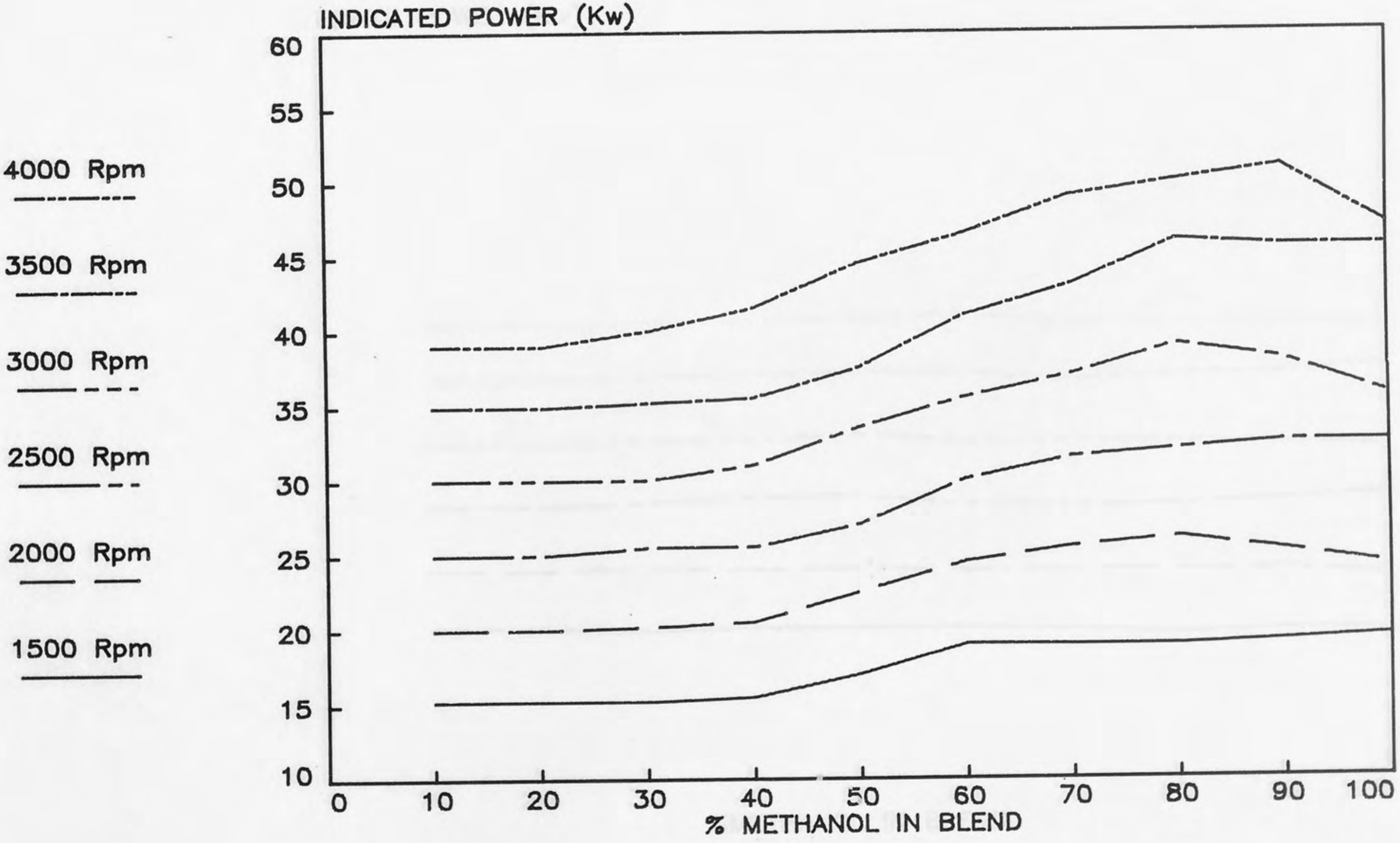

FIG: 4.1.25

EFFECT OF ALCHOL CONTENT ON BRAKE POWERAT
STOICHIOMETRIC F/A RATIO

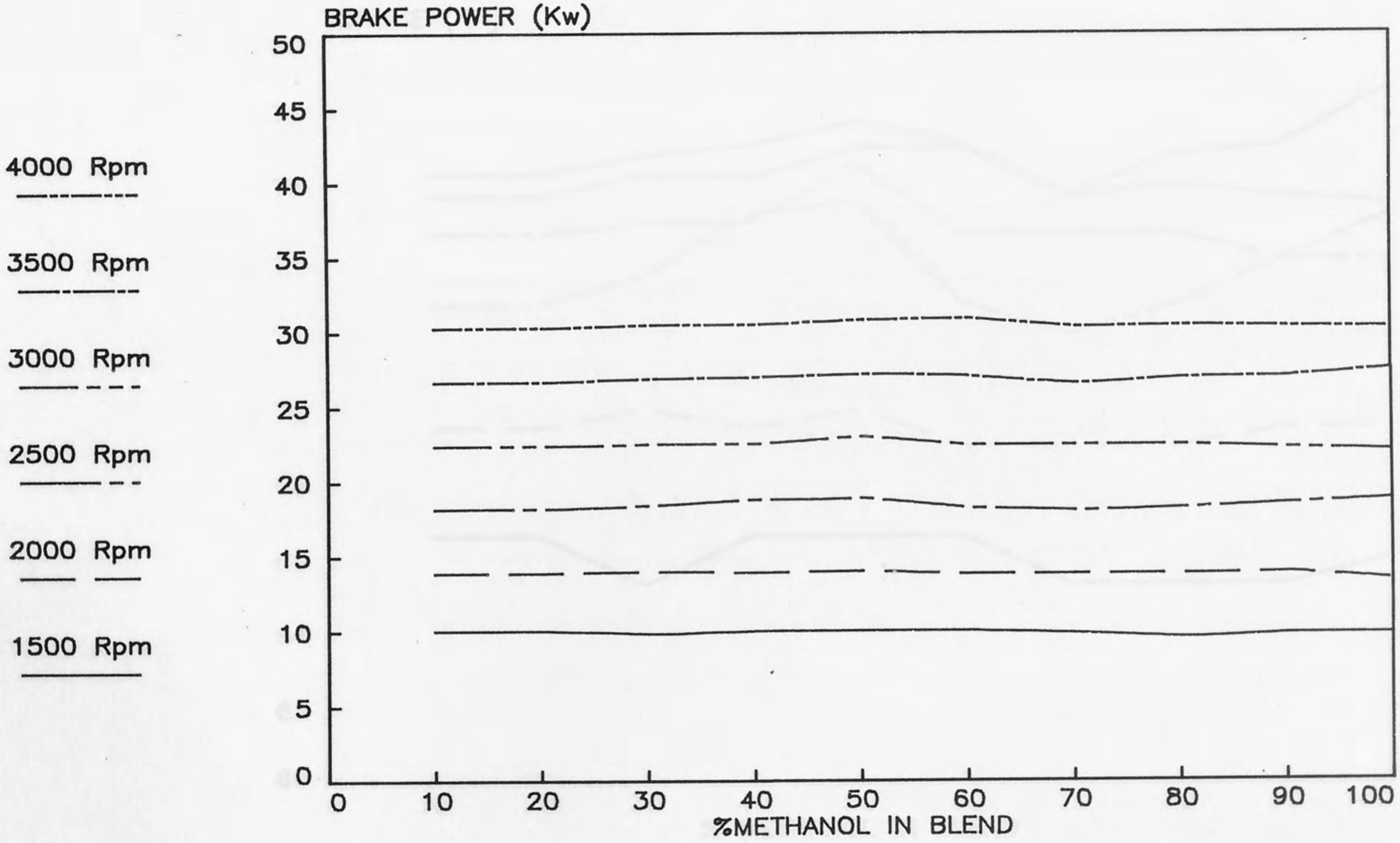

FIG: 4.1.26

EFFECT OF ALCOHOL CONTENT ON TORQUE
AT STOICHIOMETRIC F/A RATIO

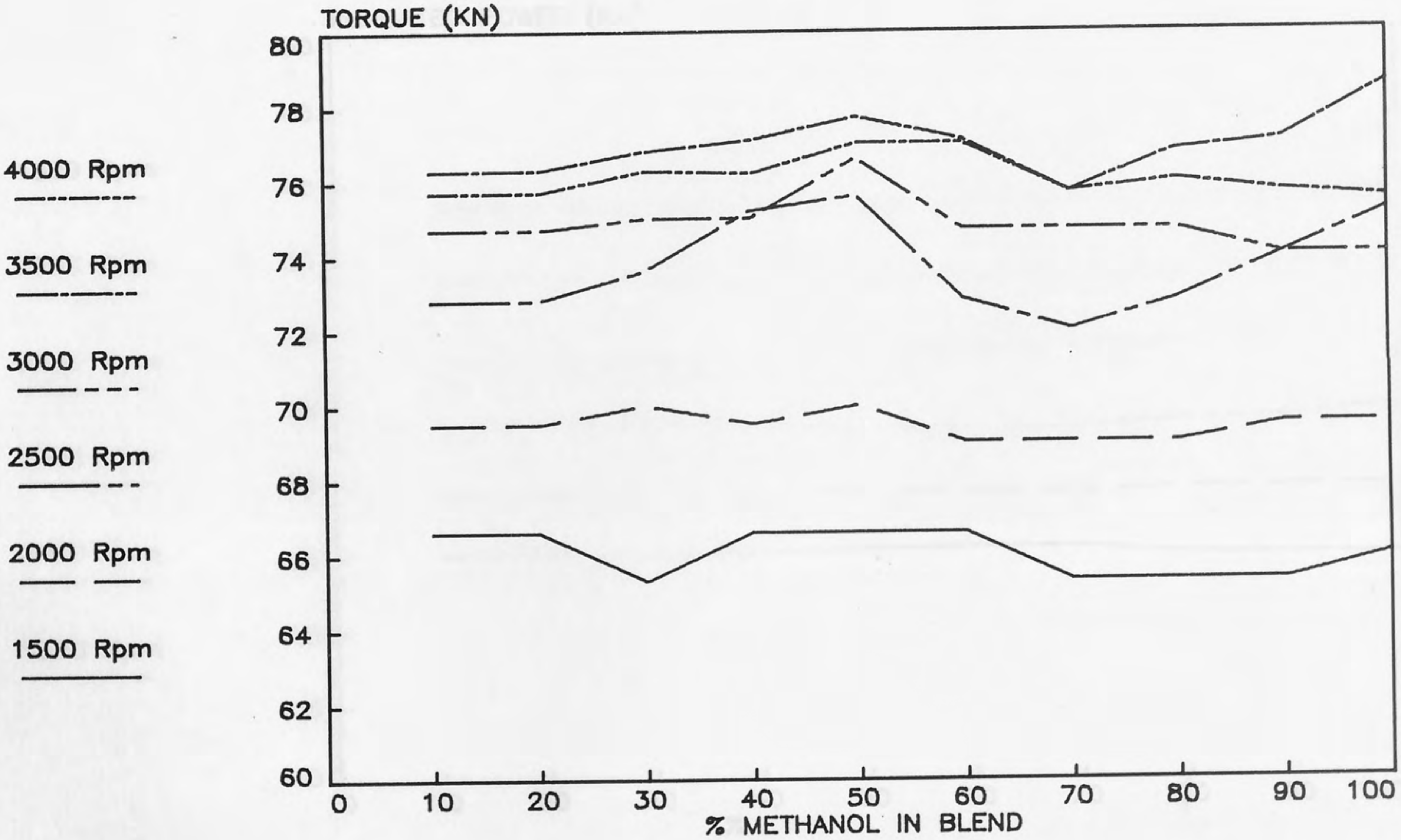

FIG: 4.1.27

EFFECT OF ALCHOL CONTENT ON INDICATED POWER
AT STOICHIOMETRIC F/A RATIO

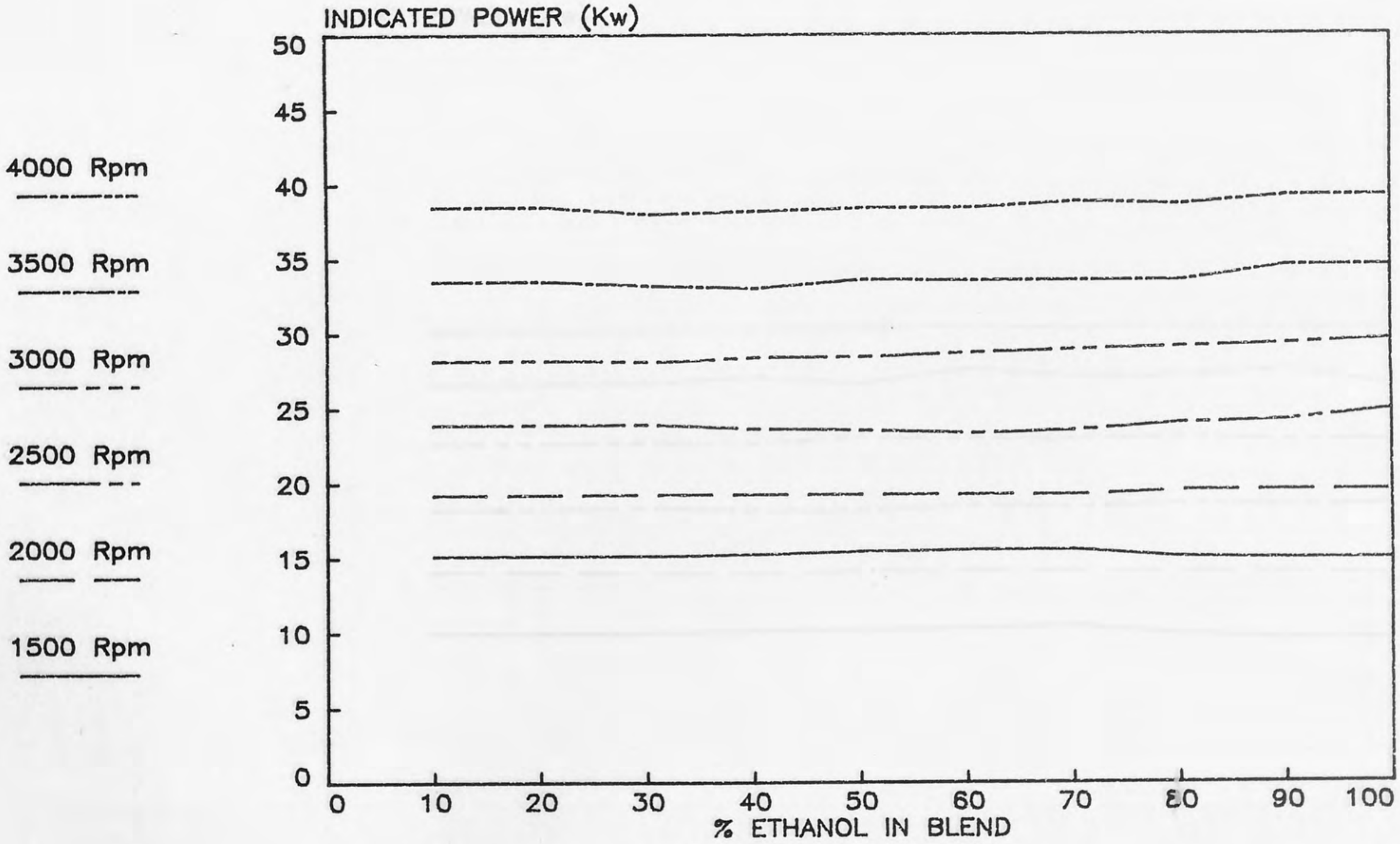

FIG: 4.1.28

EFFECT OF ALCOHOL CONTENT ON BRAKE POWER AT
STOICHIOMETRIC F/A RATIO

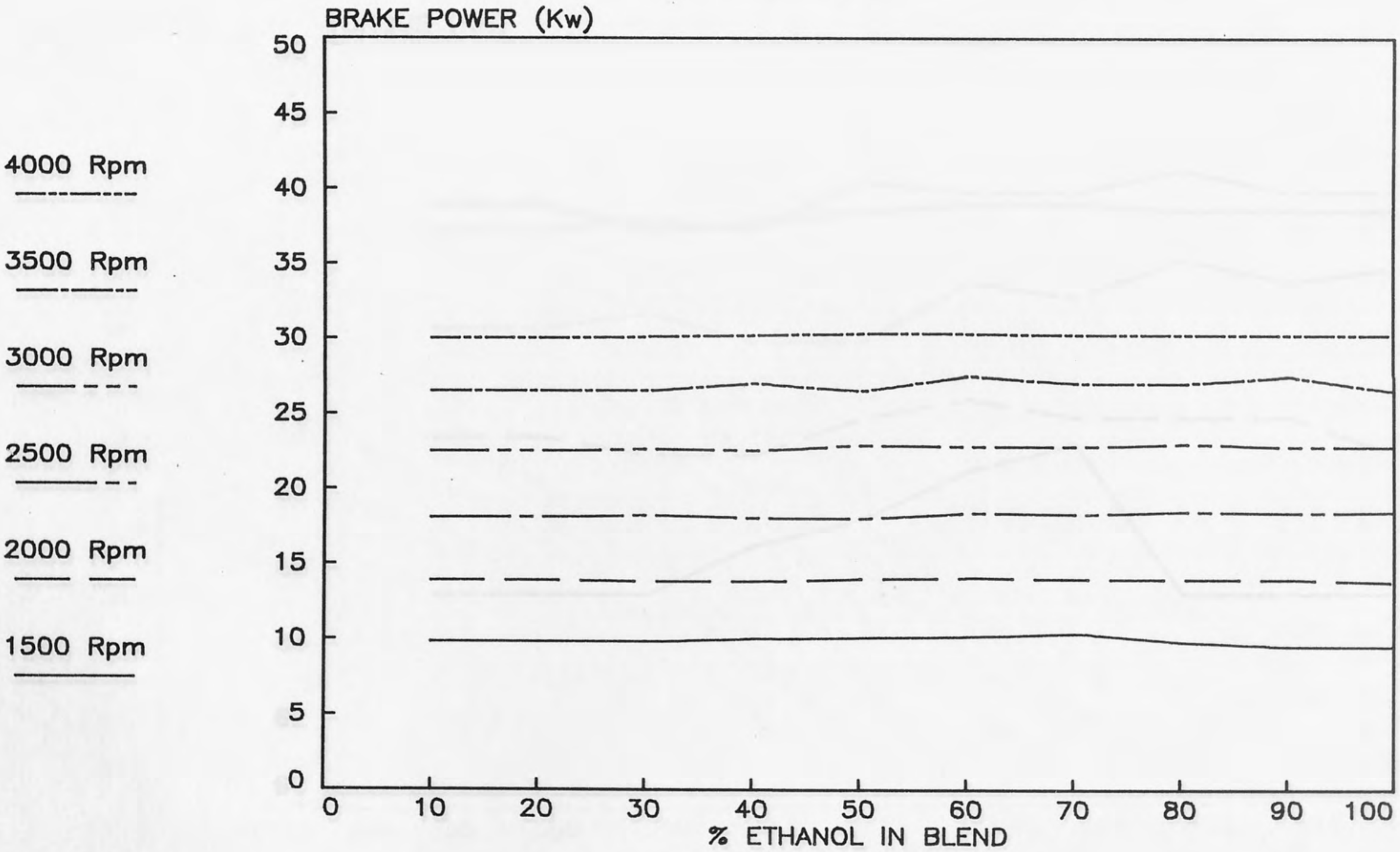

FIG: 4.1.29

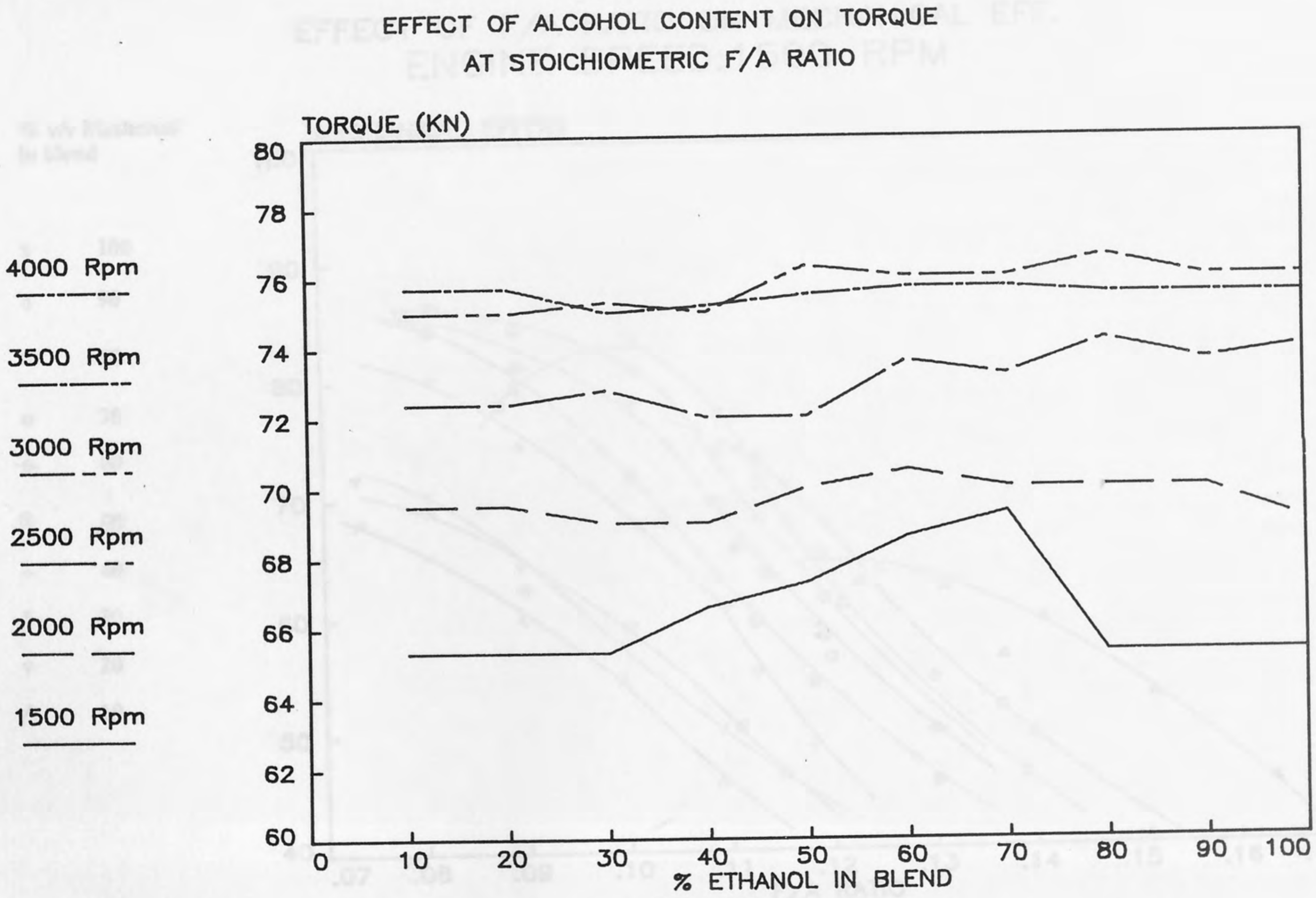
EFFECT OF ALCOHOL CONTENT ON TORQUE
AT STOICHIOMETRIC F/A RATIO
TORQUE (KN)
80
78
76
74
72
70
68
66
64
62
60
0
10
20
30
40
50
60
70
80
90
100
% ETHANOL IN BLEND
4000 Rpm
3500 Rpm
3000 Rpm
2500 Rpm
2000 Rpm
1500 Rpm

FIG: 4.1.30

EFFECT OF F/A RATIO ON MECHANICAL EFF.
ENGINE SPEED:1500 RPM

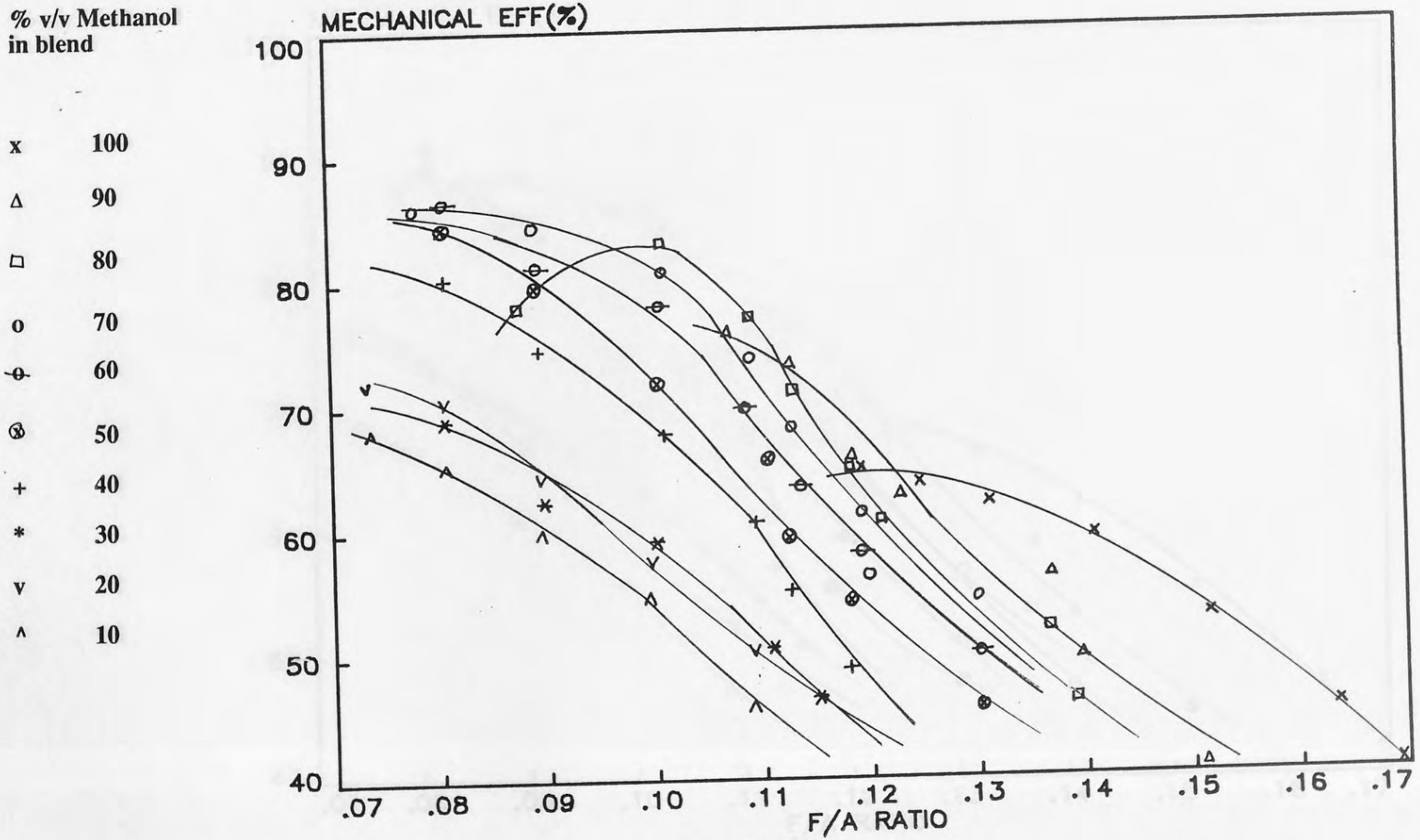

FIG: 4.1.31

EFFECT OF F/A RATIO ON MECHANICAL EFF.
ENGINE SPEED:2000 RPM

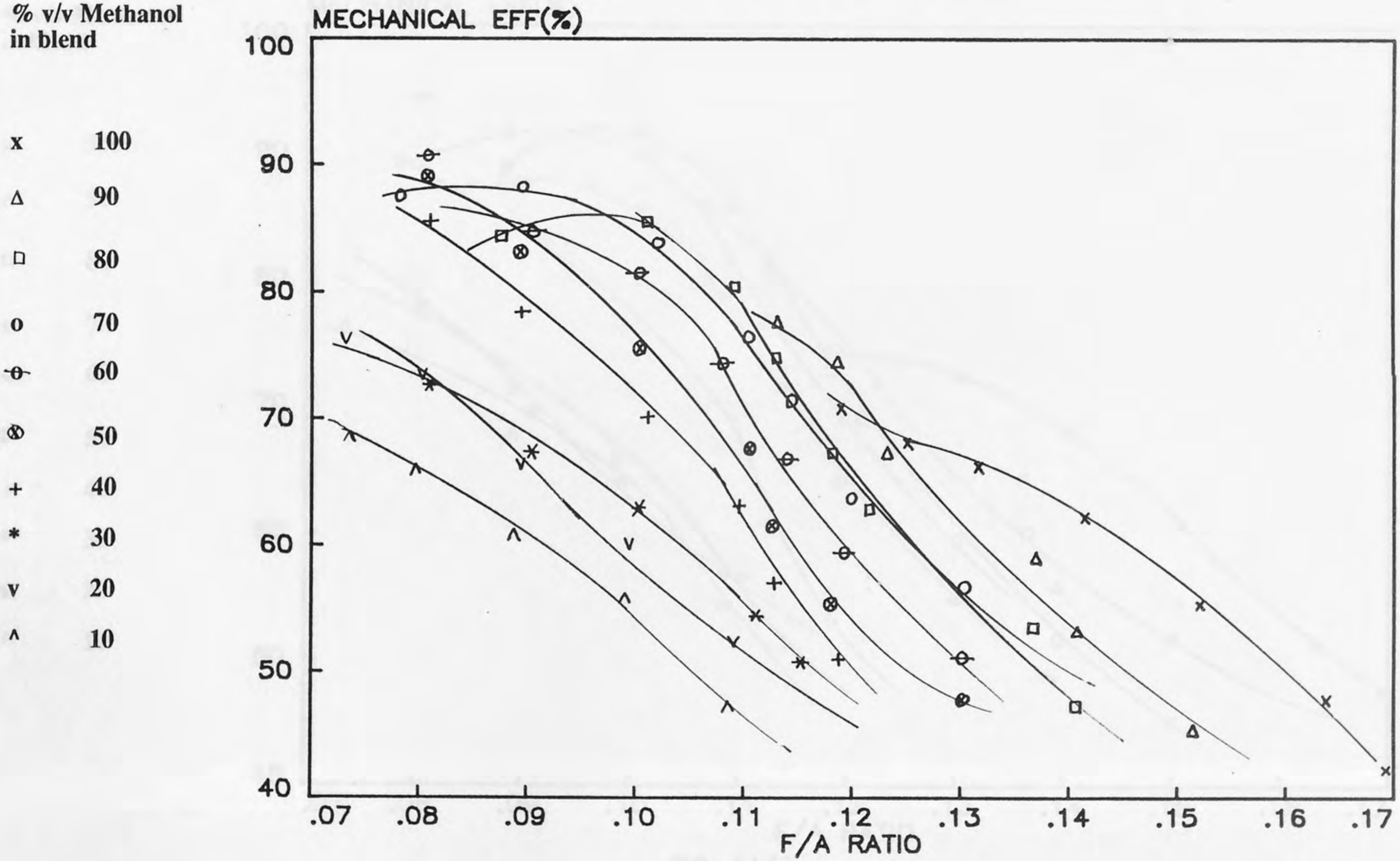

FIG: 4.1.32

EFFECT OF F/A RATIO ON MECHANICAL EFF.
ENGINE SPEED:2500 RPM

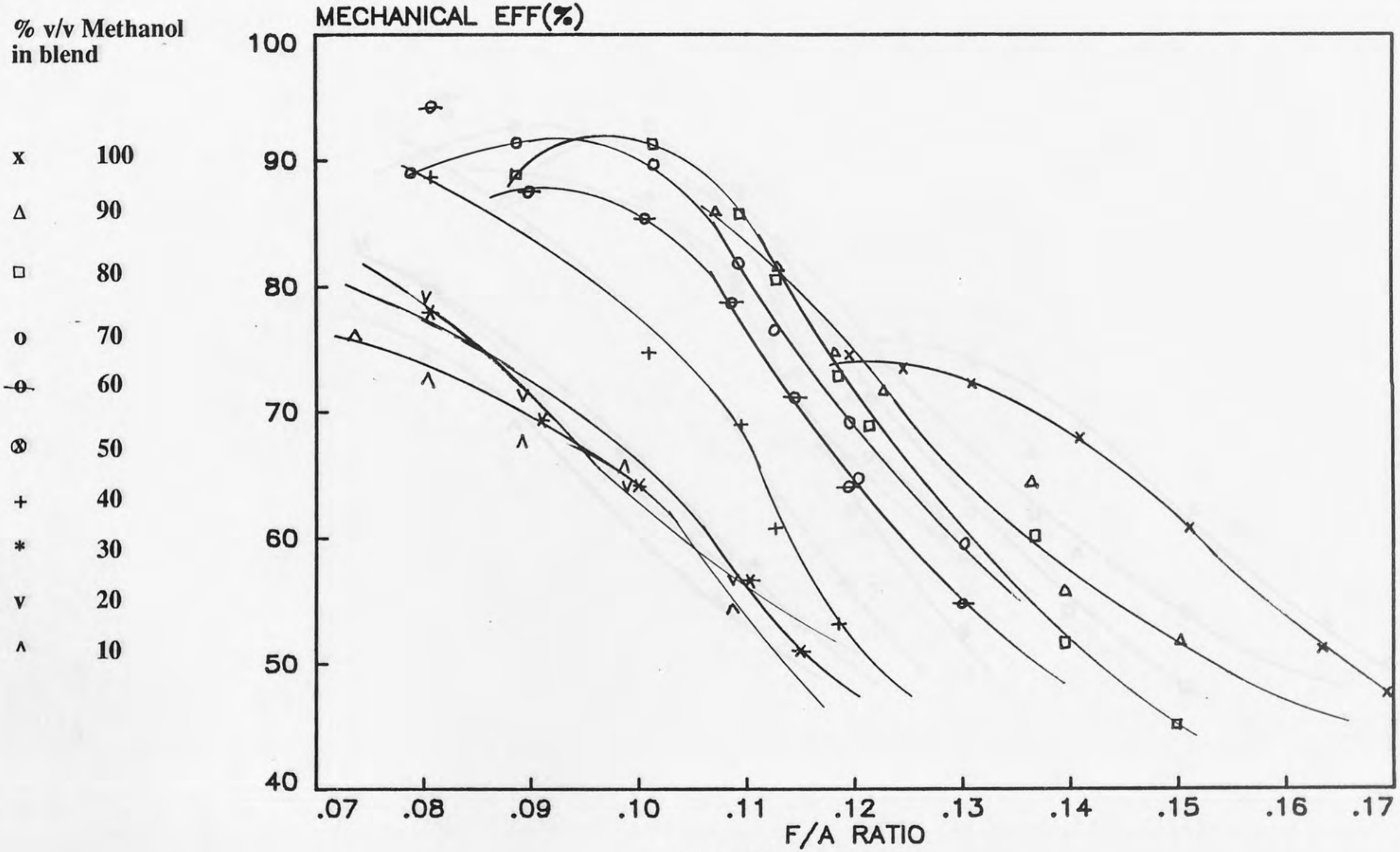

FIG: 4.1.33

EFFECT OF F/A RATIO ON MECHANICAL EFF.
ENGINE SPEED:3000 RPM

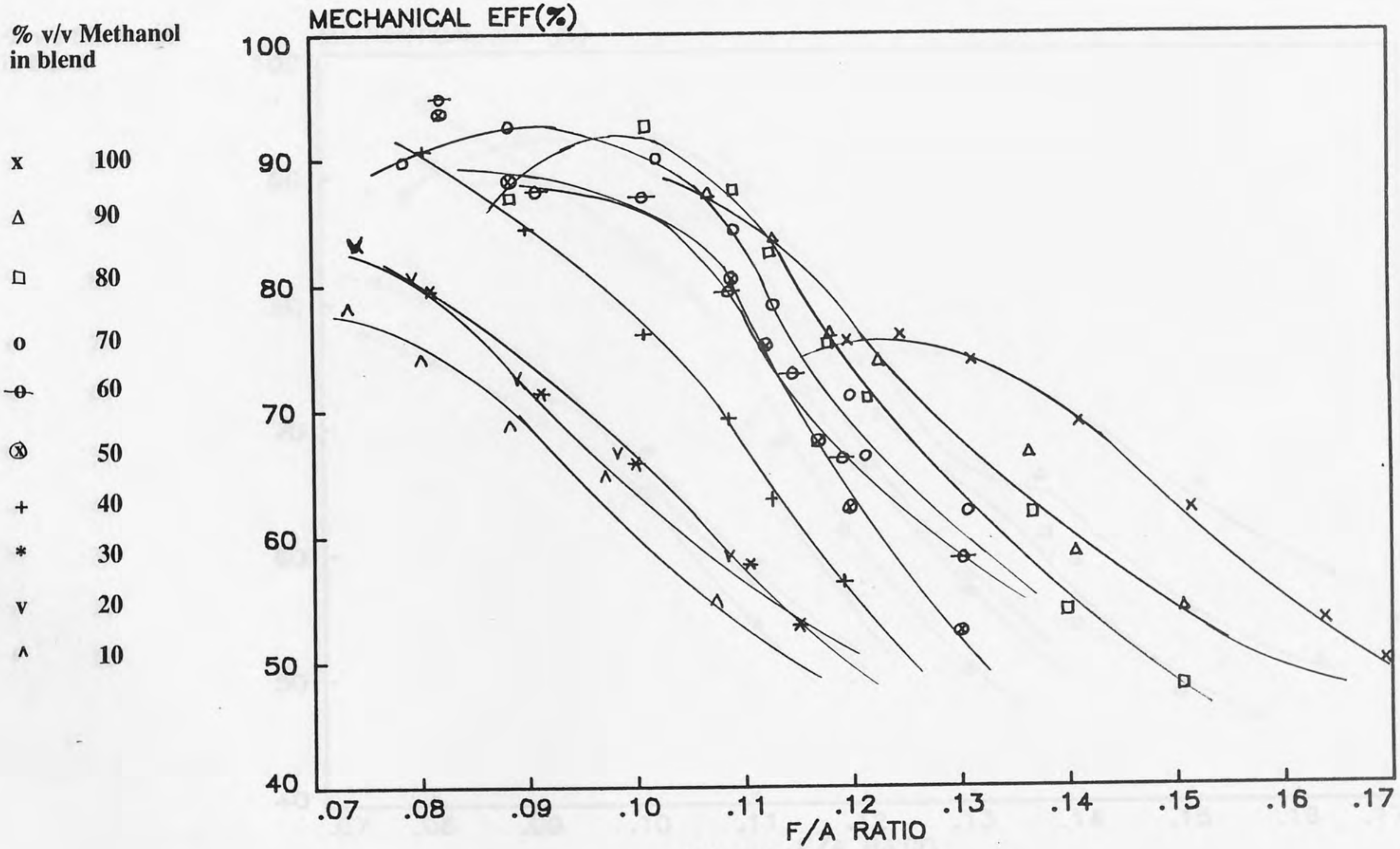

FIG: 4.1.34

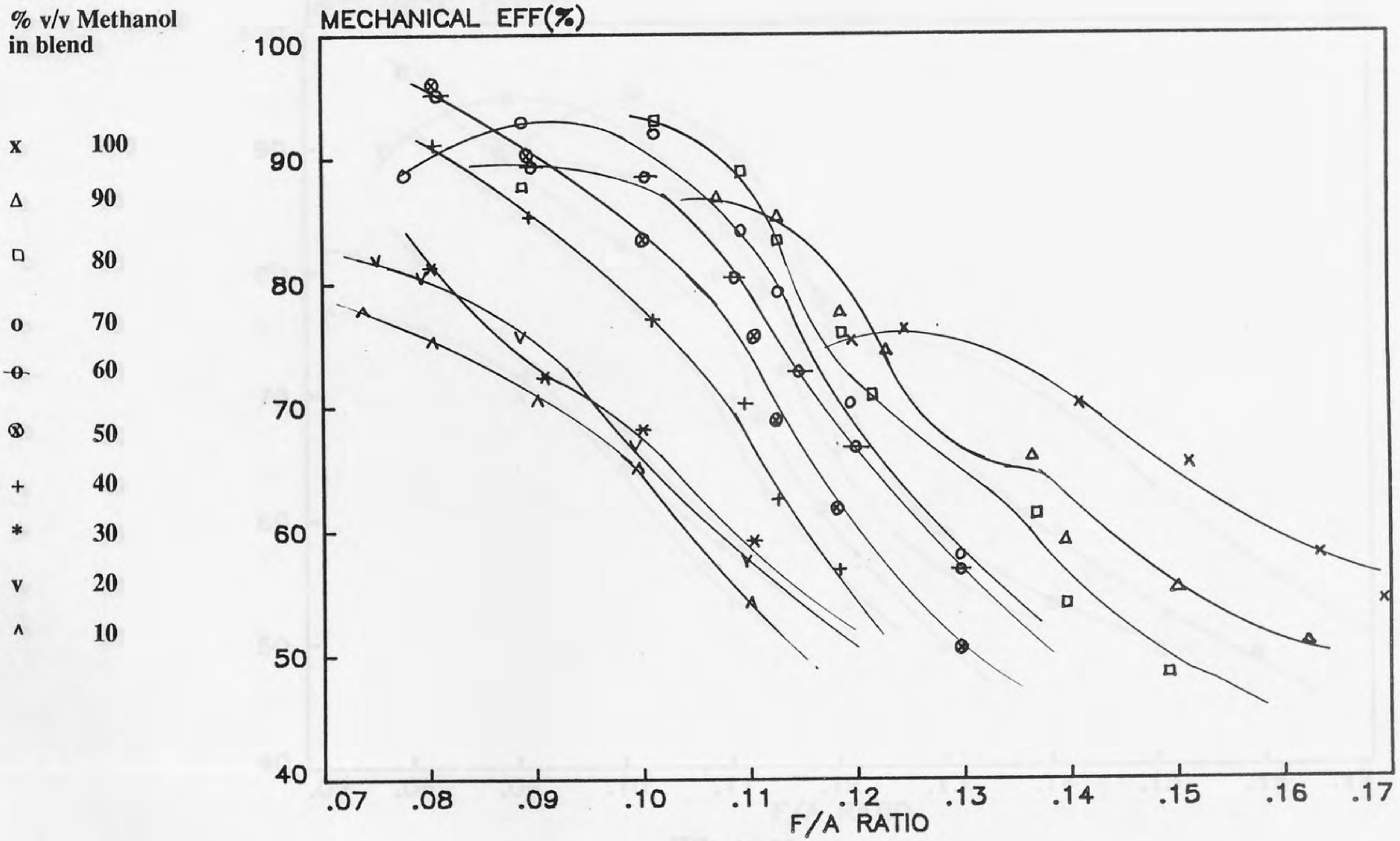

EFFECT OF F/A RATIO ON MECHANICAL EFF.
ENGINE SPEED:3500 RPM

FIG: 4.1.35

EFFECT OF F/A RATIO ON MECHANICAL EFF.
ENGINE SPEED:4000 RPM

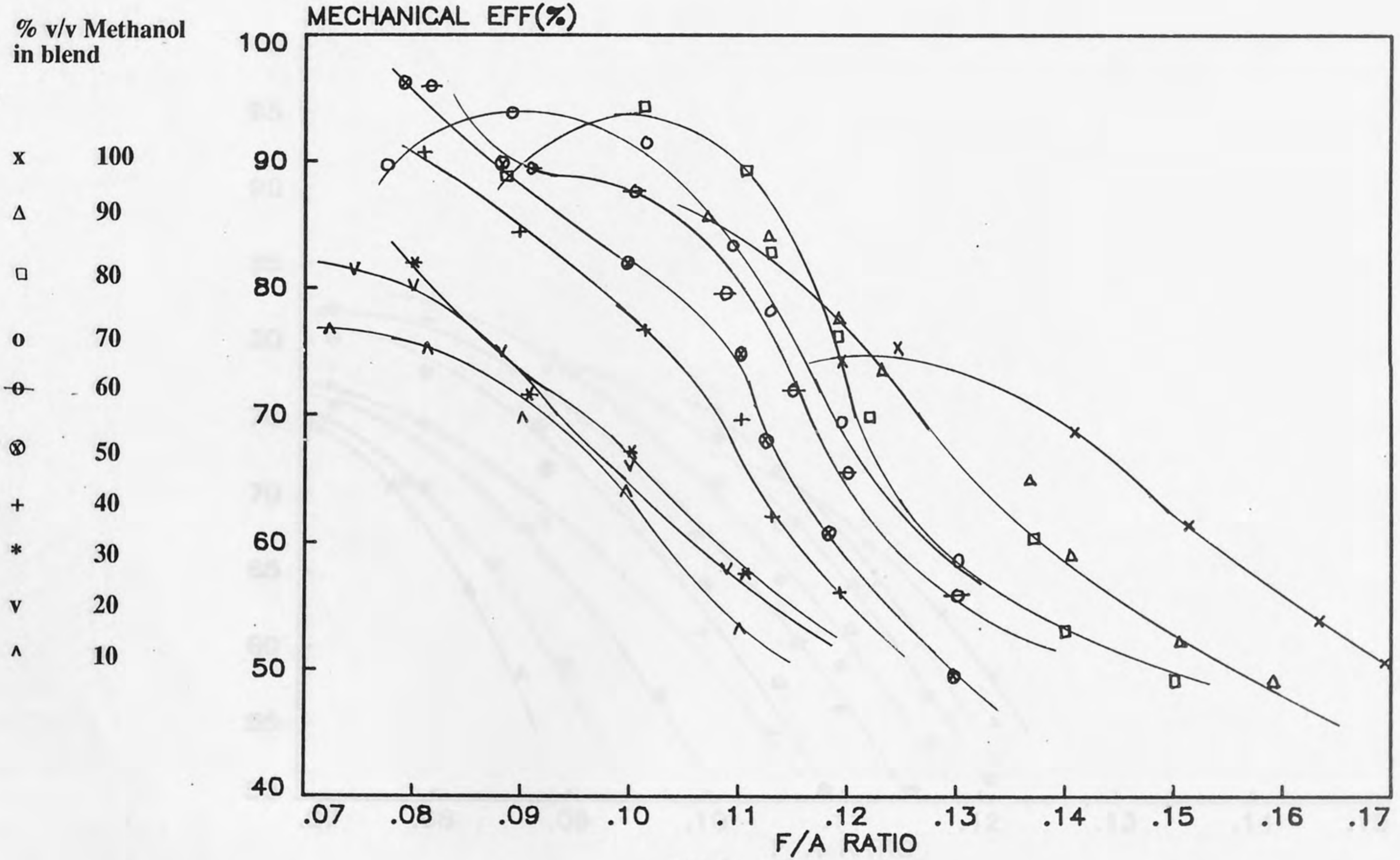

FIG: 4.1.36

EFFECT OF F/A RATIO ON MECHANICAL EFF.
ENGINE SPEED:1500 RPM

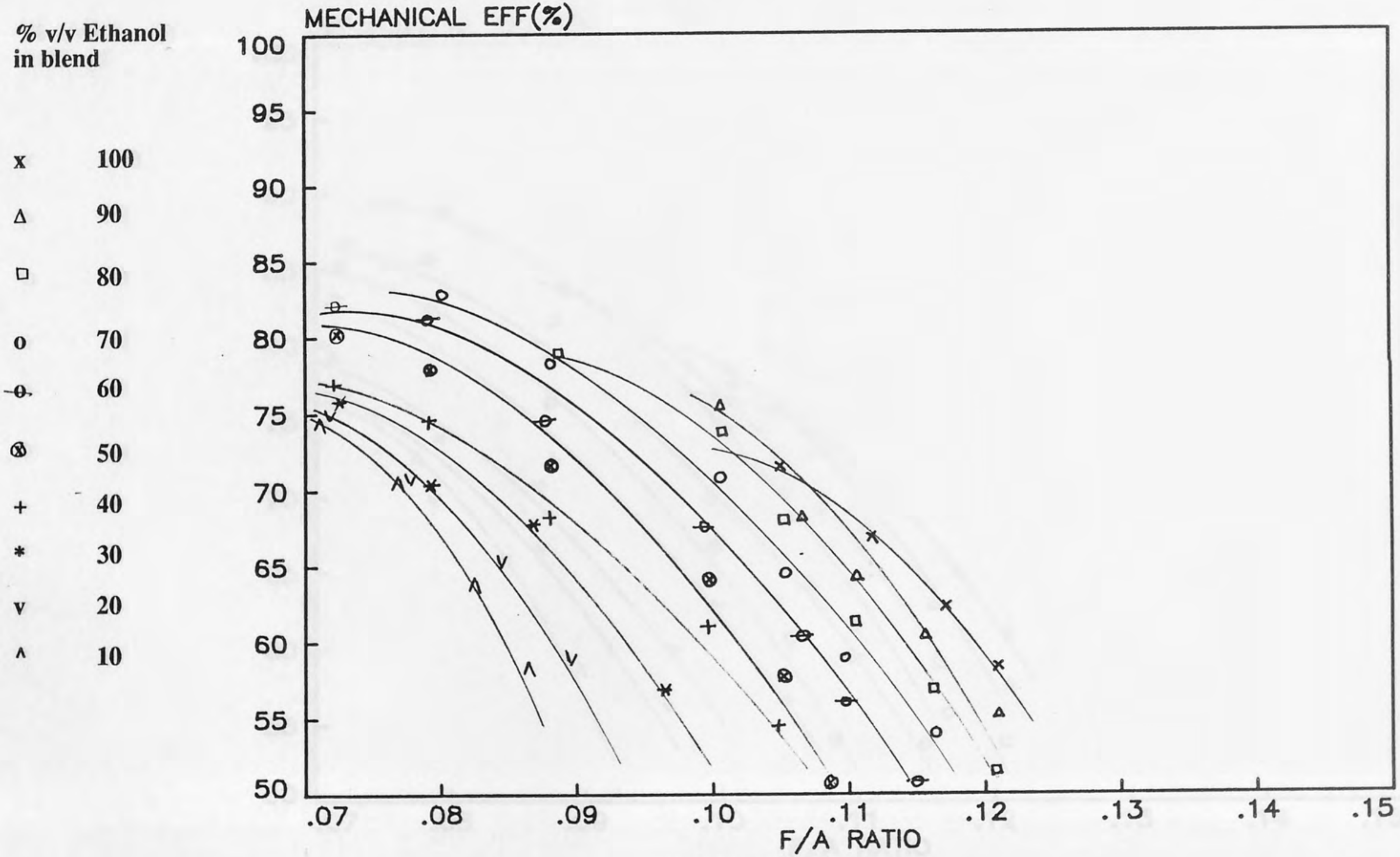

FIG: 4.1.37

EFFECT OF F/A RATIO ON MECHANICAL EFF.
ENGINE SPEED:2000 RPM

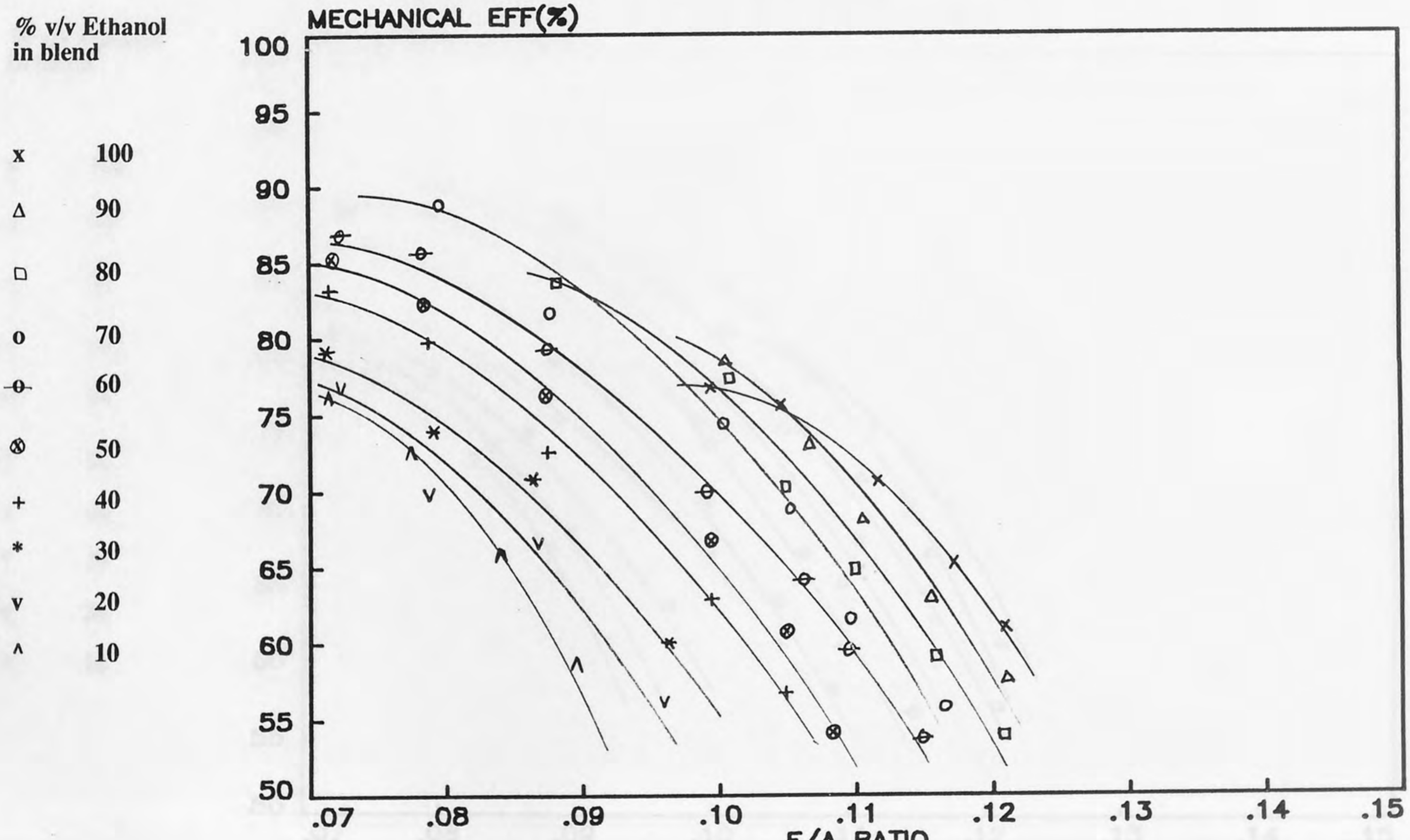

FIG: 4.1.38

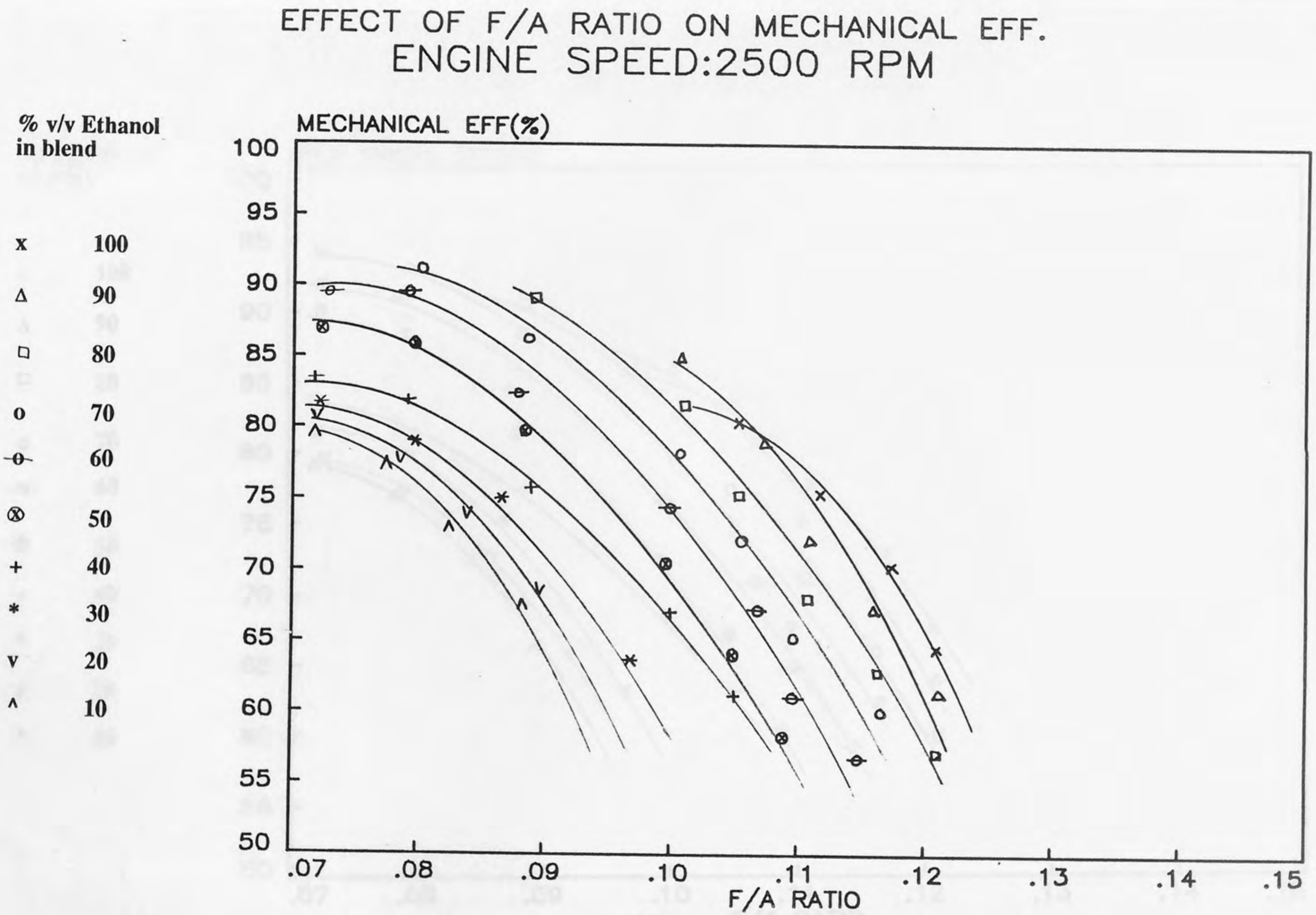
EFFECT OF F/A RATIO ON MECHANICAL EFF.
ENGINE SPEED:2500 RPM
% v/v Ethanol in blend
x 100
Δ 90
□ 80
o 70
-ϕ- 60
⊗ 50
+ 40
* 30
v 20
^ 10
MECHANICAL EFF(%)
100
95
90
85
80
75
70
65
60
55
50
.07
.08
.09
.10
.11
.12
.13
.14
.15
F/A RATIO

FIG: 4.1.39

EFFECT OF F/A RATIO ON MECHANICAL EFF.
ENGINE SPEED:3000 RPM

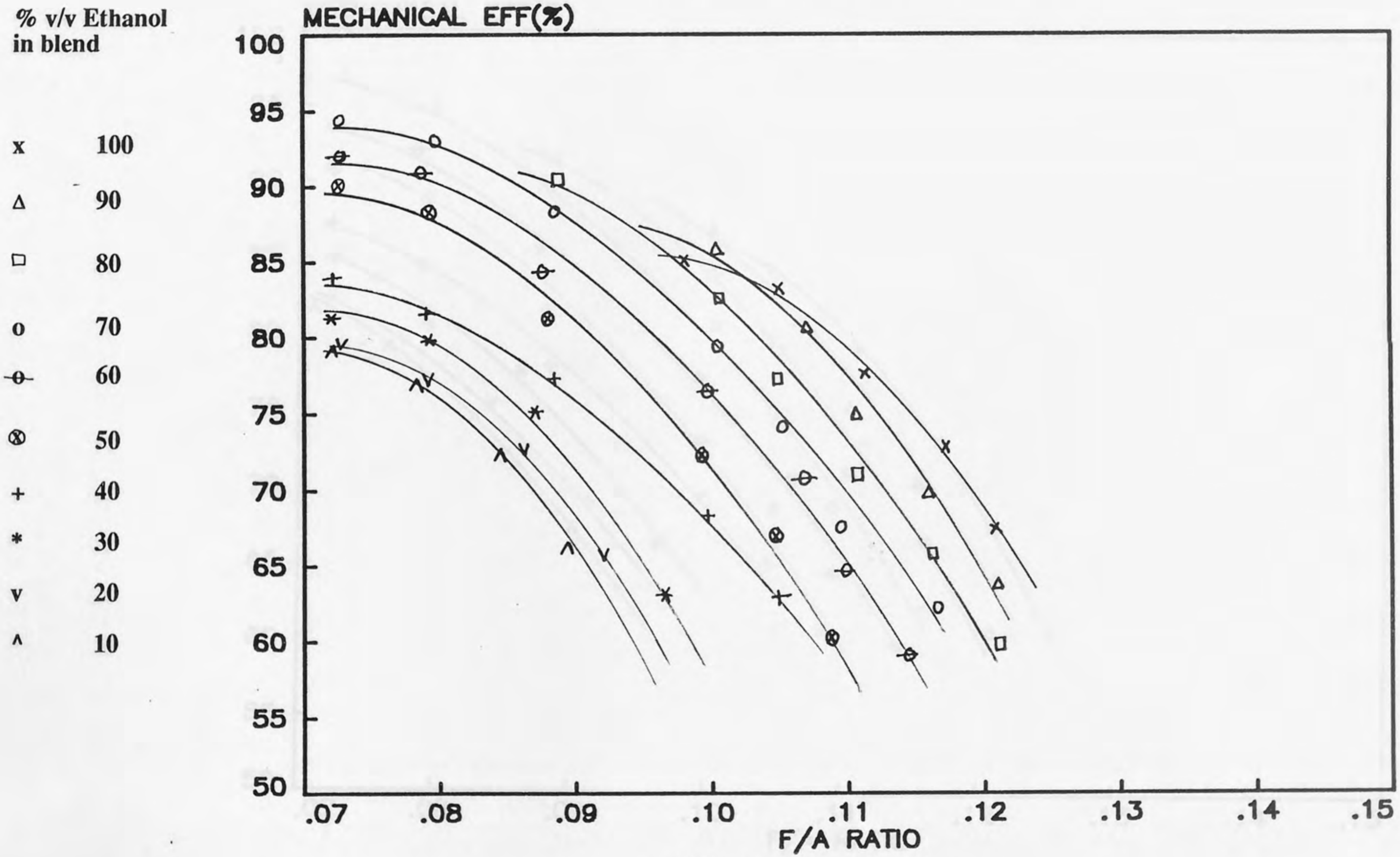

FIG: 4.1.40

EFFECT OF F/A RATIO ON MECHANICAL EFF.
ENGINE SPEED:3500 RPM

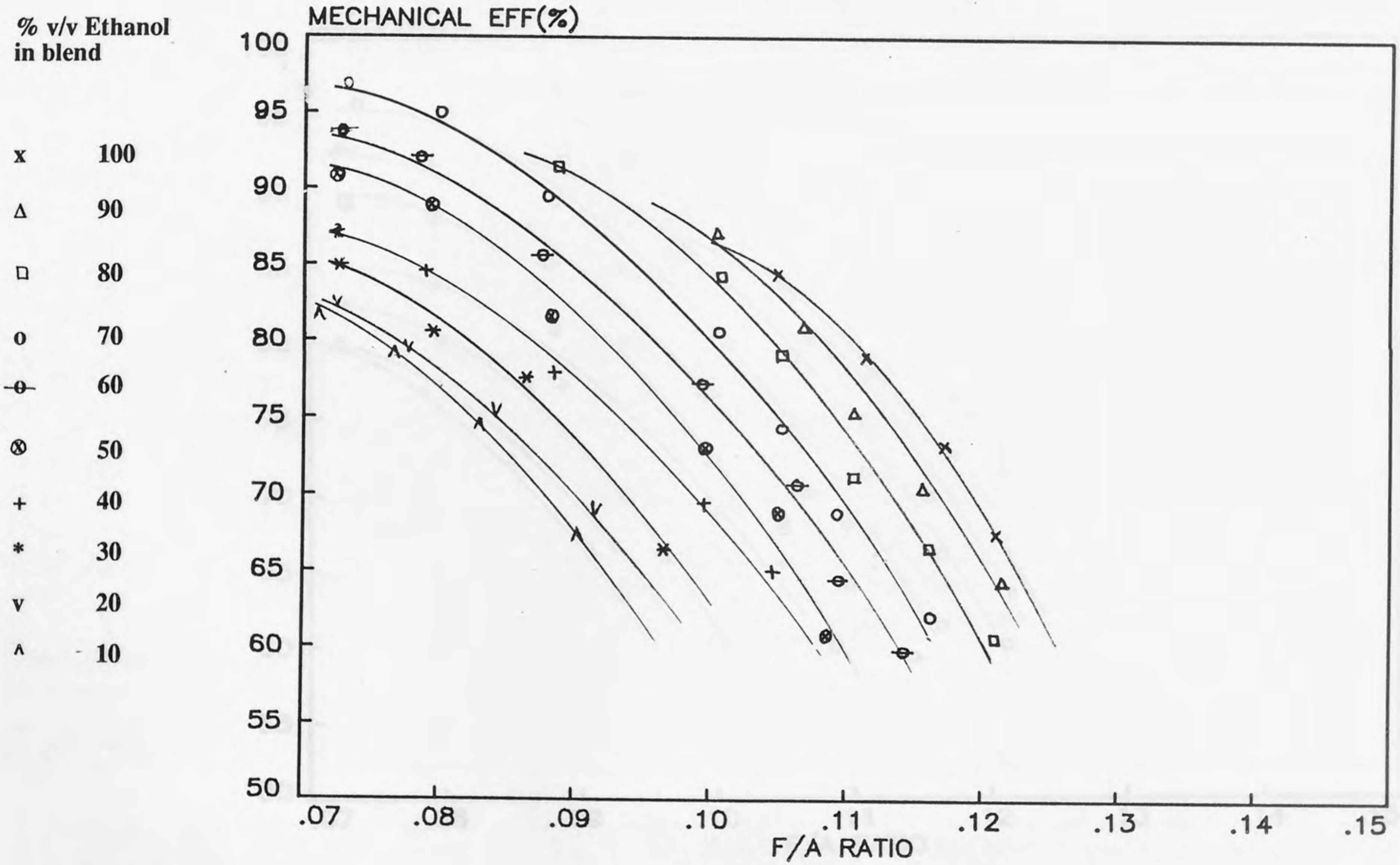

FIG: 4.1.41

EFFECT OF F/A RATIO ON MECHANICAL EFF.
ENGINE SPEED:4000 RPM

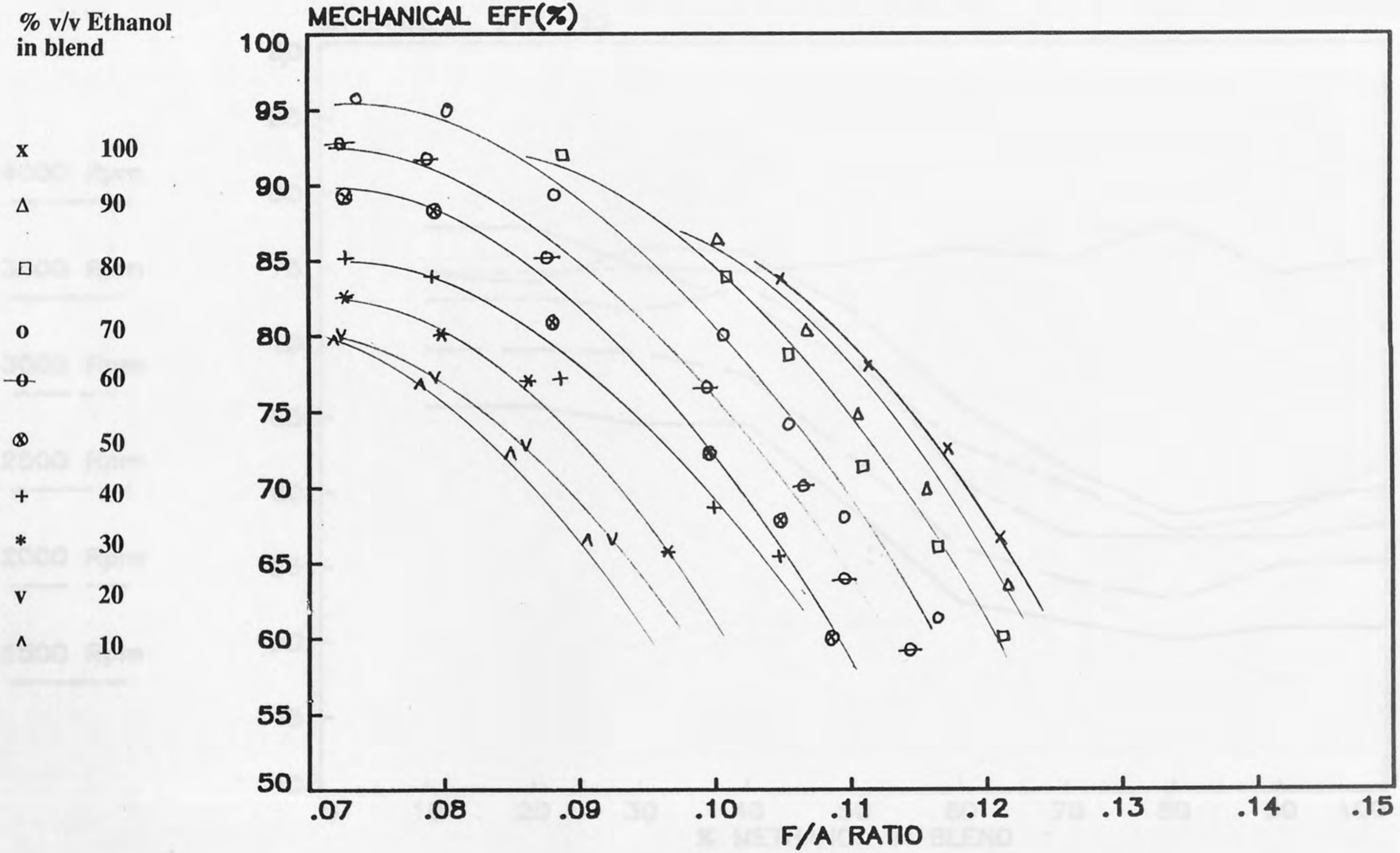

FIG: 4.1.42

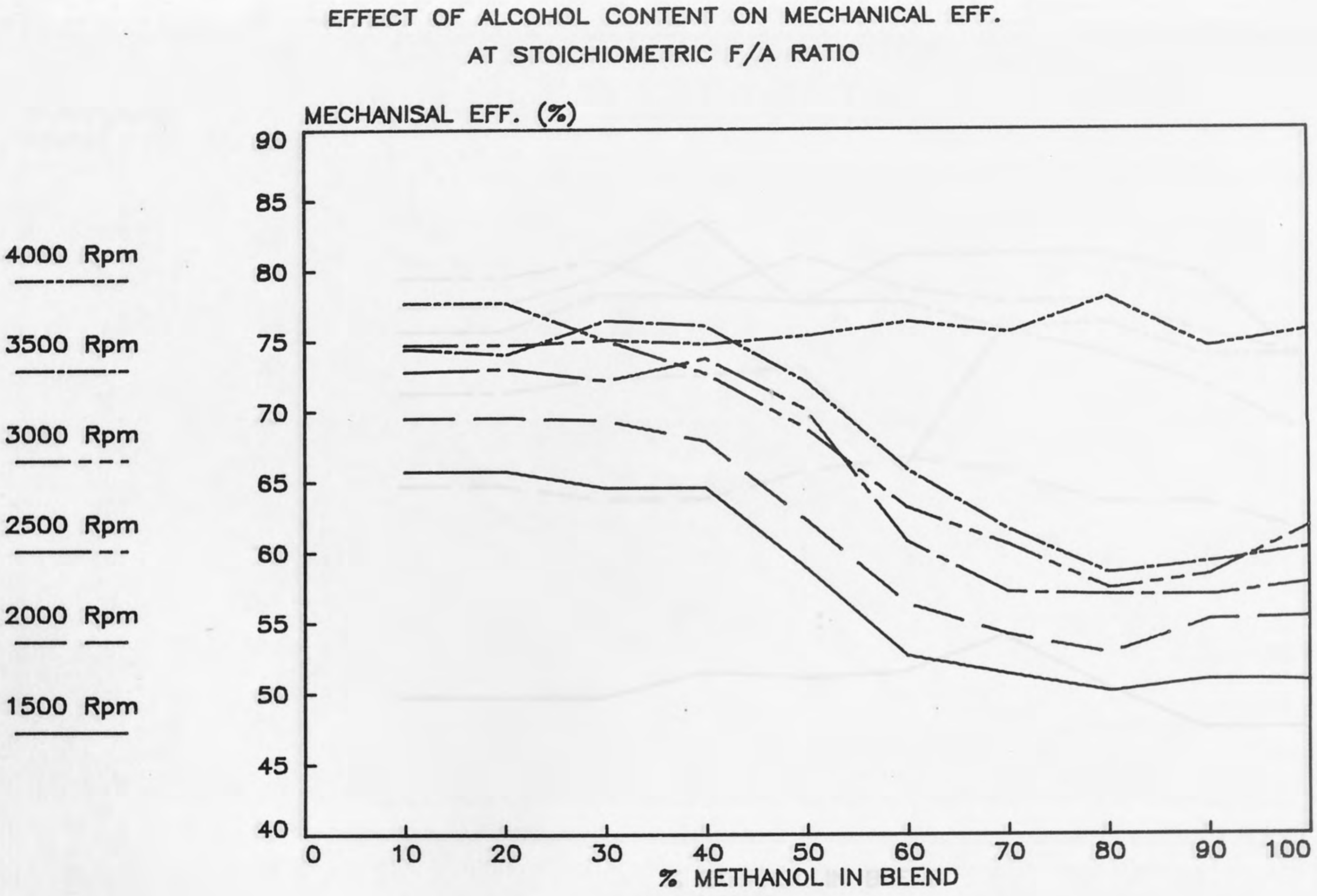
EFFECT OF ALCOHOL CONTENT ON MECHANICAL EFF.
AT STOICHIOMETRIC F/A RATIO
MECHANISAL EFF. (%)
90
85
80
75
70
65
60
55
50
45
40
0
10
20
30
40
50
60
70
80
90
100
% METHANOL IN BLEND
4000 Rpm
3500 Rpm
3000 Rpm
2500 Rpm
2000 Rpm
1500 Rpm

FIG: 4.1.43

EFFECT OF ALCOHOL CONTENT ON MECHANICAL EFF.
AT STOICHIOMETRIC F/A RATIO

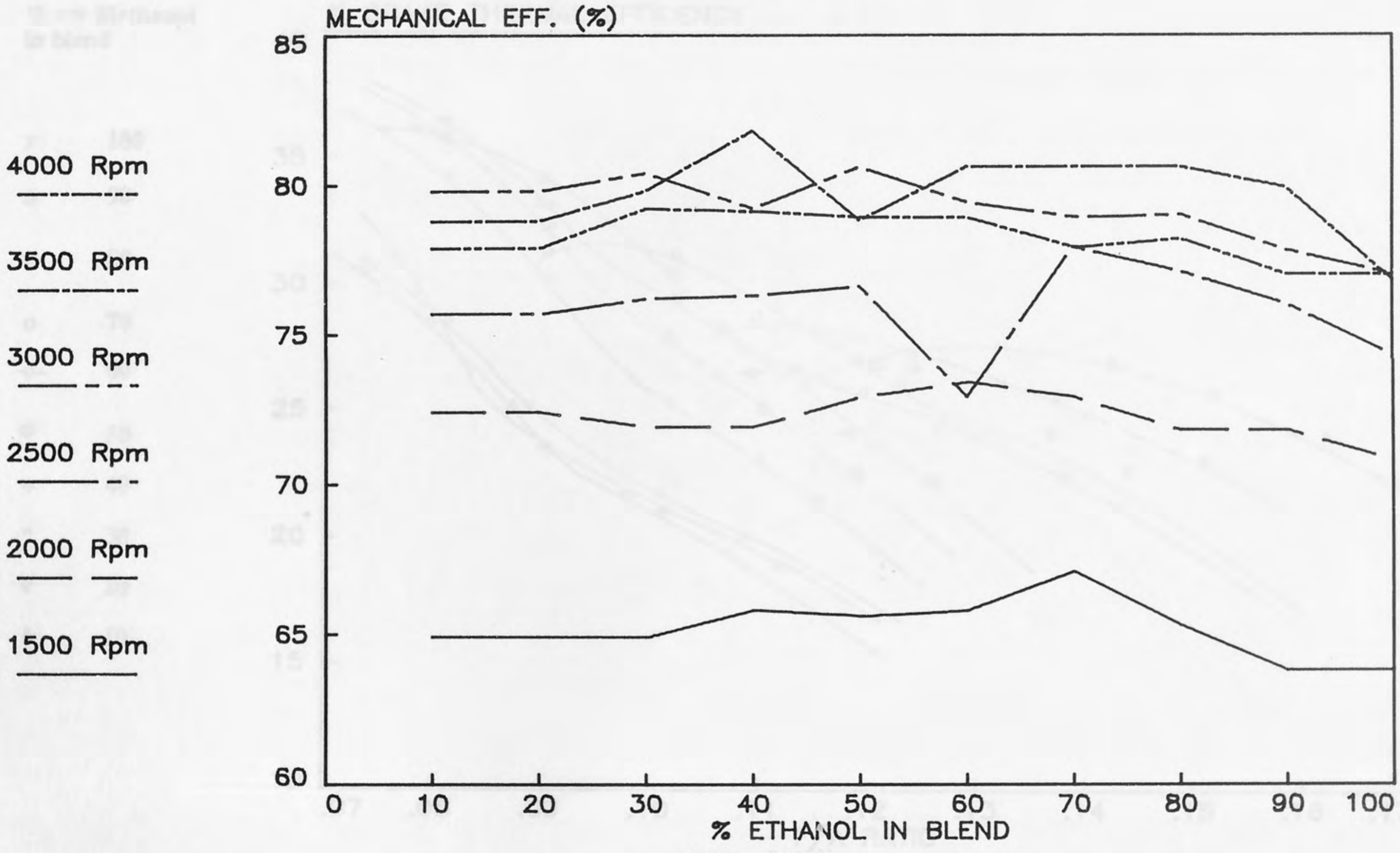

FIG: 4.1.44

EFFECT OF F/A RATIO ON BRAKE THERMAL EFF.
ENGINE SPEED:1500 RPM

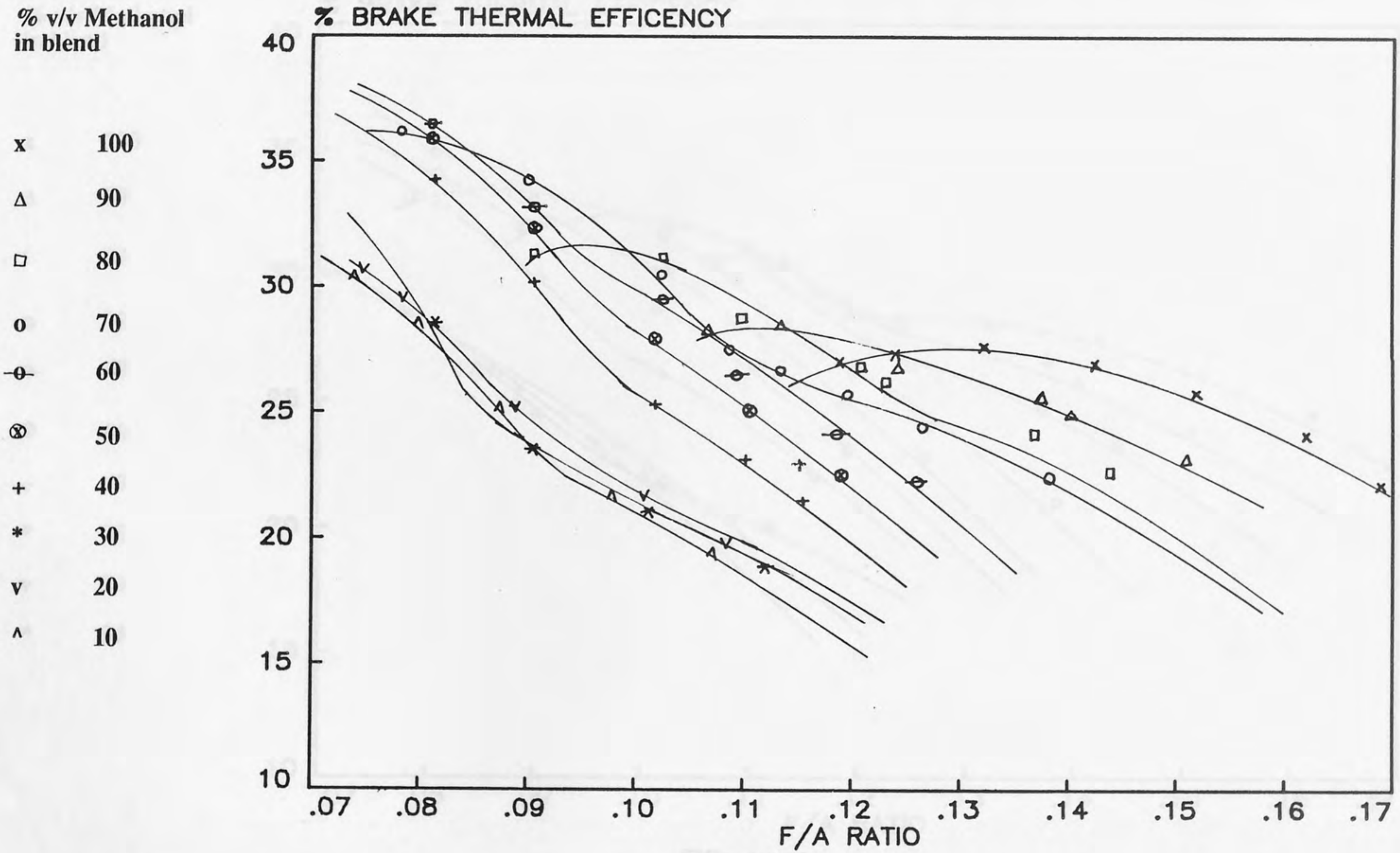

FIG: 4.1.45

EFFECT OF F/A RATIO ON BRAKE THERMAL EFF.
ENGINE SPEED:2000 RPM

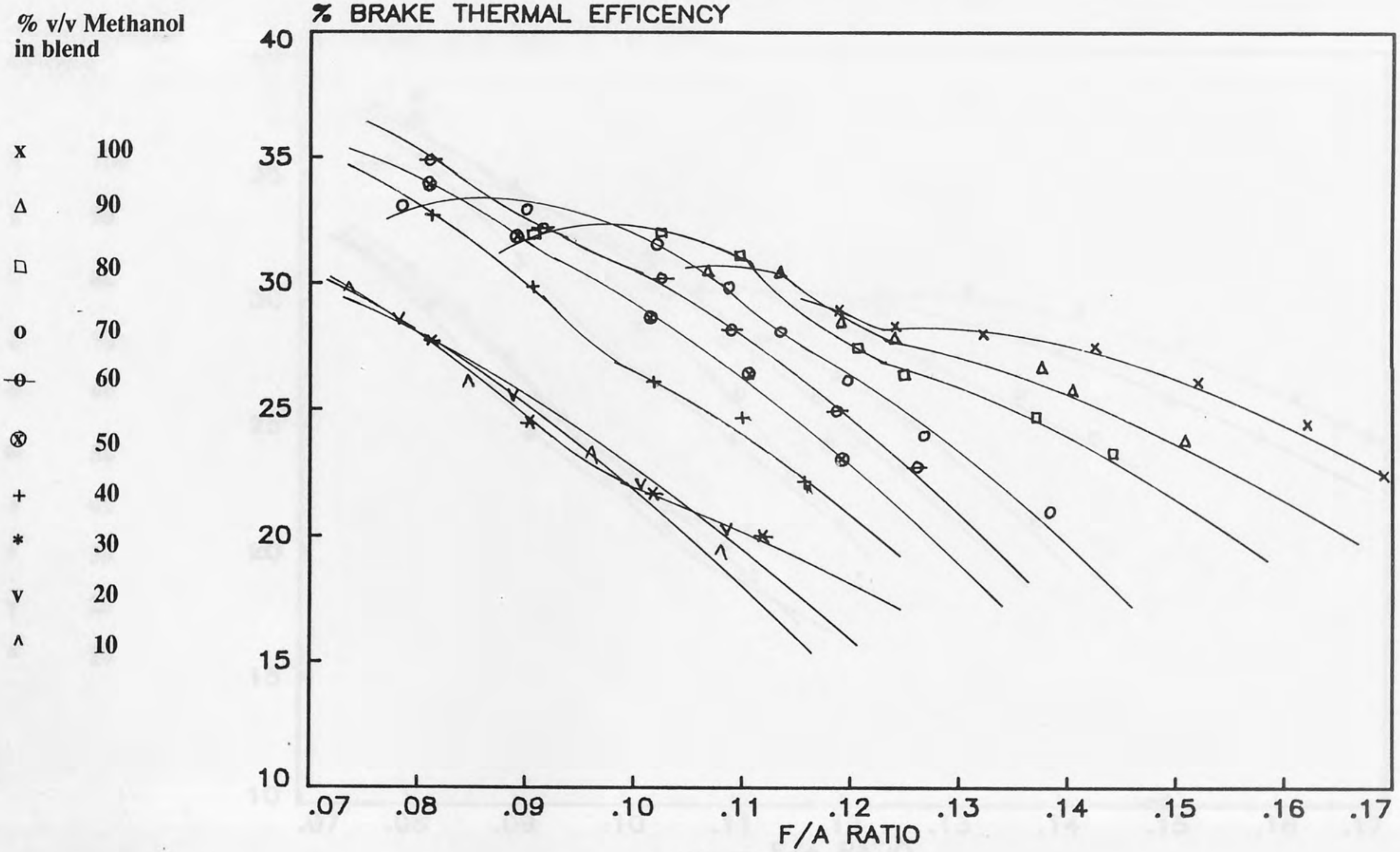

FIG: 4.1.46

EFFECT OF F/A RATIO ON BRAKE THERMAL EFF.
ENGINE SPEED:2500 RPM

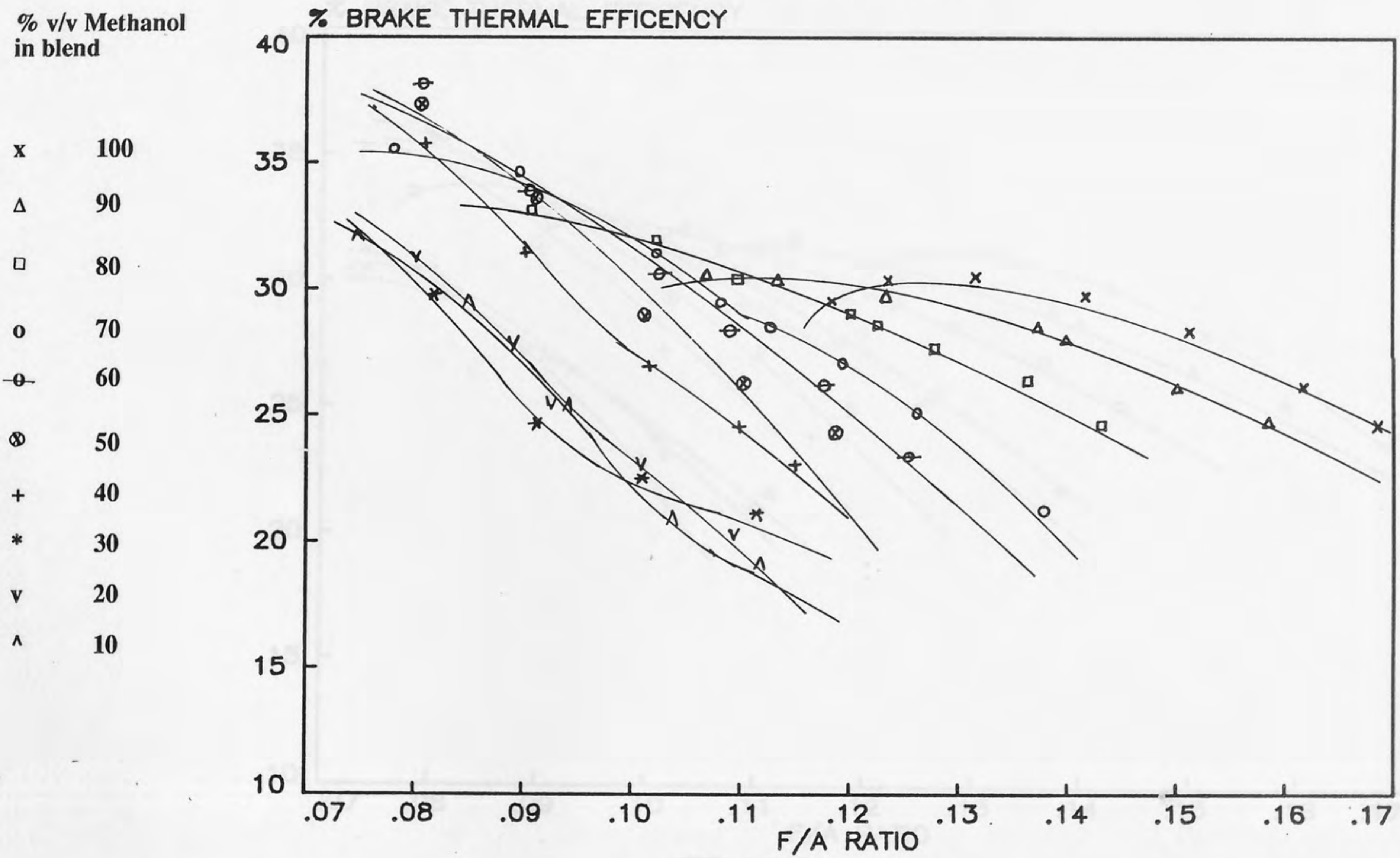

FIG: 4.1.47

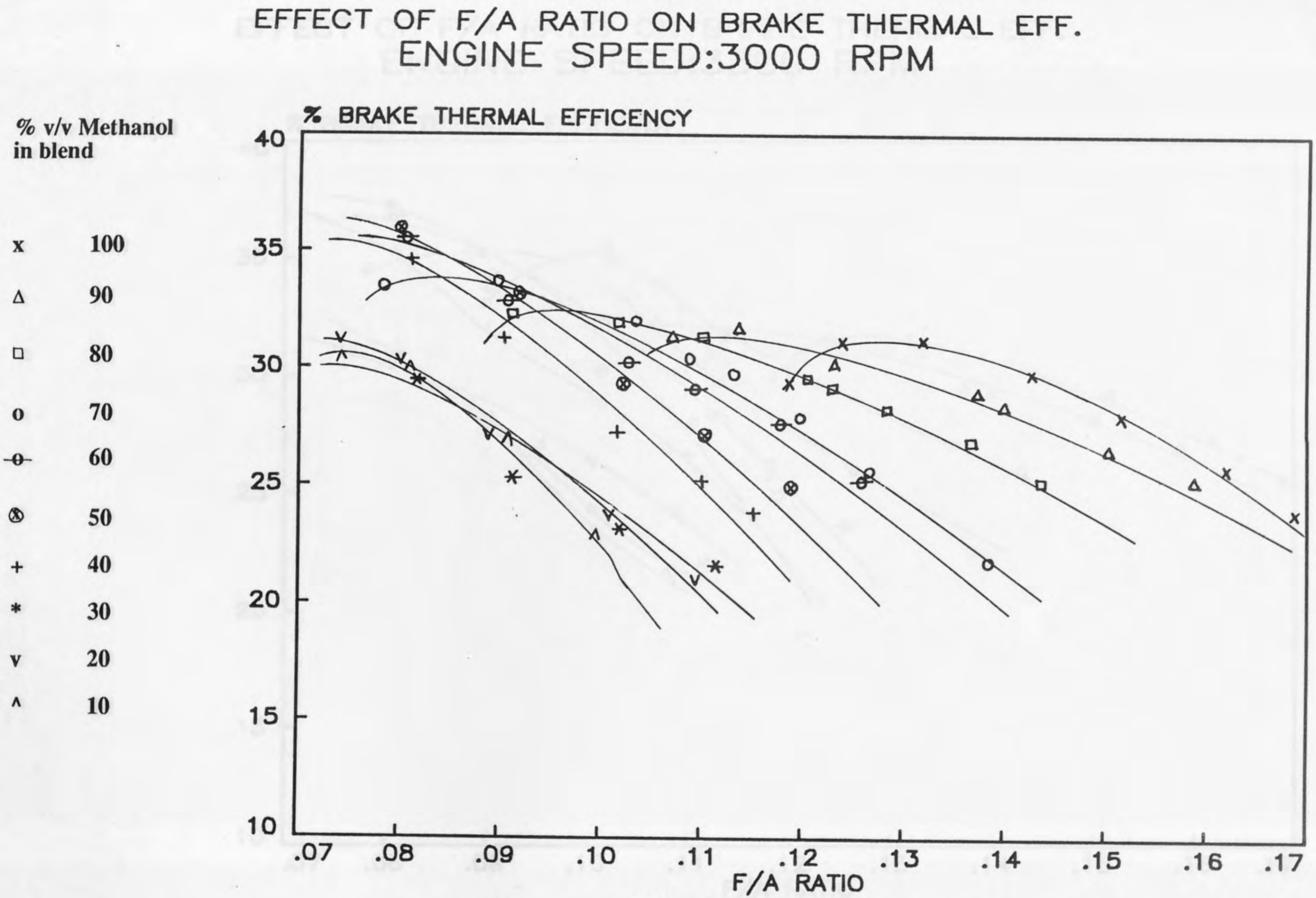
EFFECT OF F/A RATIO ON BRAKE THERMAL EFF.
ENGINE SPEED:3000 RPM
% v/v Methanol in blend
x 100
Δ 90
□ 80
o 70
-θ- 60
⊗ 50
+ 40
* 30
v 20
^ 10
% BRAKE THERMAL EFFICENCY
40
35
30
25
20
15
10
.07
.08
.09
.10
.11
.12
.13
.14
.15
.16
.17
F/A RATIO

FIG: 4.1.48

EFFECT OF F/A RATIO ON BRAKE THERMAL EFF.
ENGINE SPEED:3500 RPM

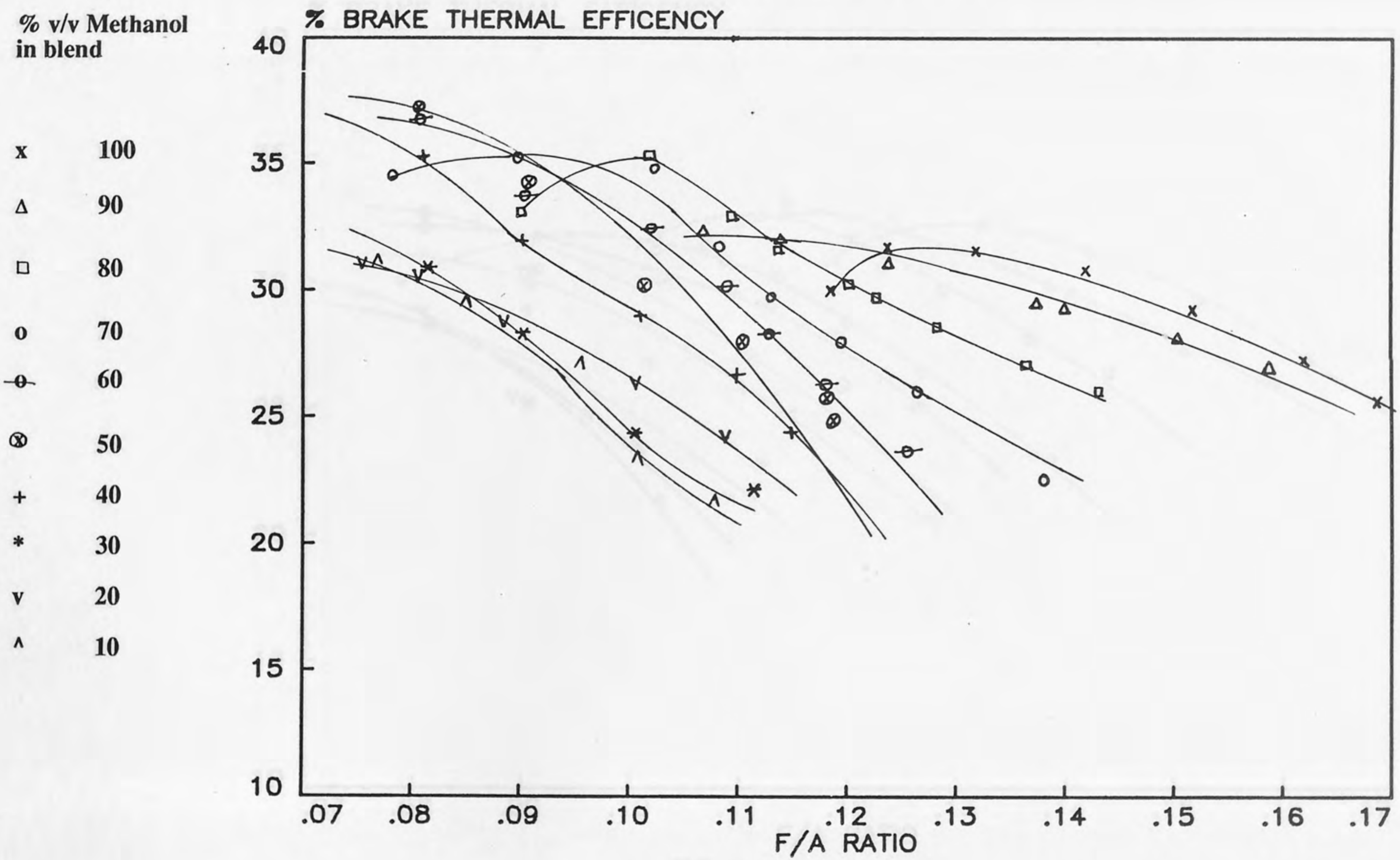

FIG: 4.1.49

EFFECT OF F/A RATIO ON BRAKE THERMAL EFF.
ENGINE SPEED:4000 RPM

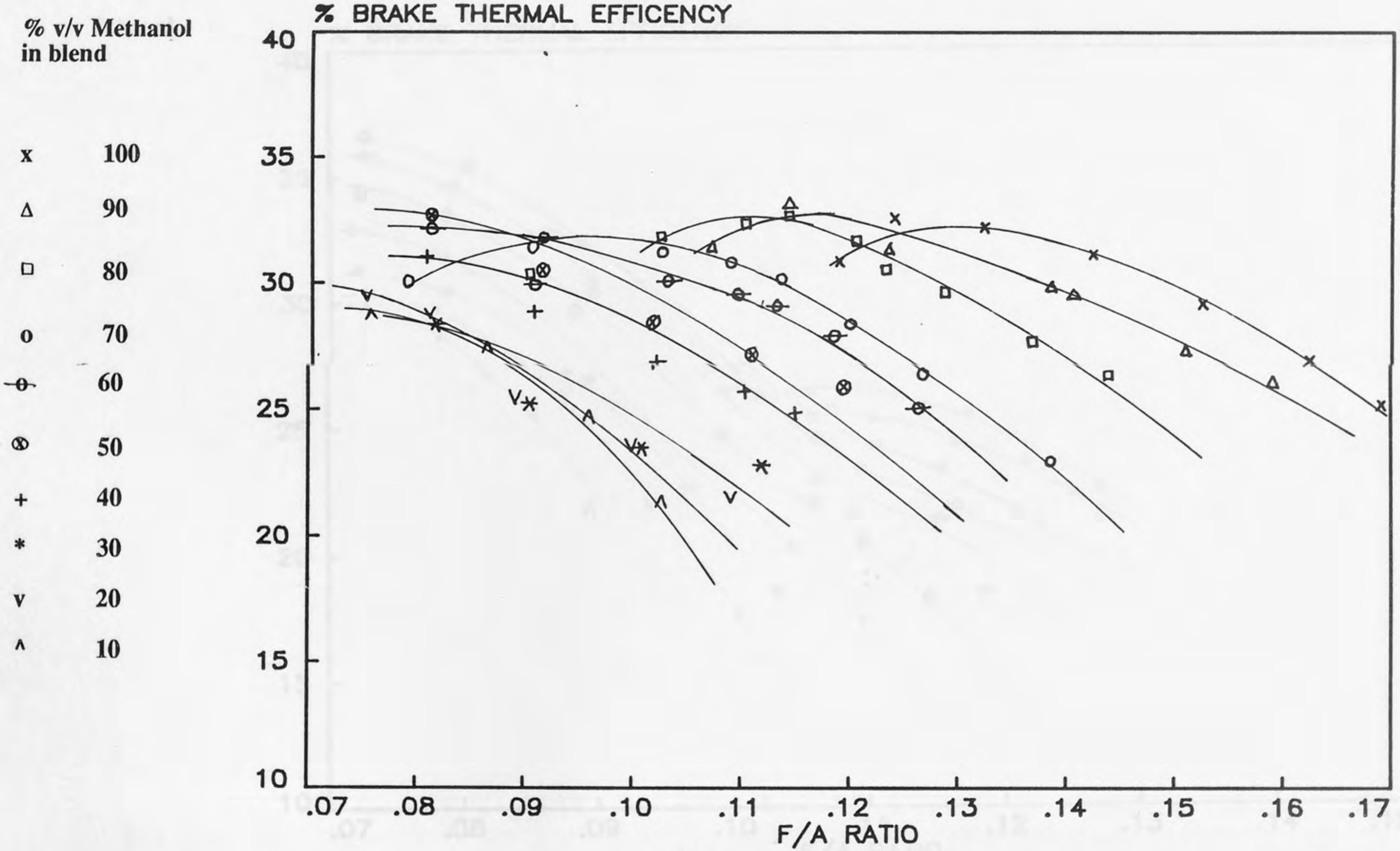

FIG: 4.1.50

EFFECT OF F/A RATIO ON BRAKE THERMAL EFF.
ENGINE SPEED:1500 RPM

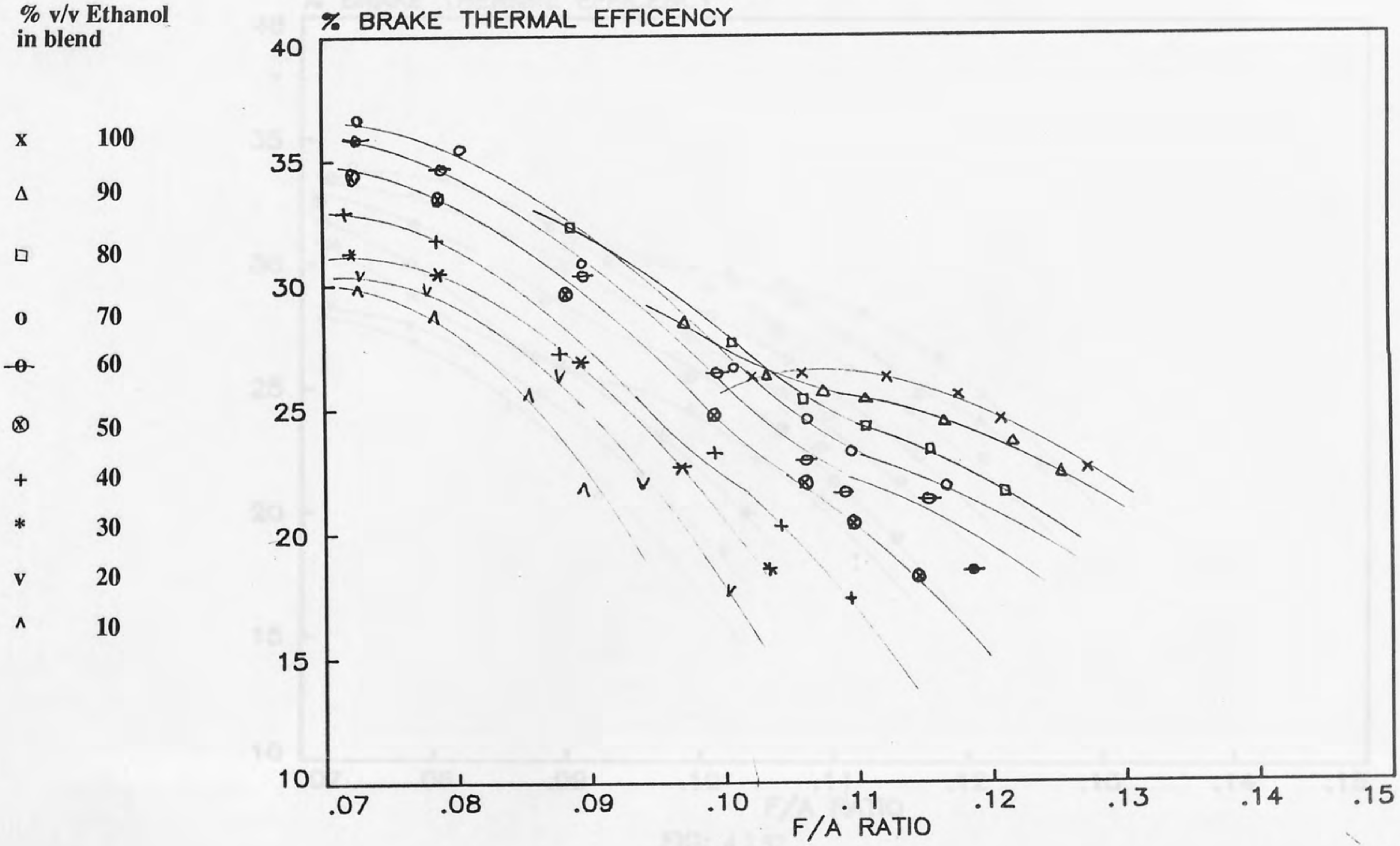

FIG: 4.1.51

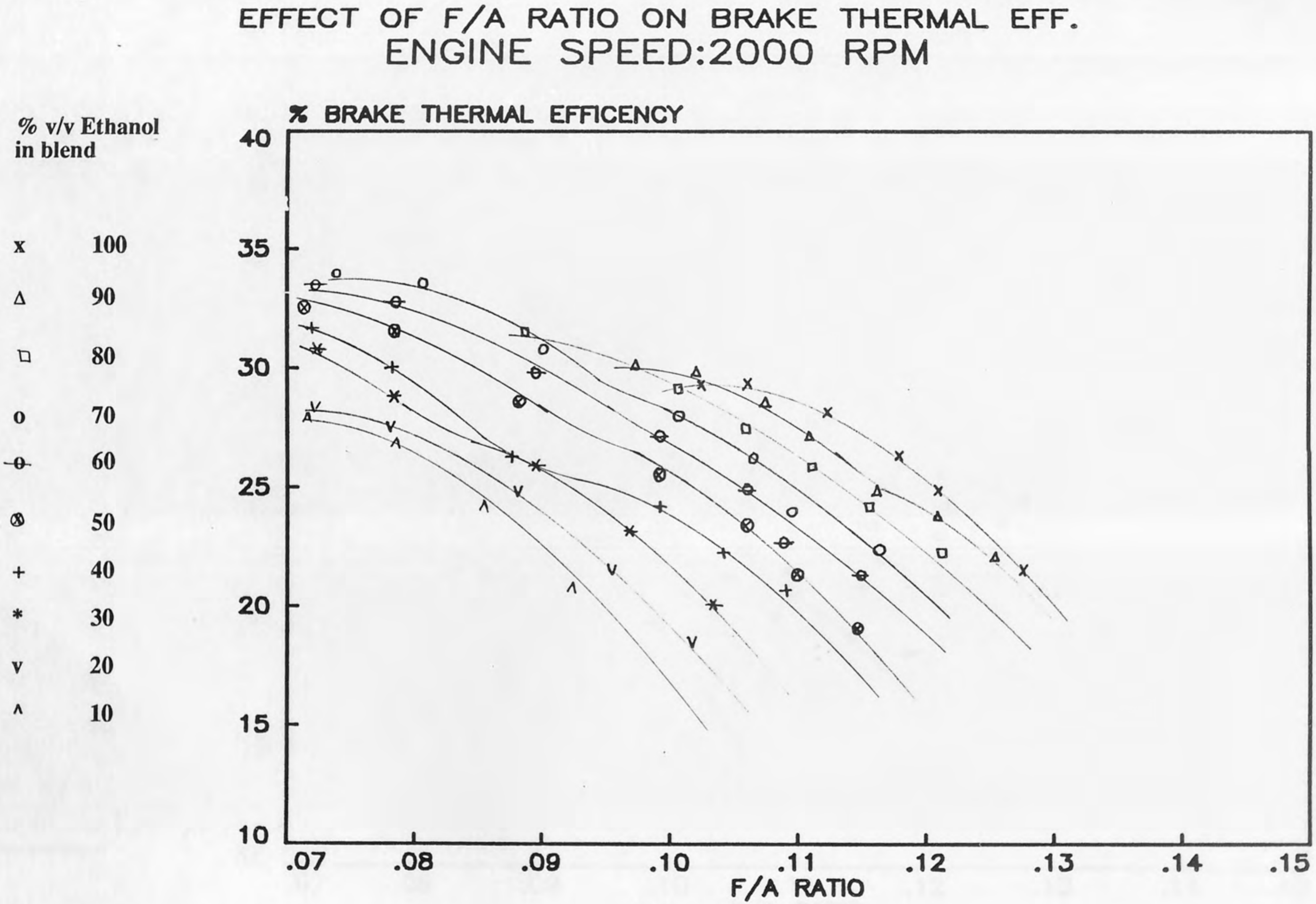

EFFECT OF F/A RATIO ON BRAKE THERMAL EFF.
ENGINE SPEED:2000 RPM

FIG: 4.1.52

This page has been left intentionally blank

EFFECT OF F/A RATIO ON BRAKE THERMAL EFF.
ENGINE SPEED:2500 RPM

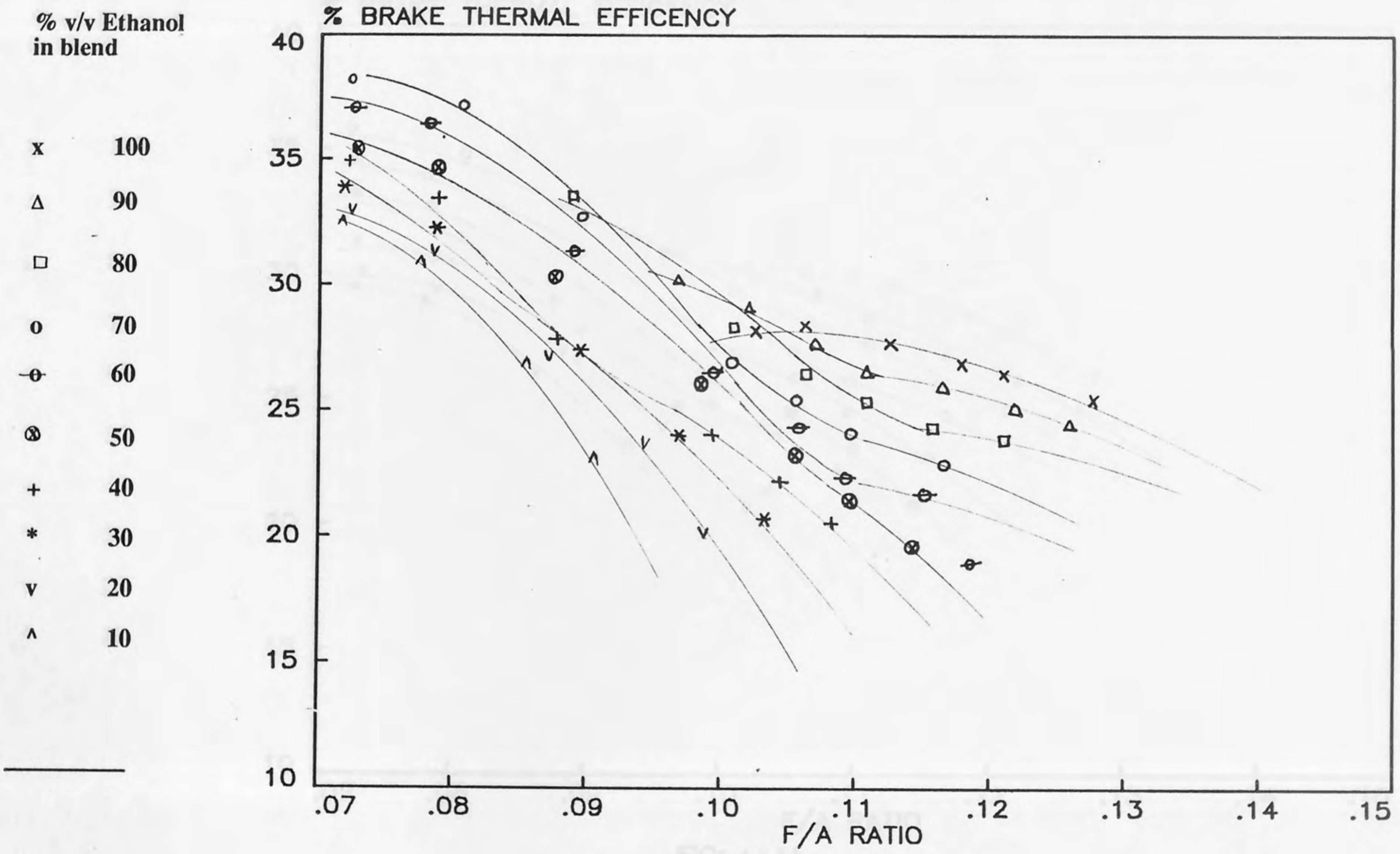

FIG: 4.1.53

EFFECT OF F/A RATIO ON BRAKE THERMAL EFF.
ENGINE SPEED:3000 RPM

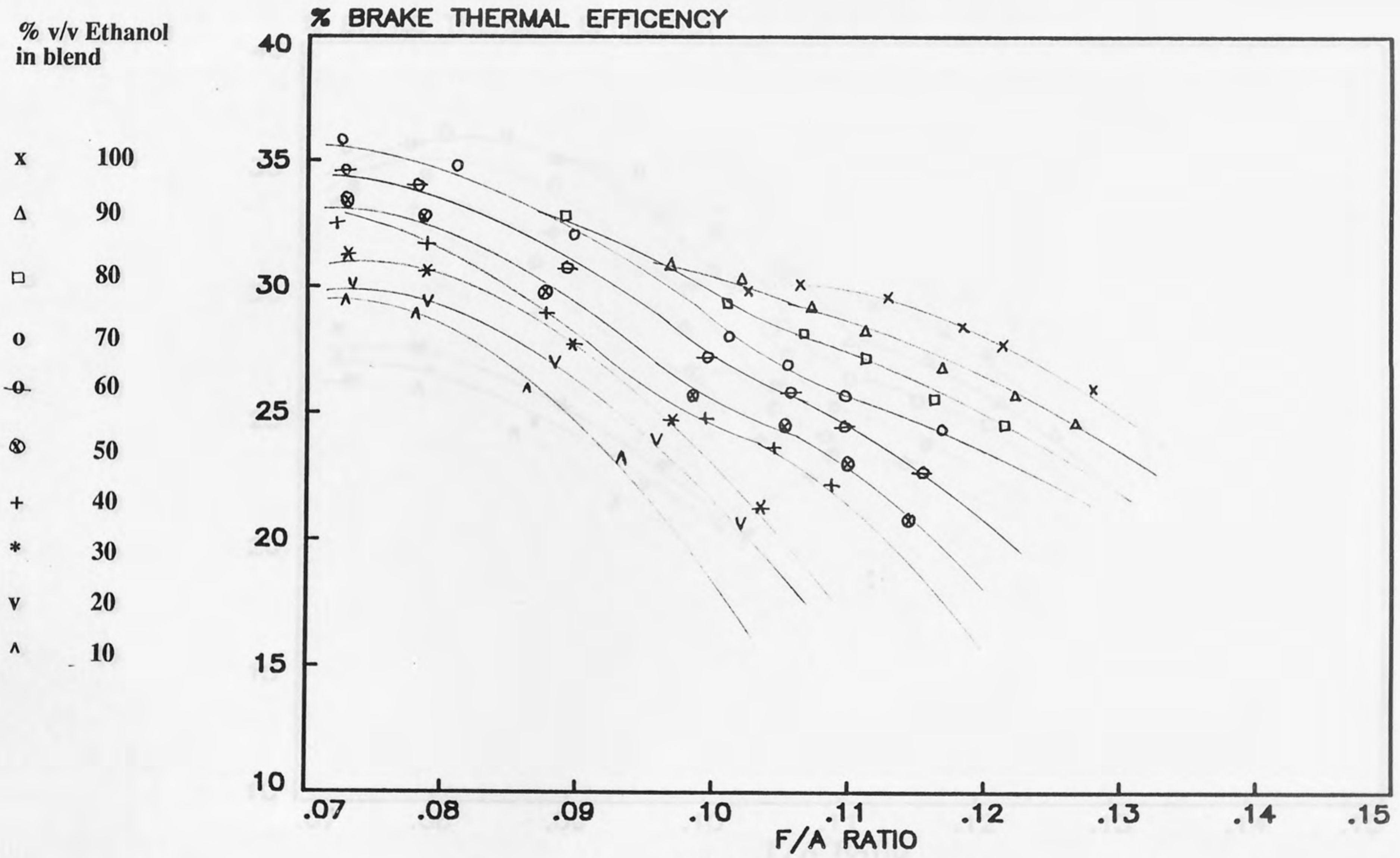

FIG: 4.1.54

EFFECT OF F/A RATIO ON BRAKE THERMAL EFF.
ENGINE SPEED:3500 RPM

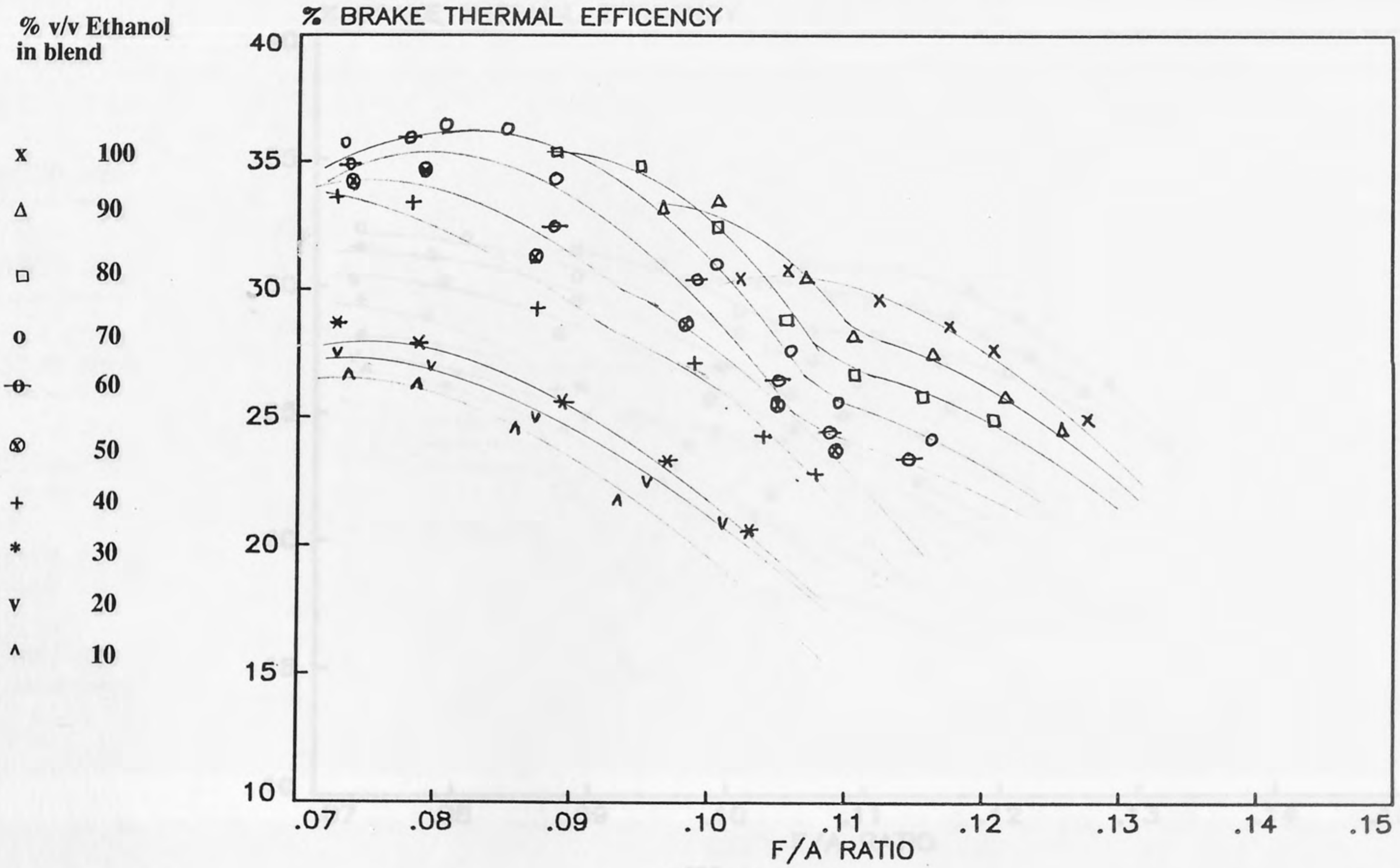

FIG: 4.1.55

EFFECT OF F/A RATIO ON BRAKE THERMAL EFF.
ENGINE SPEED:4000 RPM

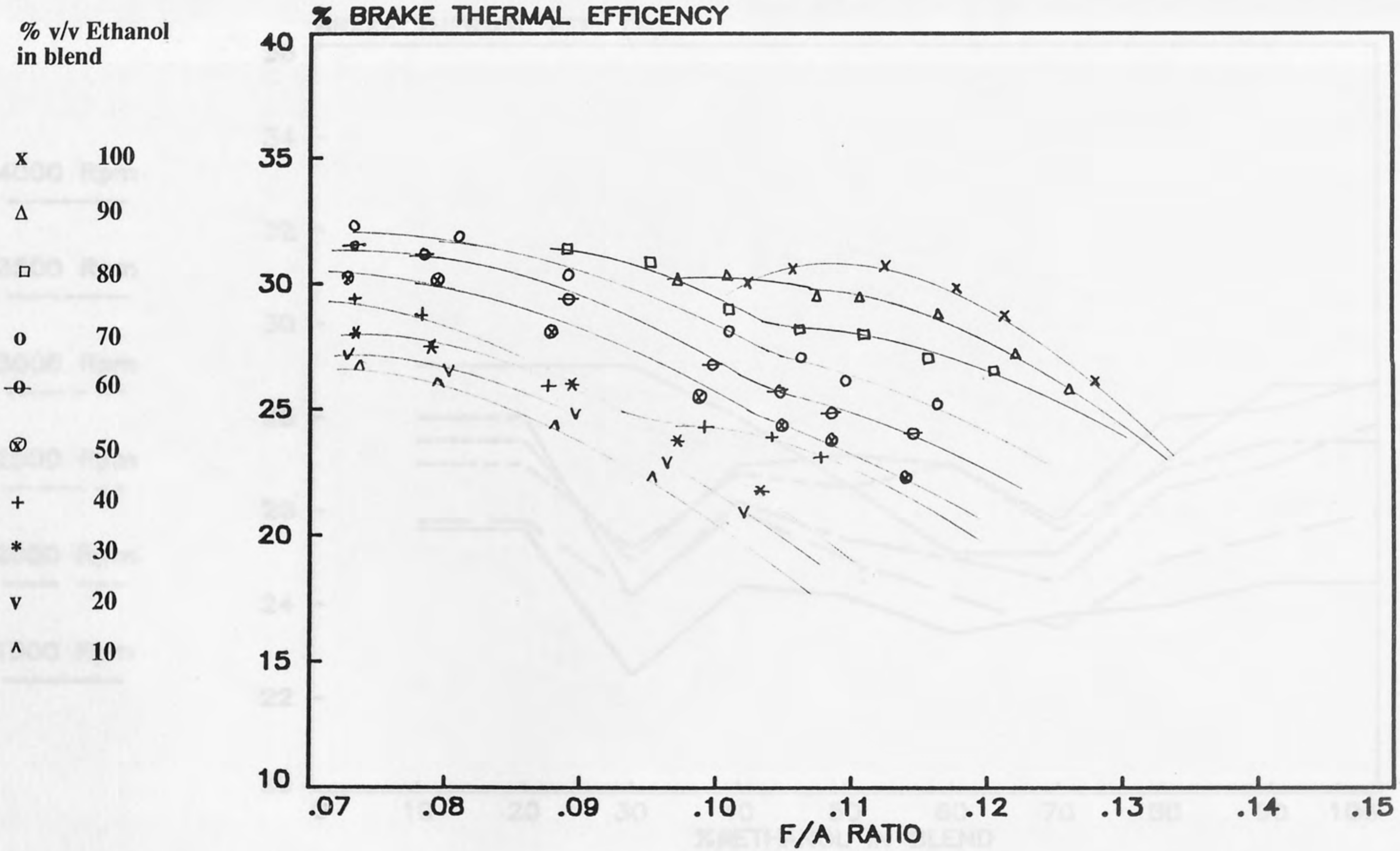

FIG: 4.1.56

EFFECT OF ALCOHOL CONTENT ON THERMAL EFF.
AT STOICHIOMETRIC F/A RATIO

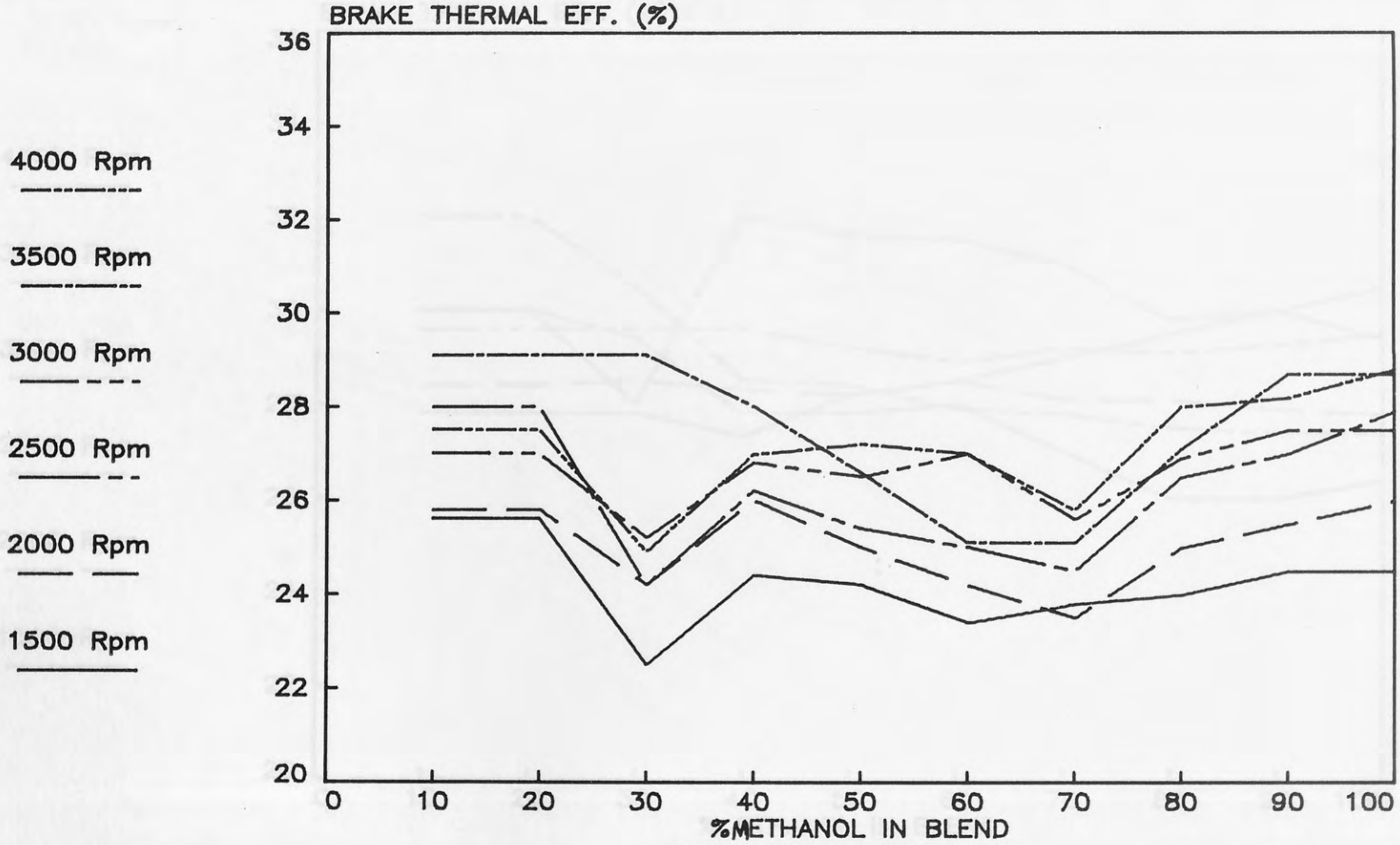

FIG: 4.1.57

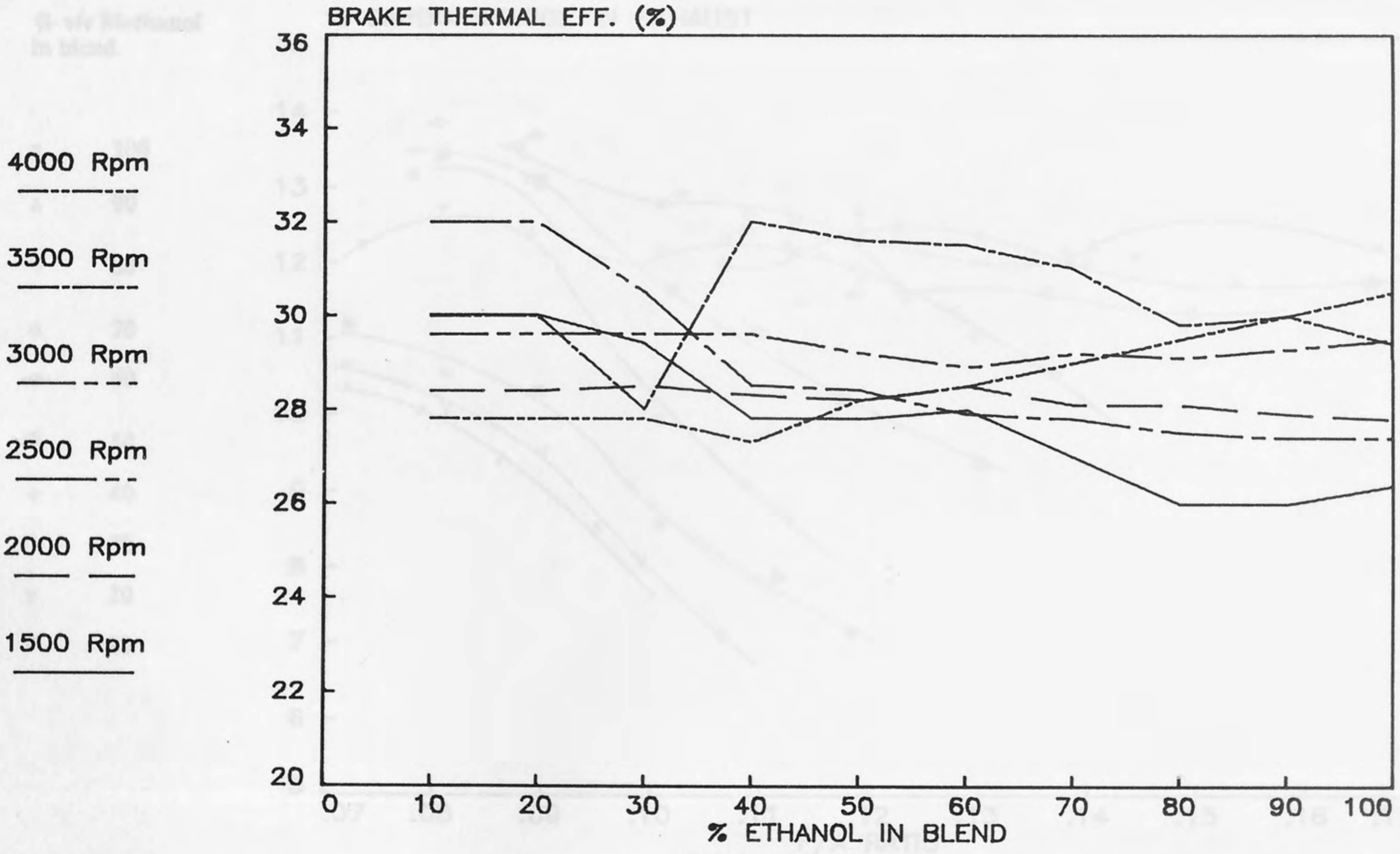

EFFECT OF ALCOHOL CONTENT ON THERMAL EFF.
AT STOICHIOMETRIC F/A RATIO

FIG: 4.1.58

EFFECT OF F/A RATIO ON CARBONDIOXIDE EMISSION
ENGINE SPEED:1500 RPM

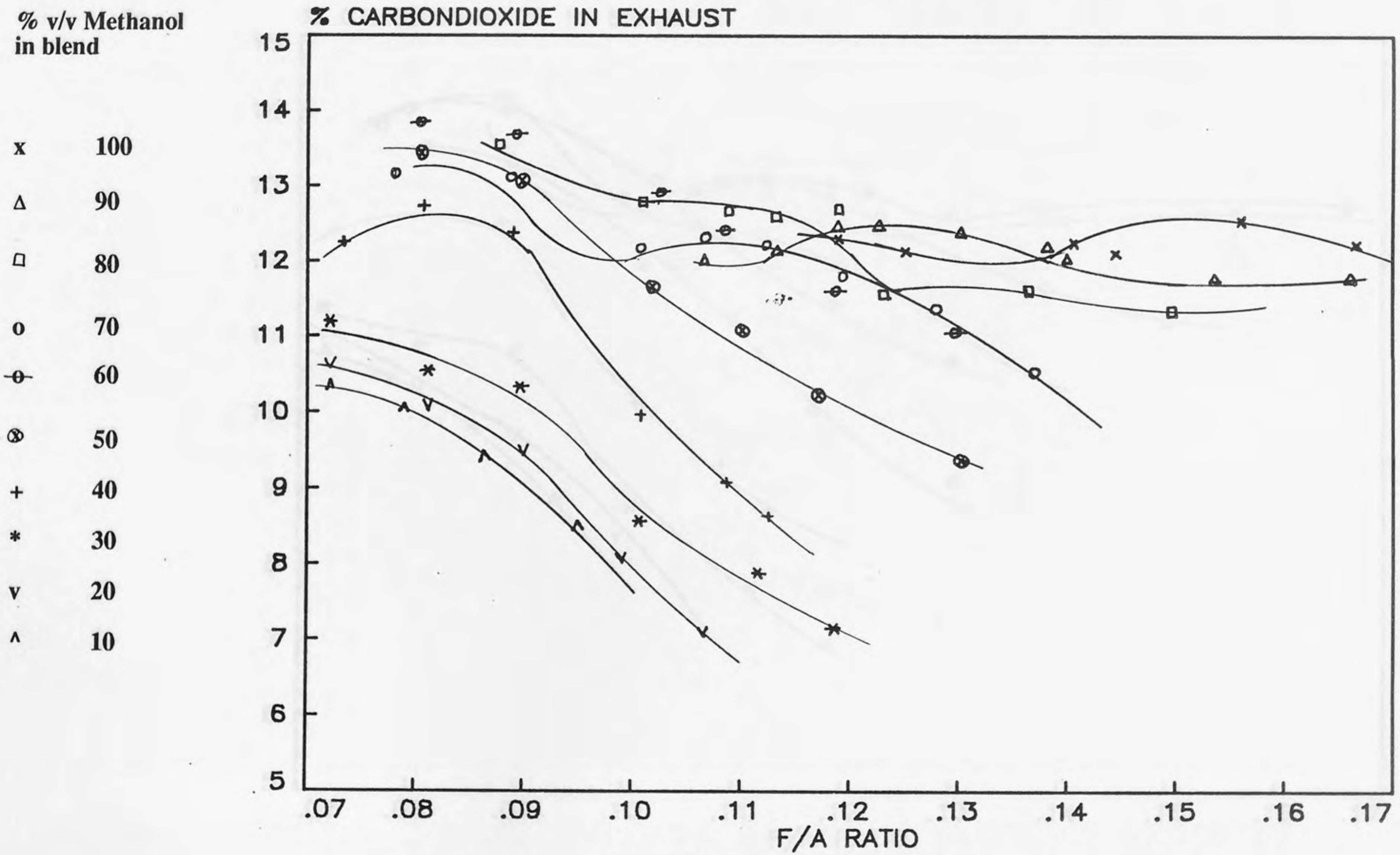

FIG: 4.1.59

EFFECT OF F/A RATIO ON CARBONDIOXIDE EMISSION
ENGINE SPEED:2000 RPM

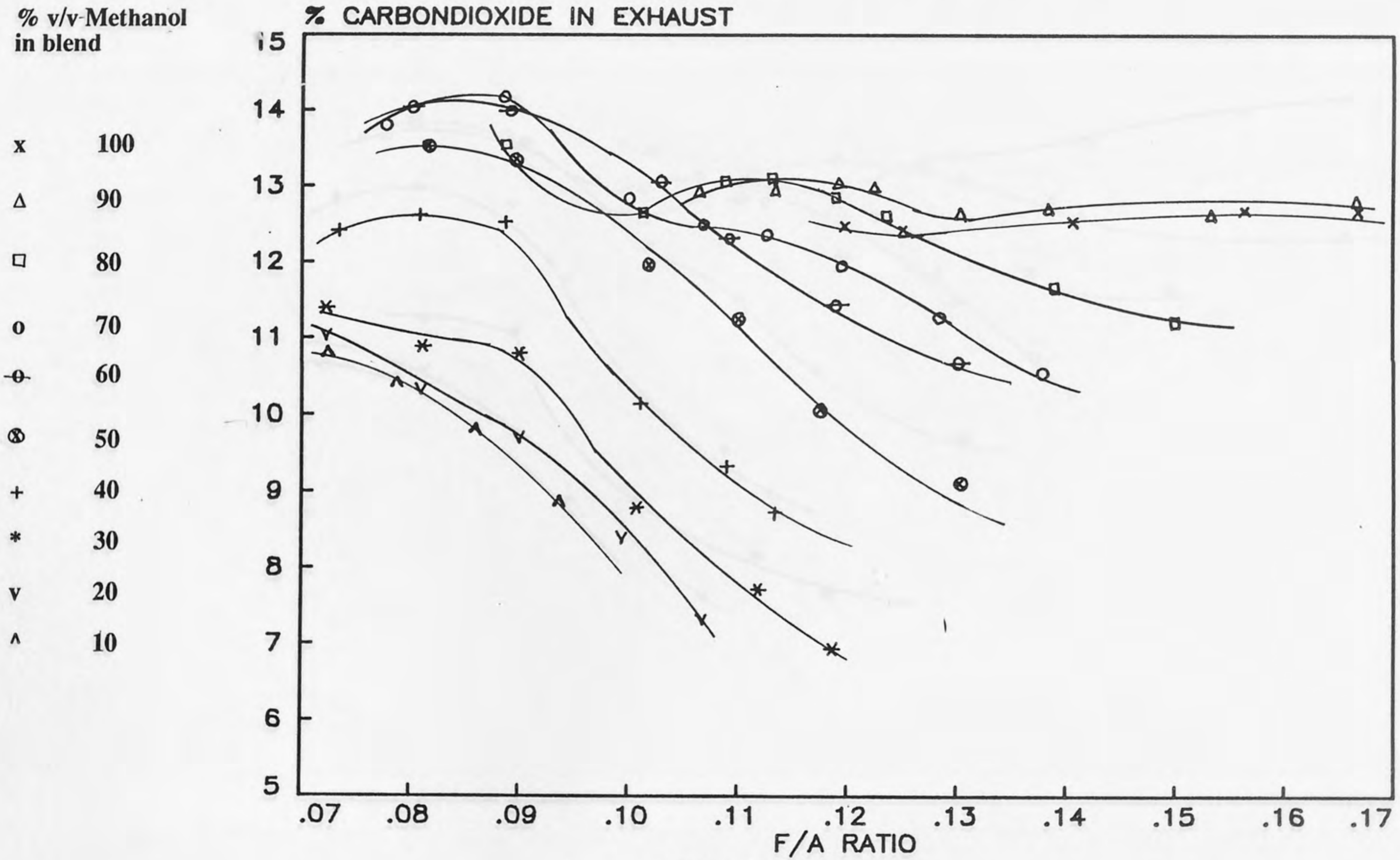

FIG: 4.1.60

EFFECT OF F/A RATIO ON CARBONDIOXIDE EMISSION
ENGINE SPEED:2500 RPM

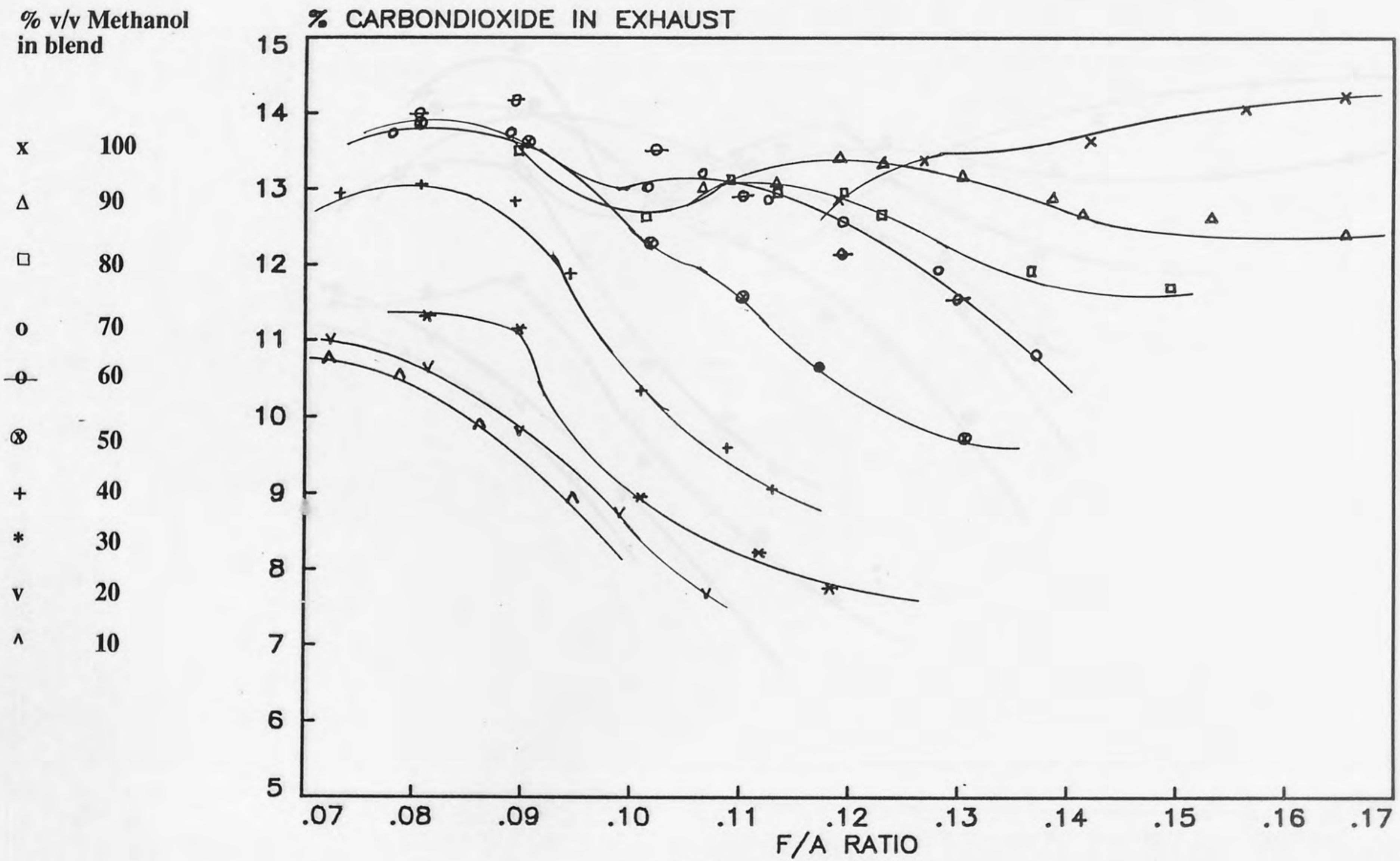

FIG: 4.1.61

EFFECT OF F/A RATIO ON CARBONDIOXIDE EMISSION
ENGINE SPEED:3000 RPM

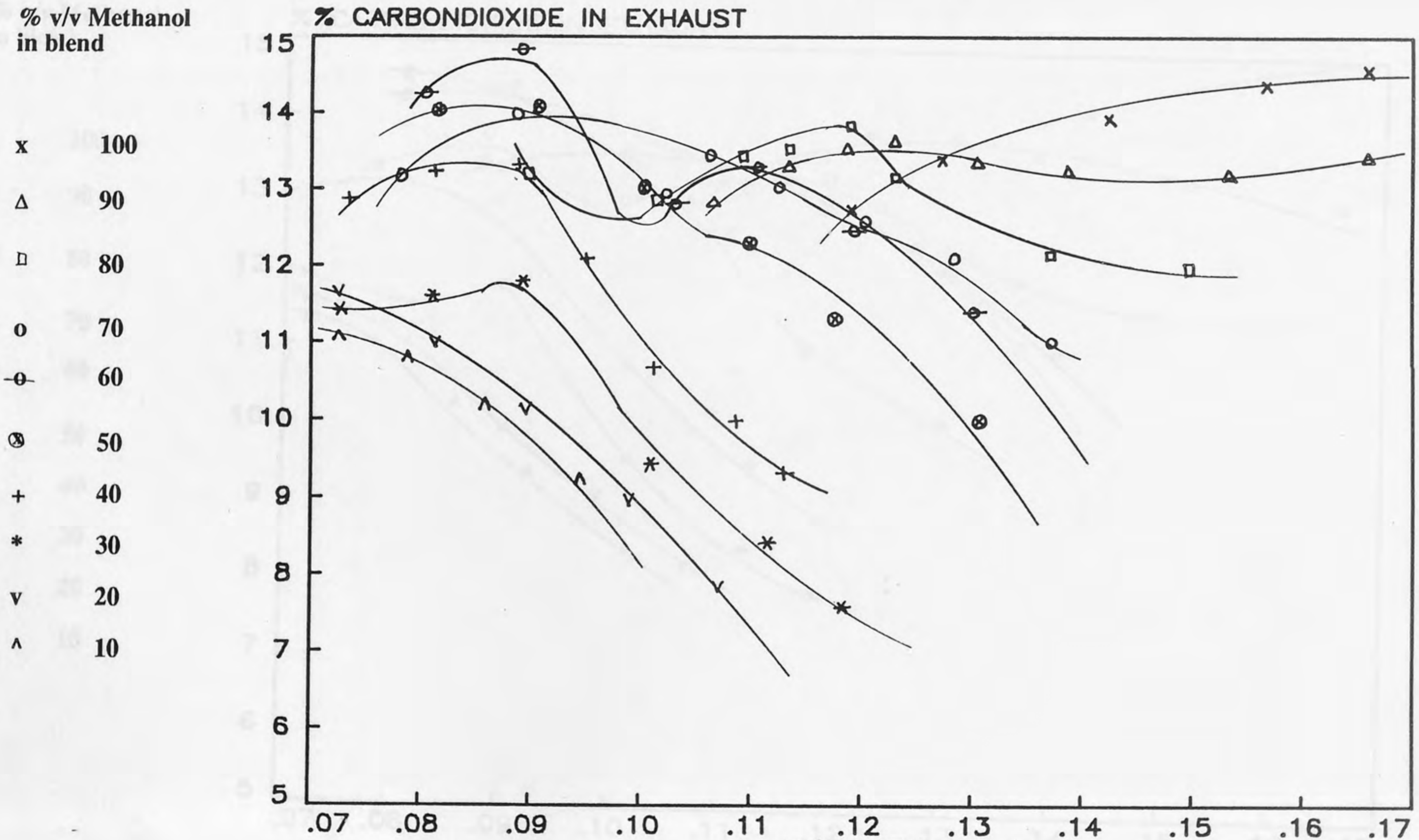

FIG: 4.1.62

EFFECT OF F/A RATIO ON CARBONDIOXIDE EMISSION
ENGINE SPEED:3500 RPM

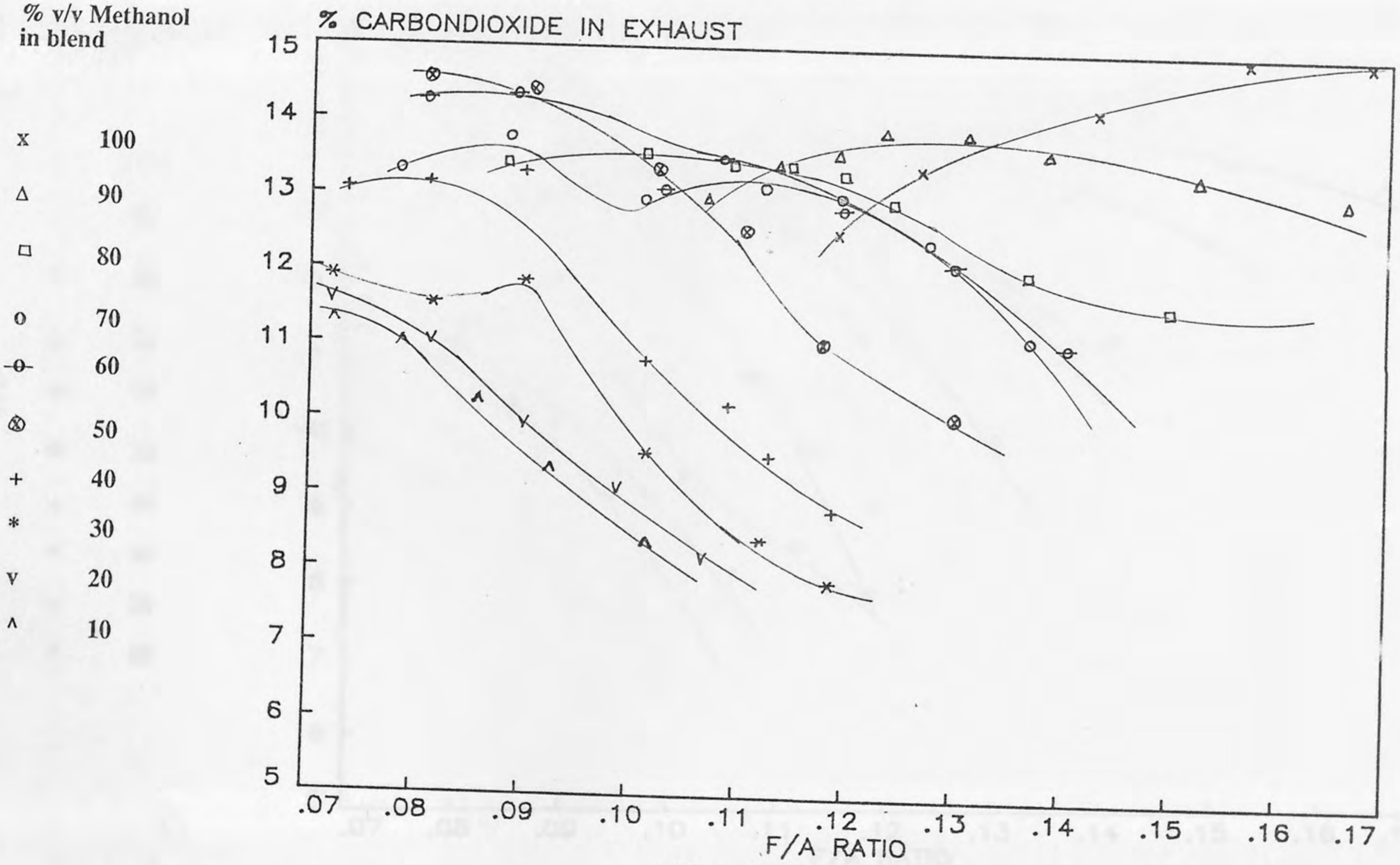

FIG: 4.1.63

EFFECT OF F/A RATIO ON CARBONDIOXIDE EMISSION
ENGINE SPEED:4000 RPM

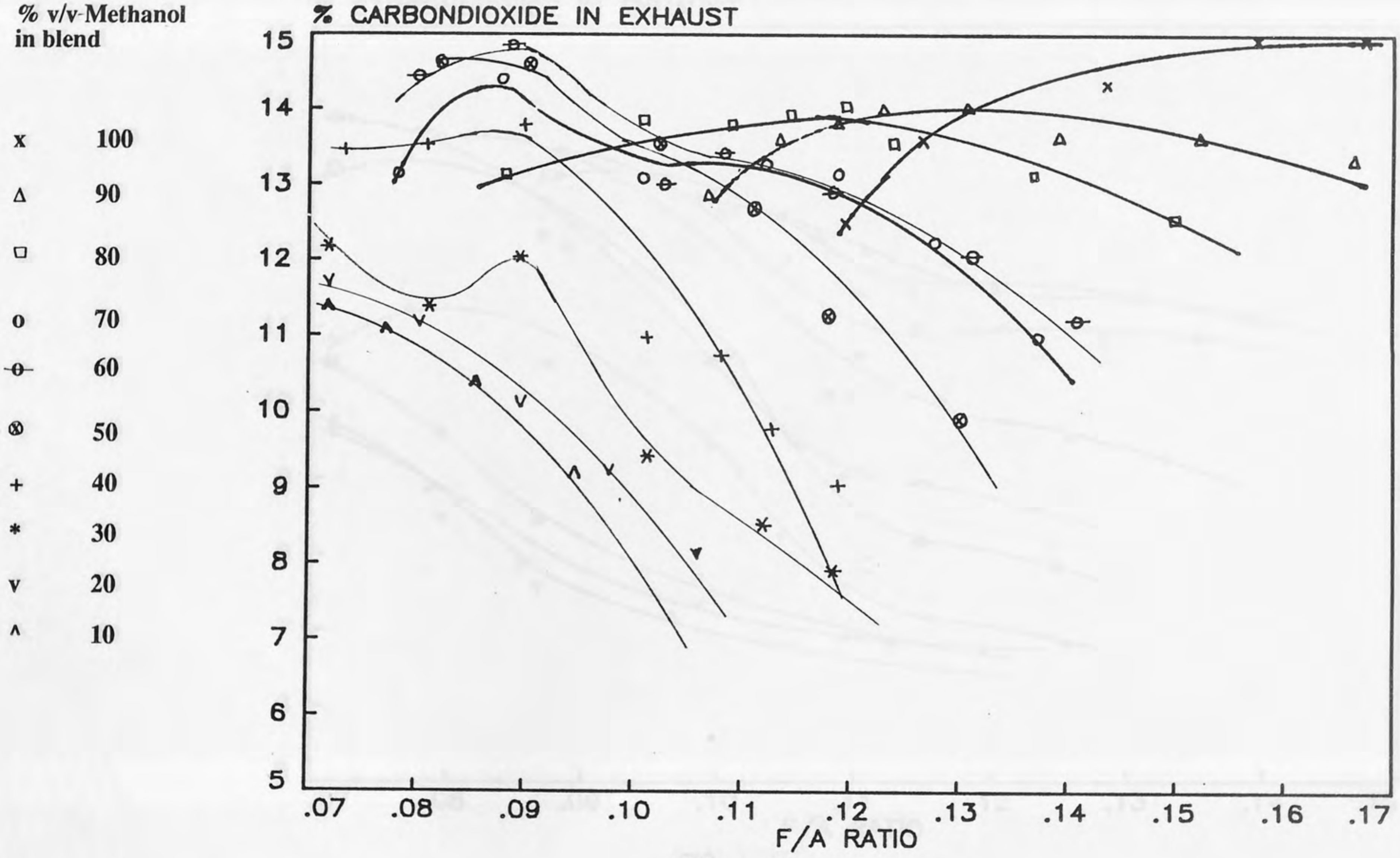

FIG: 4.1.64

Ethanol

EFFECT OF F/A RATIO ON CARBONDIOXIDE EMISSION
ENGINE SPEED:1500 RPM

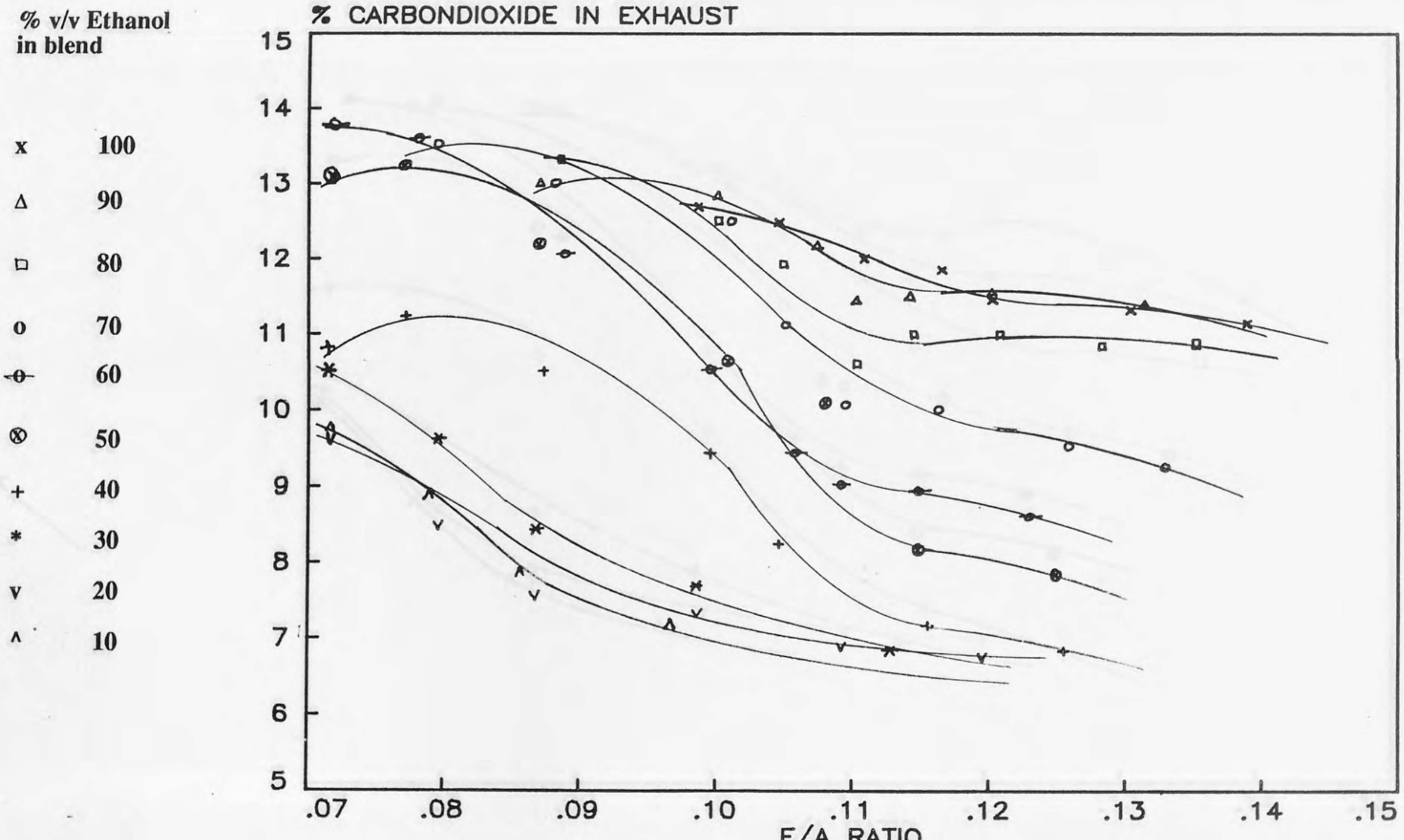

FIG: 4.1.65

EFFECT OF F/A RATIO ON CARBONDIOXIDE EMISSION
ENGINE SPEED:2000 RPM

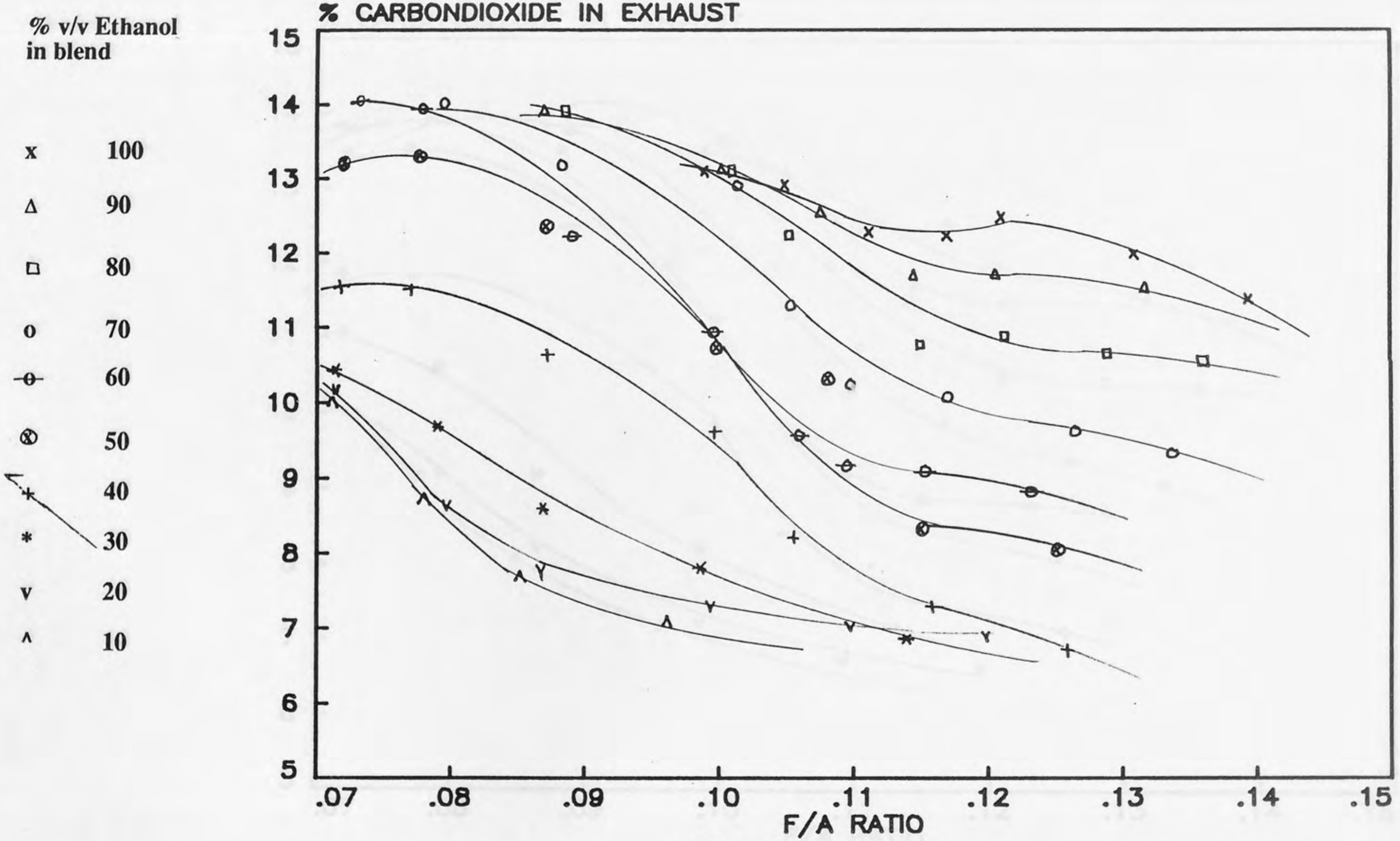

FIG: 4.1.66

Ethanol

EFFECT OF F/A RATIO ON CARBONDIOXIDE EMISSION
ENGINE SPEED:2500 RPM

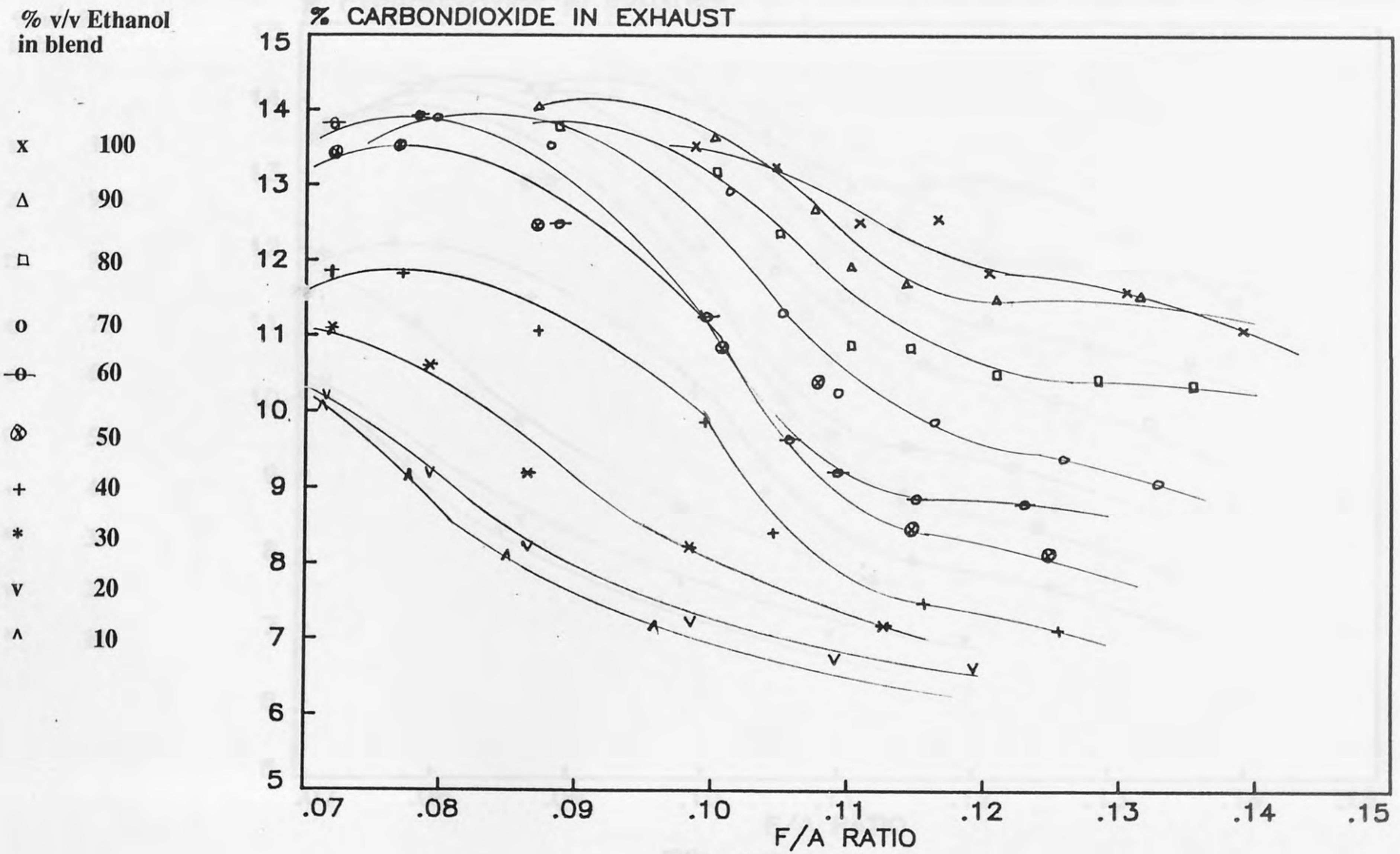

FIG: 4.1.67

EFFECT OF F/A RATIO ON CARBONDIOXIDE EMISSION
ENGINE SPEED:3000 RPM

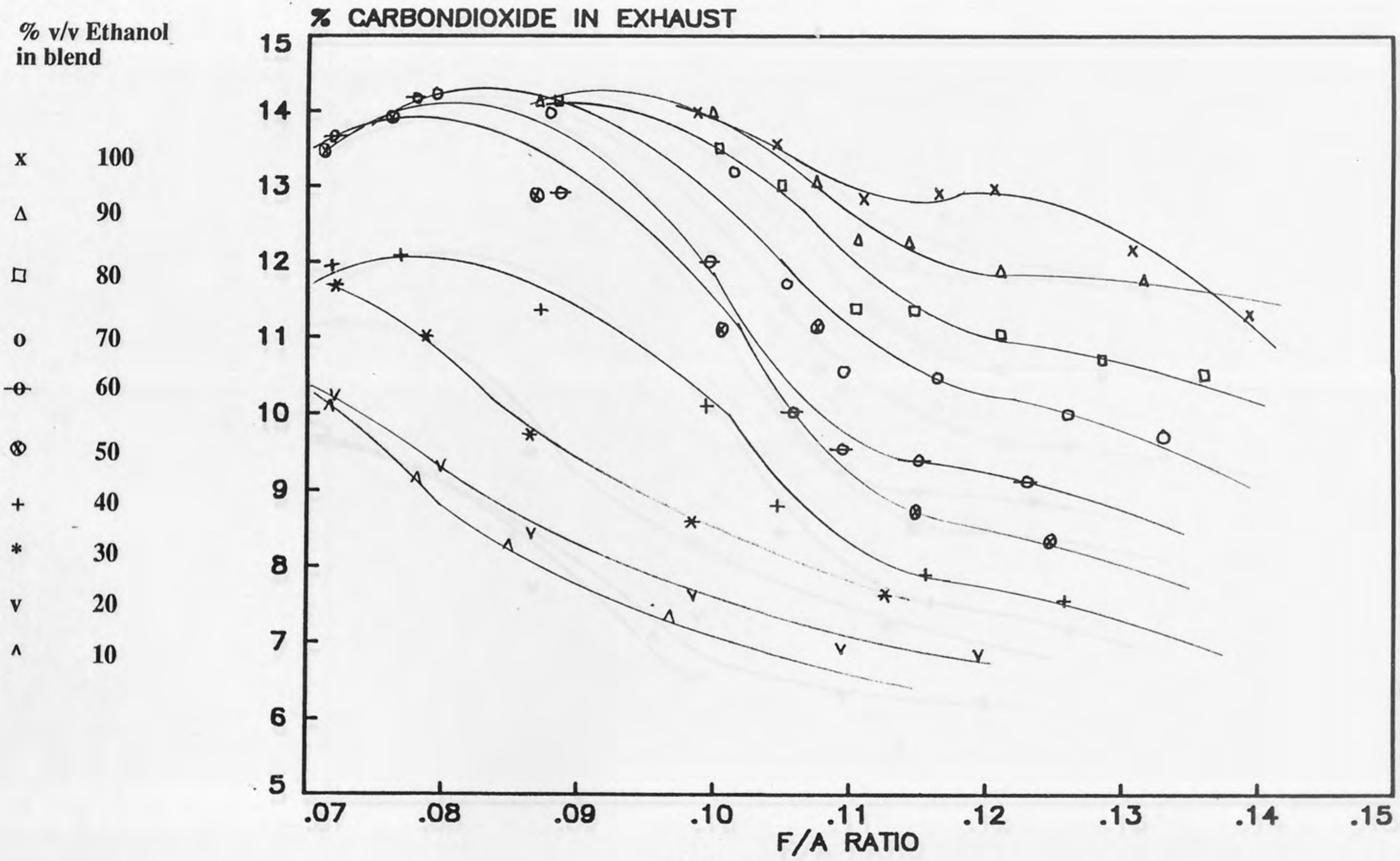

FIG: 4.1.68

Ethanol

EFFECT OF F/A RATIO ON CARBONDIOXIDE EMISSION
ENGINE SPEED:3500 RPM

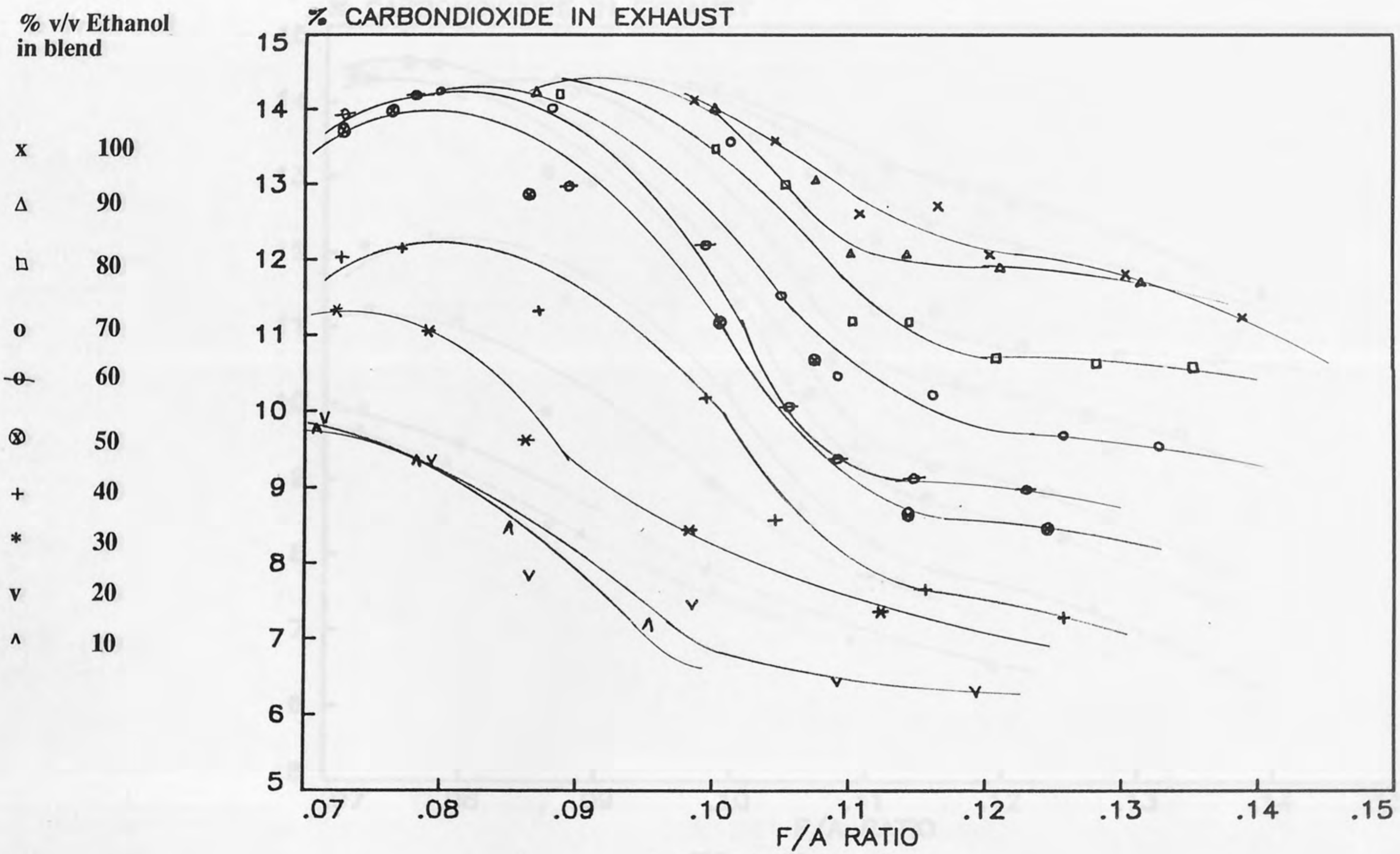

FIG: 4.1.69

EFFECT OF F/A RATIO ON CARBONDIOXIDE EMISSION
ENGINE SPEED:4000 RPM

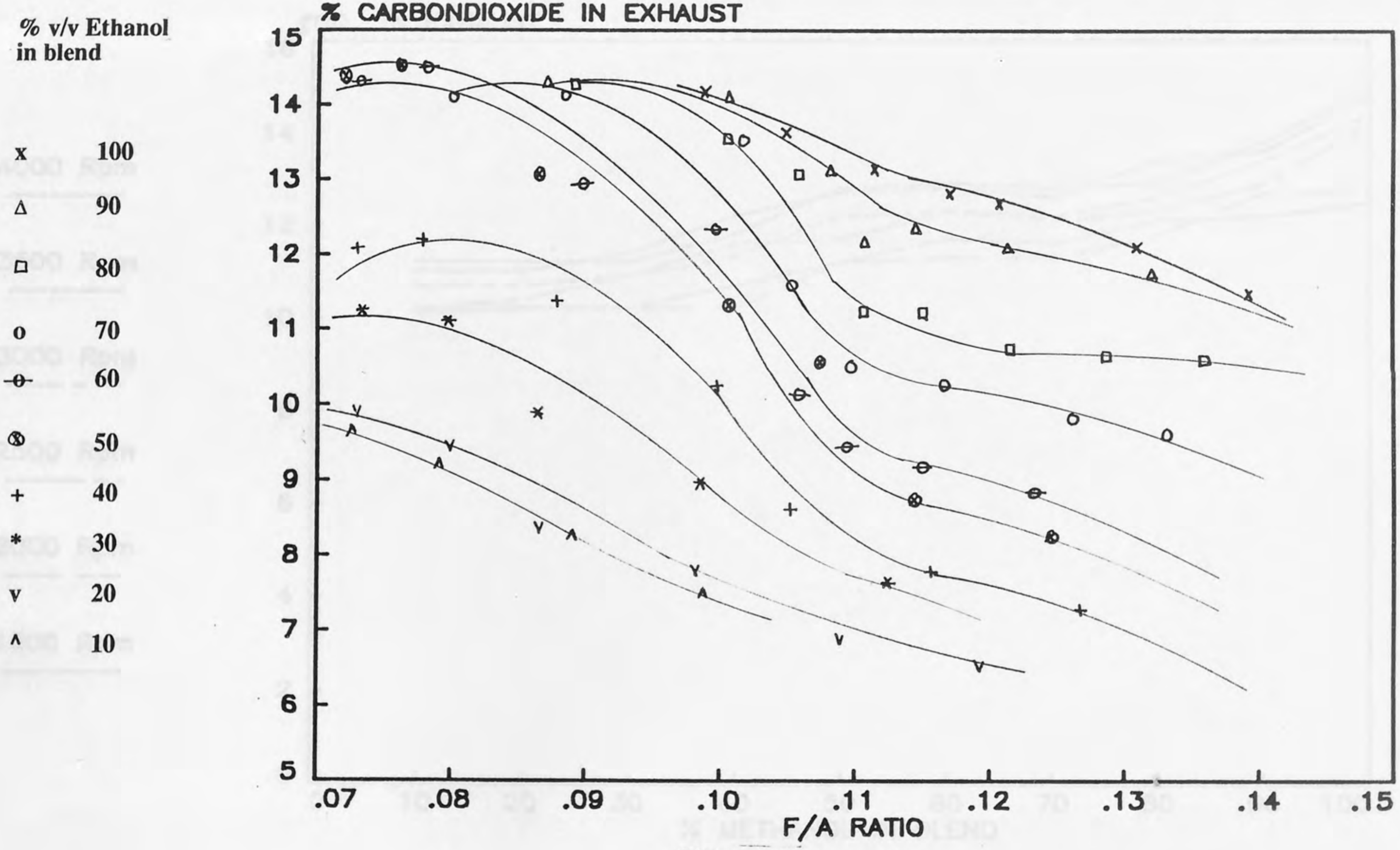

FIG: 4.1.70

EFFECT OF ALCOHOL CONTENT ON CO.. EMISSION
AT STOICHIOMETRIC F/A RATIO

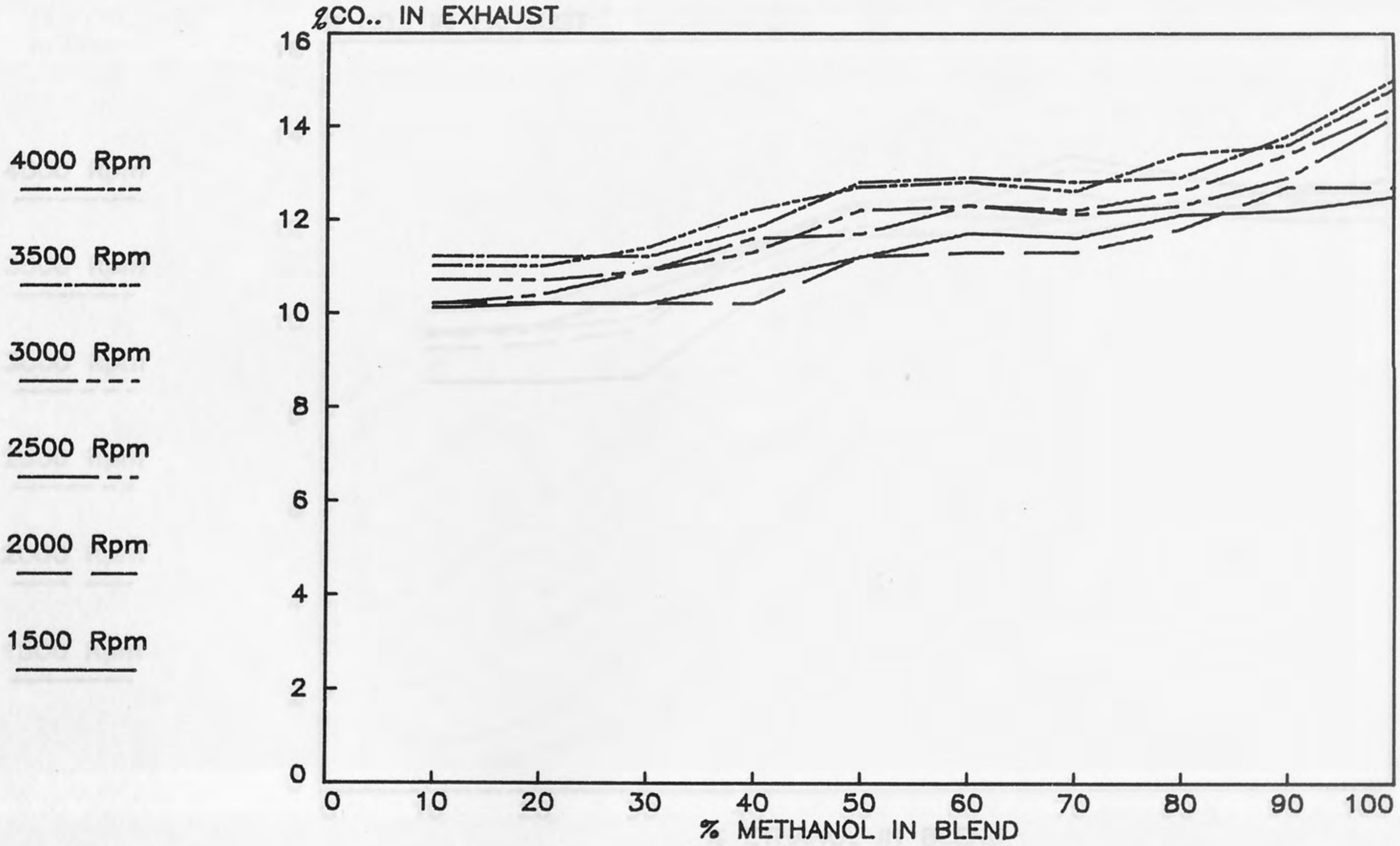

FIG: 4.1.71

EFFECT OF ALCOHOL CONTENT ON CO.. EMISSION
AT STOICHIOMETRIC F/A RATIO

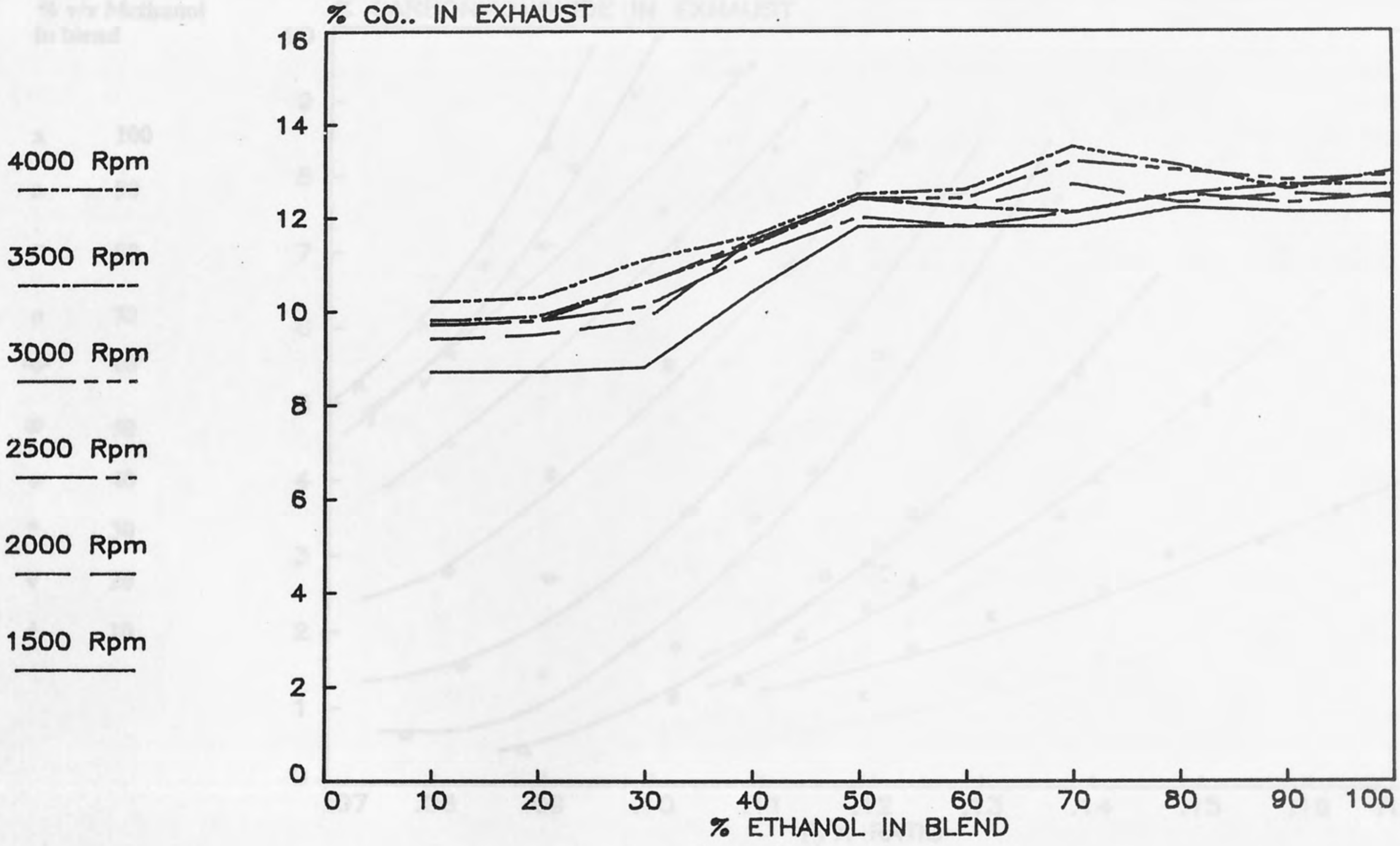

FIG: 4.1.72

Methanol

EFFECT OF F/A RATIO ON CO EMISSION
ENGINE SPEED:1500 RPM

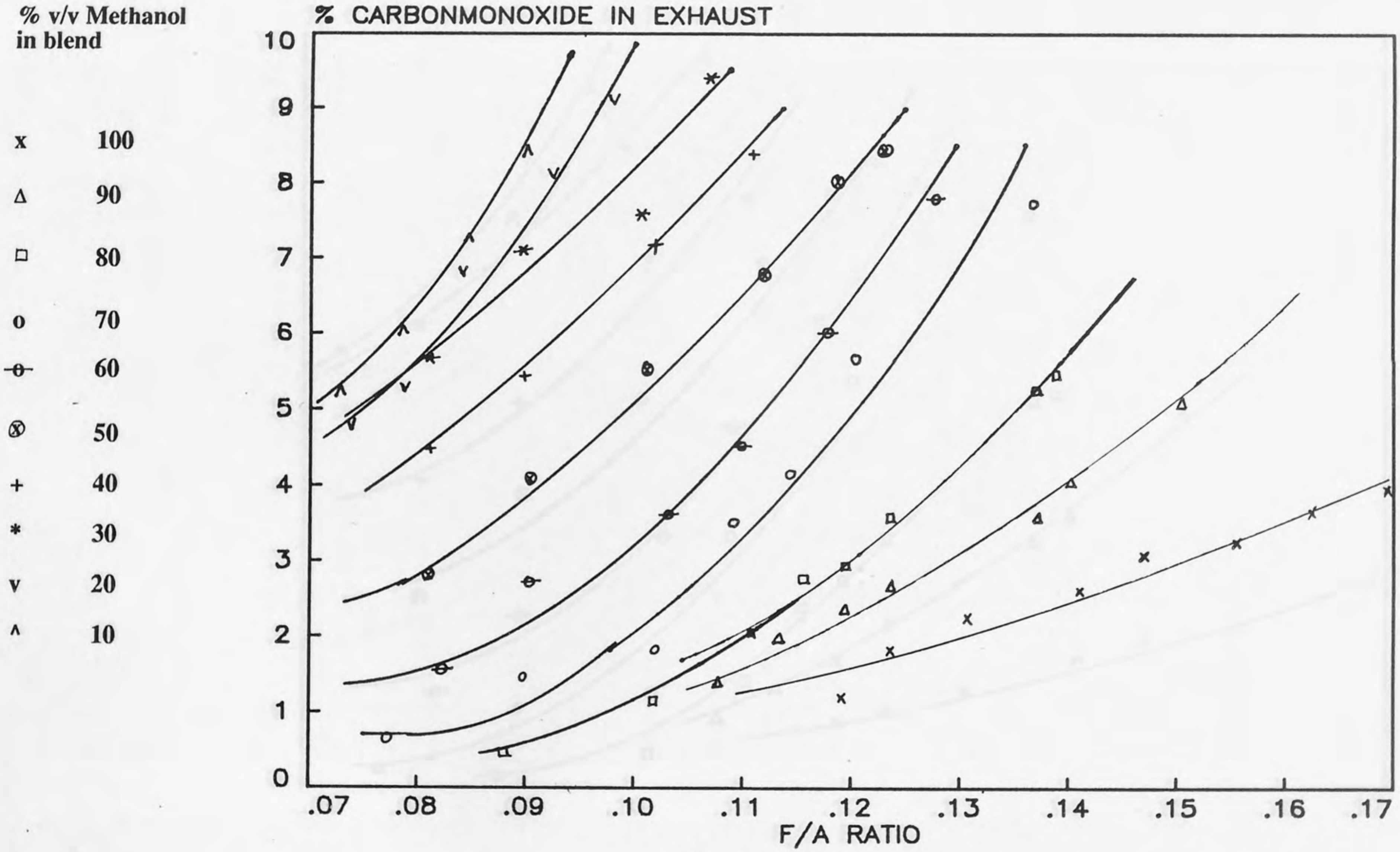

FIG: 4.1.73

EFFECT OF F/A RATIO ON CO EMISSION
ENGINE SPEED:2000 RPM

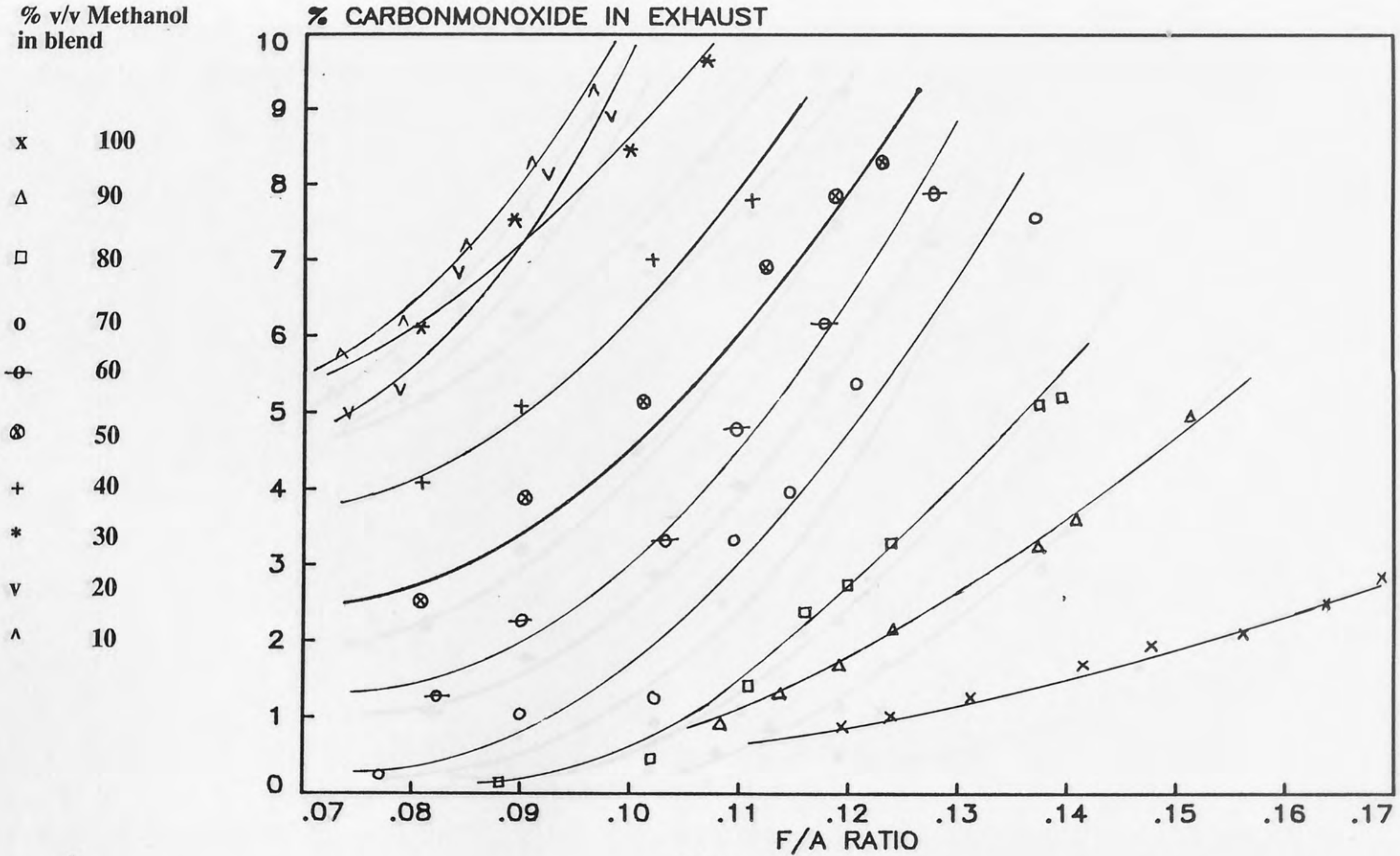

FIG: 4.1.74

Methanol

EFFECT OF F/A RATIO ON CO EMISSION
ENGINE SPEED:2500 RPM

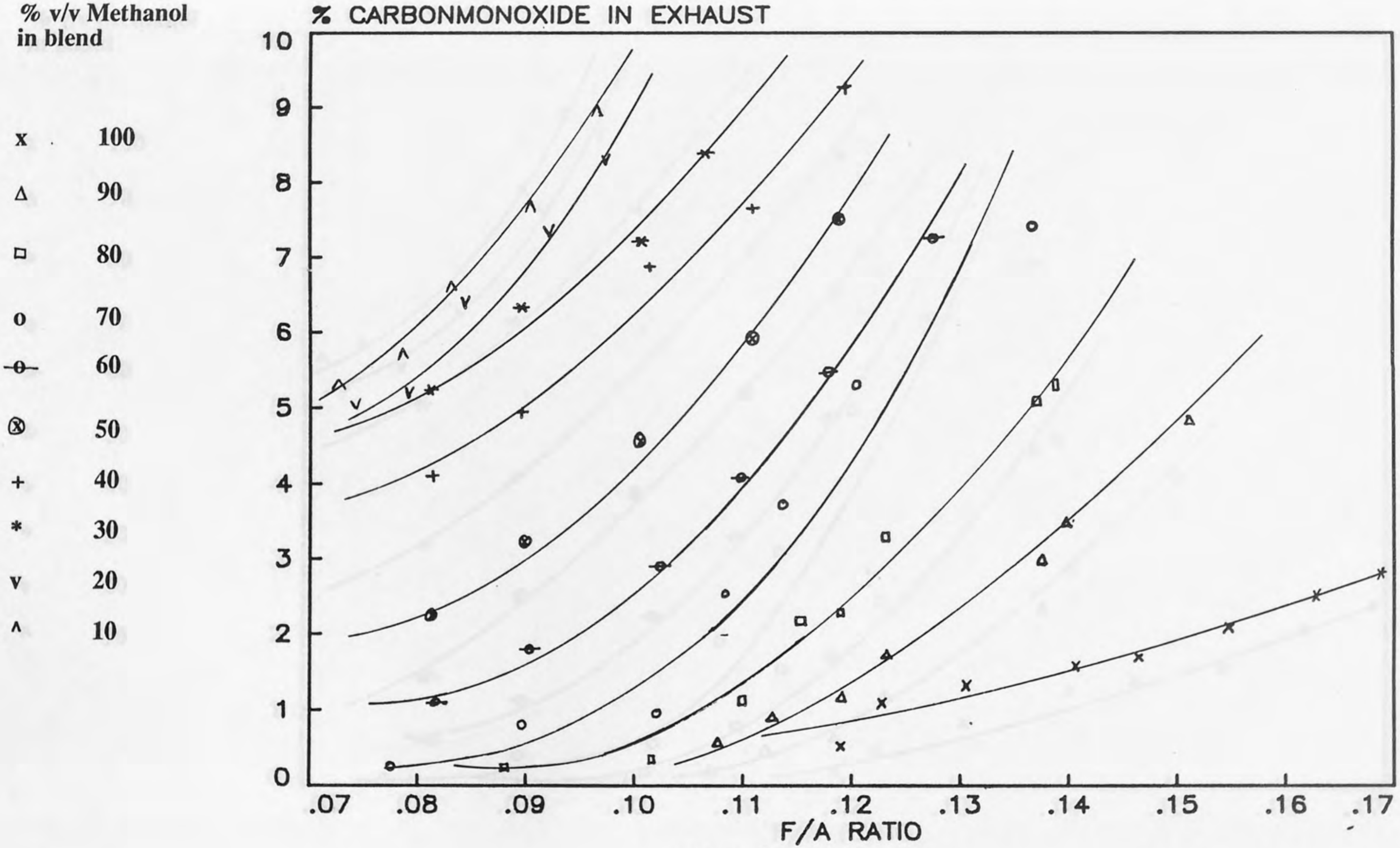

FIG: 4.1.75

EFFECT OF F/A RATIO ON CO EMISSION
ENGINE SPEED:3000 RPM

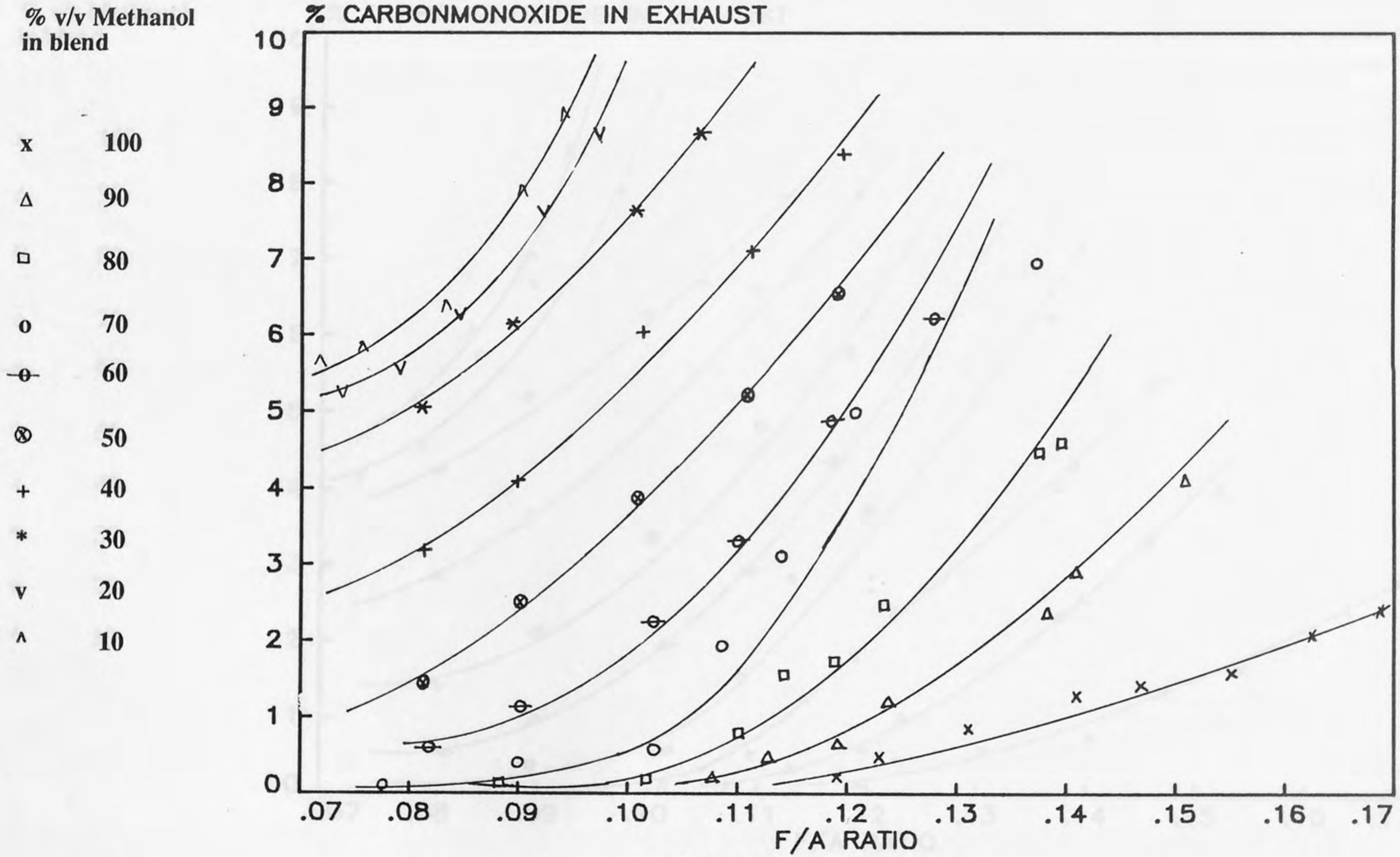

FIG: 4.1.76

MeOh

EFFECT OF F/A RATIO ON CO EMISSION
ENGINE SPEED:3500 RPM

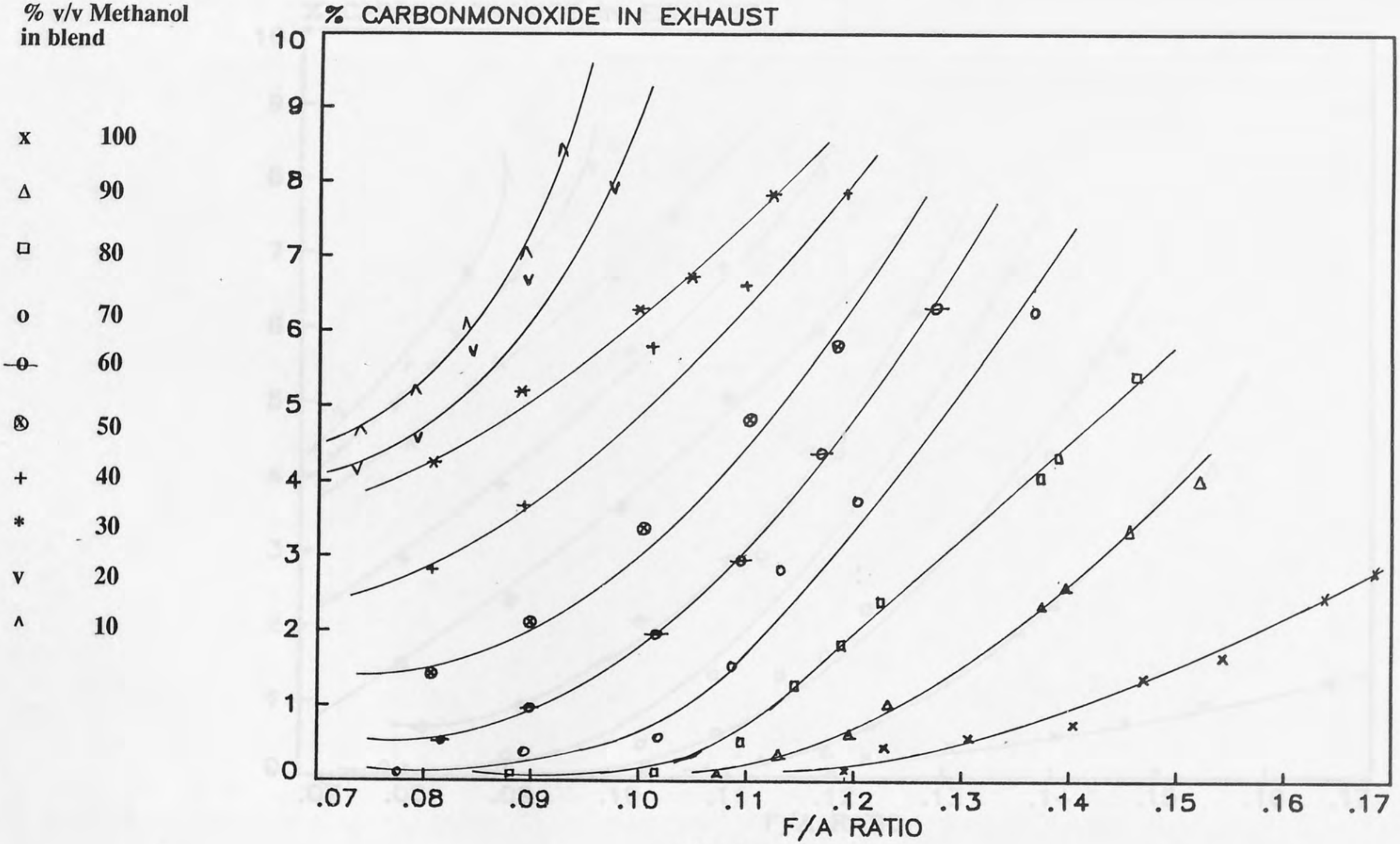

FIG: 4.1.77

EFFECT OF F/A RATIO ON CO EMISSION
ENGINE SPEED:4000 RPM

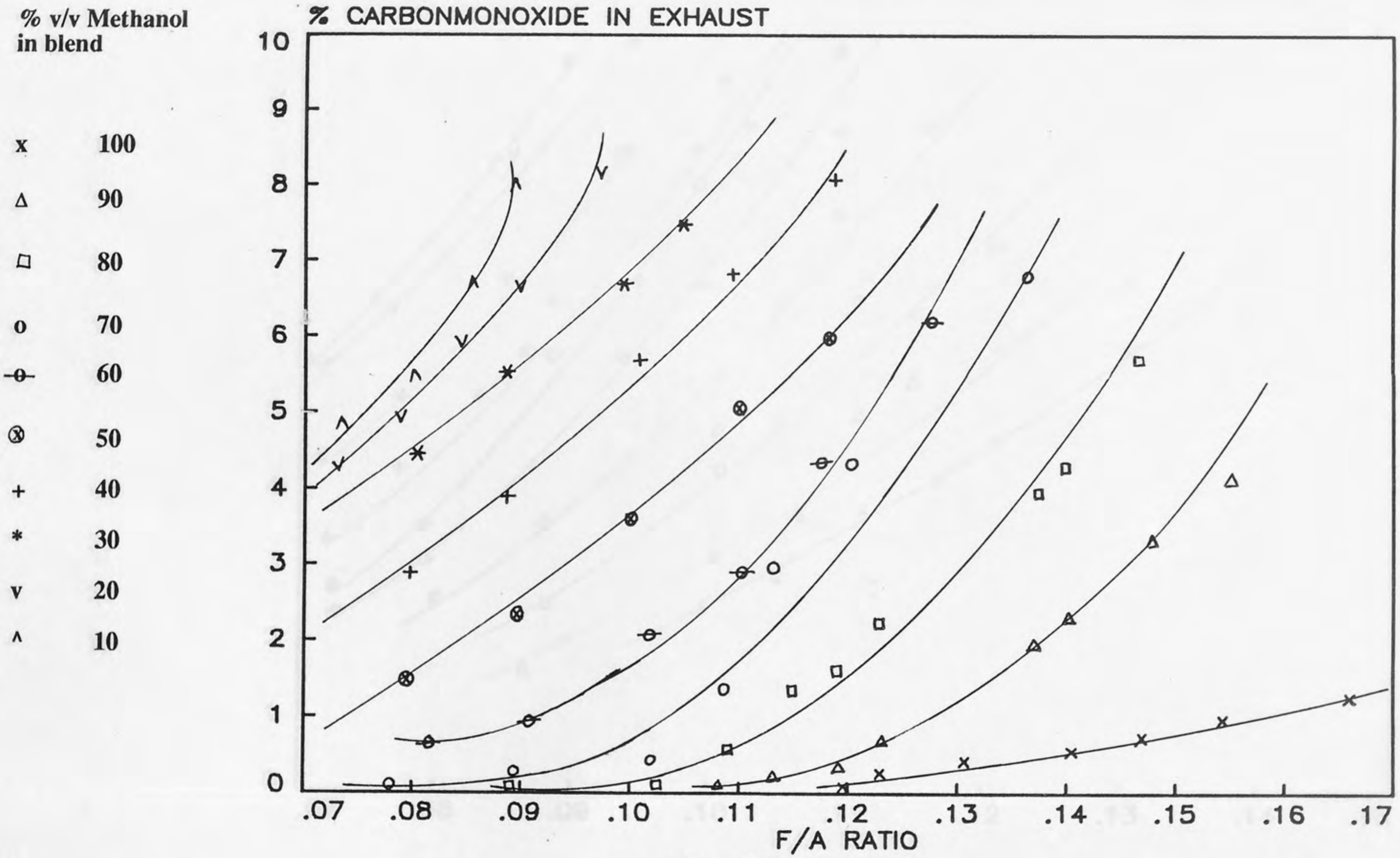

FIG: 4.1.78

Ethanol

EFFECT OF F/A RATIO ON CO EMISSION
ENGINE SPEED:1500 RPM

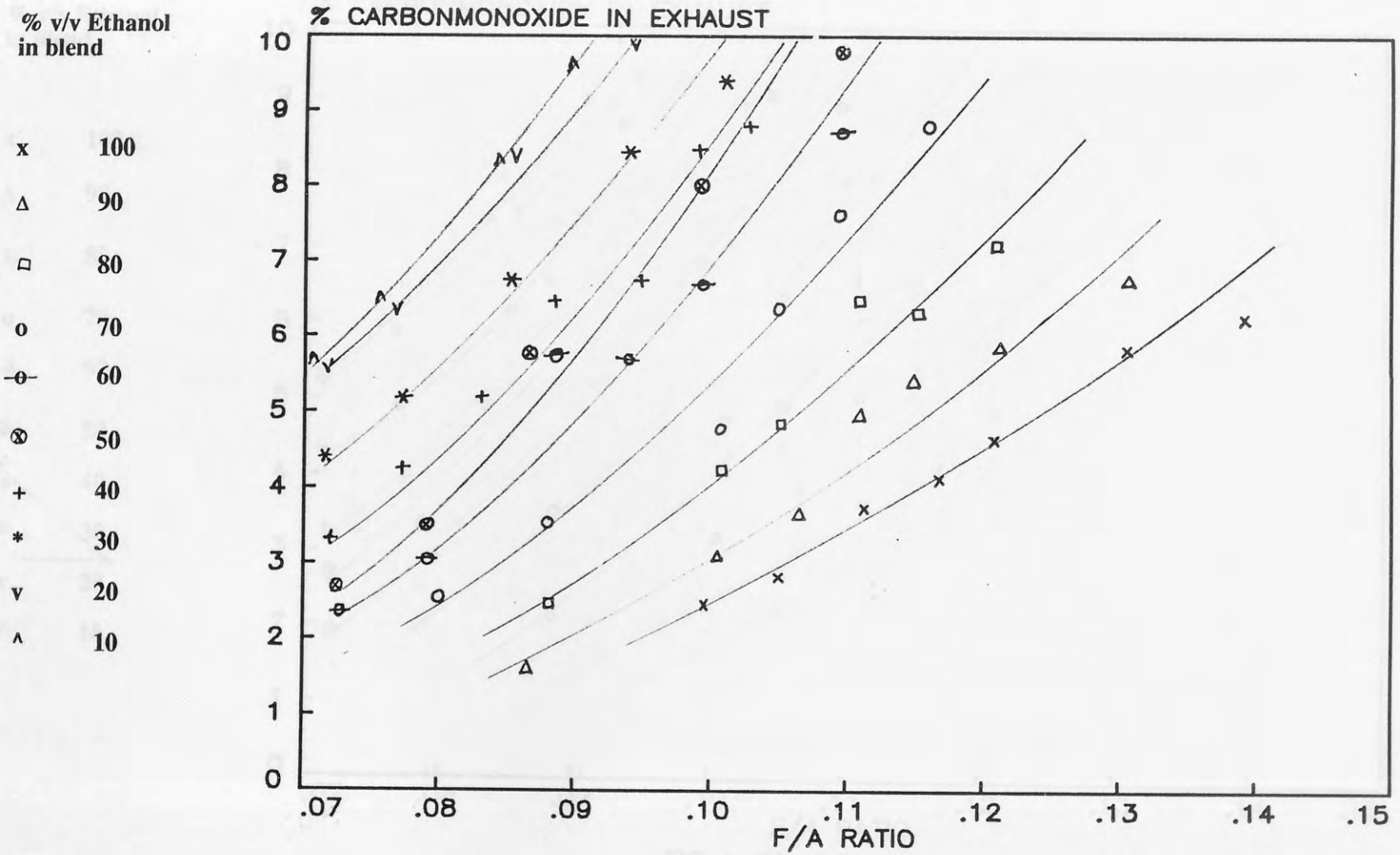

FIG: 4.1.79

EFFECT OF F/A RATIO ON CO EMISSION
ENGINE SPEED:2000 RPM

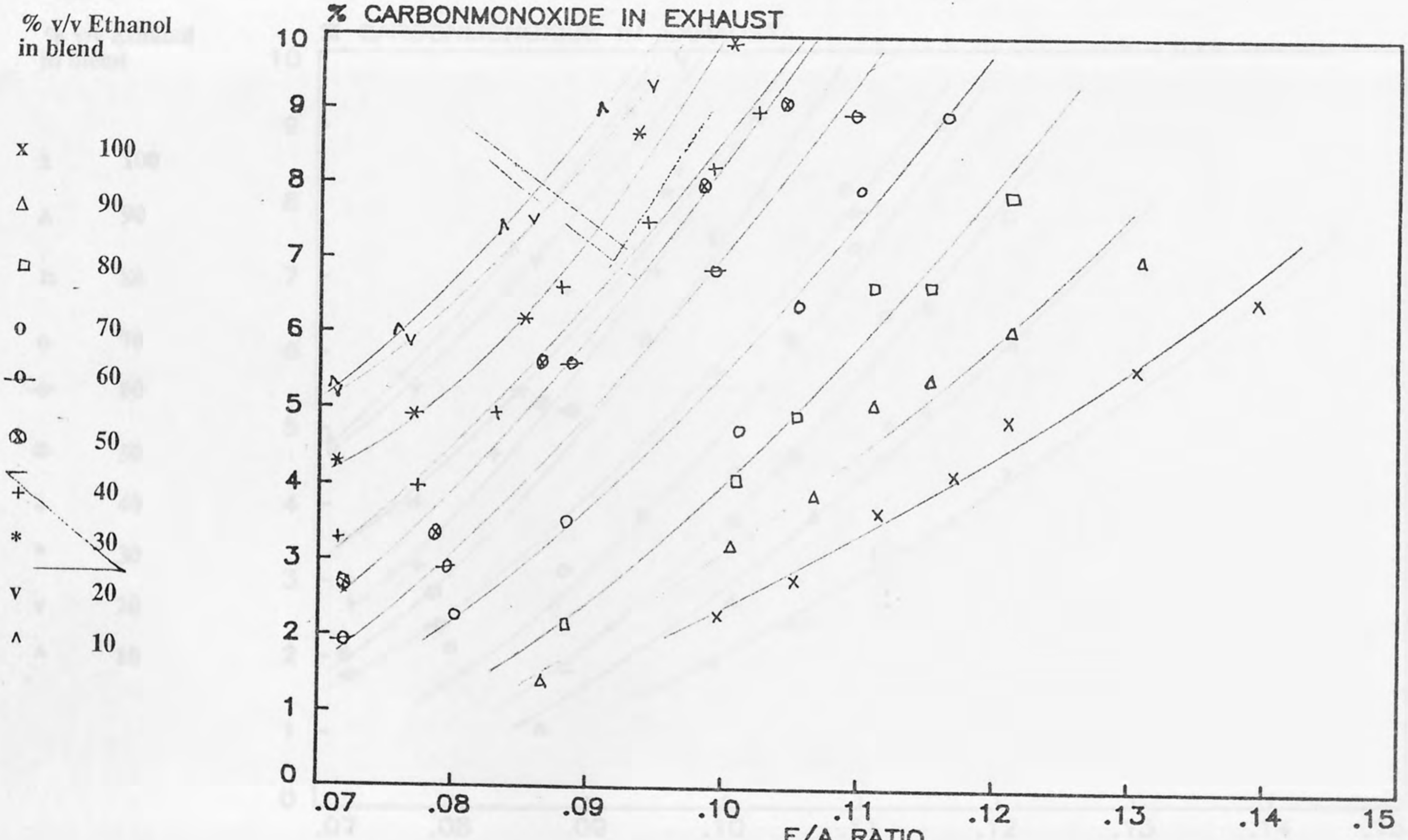

FIG: 4.1.80

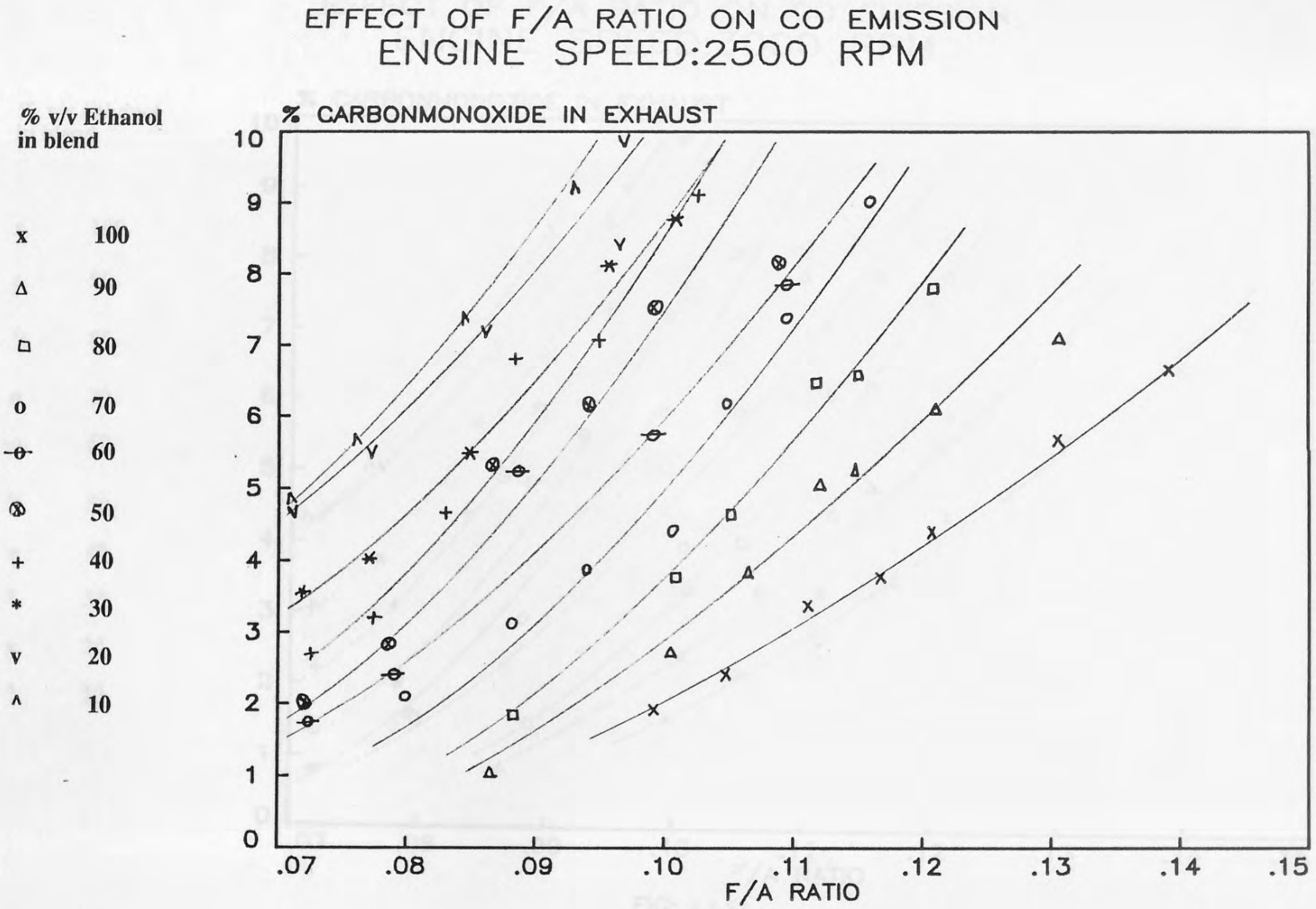
EFFECT OF F/A RATIO ON CO EMISSION
ENGINE SPEED:2500 RPM
% v/v Ethanol in blend
x 100
Δ 90
□ 80
o 70
-θ- 60
⊗ 50
+ 40
* 30
v 20
^ 10
% CARBONMONOXIDE IN EXHAUST
0
1
2
3
4
5
6
7
8
9
10
.07
.08
.09
.10
.11
.12
.13
.14
.15
F/A RATIO

FIG: 4.1.81

EFFECT OF F/A RATIO ON CO EMISSION
ENGINE SPEED:3000 RPM

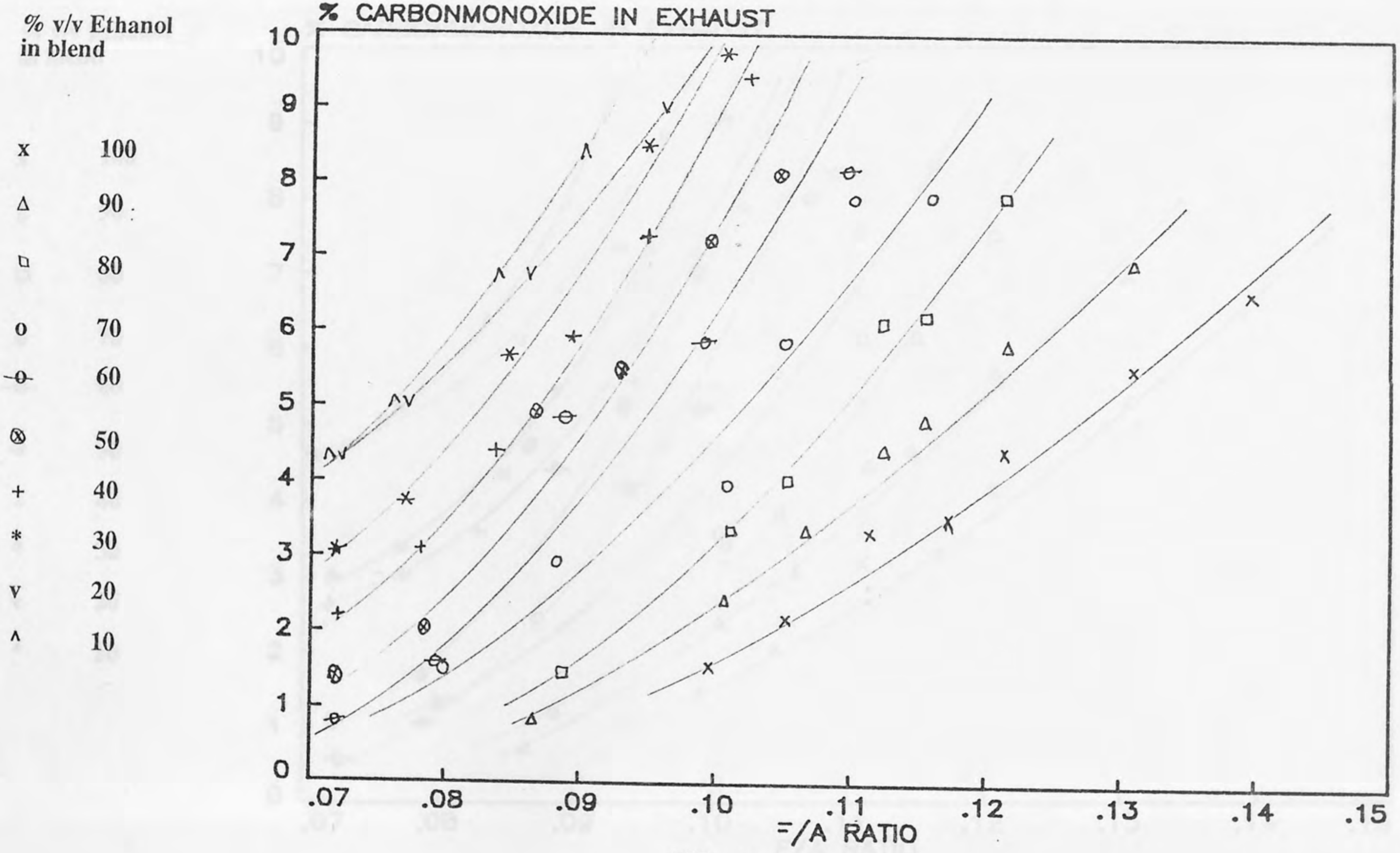

FIG: 4.1.82

Ethanol

EFFECT OF F/A RATIO ON CO EMISSION
ENGINE SPEED:3500 RPM

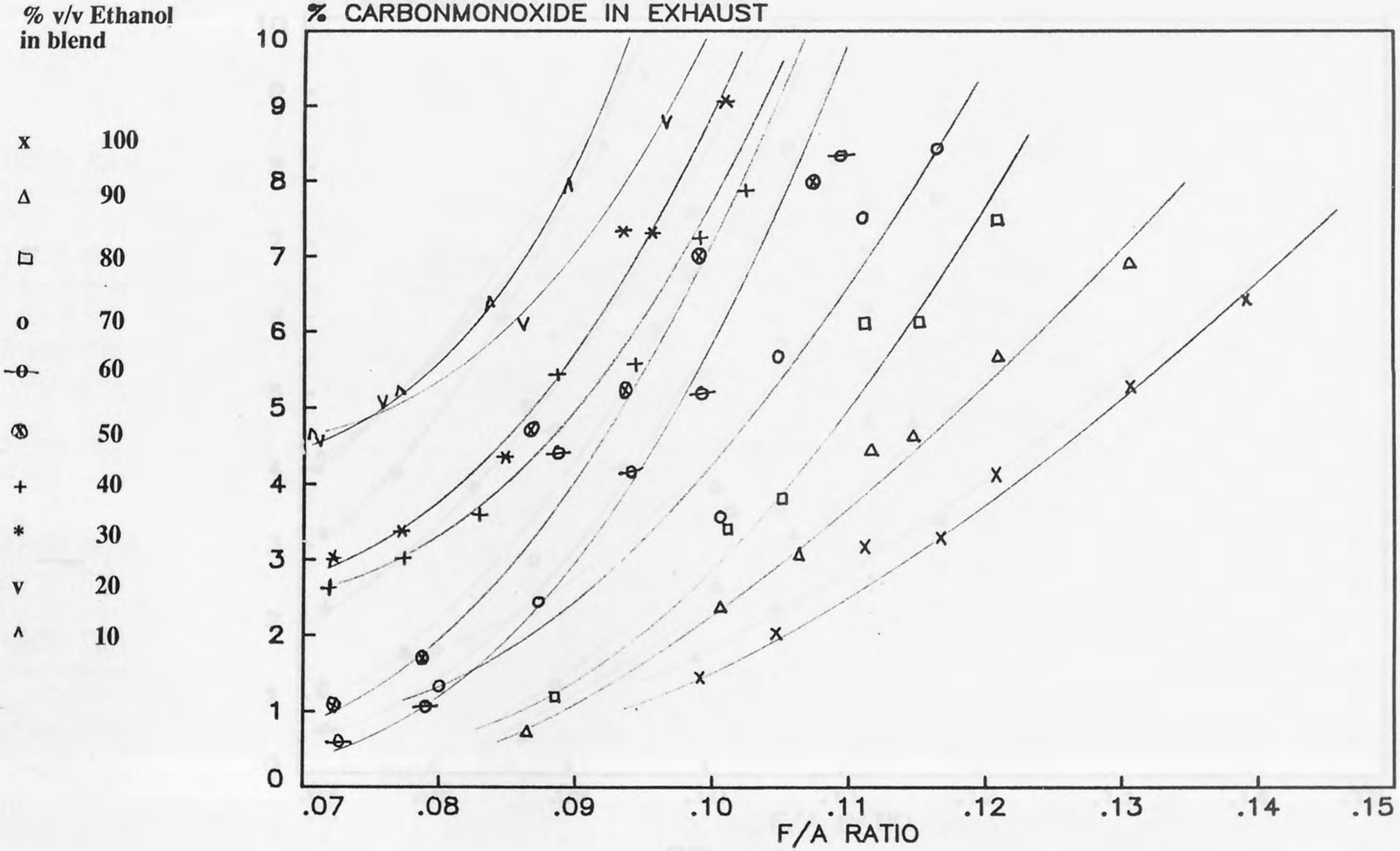

FIG: 4.1.83

EFFECT OF F/A RATIO ON CO EMISSION
ENGINE SPEED:4000 RPM

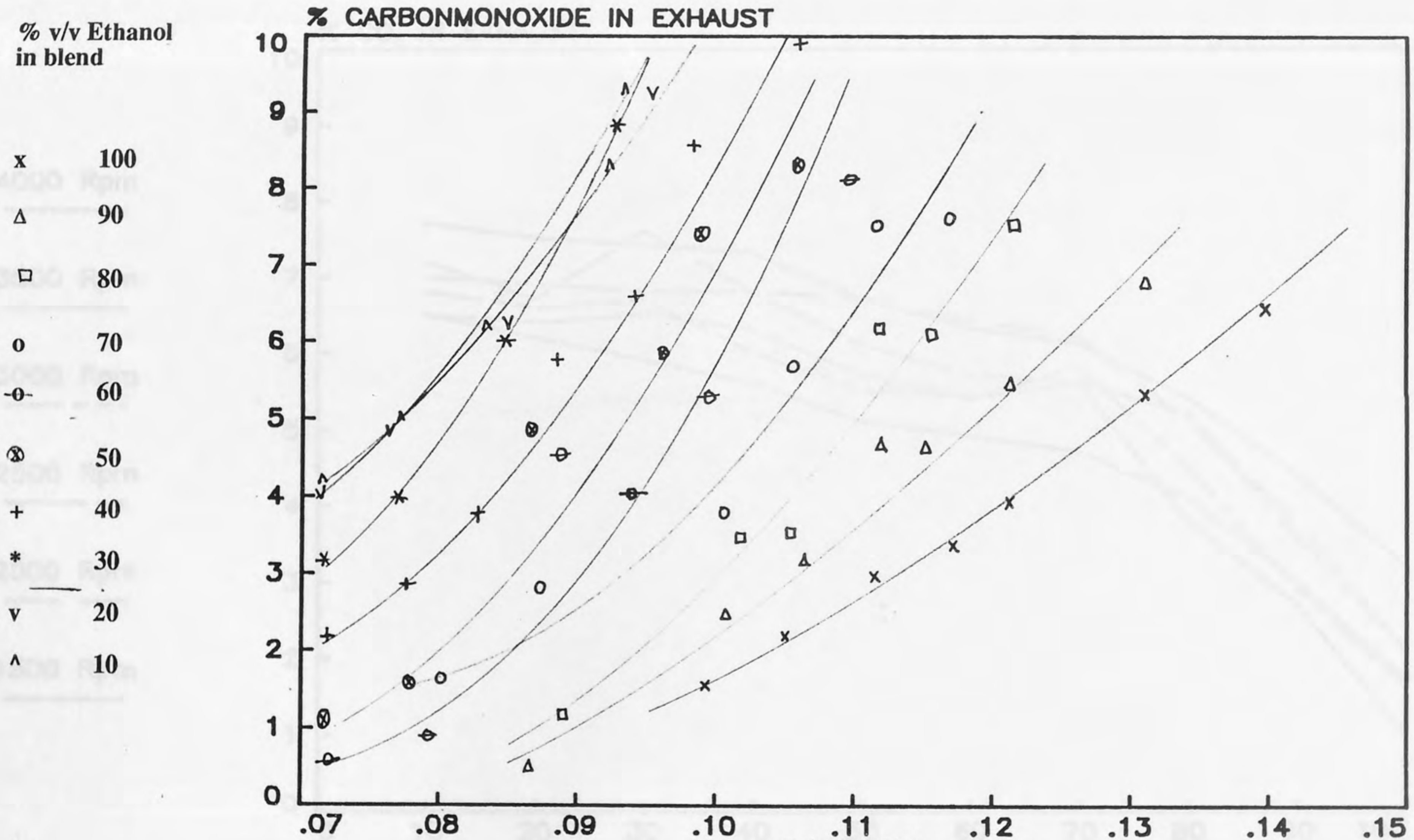

FIG: 4.1.84

EFFECT OF ALCOHOL CONTENT ON CO. EMISSION
AT STOICHIOMETRIC F/A RATIO

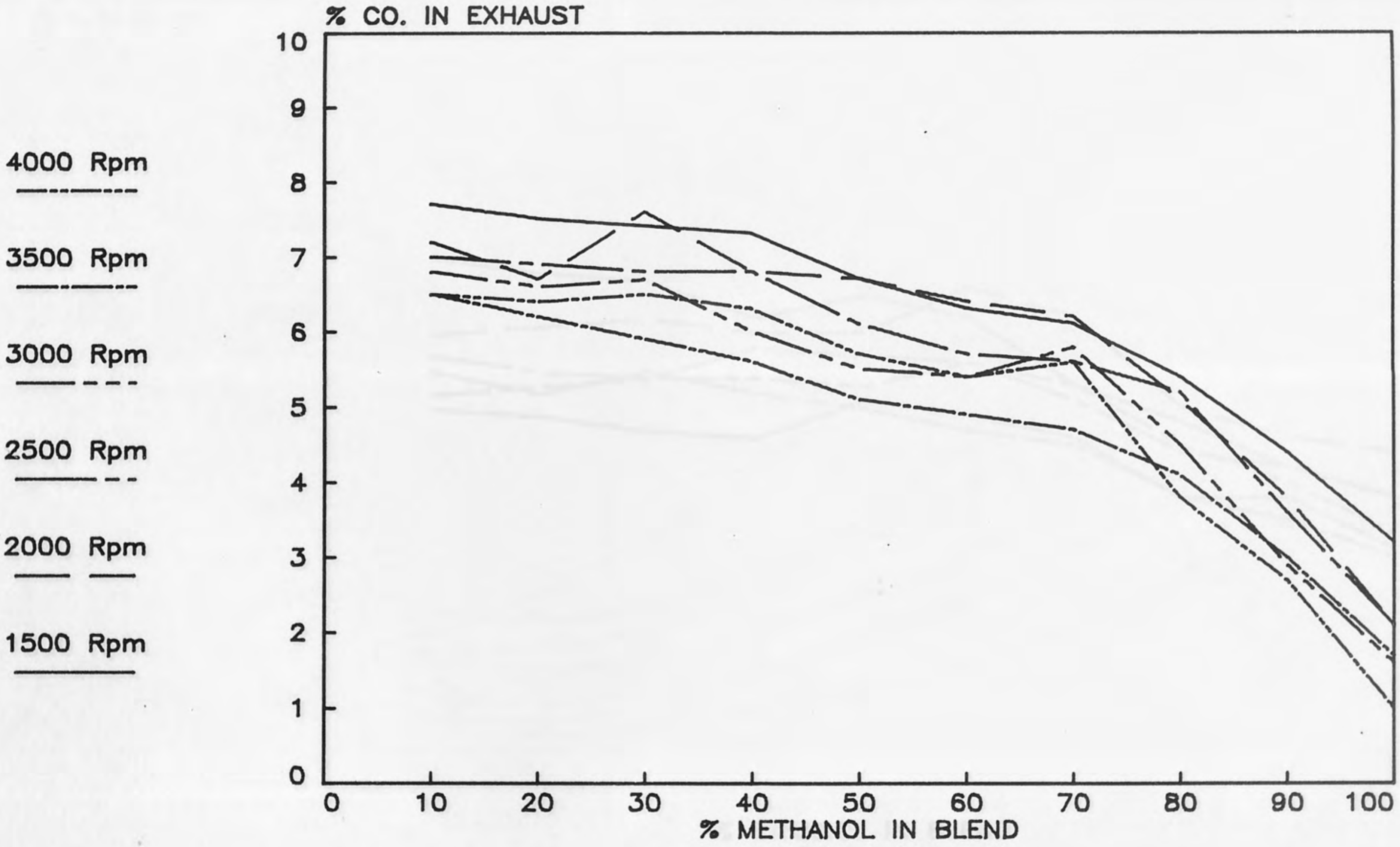

FIG: 4.1.85

EFFECT OF ALCOHOL CONTENT ON CO. EMISSION
AT STOICHIOMETRIC F/A RATIO

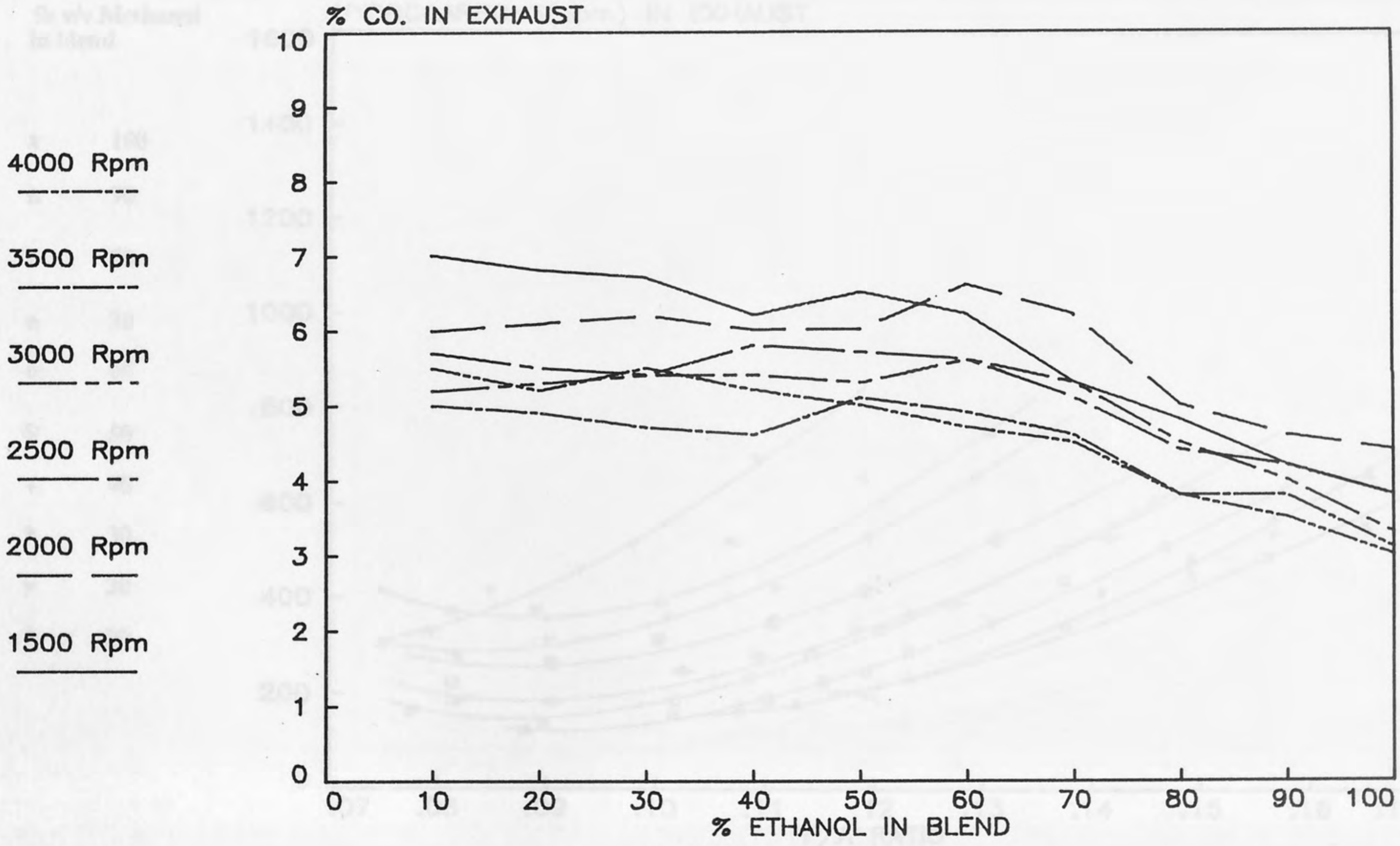

FIG: 4.1.86

Mesh

EFFECT OF F/A RATIO ON HC. EMISSION
ENGINE SPEED:1500 RPM

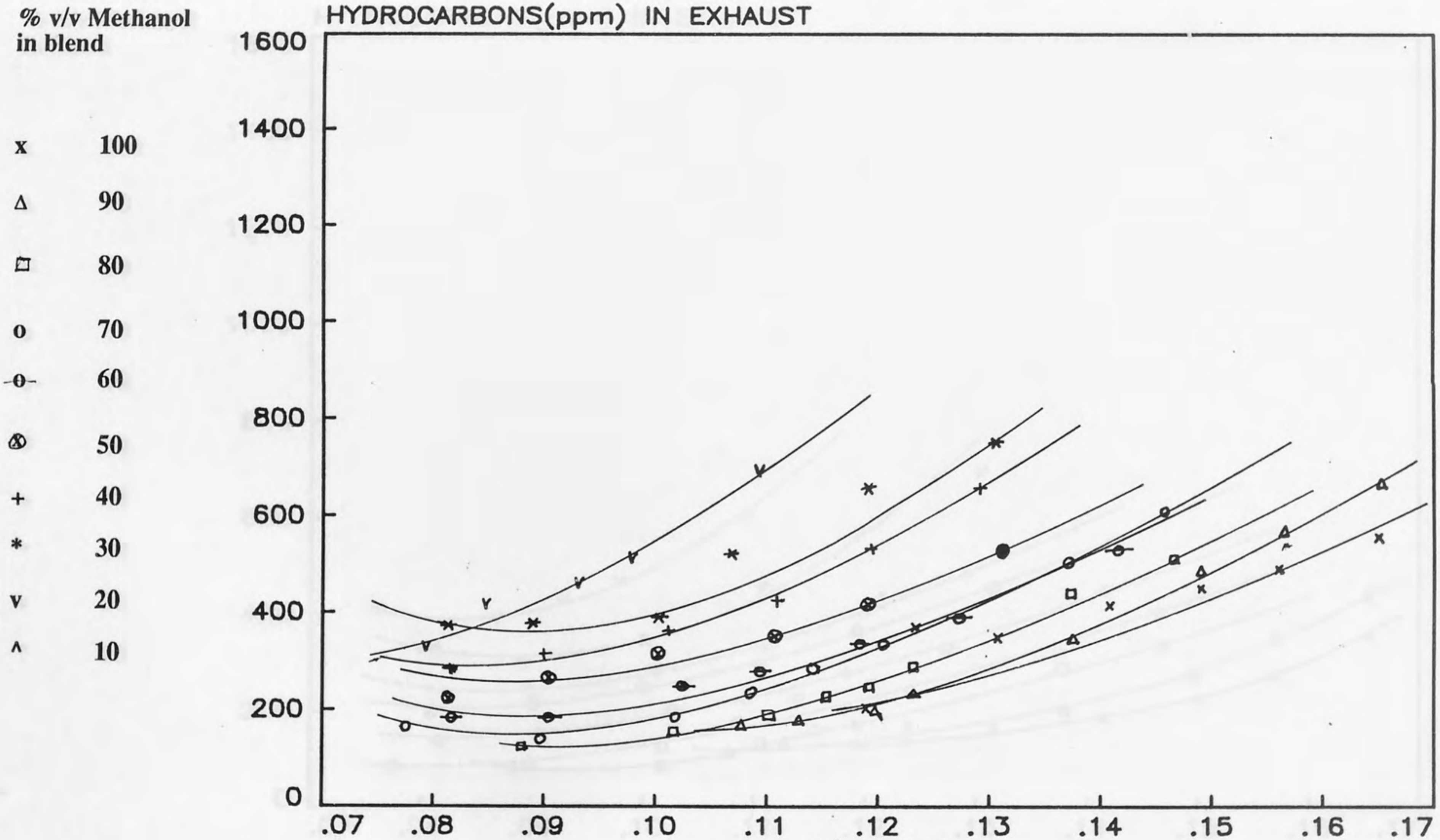

FIG: 4.1.87

EFFECT OF F/A RATIO ON HC. EMISSION
ENGINE SPEED:2000 RPM

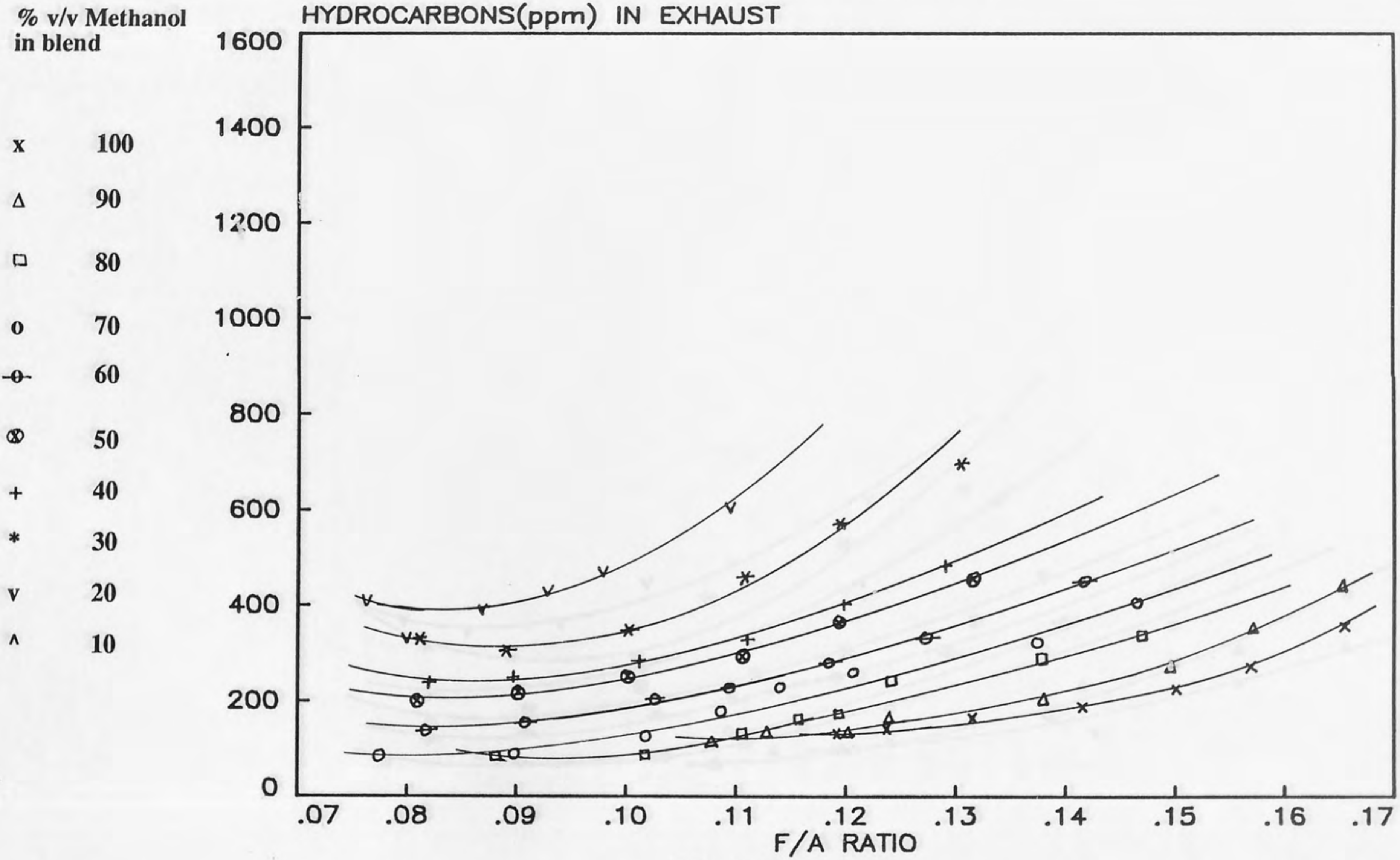

FIG: 4.1.88

EFFECT OF F/A RATIO ON HC. EMISSION
ENGINE SPEED:2500 RPM

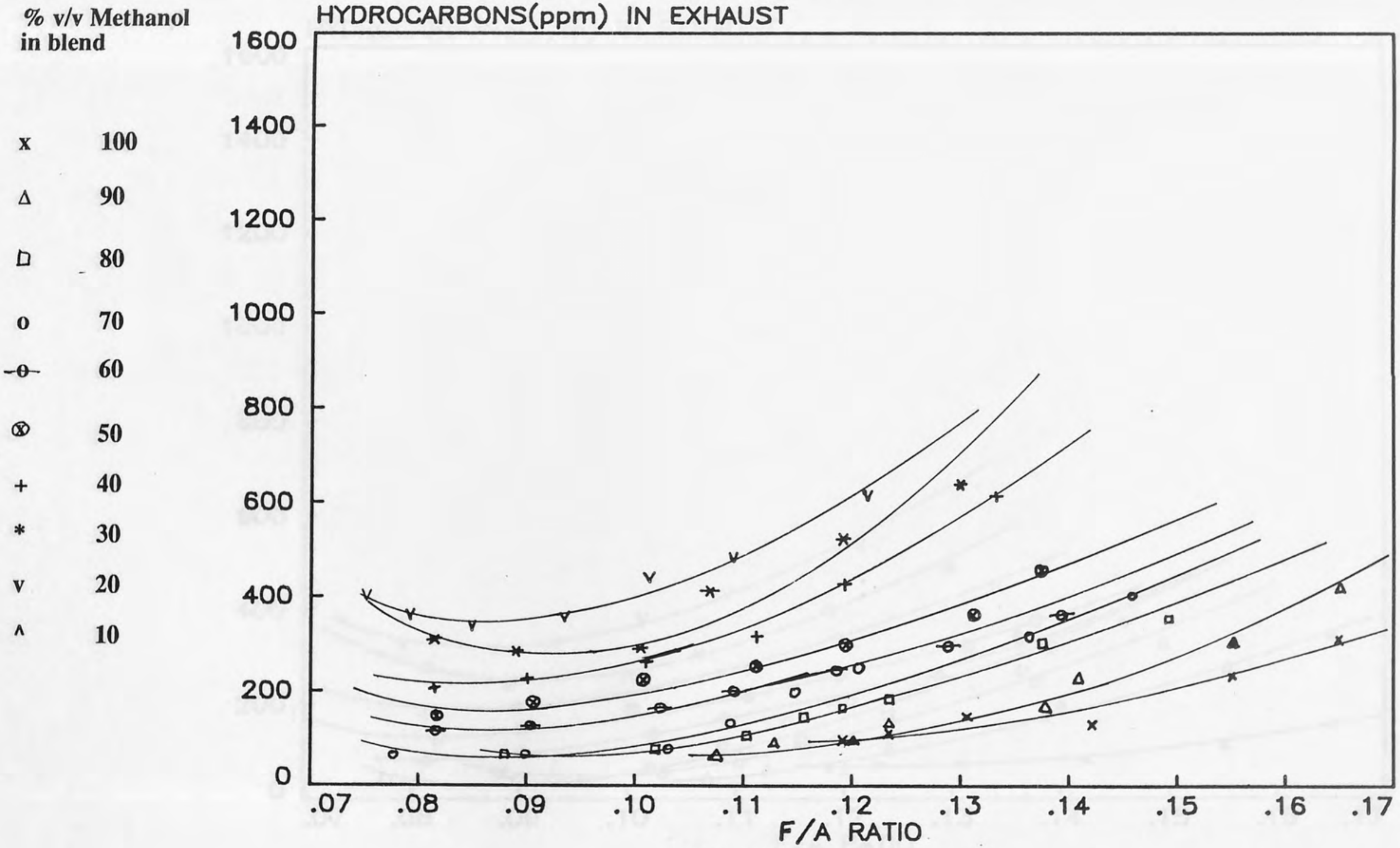

FIG: 4.1.89

EFFECT OF F/A RATIO ON HC. EMISSION
ENGINE SPEED:3000 RPM

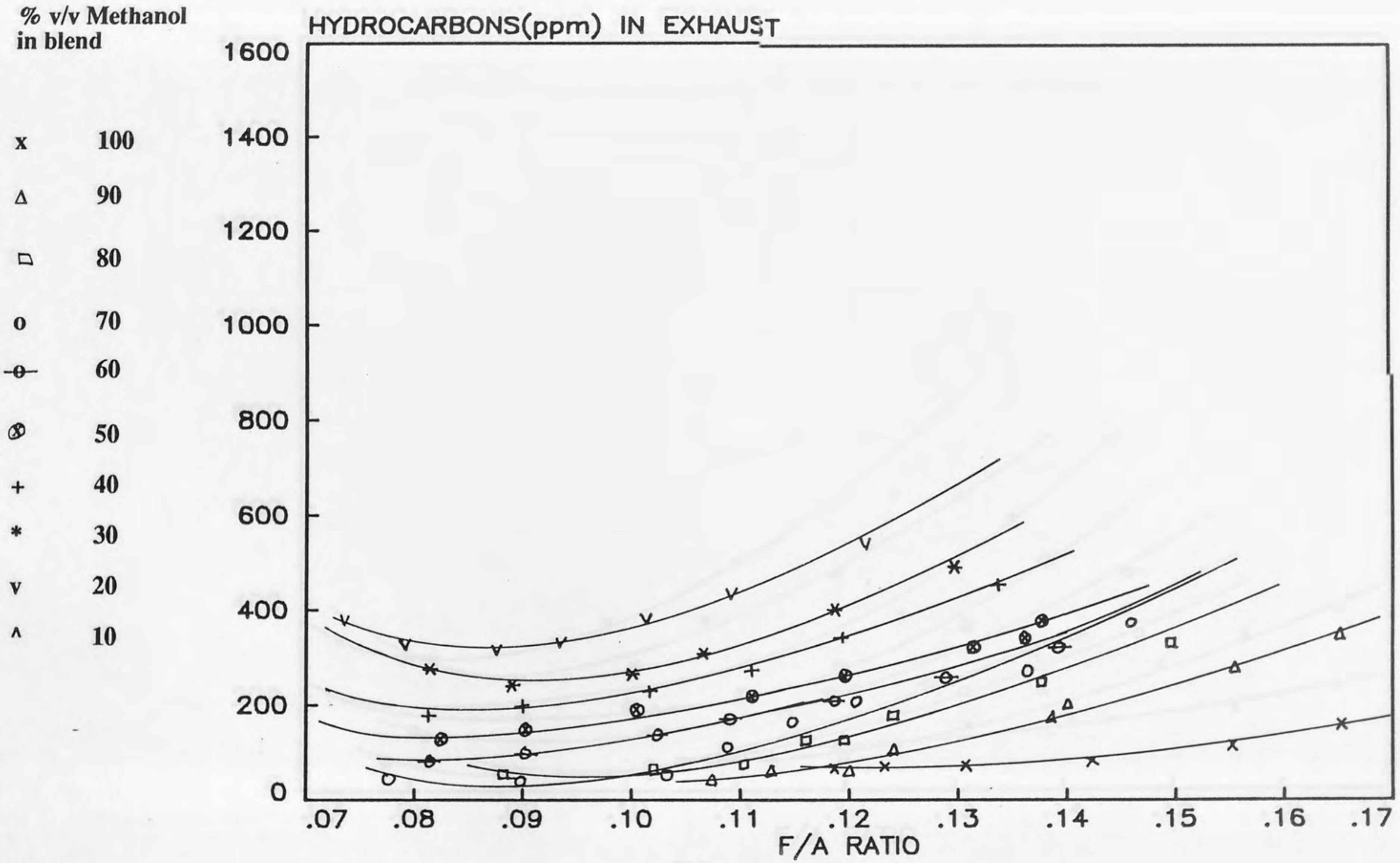

FIG: 4.1.90

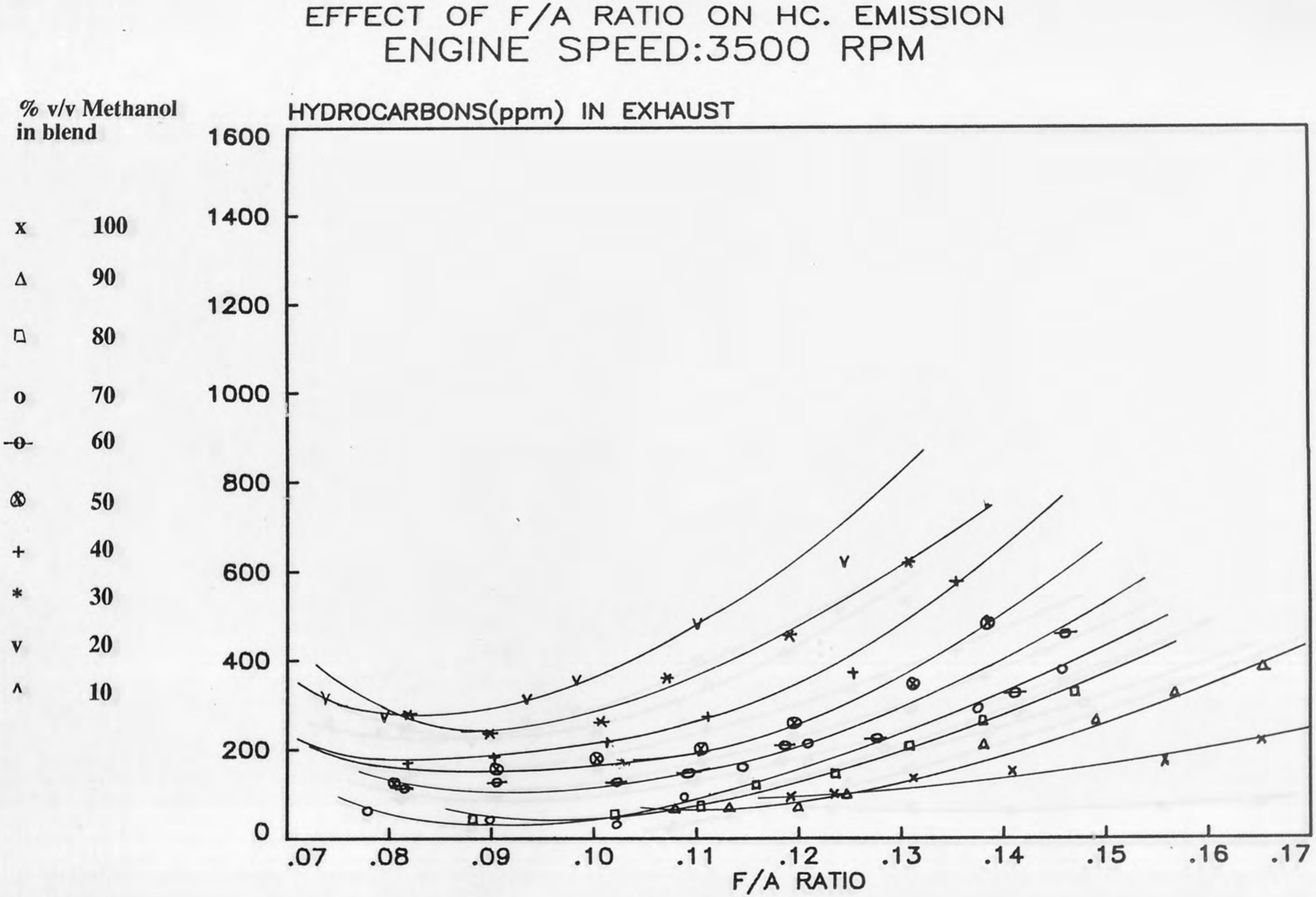
EFFECT OF F/A RATIO ON HC. EMISSION
ENGINE SPEED:3500 RPM
% v/v Methanol in blend
x 100
Δ 90
□ 80
o 70
-θ- 60
⊗ 50
+ 40
* 30
v 20
^ 10
HYDROCARBONS(ppm) IN EXHAUST
1600
1400
1200
1000
800
600
400
200
0
.07
.08
.09
.10
.11
.12
.13
.14
.15
.16
.17
F/A RATIO

FIG: 4.1.91

EFFECT OF F/A RATIO ON HC. EMISSION
ENGINE SPEED:4000 RPM

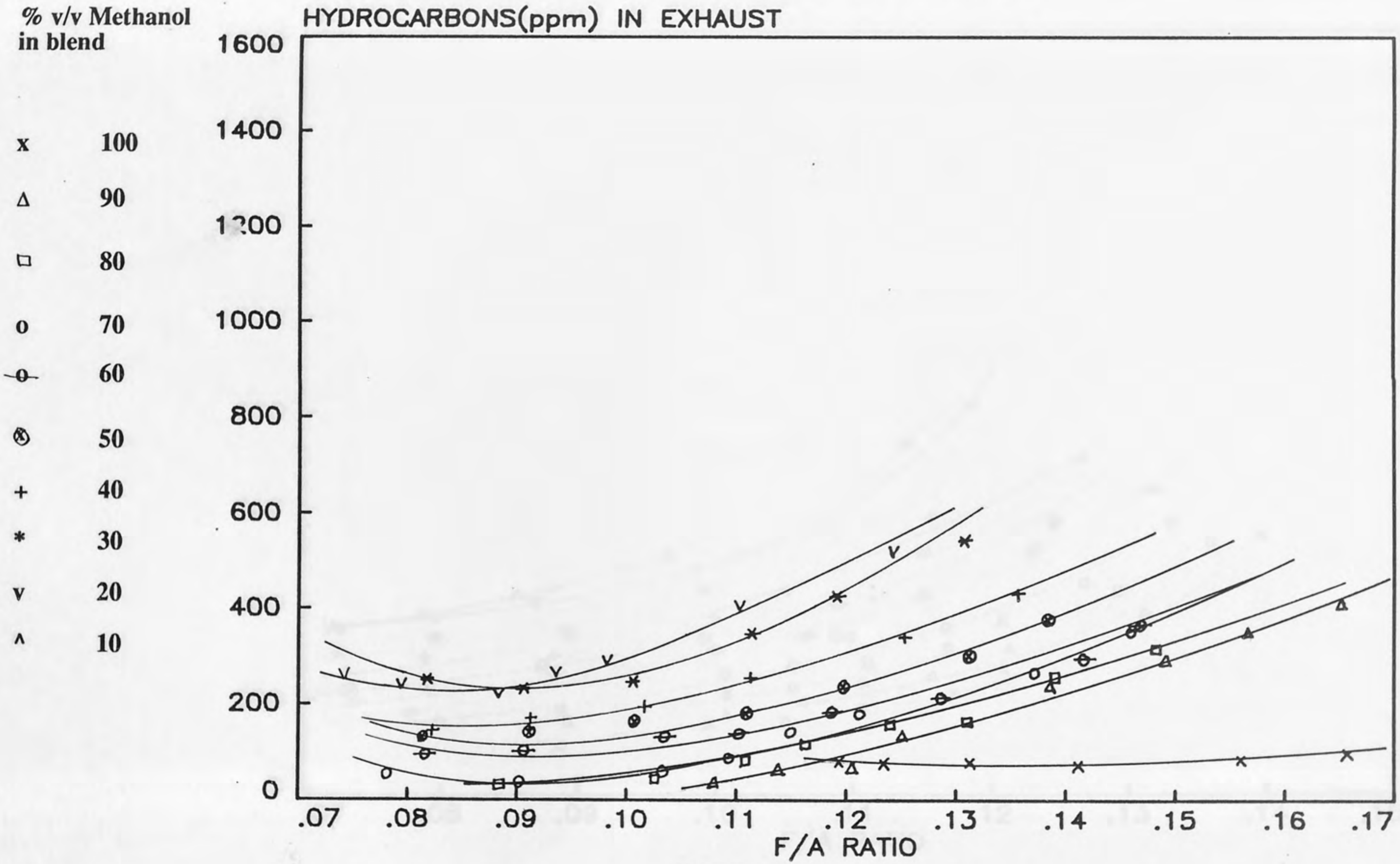

FIG: 4.1.92

EFFECT OF F/A RATIO ON HC. EMISSION
ENGINE SPEED:1500 RPM

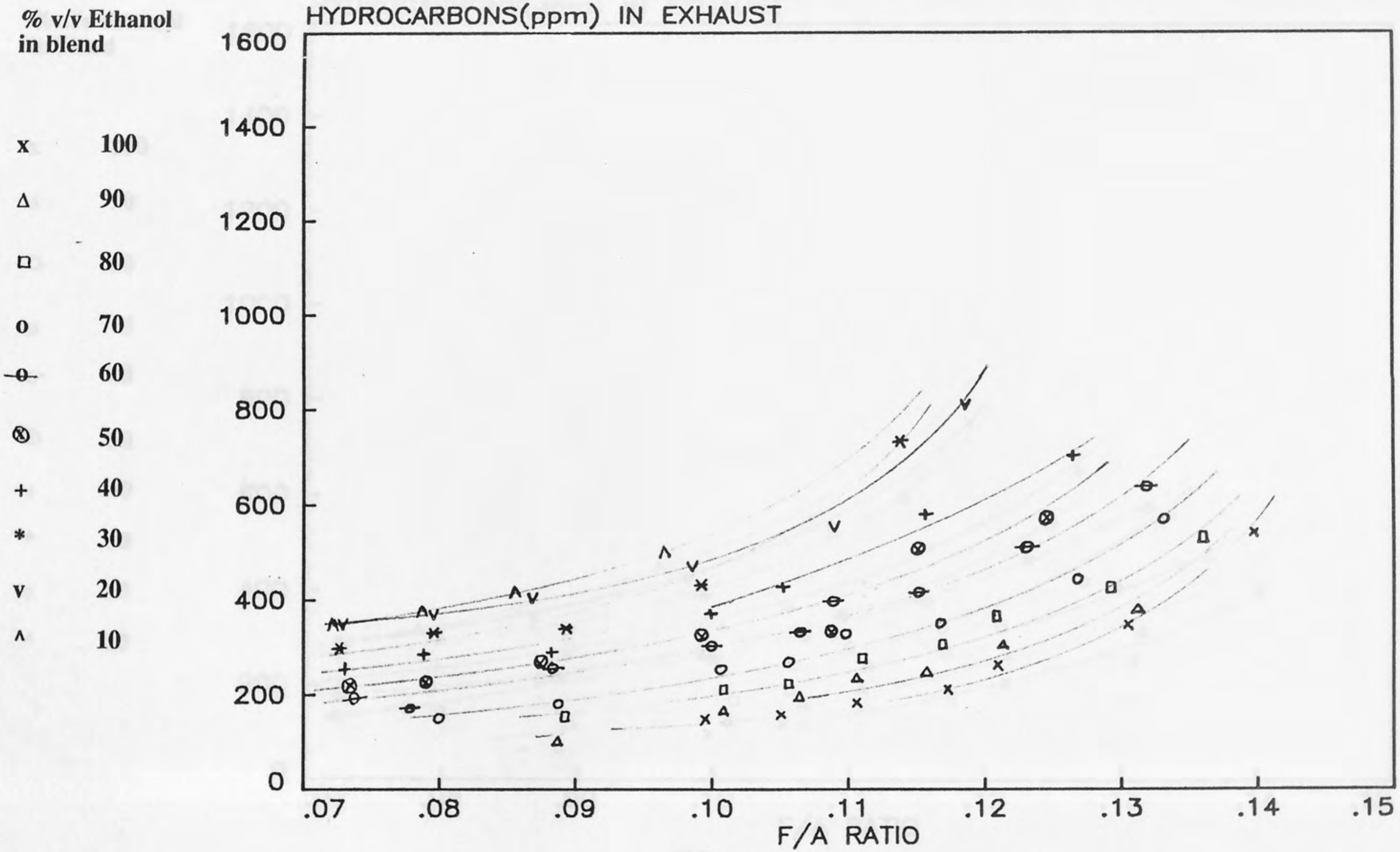

FIG: 4.1.93

EFFECT OF F/A RATIO ON HC. EMISSION
ENGINE SPEED:2000 RPM

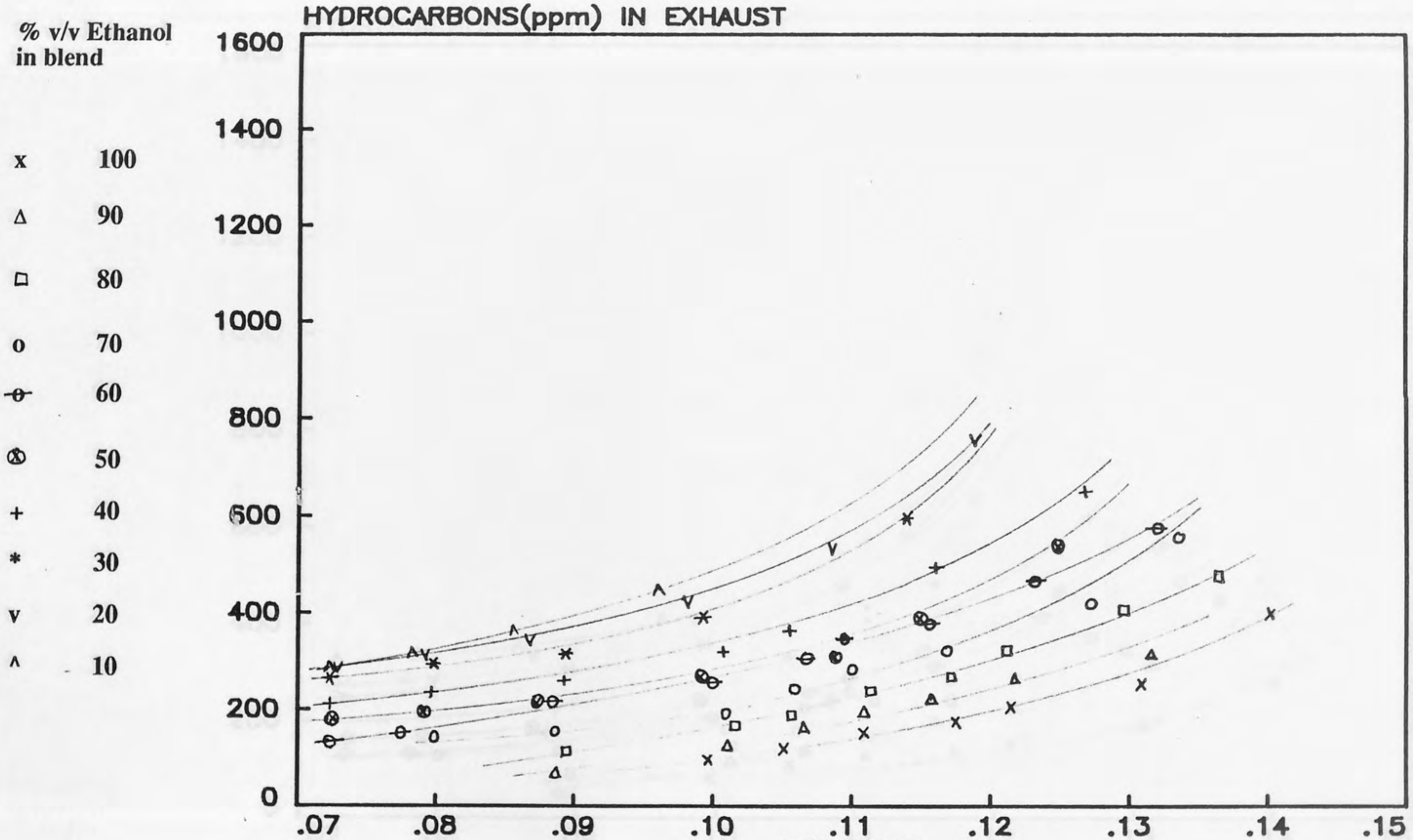

FIG: 4.1.94

EFFECT OF F/A RATIO ON HC. EMISSION
ENGINE SPEED:2500 RPM

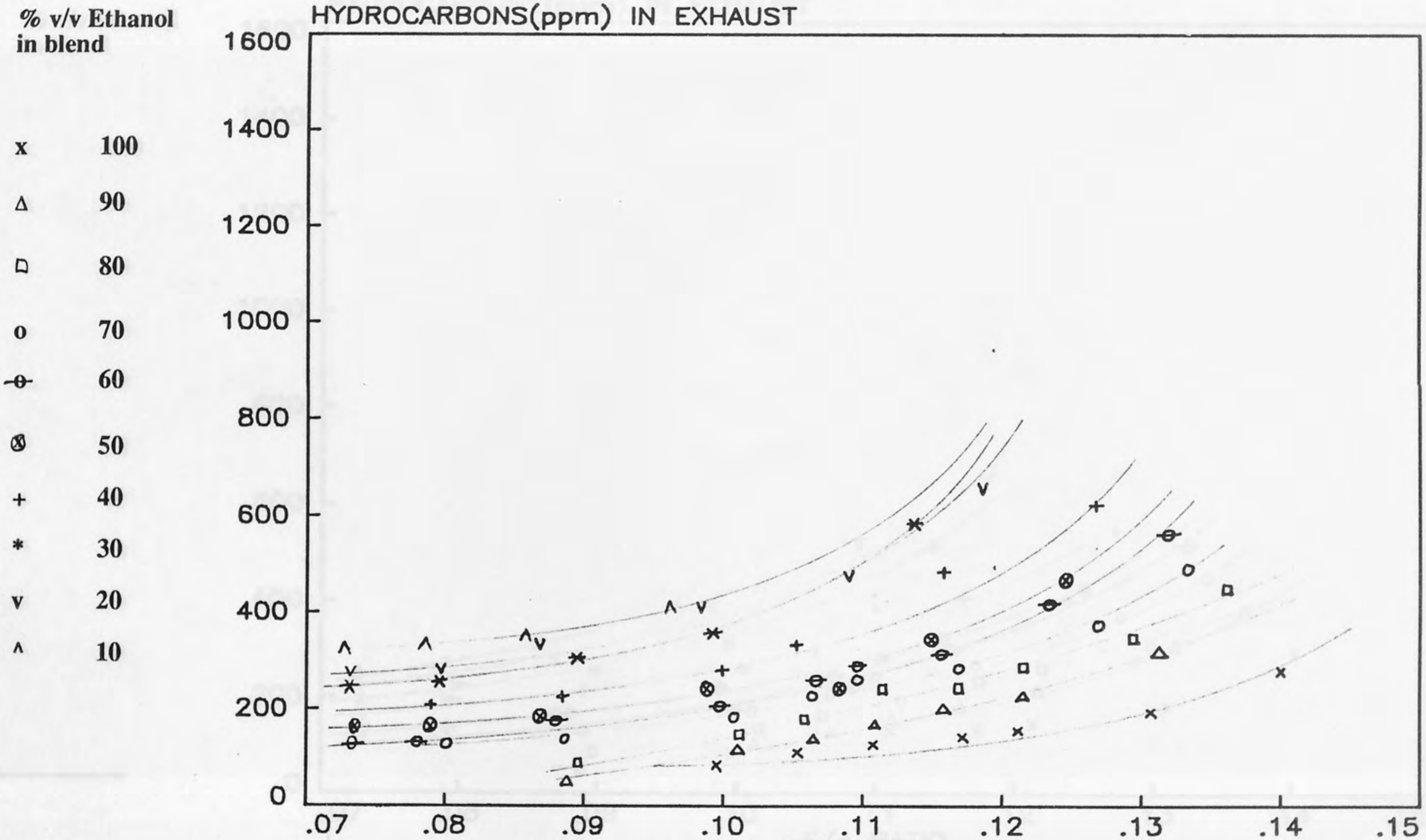

FIG: 4.1.95

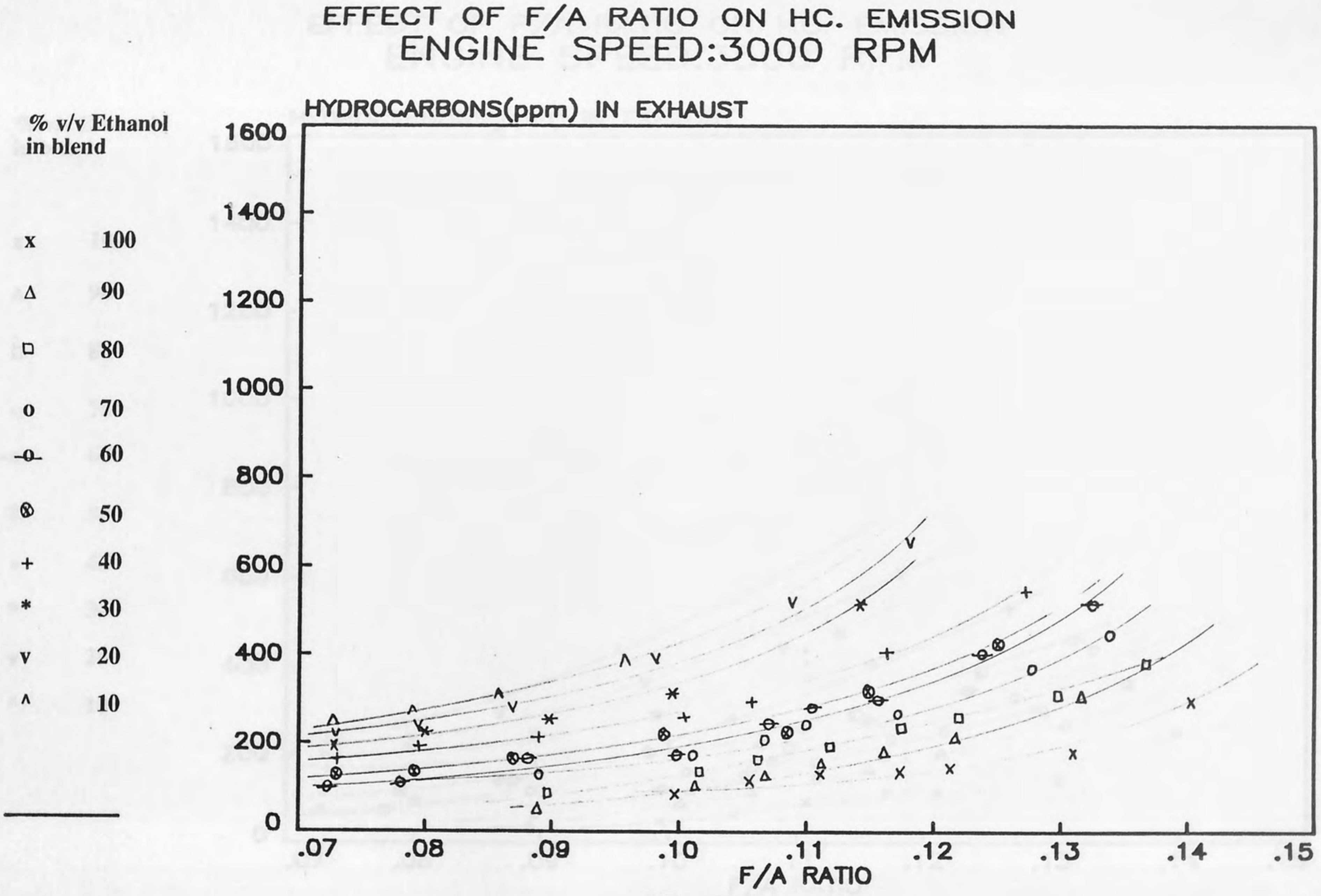
EFFECT OF F/A RATIO ON HC. EMISSION
ENGINE SPEED:3000 RPM
HYDROCARBONS(ppm) IN EXHAUST
% v/v Ethanol in blend
x 100
Δ 90
□ 80
o 70
-o- 60
⊗ 50
+ 40
* 30
v 20
^ 10
1600
1400
1200
1000
800
600
400
200
0
.07
.08
.09
.10
.11
.12
.13
.14
.15
F/A RATIO

FIG: 4.1.96

EFFECT OF F/A RATIO ON HC. EMISSION
ENGINE SPEED:3500 RPM

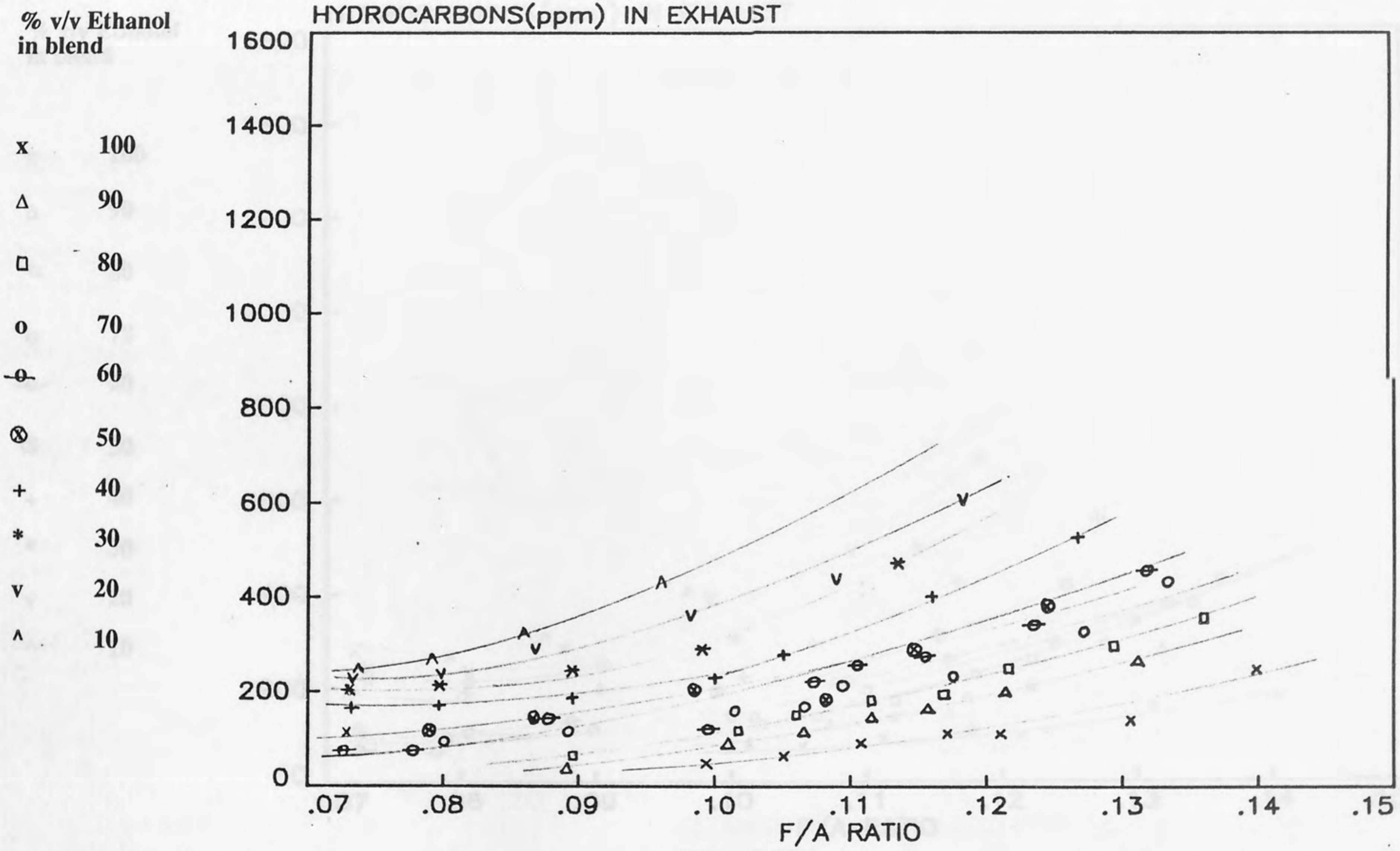

FIG: 4.1.97

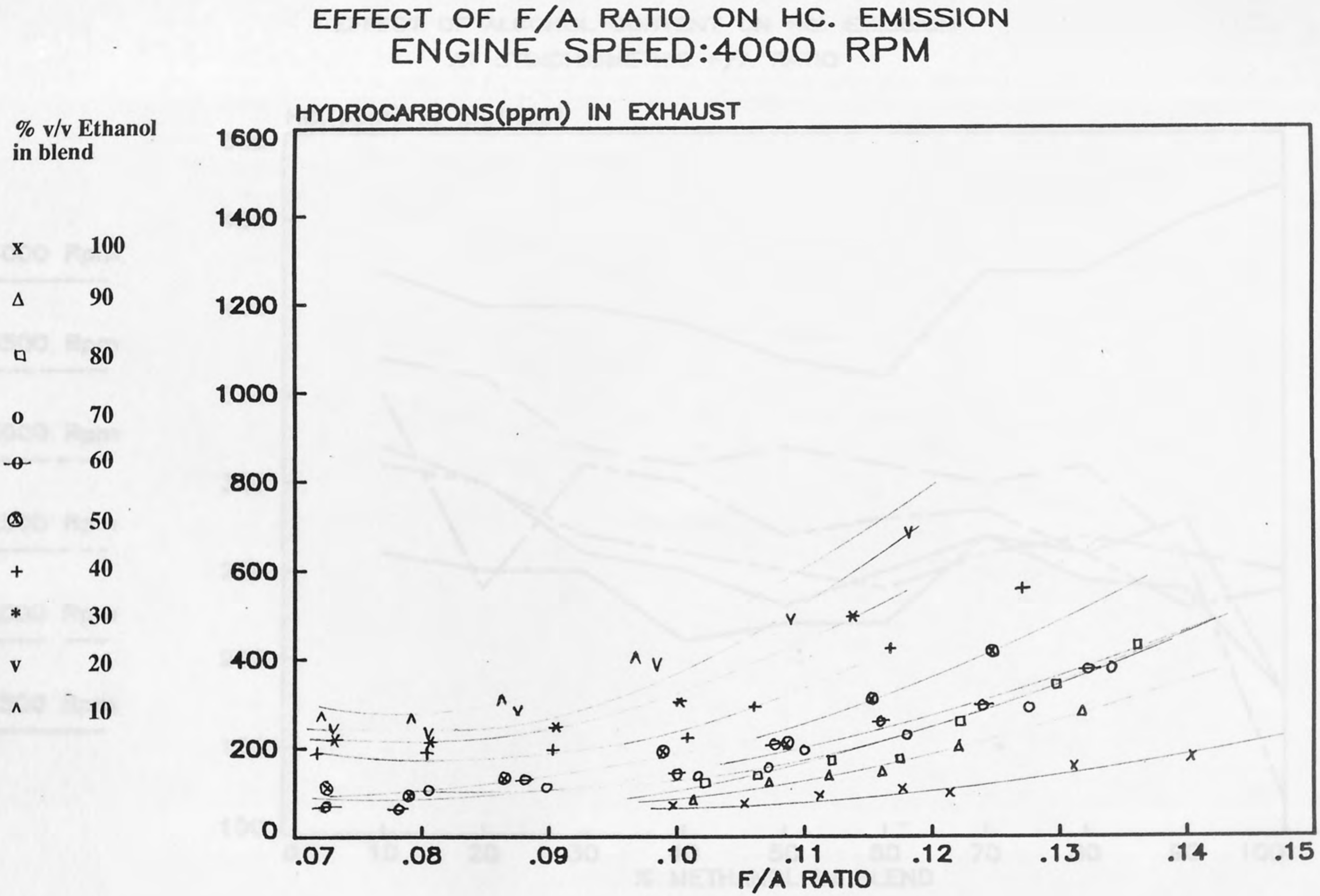
EFFECT OF F/A RATIO ON HC. EMISSION
ENGINE SPEED:4000 RPM
HYDROCARBONS(ppm) IN EXHAUST
% v/v Ethanol in blend
x 100
Δ 90
□ 80
o 70
-θ- 60
⊗ 50
+ 40
* 30
v 20
^ 10
1600
1400
1200
1000
800
600
400
200
0
.07
.08
.09
.10
.11
.12
.13
.14
.15
F/A RATIO

FIG: 4.1.98

EFFECT OF ALCOHOL CONTENT ON HC. EMISSION
AT STOICHIOMETRIC F/A RATIO

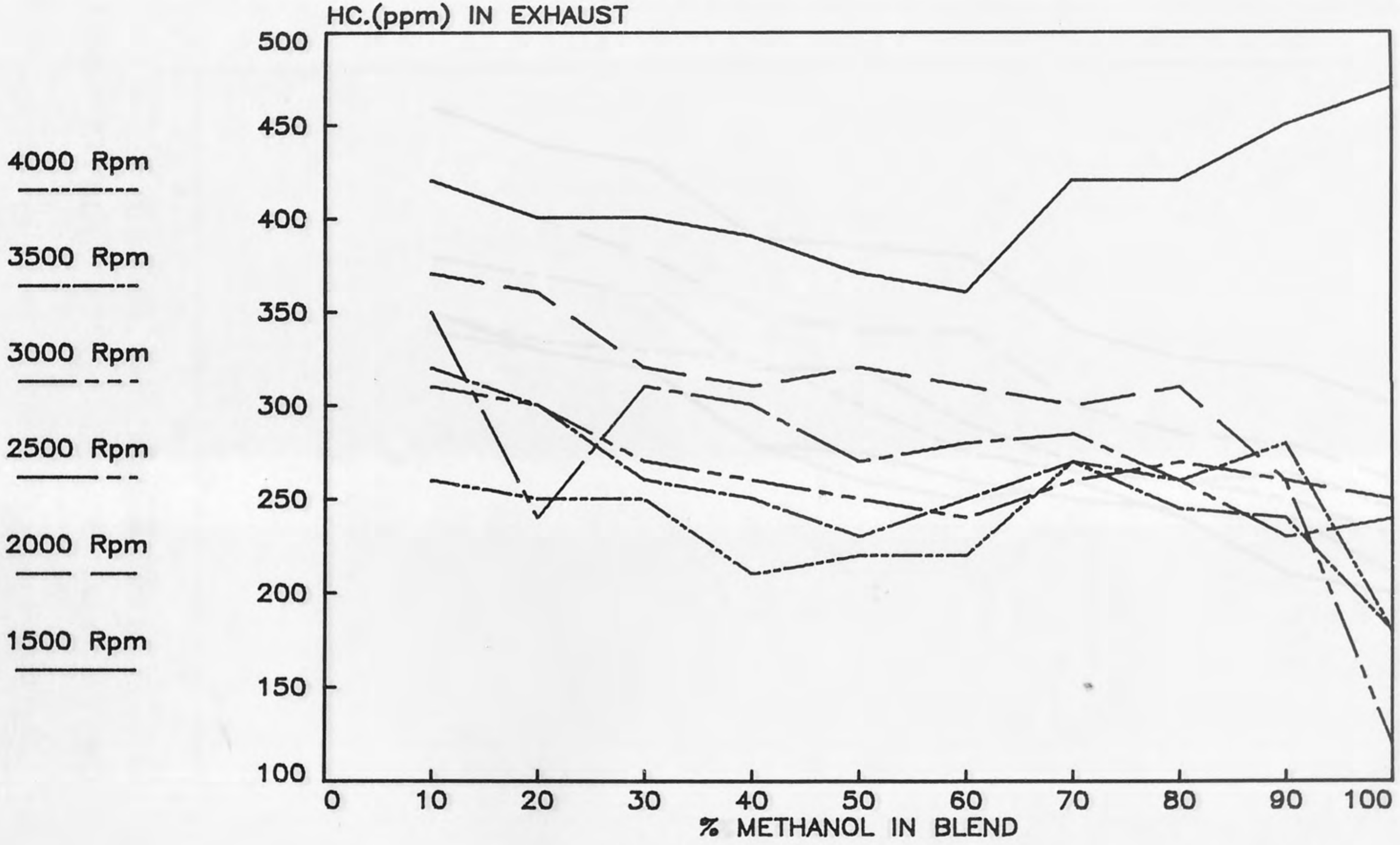

FIG: 4.1.99

EFFECT OF ALCOHOL CONTENT ON HC. EMISSION
AT STOICHIOMETRIC F/A RATIO

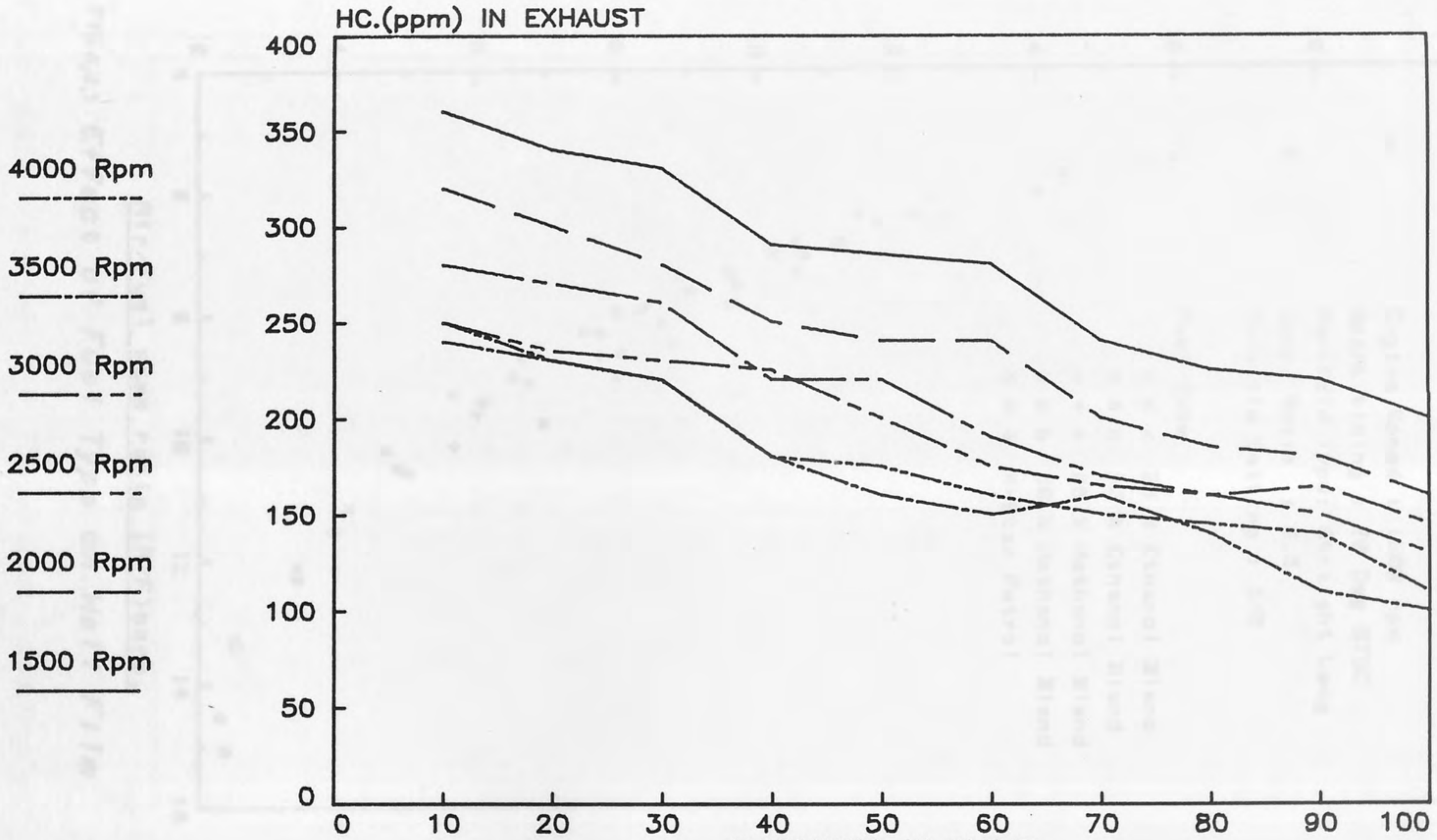

FIG: 4.1.100

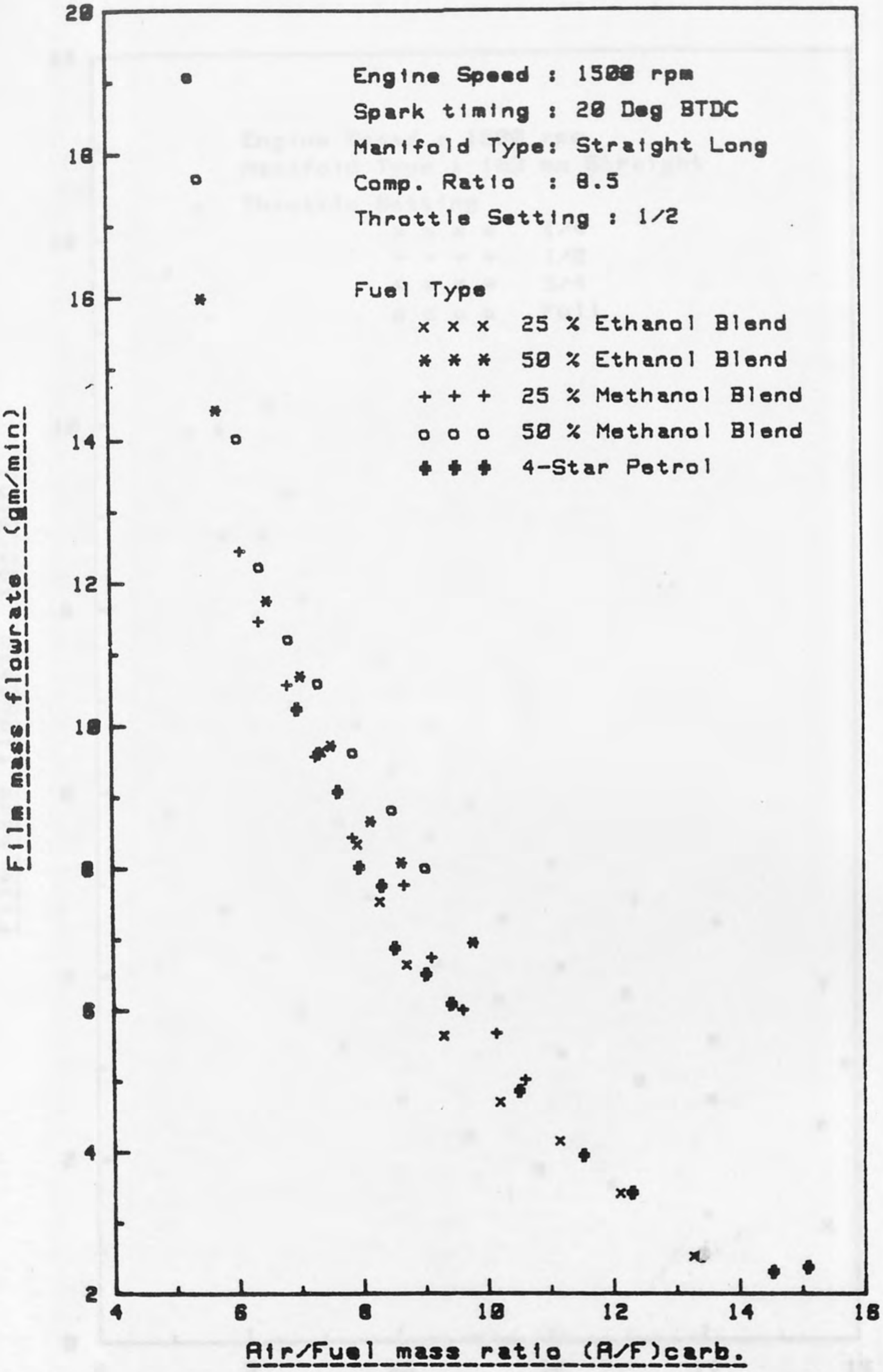

FIG 4.2.1 *Effect of Fuel Type on Wall Film*

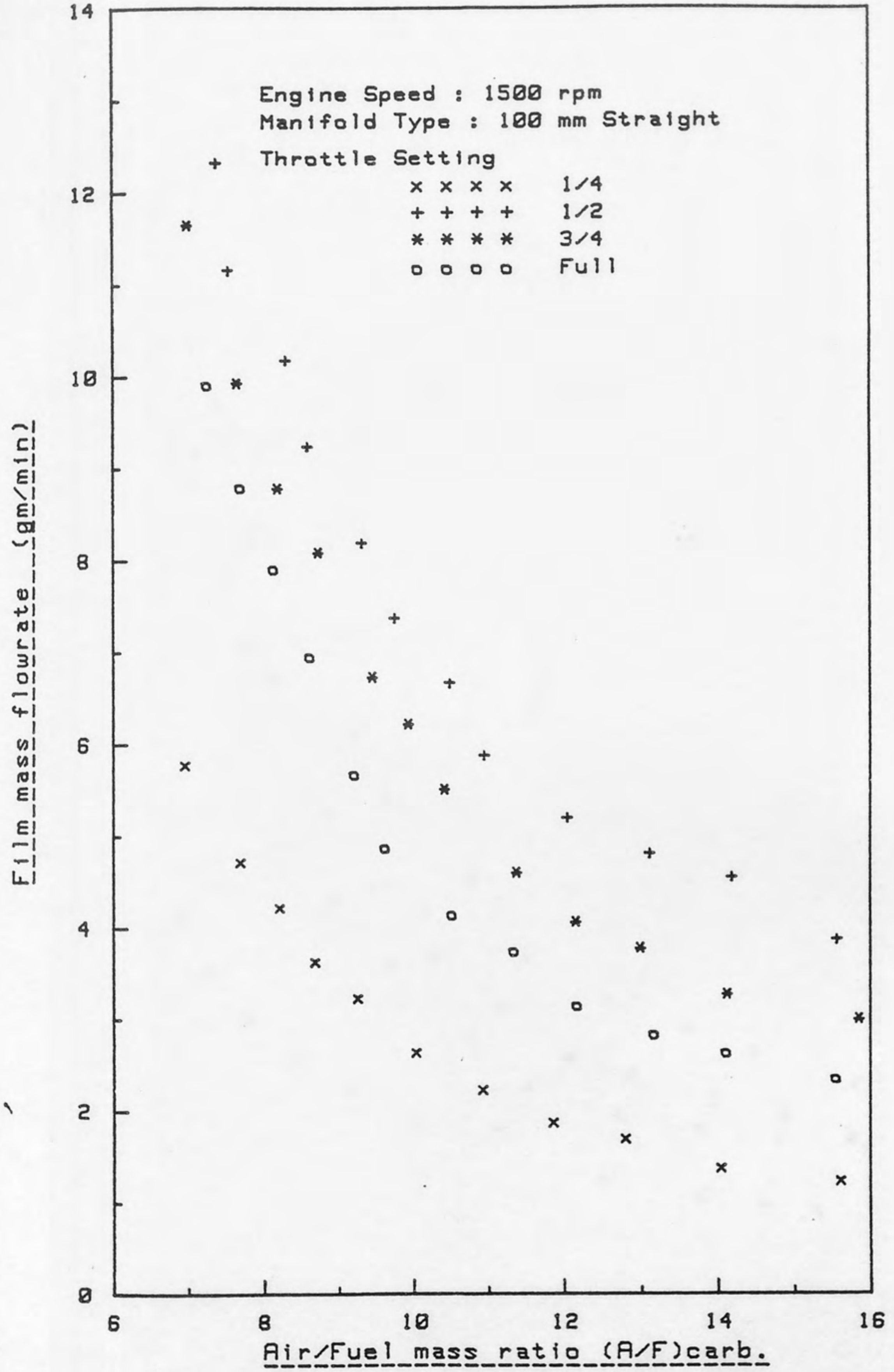

FIG. (4.2.2) *Effect of Throttle Setting on Film Flowrate*

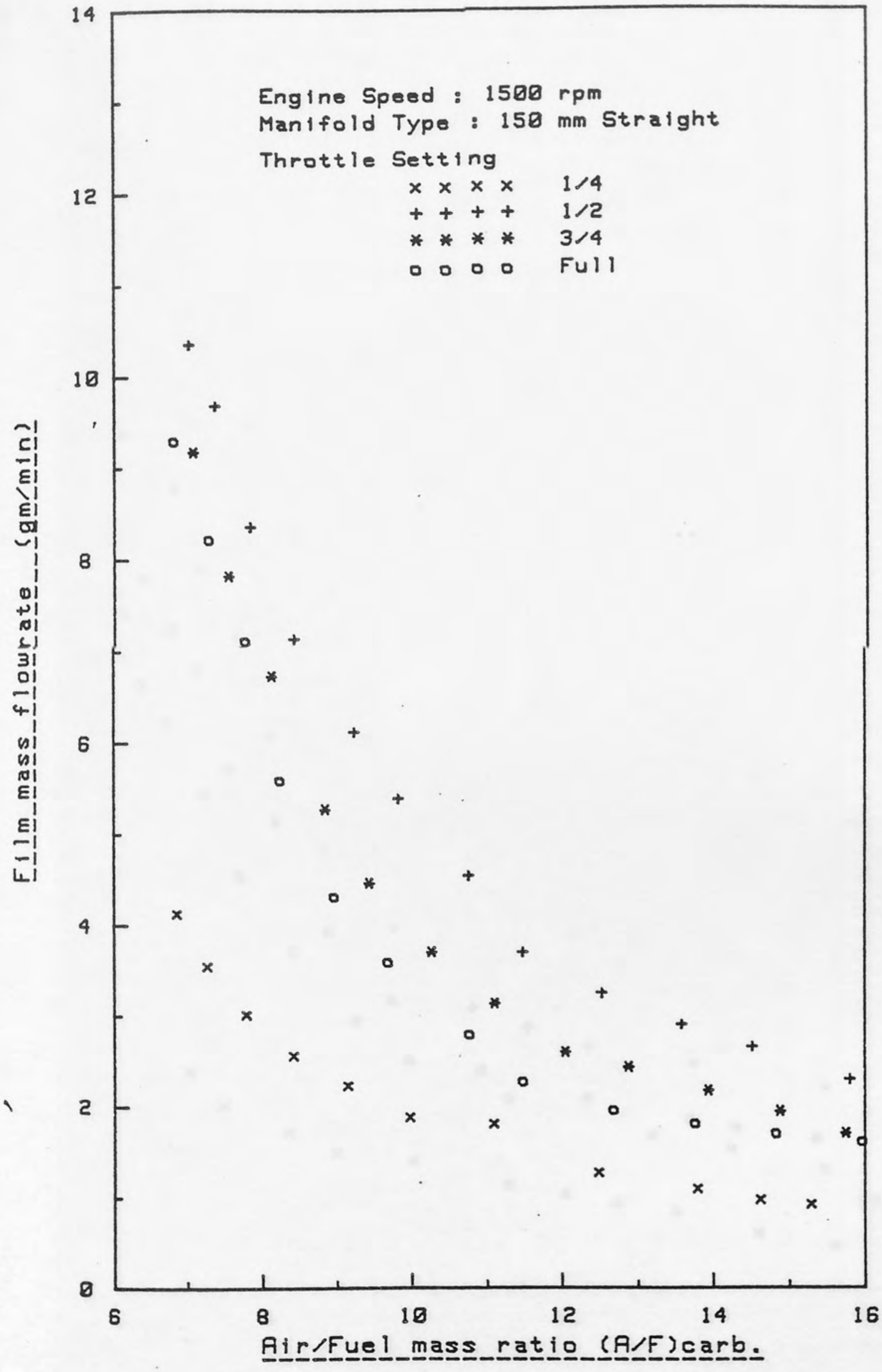

FIG. (4.2.3) *Effect of Throttle Setting on Film Flowrate*

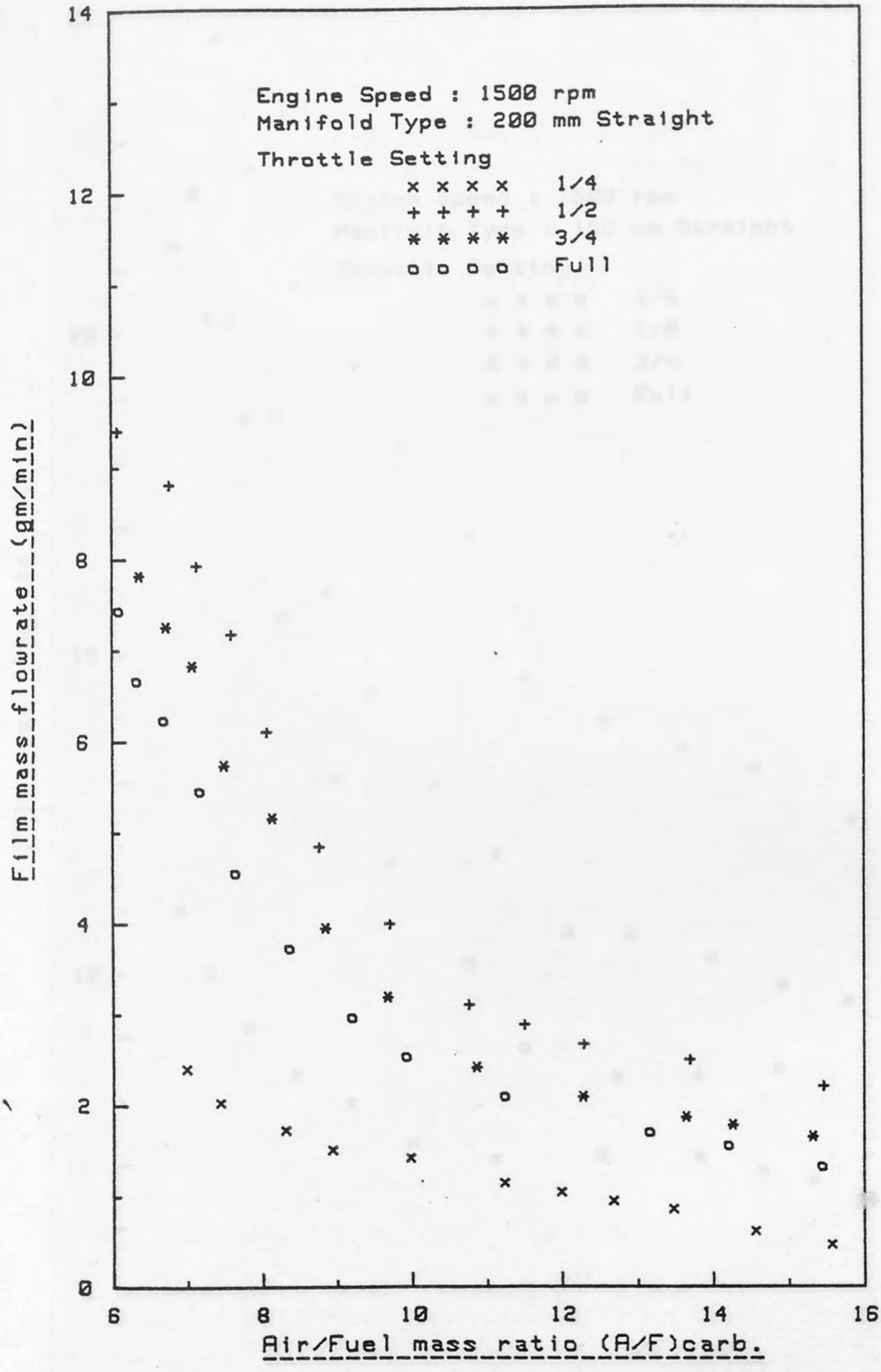

FIG. (4.2.4) Effect of Throttle Setting on Film Flowrate

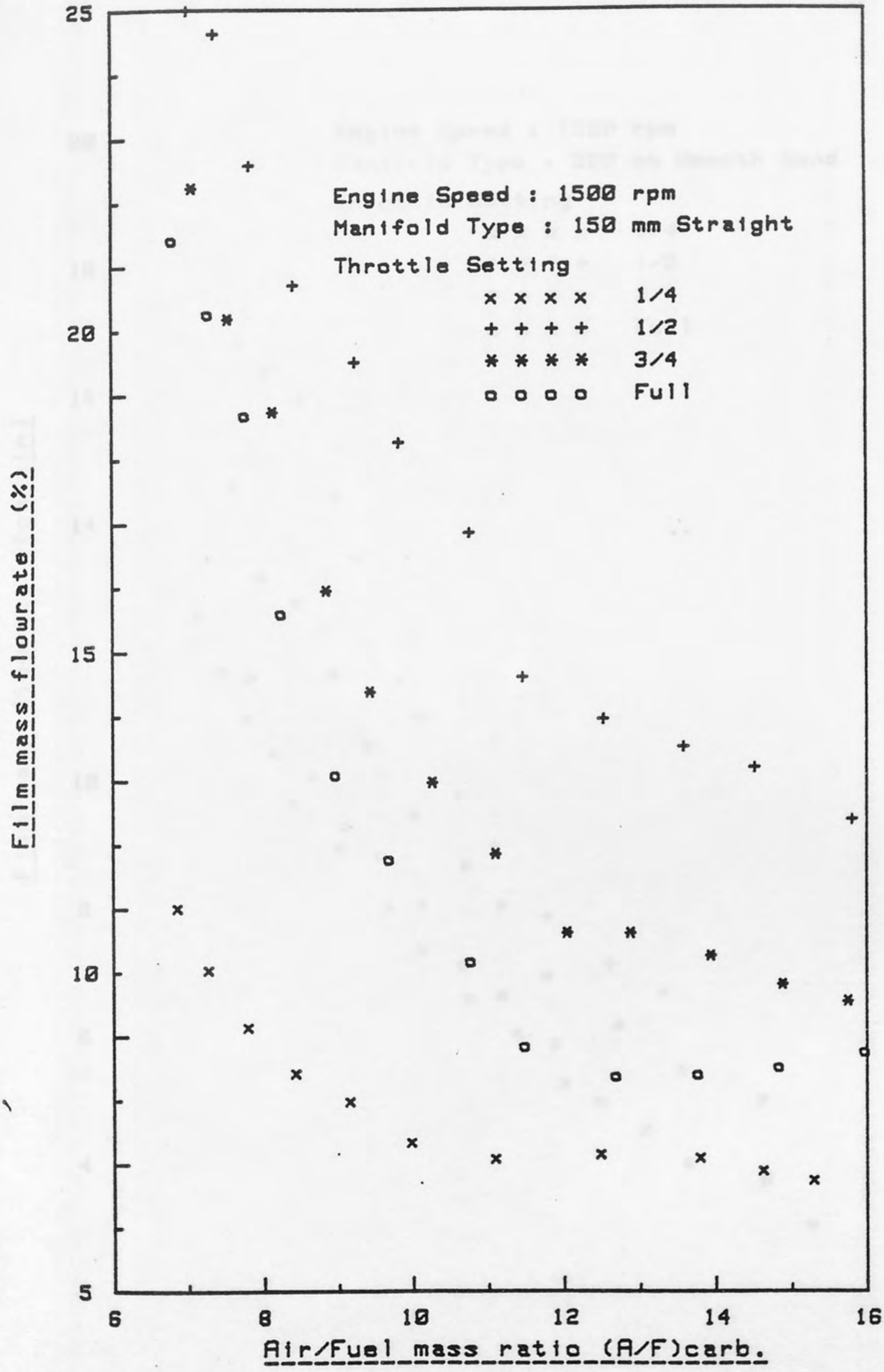

FIG. (4.2.5) *Effect of Throttle Setting on % Film Flowrate*

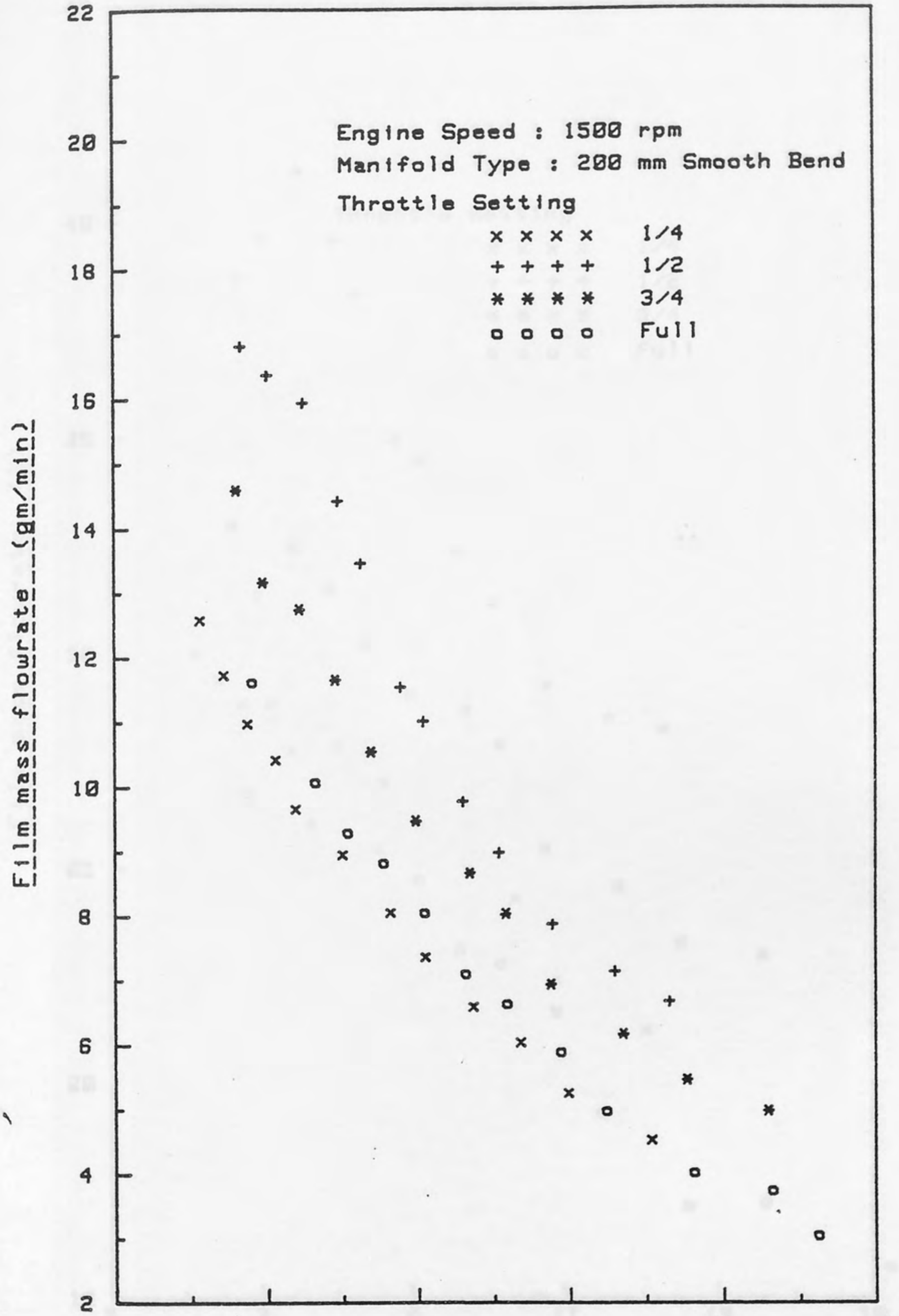

FIG. (4.2.6) Effect of Throttle Setting on Film Flowrate

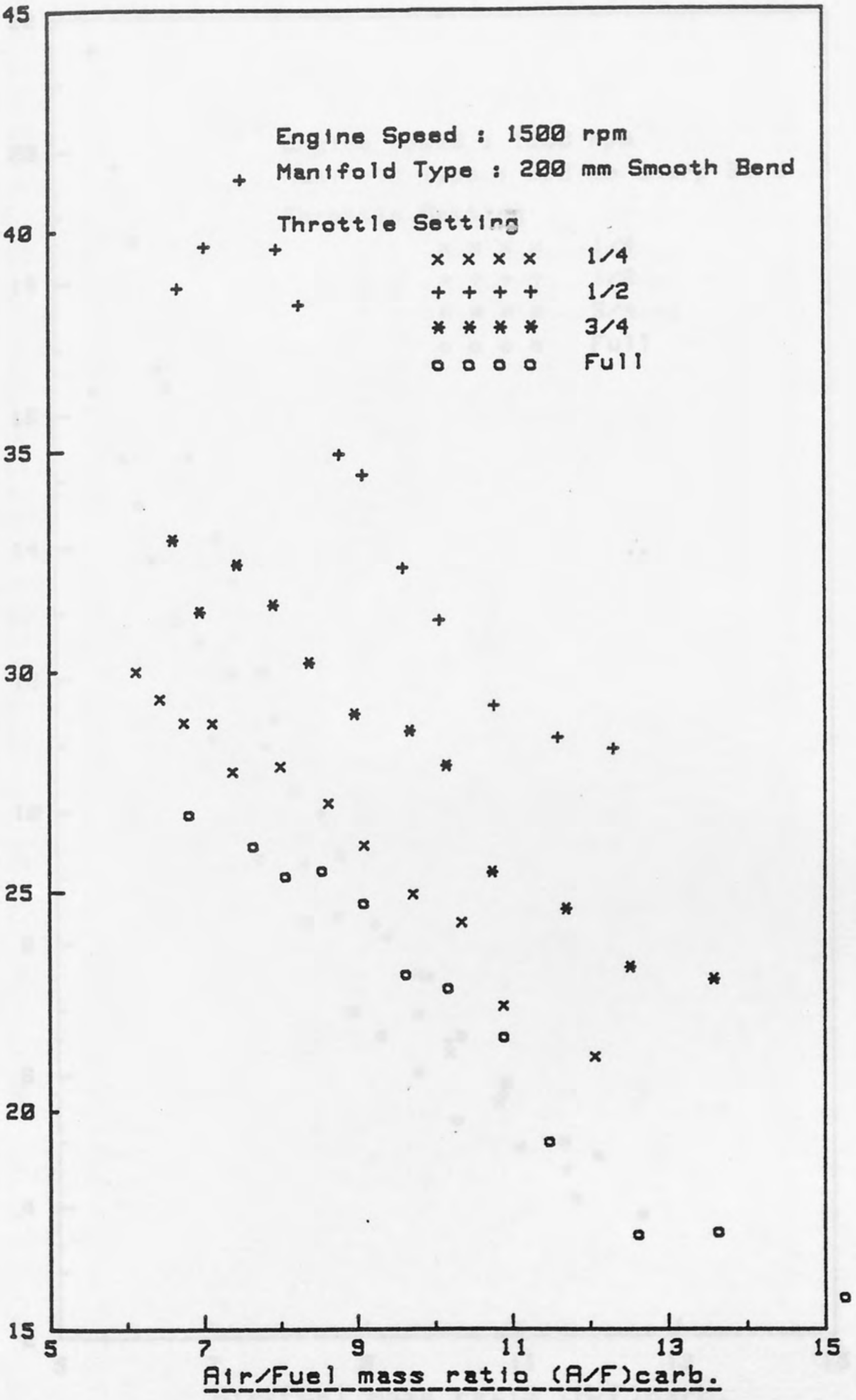

FIG. (4.2.7) *Effect of Throttle Setting on % Film Flowrate*

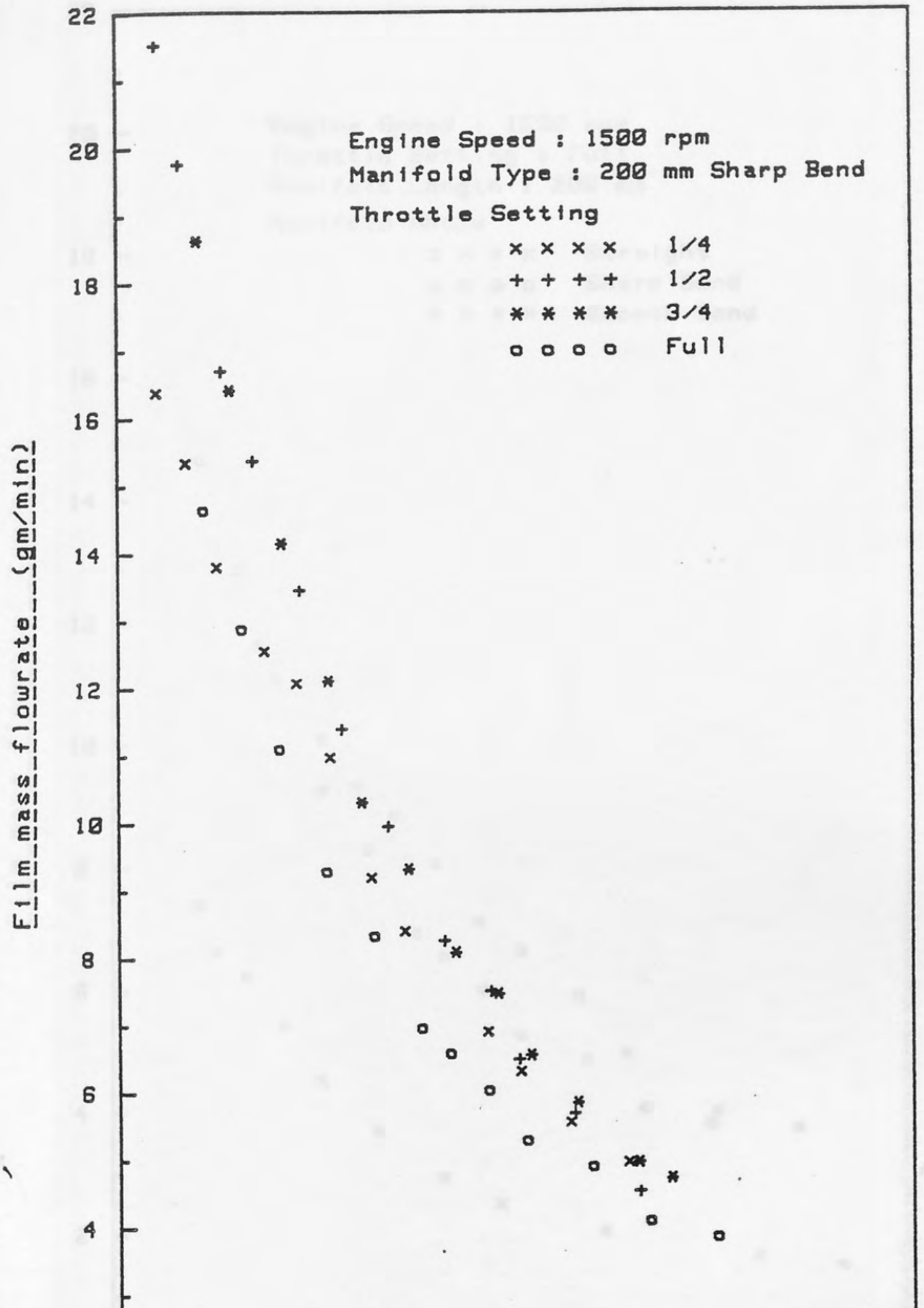

FIG. (4.2.8) *Effect of Throttle Setting on Film Flowrate*

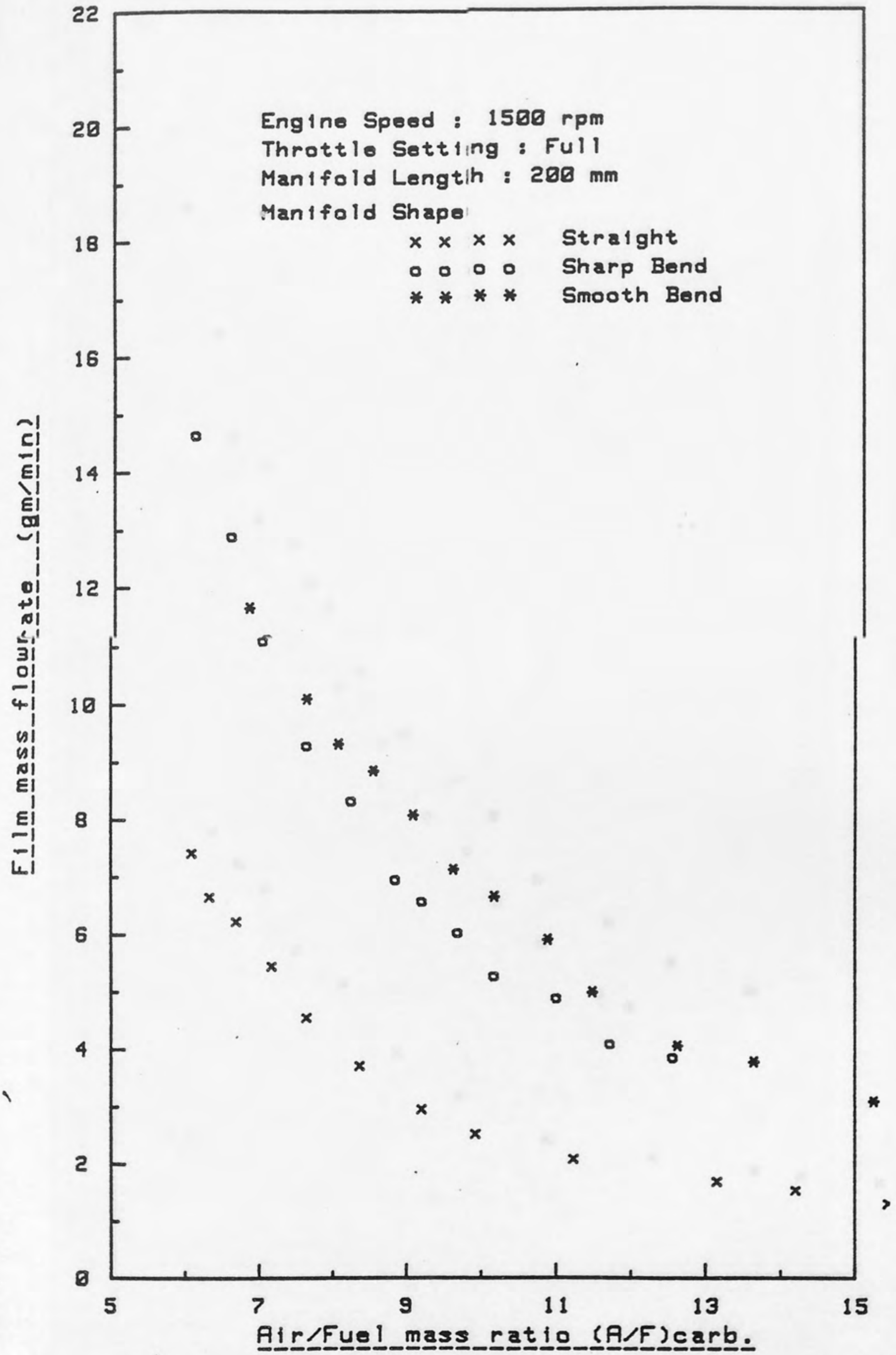

FIG. (4.2.9) Effect of Manifold Shape on Film Flowrate

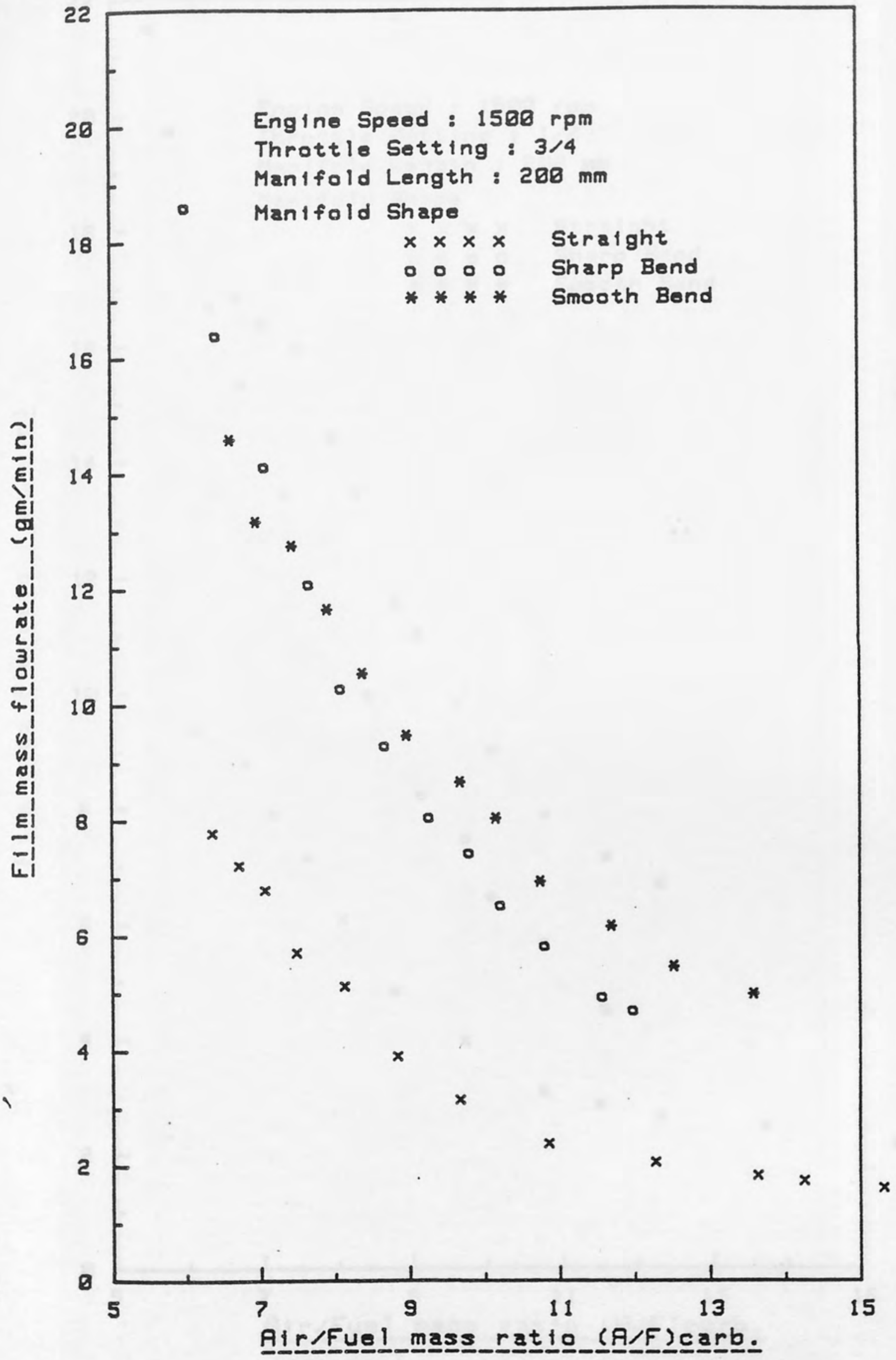

FIG. 4.2.10) Effect of Manifold Shape on Film Flowrate

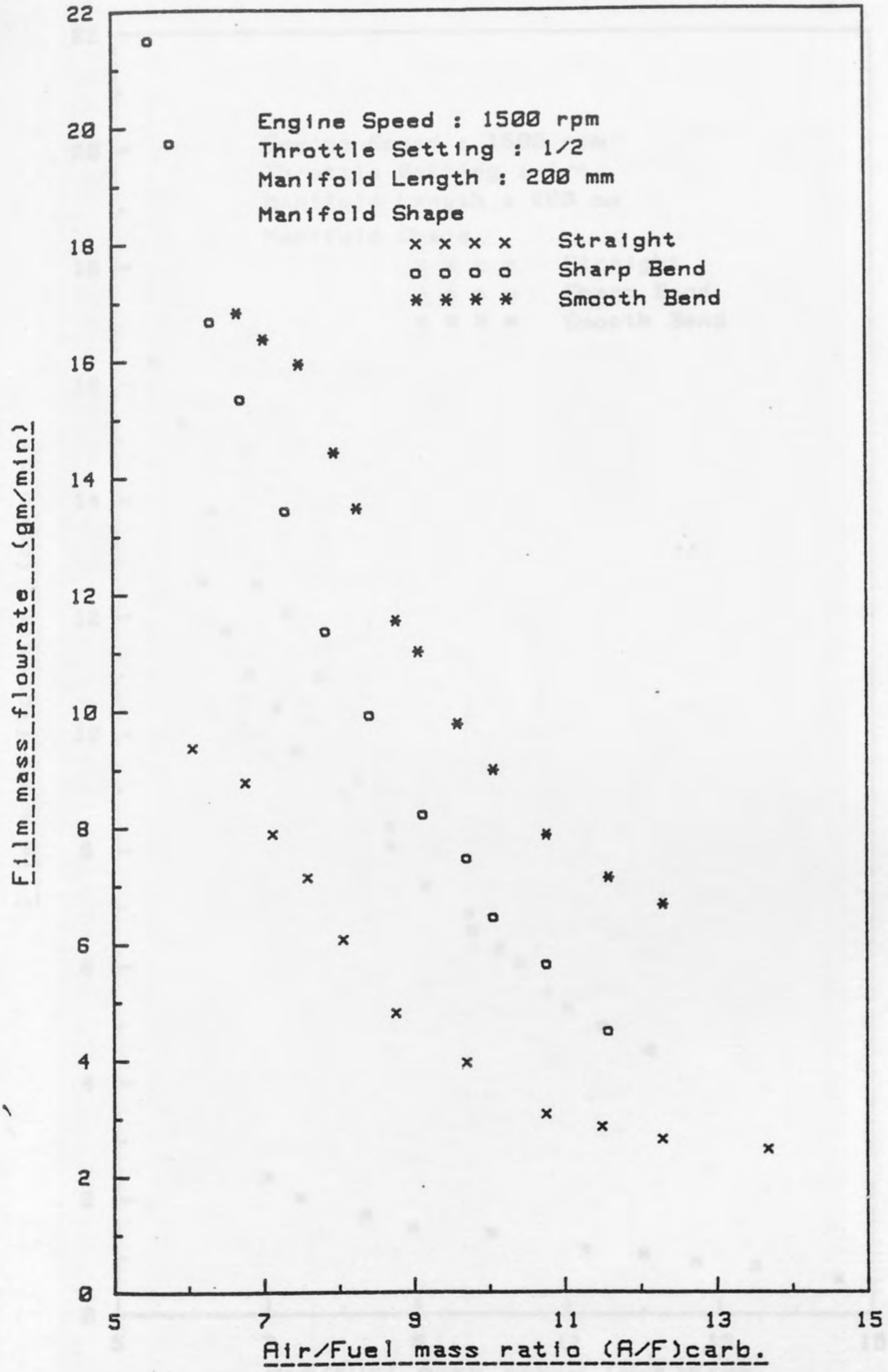

FIG. 4.2.11 *Effect of Manifold Shape on Film Flowrate*

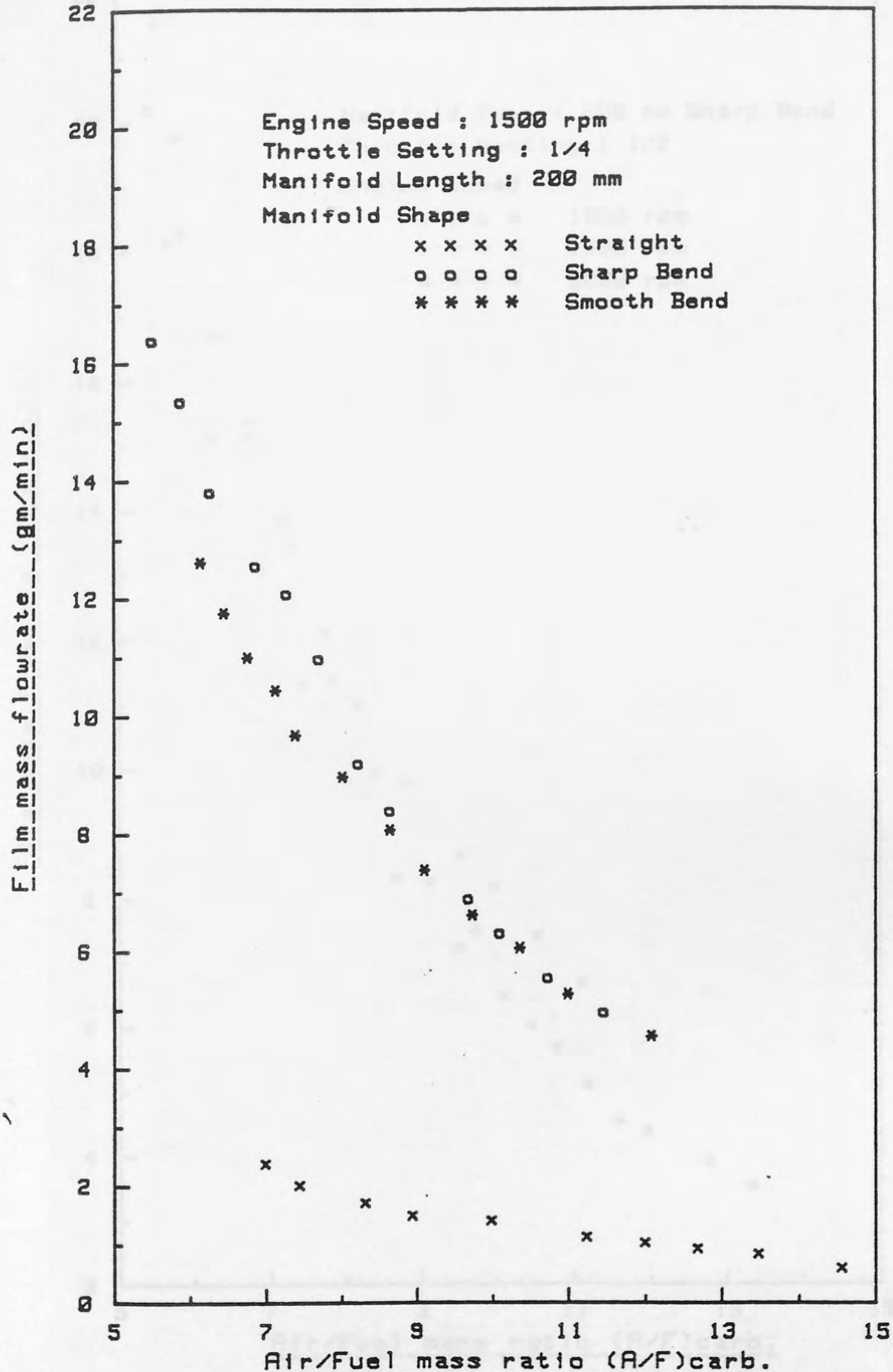

FIG. 4.2.12 Effect of Manifold Shape on Film Flowrate

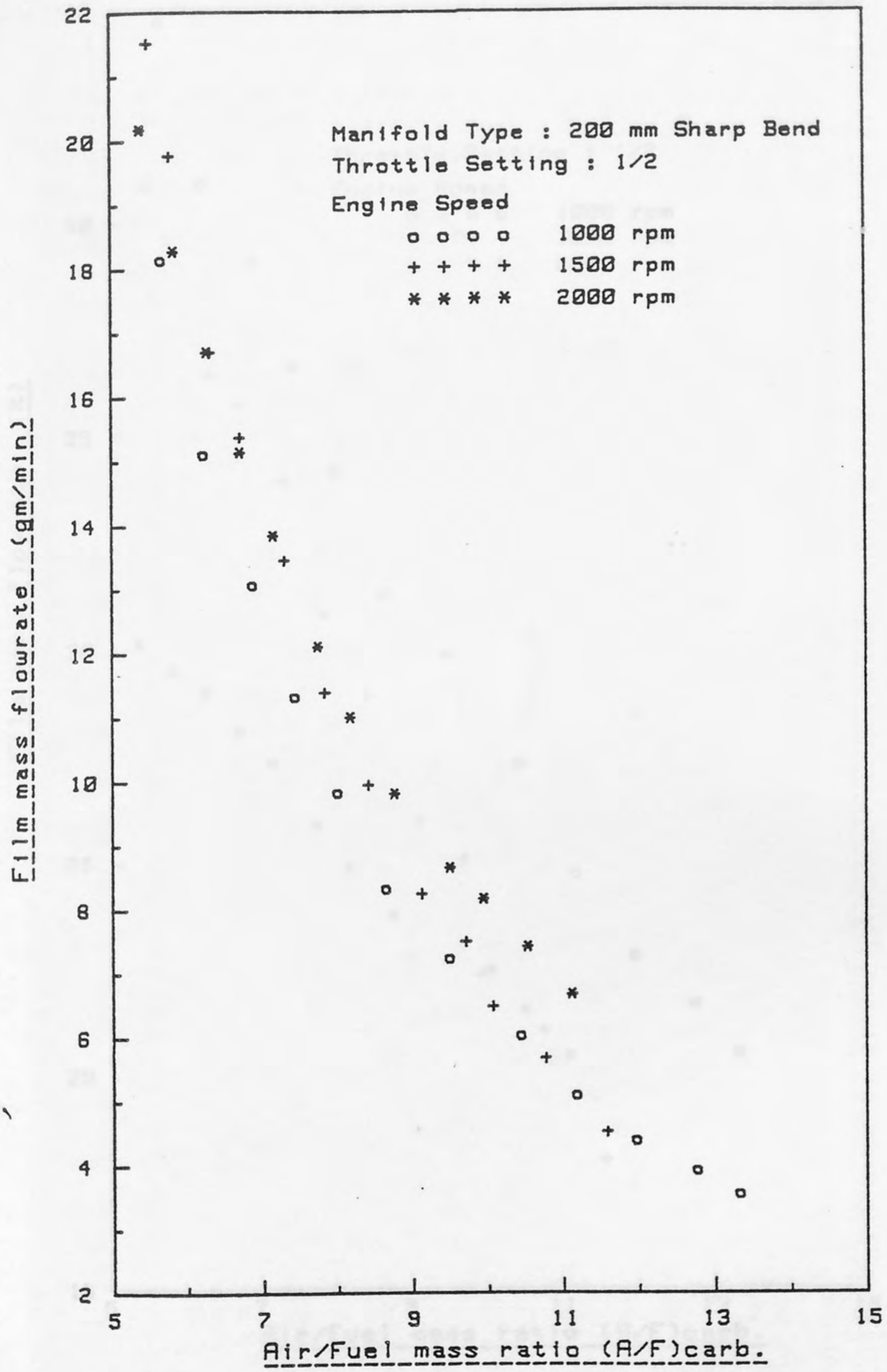

FIG. 4.2.13 *Effect of Engine Speed on Film Flowrate*

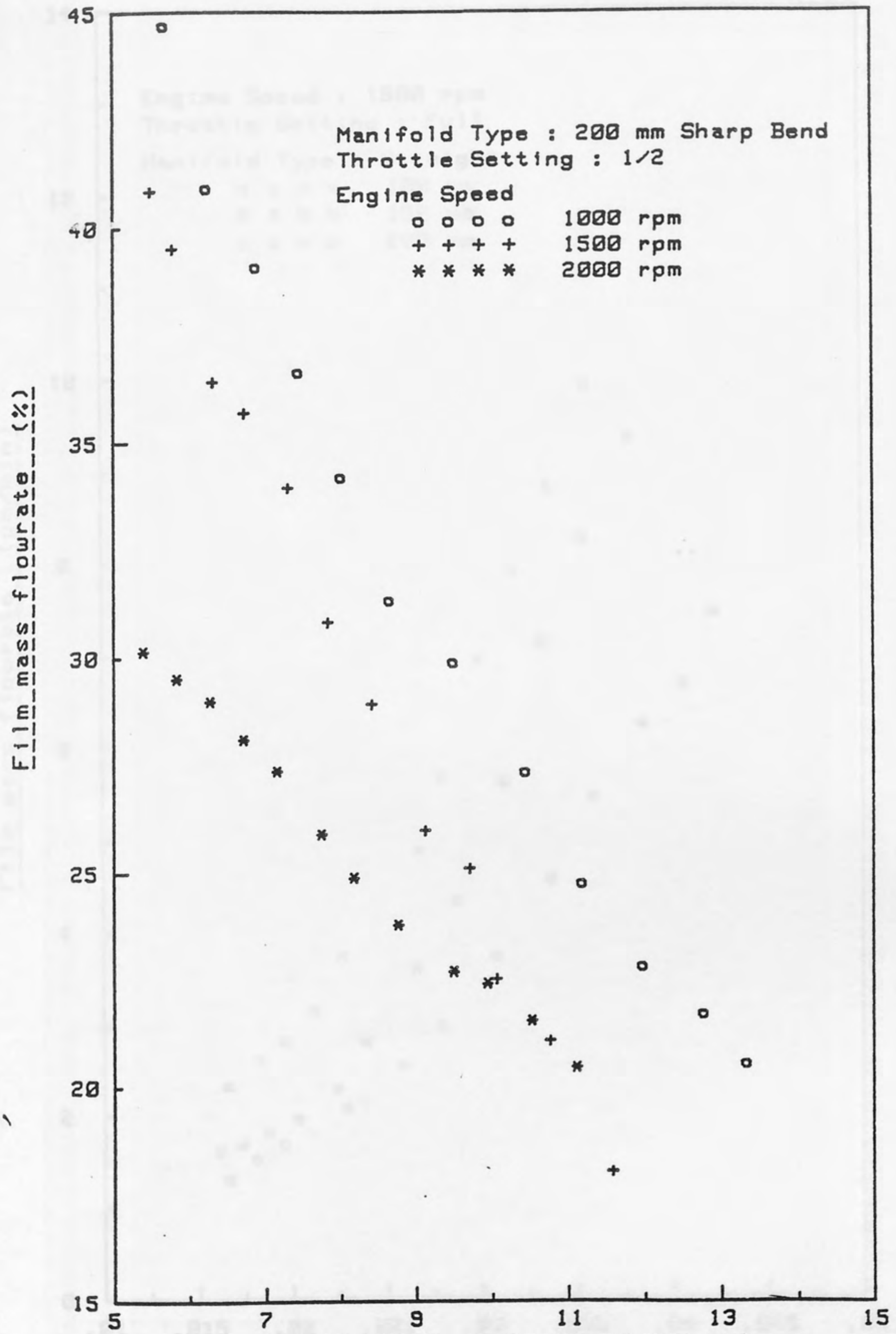

FIG. 4.2.14 *Effect of Engine Speed on % Film Flowrate*

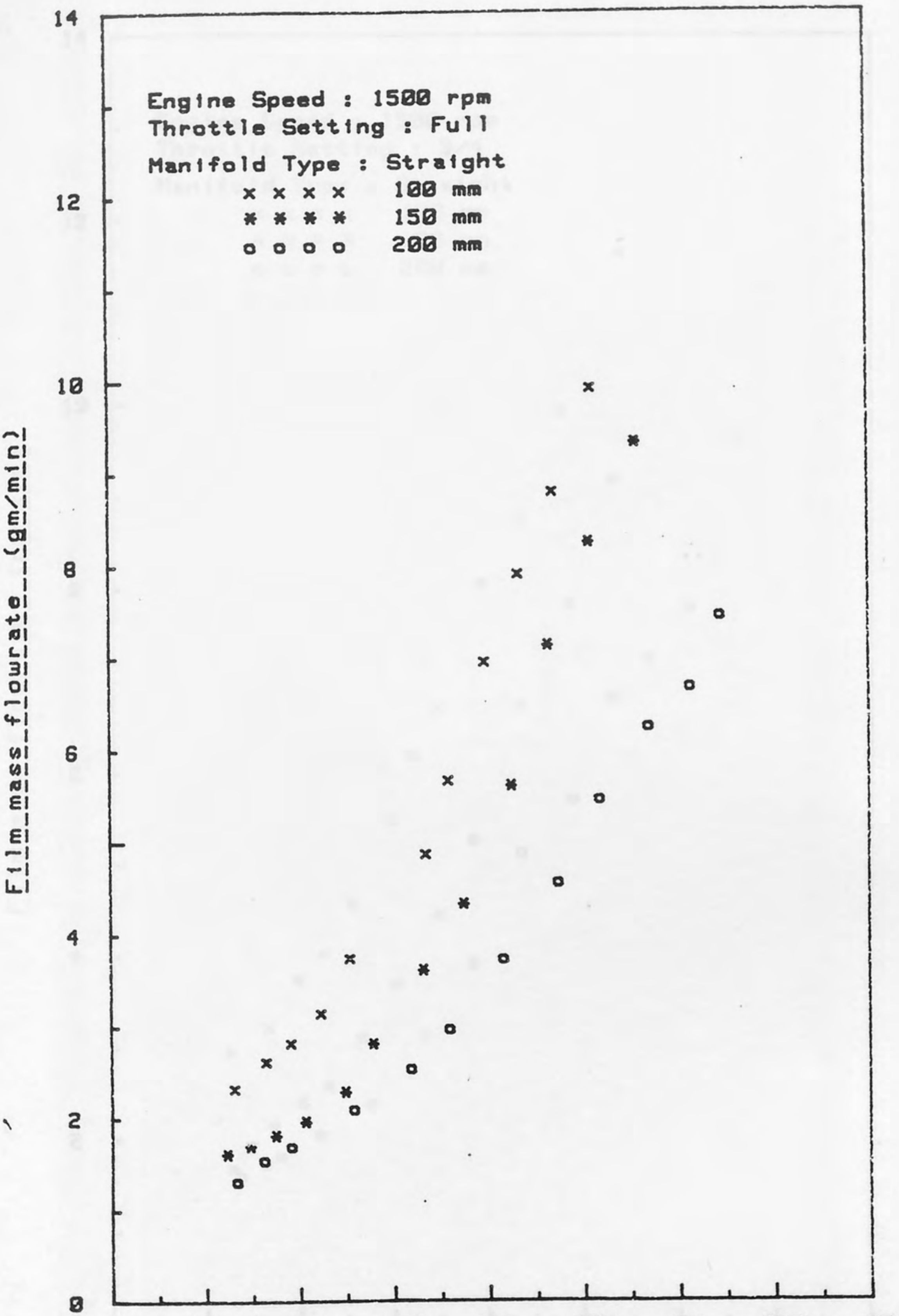

FIG. 4.2.15 *Effect of Manifold Length on Film Flowrate*

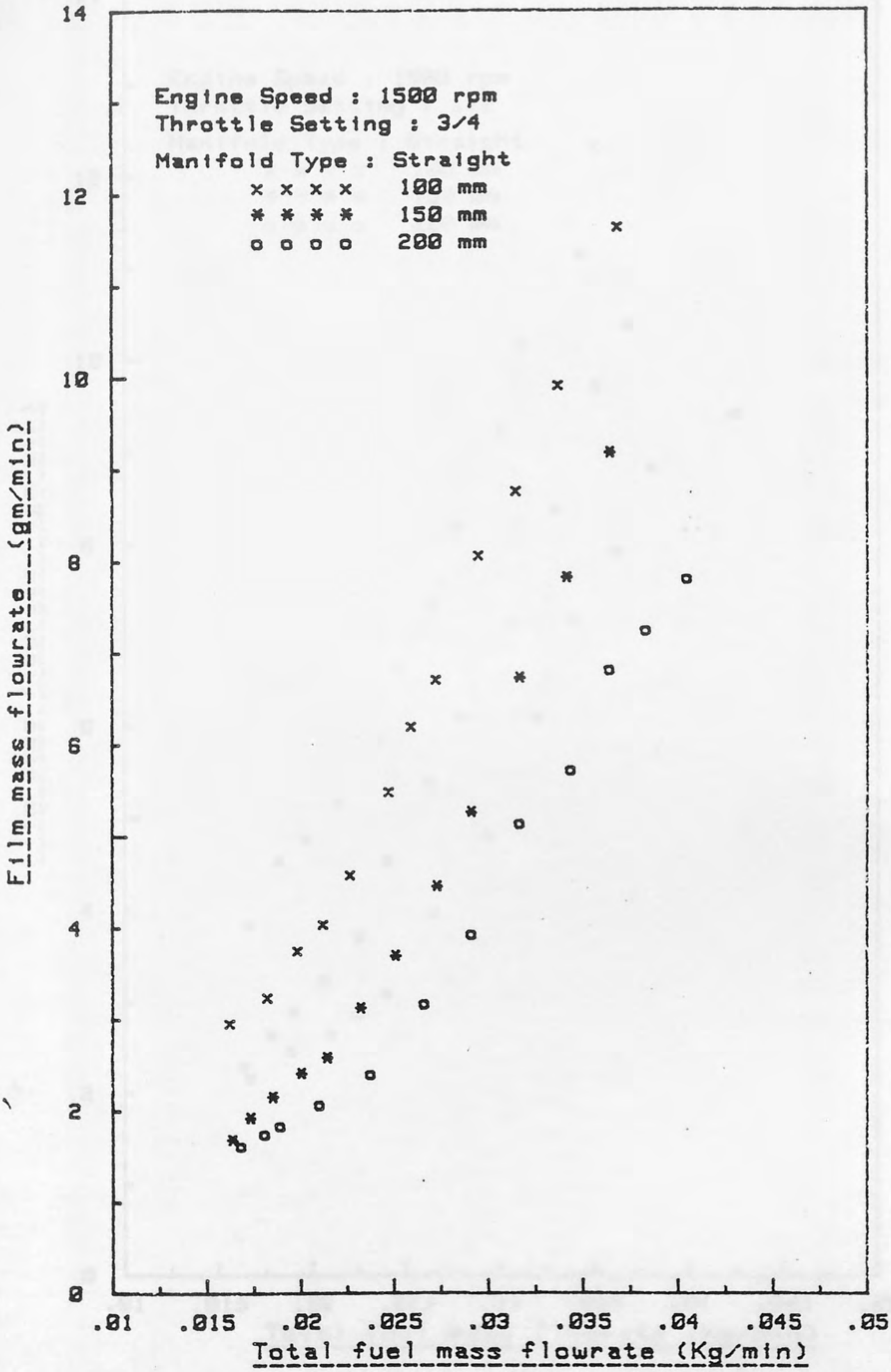

FIG. 4.2.16 *Effect of Manifold Length on Film Flowrate*

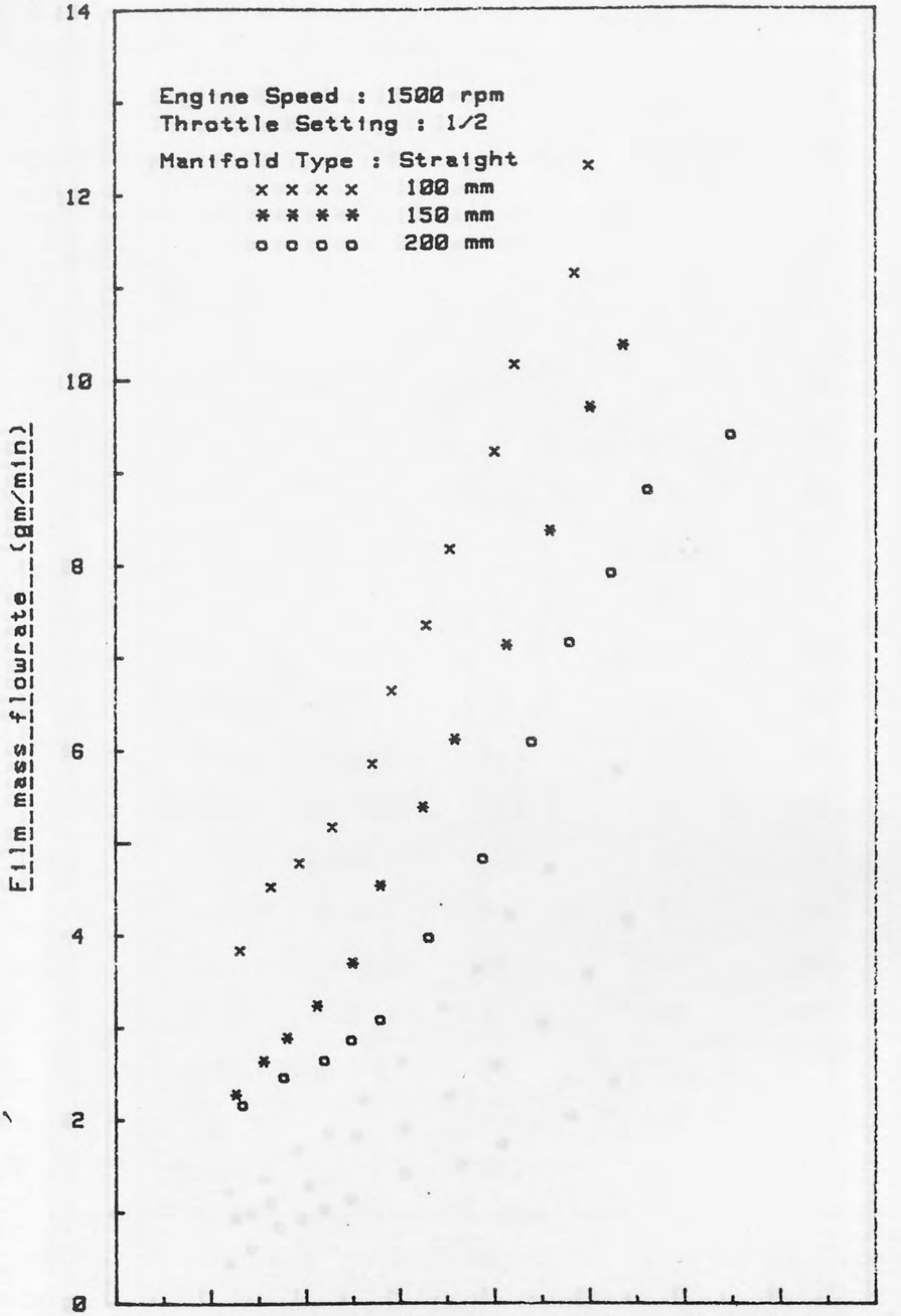

FIG. 4.2.17 *Effect of Manifold Length on Film Flowrate*

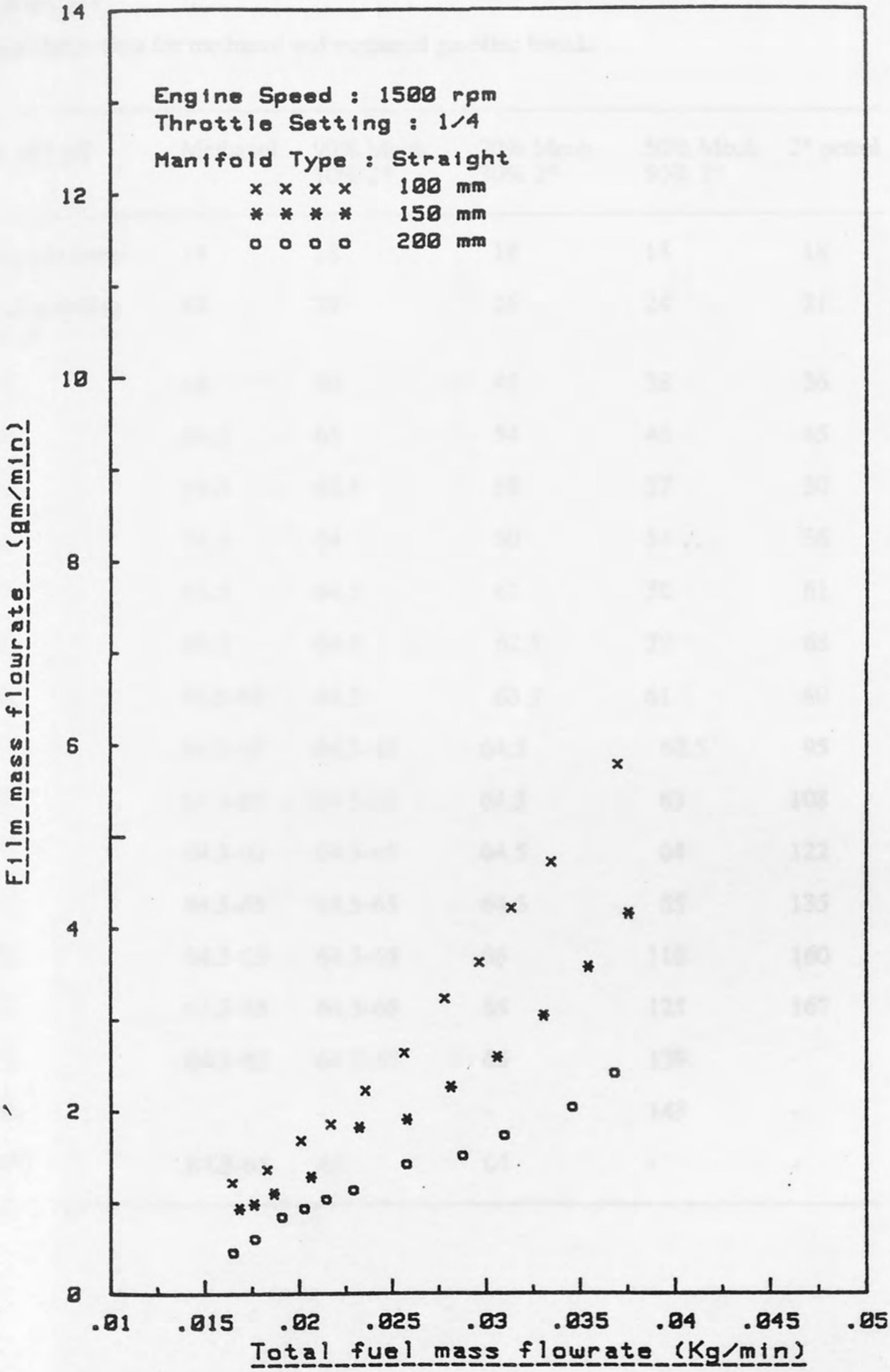

FIG. 4.2.18 *Effect of Manifold Length on Film Flowrate*

Table 4.3.1

Distillation data for methanol and methanol gasoline blends

% take off	Methanol	90% Meoh 10% 2*	70% Meoh 30% 2*	50% Meoh 50% 2*	2* petrol
Starting temp	18	18	18	18	18
Initial boiling point	62	29	26	24	21
5	64	60	45	38	36
10	64.5	63	54	46	45
15	64.5	63.5	58	57	50
20	64.5	64	60	54	56
25	64.5	64.5	61	56	61
30	64.5	64.5	62.5	59	68
40	64.5-65	64.5	63.5	61	80
50	64.5-65	64.5-65	64.5	62.5	95
60	64.5-65	64.5-65	64.5	63	108
70	64.5-65	64.5-65	64.5	64	122
80	64.5-65	64.5-65	64.5	65	135
90	64.5-65	64.5-65	65	116	160
92	64.5-65	64.5-65	65	125	167
95	64.5-65	64.5-65	66	139	-
96	-	-	-	143	-
100	64.5-65	65	67	-	-

Table 4.3.2

Distillation data for methanol and hydrated methanol

% take off	Methanol	95% Methanol 15% H_2O	90% Methanol 10% H_2O
Starting temp	18	18	18
Initial boiling point	62	61	61
5	64	64	64
10	64.5	64	64
15	64.5	64	64
20	64.5	64	64
25	64.5	64	64
30	64.5	64	64
40	64.5	64	64
50	64.5	64	64
60	64.5-65	64	64
70	64.5-65	64	64
80	64.5-65	64	64
90	64.5-65	64	64
92	64.5-65	64	-
95	64.5-65	64.5	80
96		69	-
97		88	-
98	64.5-65	-	98
100			

Table 4.3.3

Distillation data for methanol and methanol with iso- and n-pentenes

% take off	Methanol	90% Methanol 10% iso-pentene	90% Methanol 10%n-pentene
Starting temp	18	18	18
Initial boiling point	62	24	27
5	64	37	41
10	64.5	58	58
15	64.5	64	64
20	64.5	64.5	64.5
25	64.5	64.5	64.5
30	64.5	64.5	64.5
40	64.5	64.5	64.5
50	64.5	64.5	64.5
60	64.5-65	64.5	64.5
70	64.5-65	64.5	64.5
80	64.5-65	64.5	64.5
90	64.5-65	64.5	64.5
92	64.5-65	-	-
95	64.5-65	64.5	64.5
96	-	-	-
97	-	-	-
98	64.5-65	64.5	64.5
100			

Table 4.3.4

Distillation data for ethanol and ethanol gasoline blends

% take off	Ethanol	90% Ethanol 10% 2*	70% Ethanol 30% 2*	50% Ethanol 50% 2*	2* petrol
Starting temp	18	18	18	18	18
Initial boiling point	69	26	24	24	21
5	78	68	45	40	36
10	78	76	61	48.5	45
15	78	76.5	70	55.5	50
20	78	77.5	73	61.5	56
25	78	77.5	75	67.5	61
30	78	78	76	73.0	68
40	78	78	77	74.5	80
50	78	78	77.5	76	95
60	78	78	78.0	76.5	109
70	78	78	78	77.5	122
80	78	78	78.5	78.5	135
90	78	78	78.5	119	160
92	-	78.5	-	135	167
95	78	78.5	79	141	-
96	-	-	80	-	-
97	78	-	-	-	-
98	-	79	-	-	-
100					

Table 4.3.5

Distillation data for ethanol and hydrated ethanol

% take off	Ethanol	95% Ethanol 5% H_2O	90% Ethanol 10% H_2O	85% Ethanol 15% H_2O
Starting temp	18	18	18	18
Initial boiling point	69	70	70	71
5	78	78	78	78
10	78	78	78	78
15	78	78	78	78
20	78	78	78	78
25	78	78	78	78
30	78	78	78	78
40	78	78	78	78
50	78	78	78	78
60	78	78	78	78
70	78	78	78	78
80	78	78	78	78
85	78	78	78	80
90	78	78	79	82
92	78	78	-	-
95	78	78	81	85
96	-	78	85	90
97	-	-	-	-
98	78	78	95	97
100				

Table 4.3.6

Distillation data for ethanol and ethanol with iso- and n-pentane

% take off	Ethanol	90% Ethanol 10% iso-pentane	90% Ethanol 10% n-pentane
Starting temp	18	18	18
Initial boiling point	64	26	32
5	78	45	42
10	78	68	67
15	78	78	75
20	78	78	78
25	78	78	78
30	78	78	78
40	78	78	78
50	78	78	78
60	78	78	78
70	78	78	78
80	78	78	78
90	78	78	78
92	78	78	78
95	78	78	78
98	78	78	78
100			

FIG: 4.3.1 DISTILLATION CURVES FOR METHANOL, GASOLINE AND METHANOL GASOLINE BLENDS

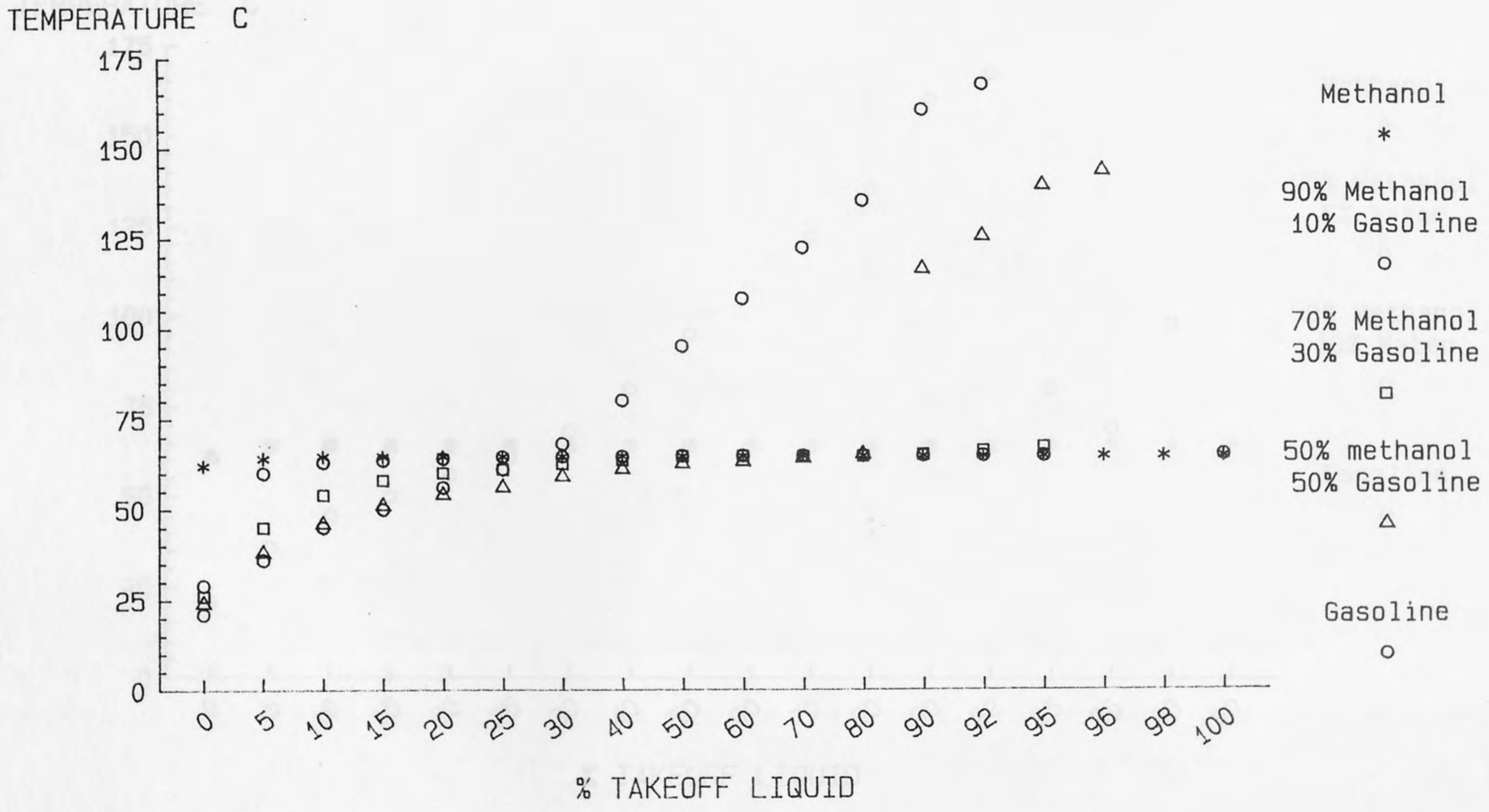

FIG: 4.3.2 DISTILLATION CURVES FOR METHANOL, GASOLINE AND HYDRATED METHANOL

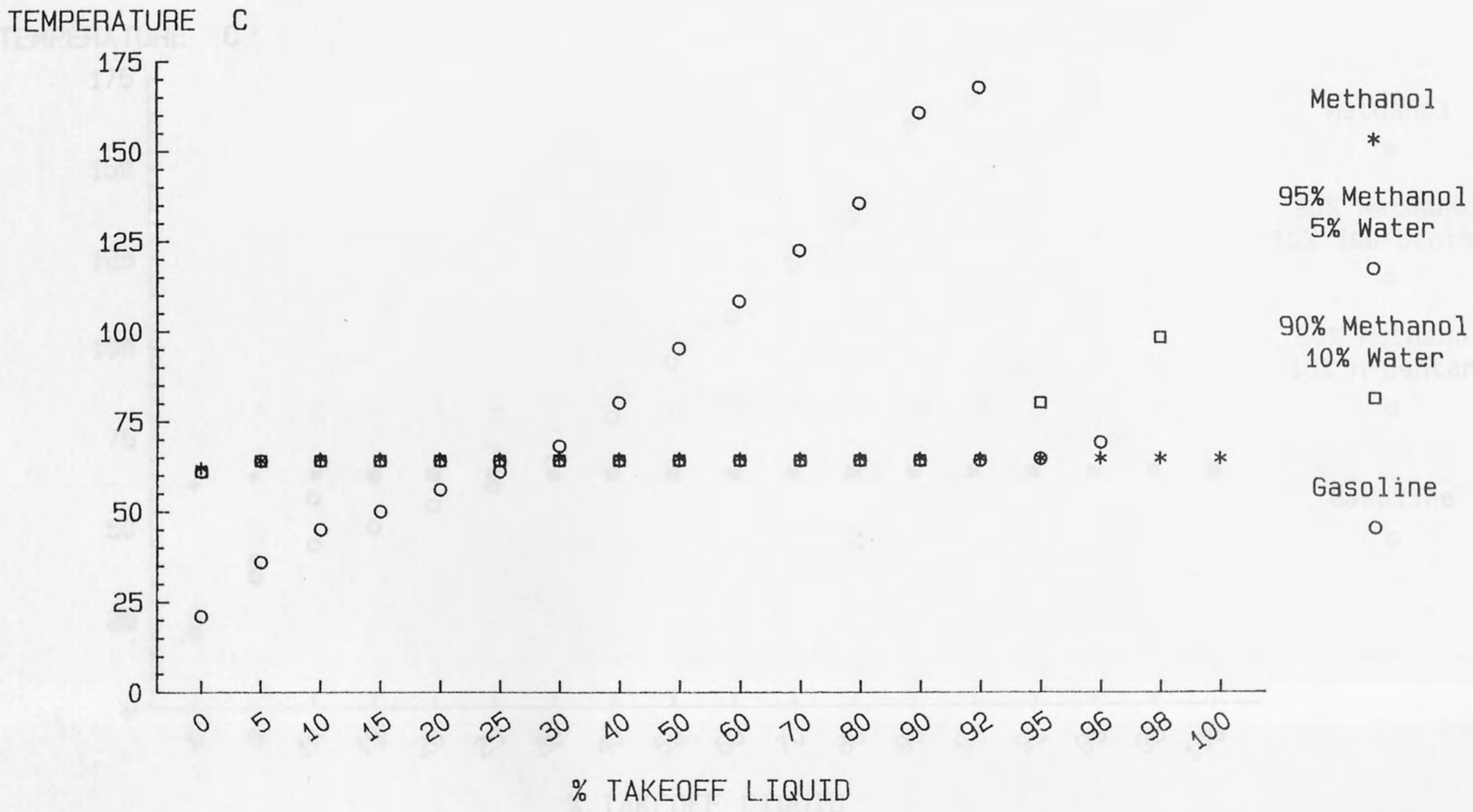

FIG: 4.3.3 DISTILLATION CURVES FOR METHANOL, GASOLINE AND METHANOL WITH ADDITIVES

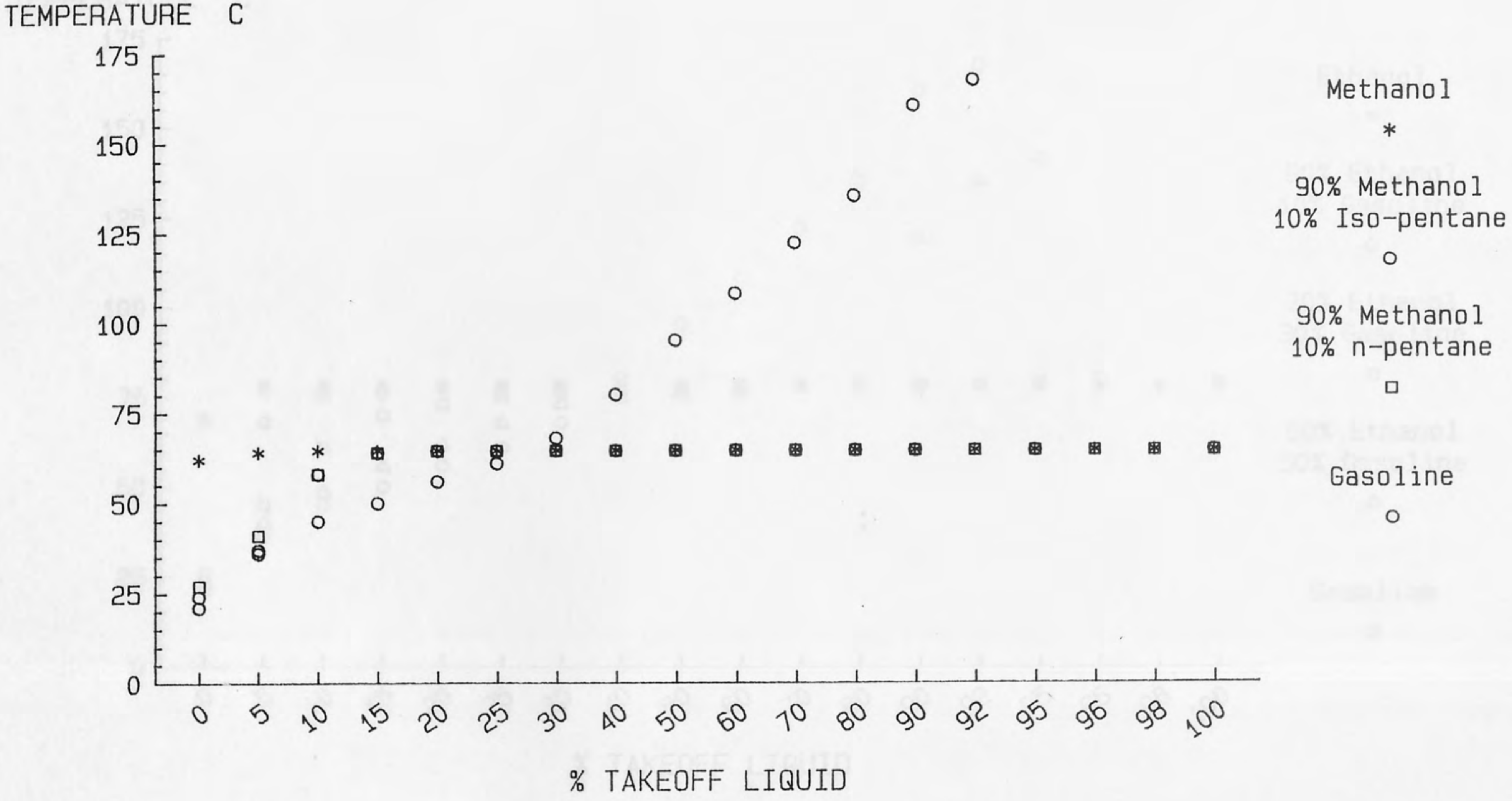

FIG: 4.3.4 DISTILLATION CURVES FOR ETHANOL, GASOLINE AND ETHANOL GASOLINE BLENDS

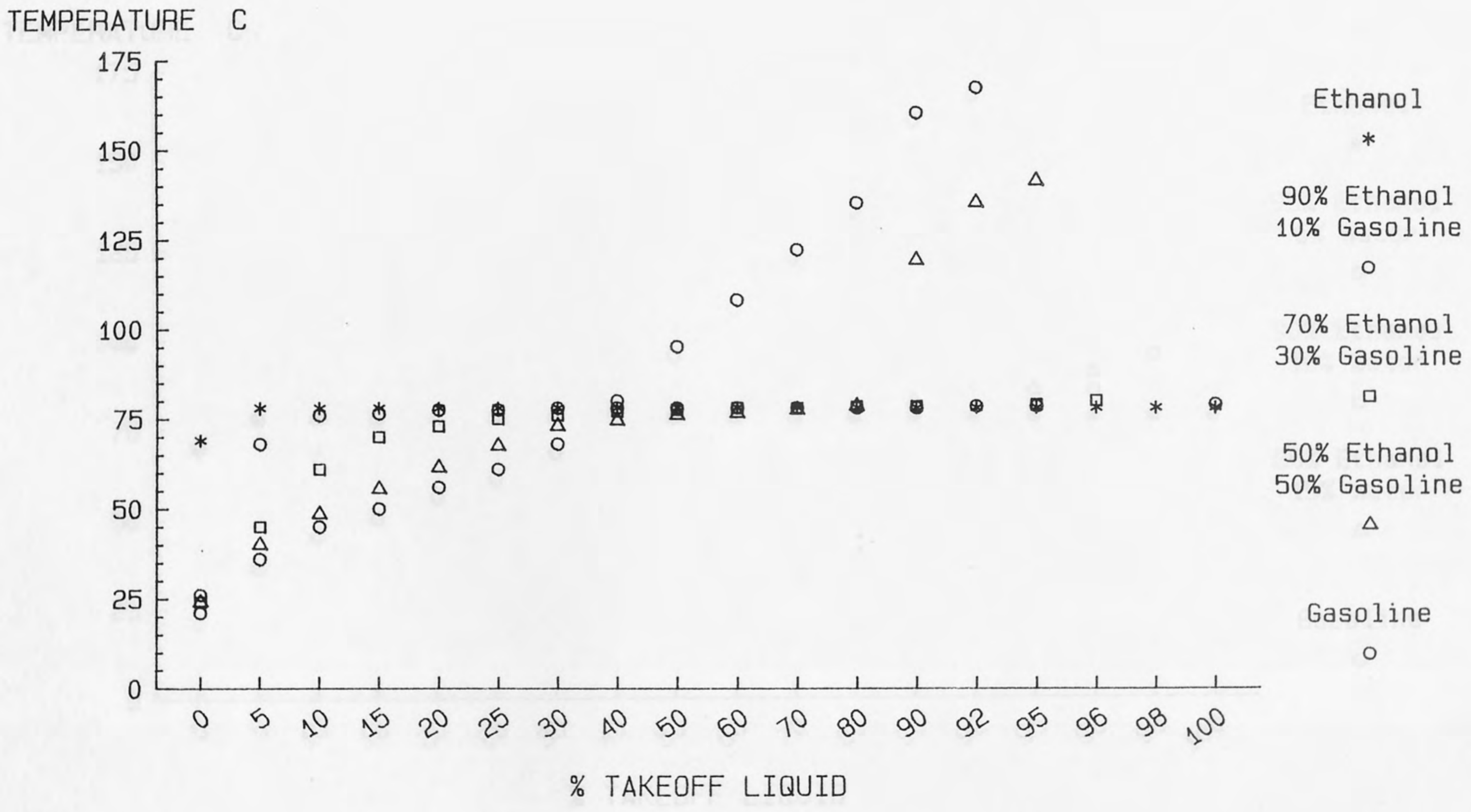

FIG: 4.3.5 DISTILLATION CURVES FOR ETHANOL, GASOLINE AND HYDRATED ETHANOL

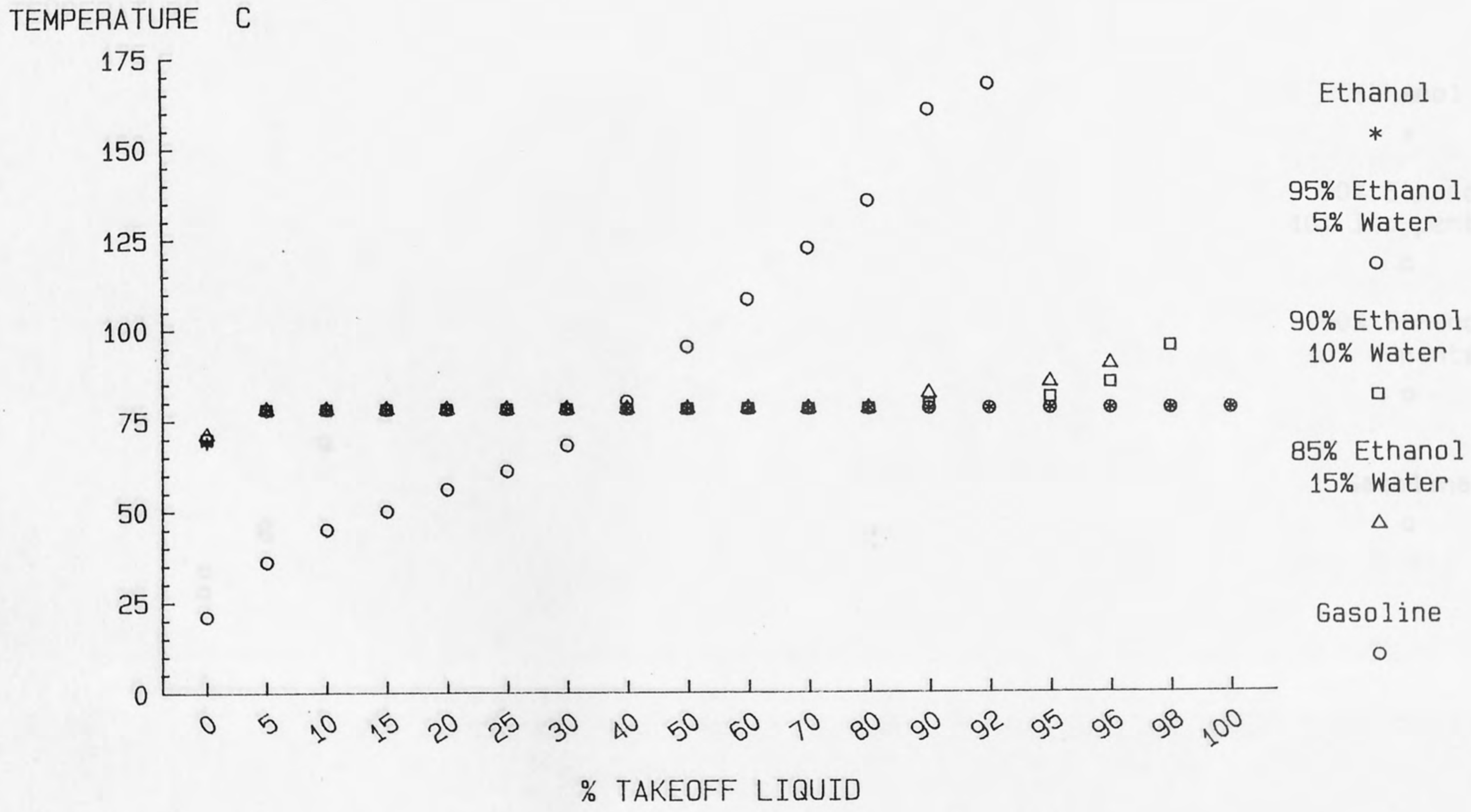

FIG: 4.3.6 DISTILLATION CURVES FOR ETHANOL, GASOLINE AND ETHANOL WITH ADDITIVES

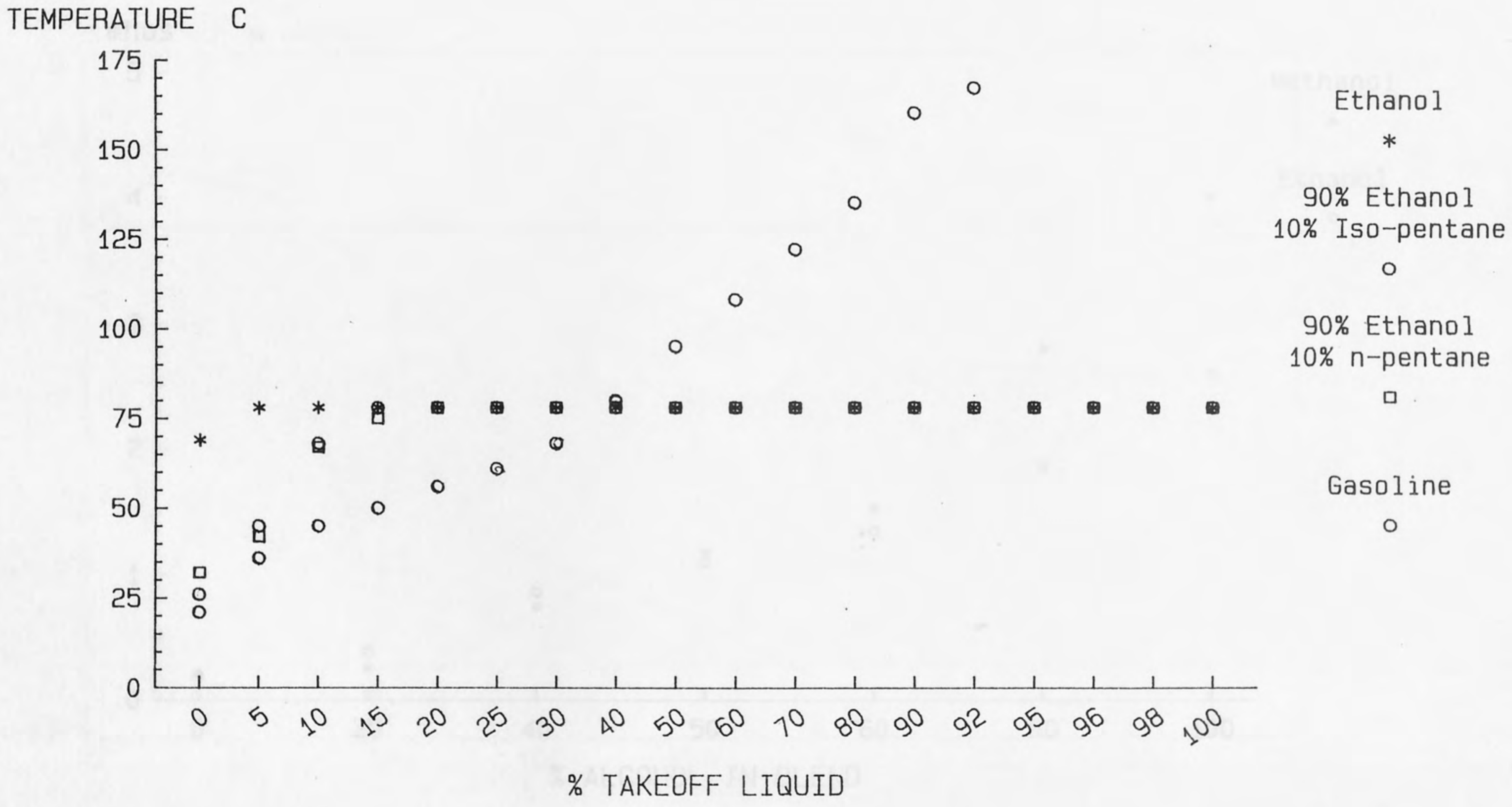

FIG:4.4.0 ELECTRICAL CONDUCTIVITY OF METHANOL AND ETHANOL GASOLINE BLENDS AT 25 C

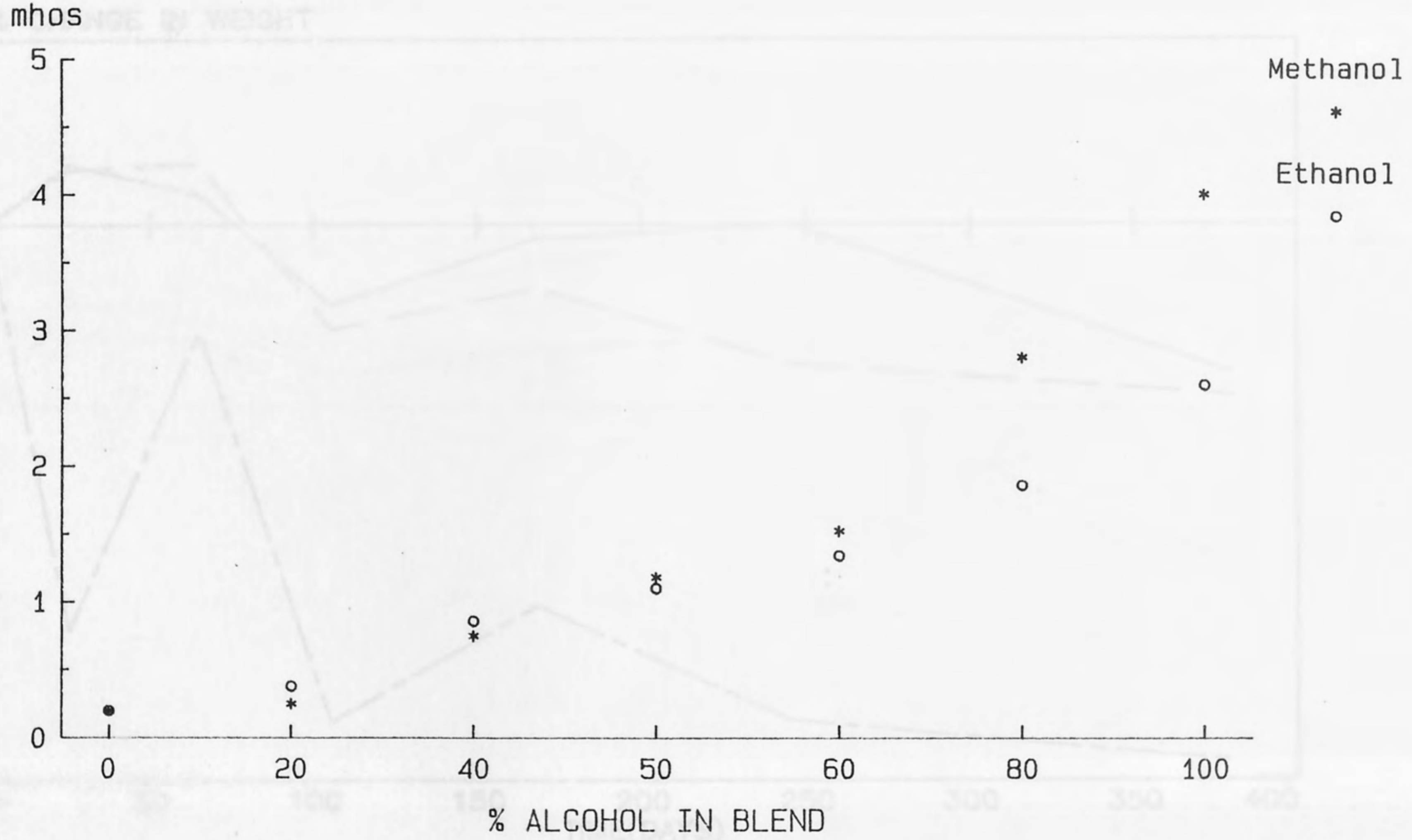

FIG: 4.4.1 EFFECT OF AERATION ON OXIDATION AND CORROSION OF BRASS

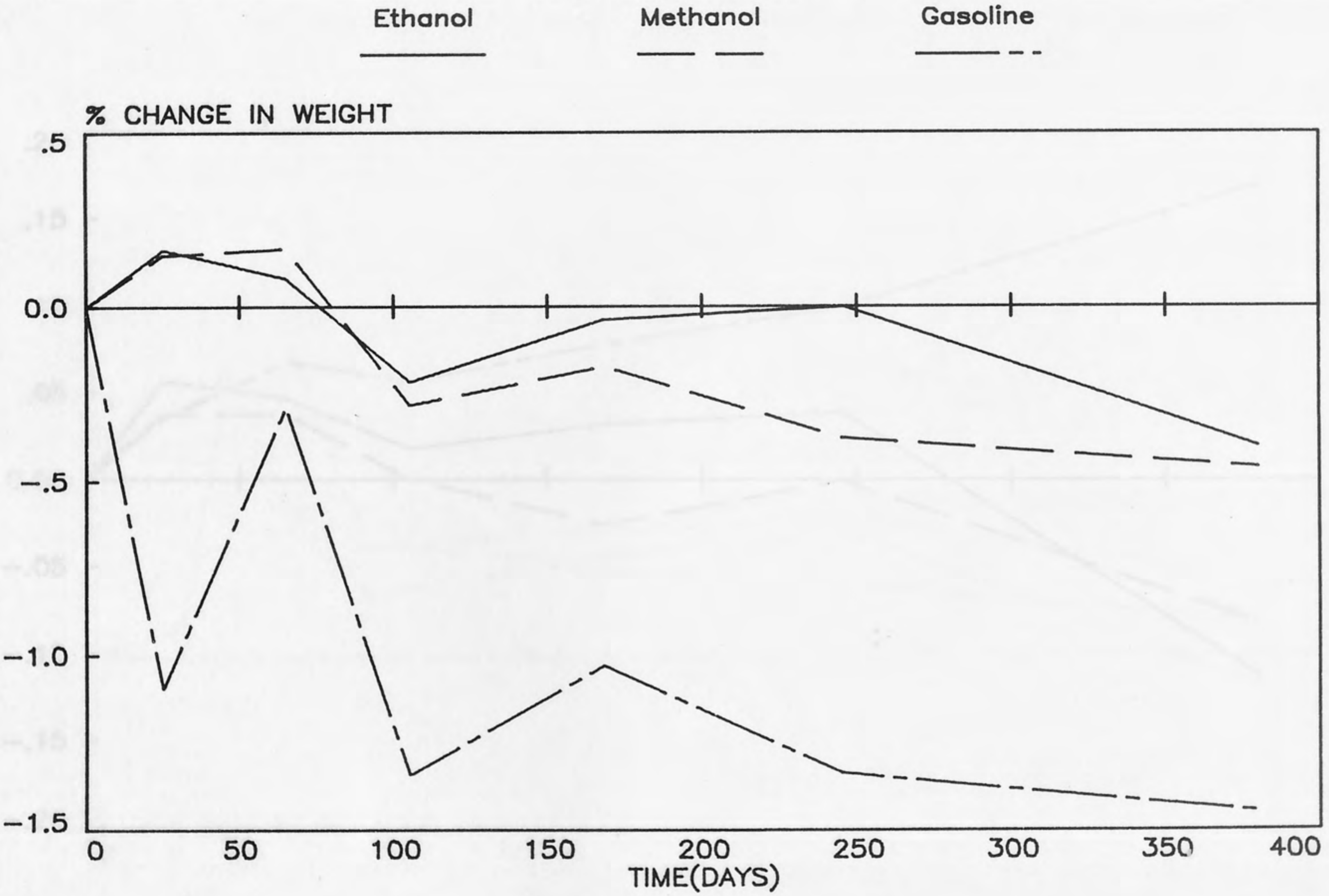

FIG: 4.4.2 EFFECT OF AERATION ON OXIDATION AND CORROSION OF ZNIC

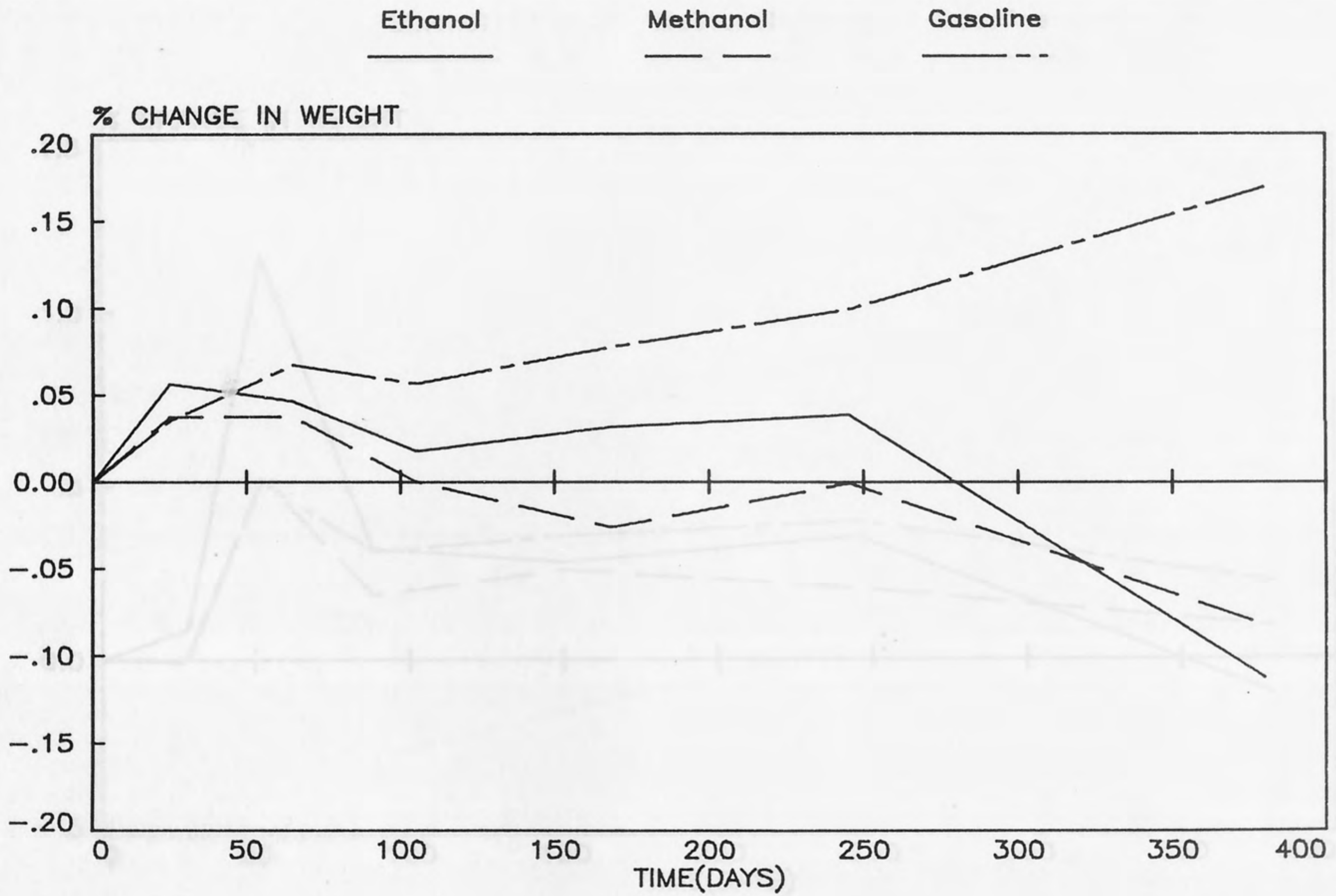

FIG:4.4.3 EFFECT OF TEMPERATURE ON OXIDATION AND CORROSION OF BRASS

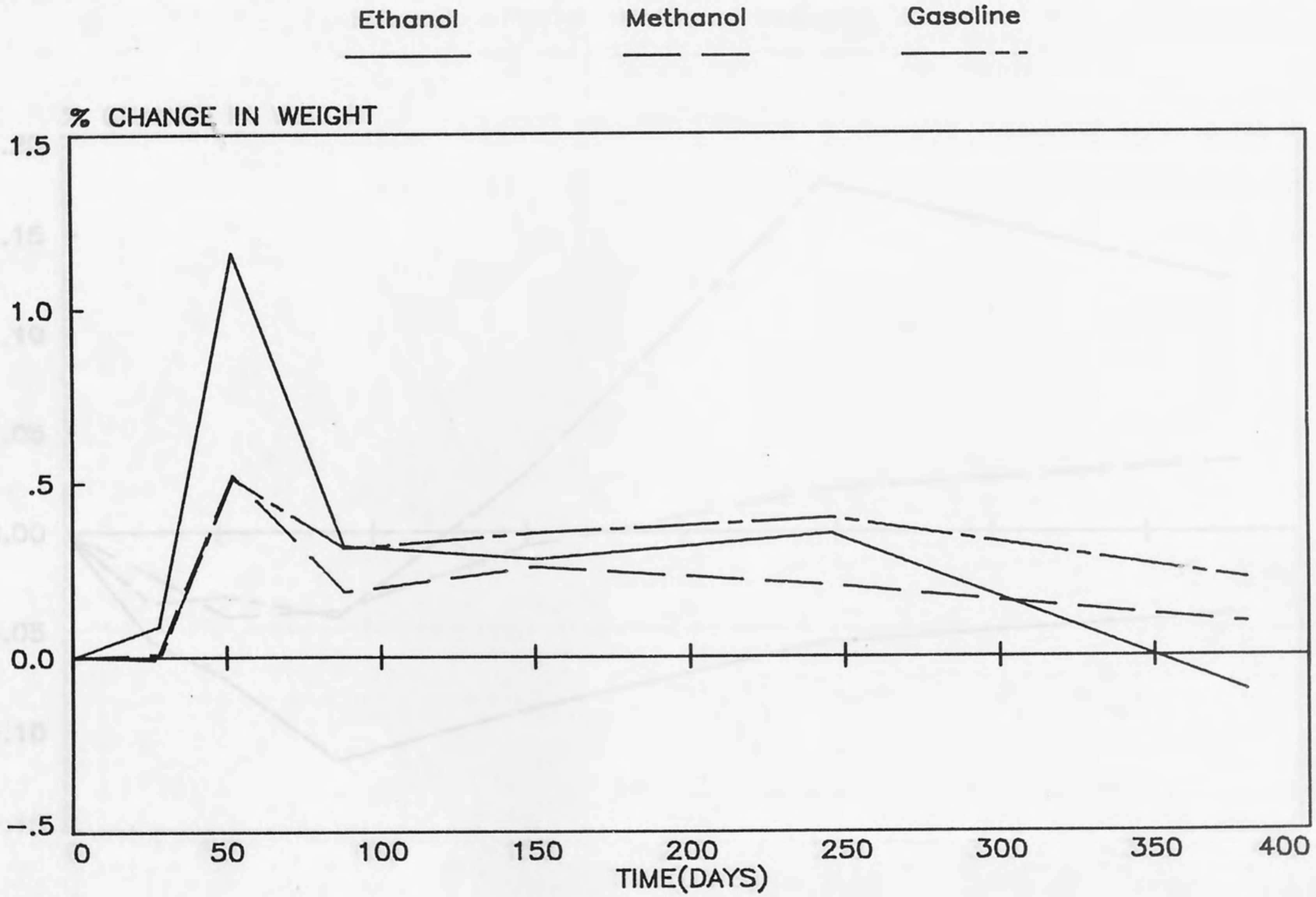

FIG: 4.4.4 EFFECT OF TEMPERATURE ON OXIDATION AND CORROSION OF ZNIC

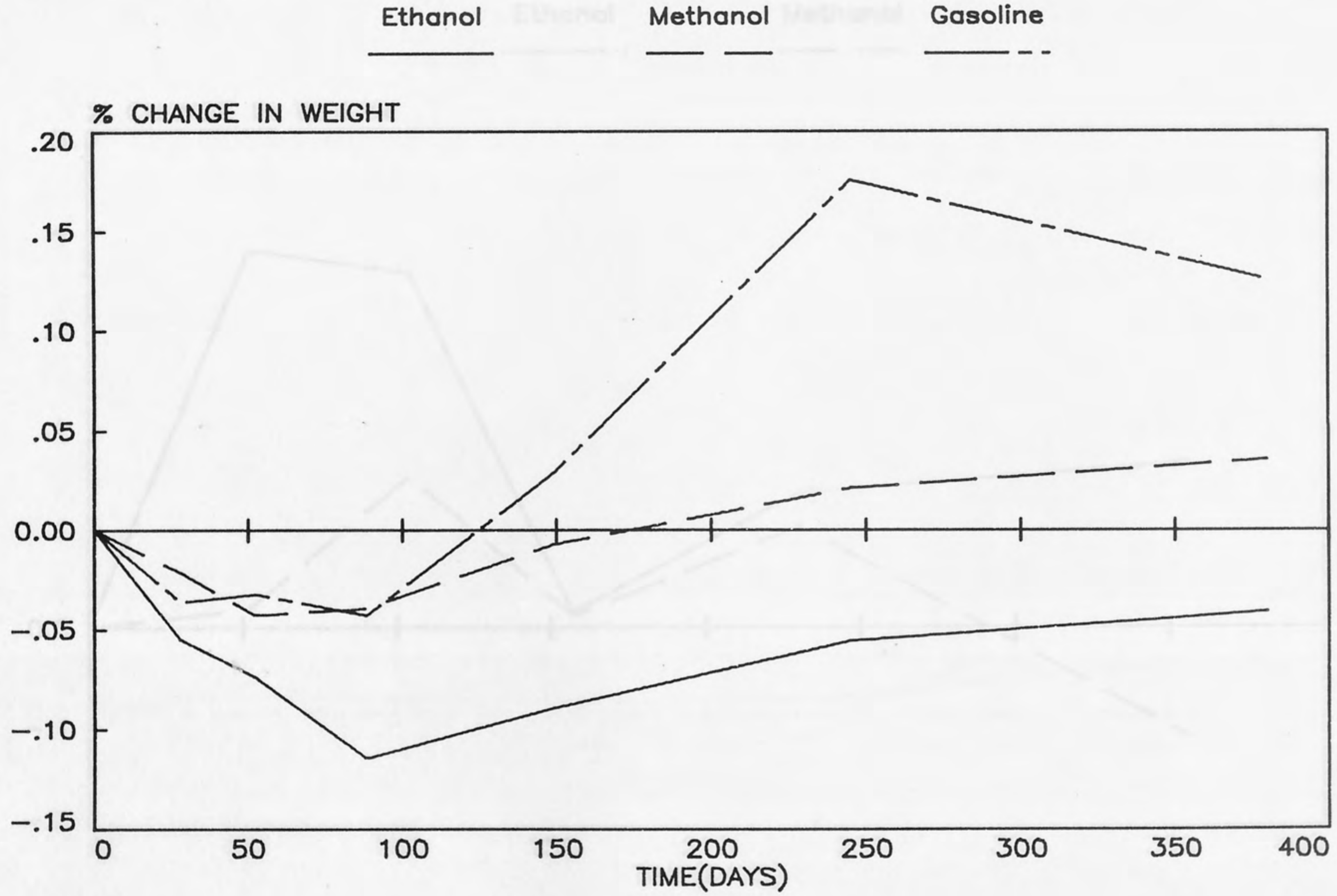

FIG: 4.4.5 EFFECT OF METALLIC CONTACT ON OXIDATION AND CORROSION OF BRASS IN AERATED SOLUTION

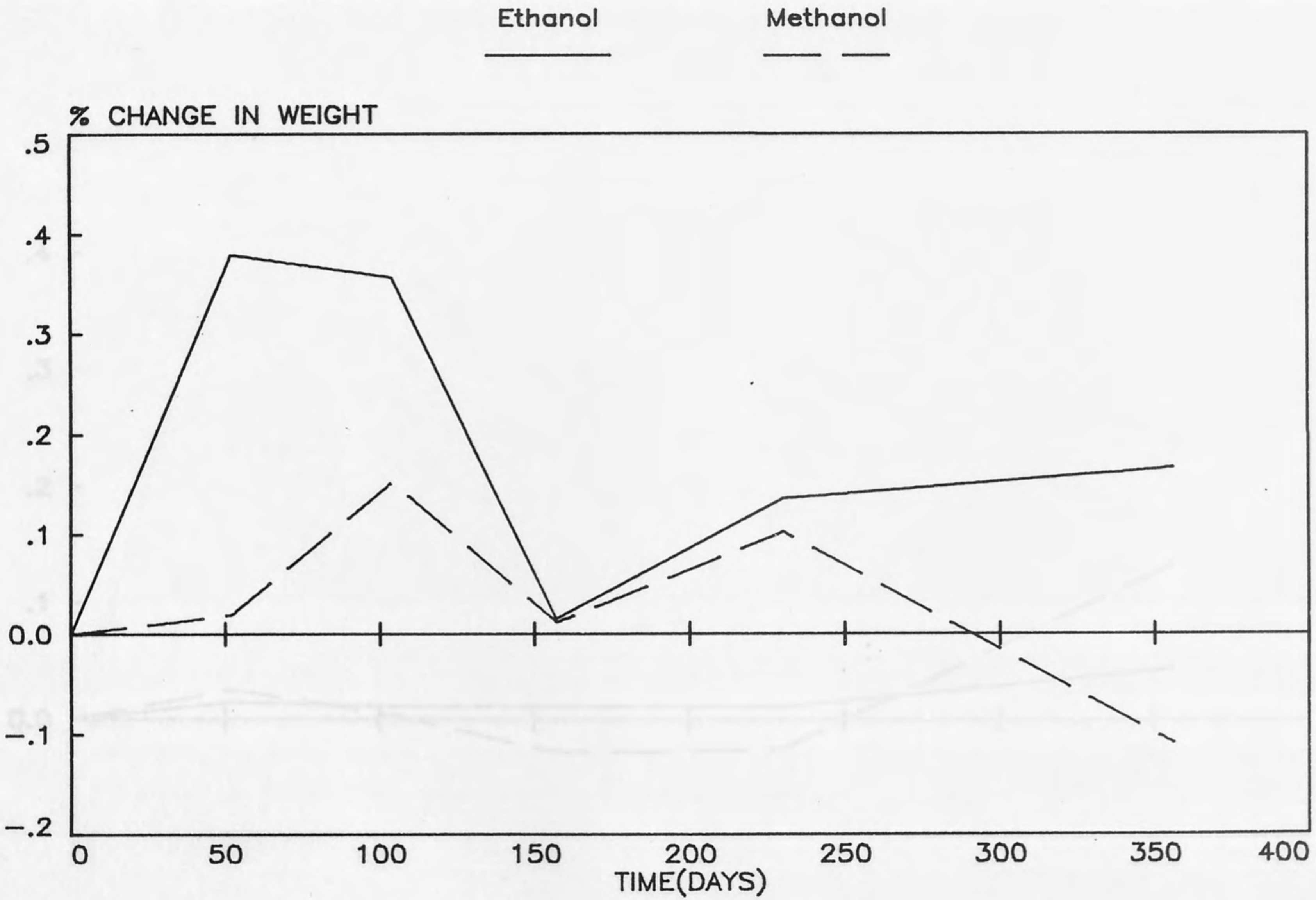

FIG: 4.4.6 EFFECT OF METALLIC CONTACT ON OXIDATION AND CORROSION OF ZNIC IN AERATED SOLUTION

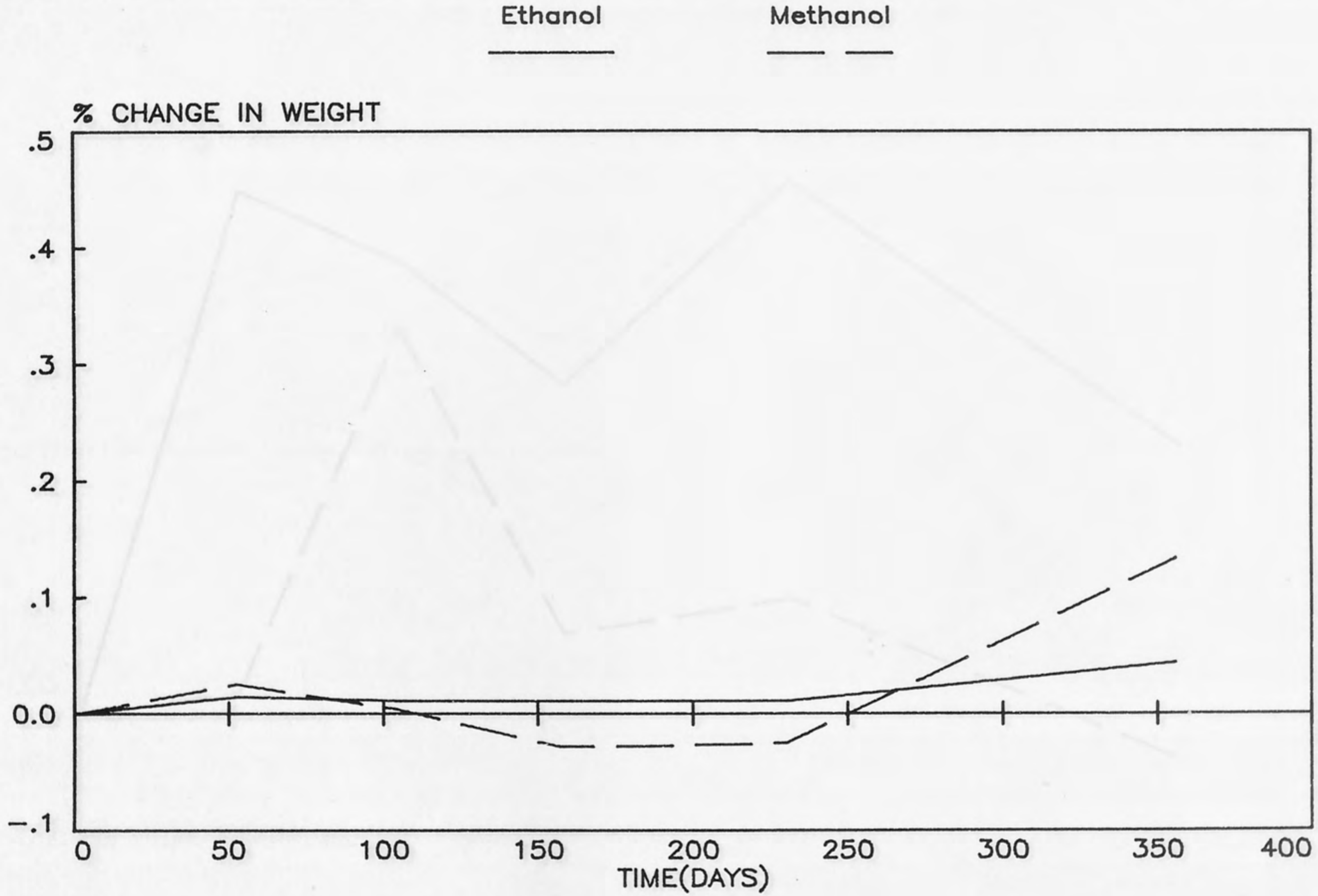

FIG: 4.4.7 EFFECT OF METALLIC CONTACT ON OXIDATION AND CORROSION OF BRASS AT 50 C

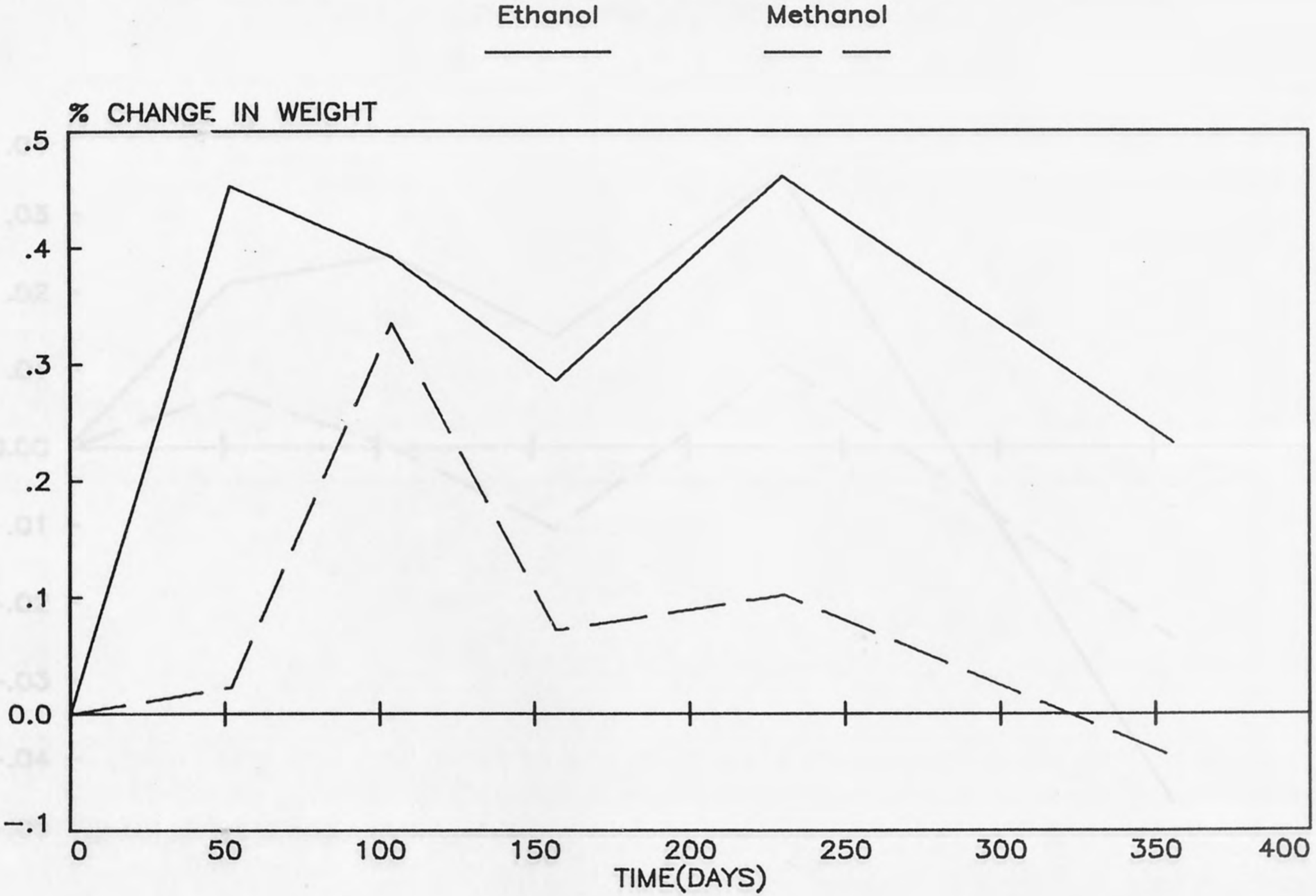

FIG: 4.4.8 EFFECT OF METALLIC CONTACT ON OXIDATION AND CORROSION OF ZNIC AT 50 C

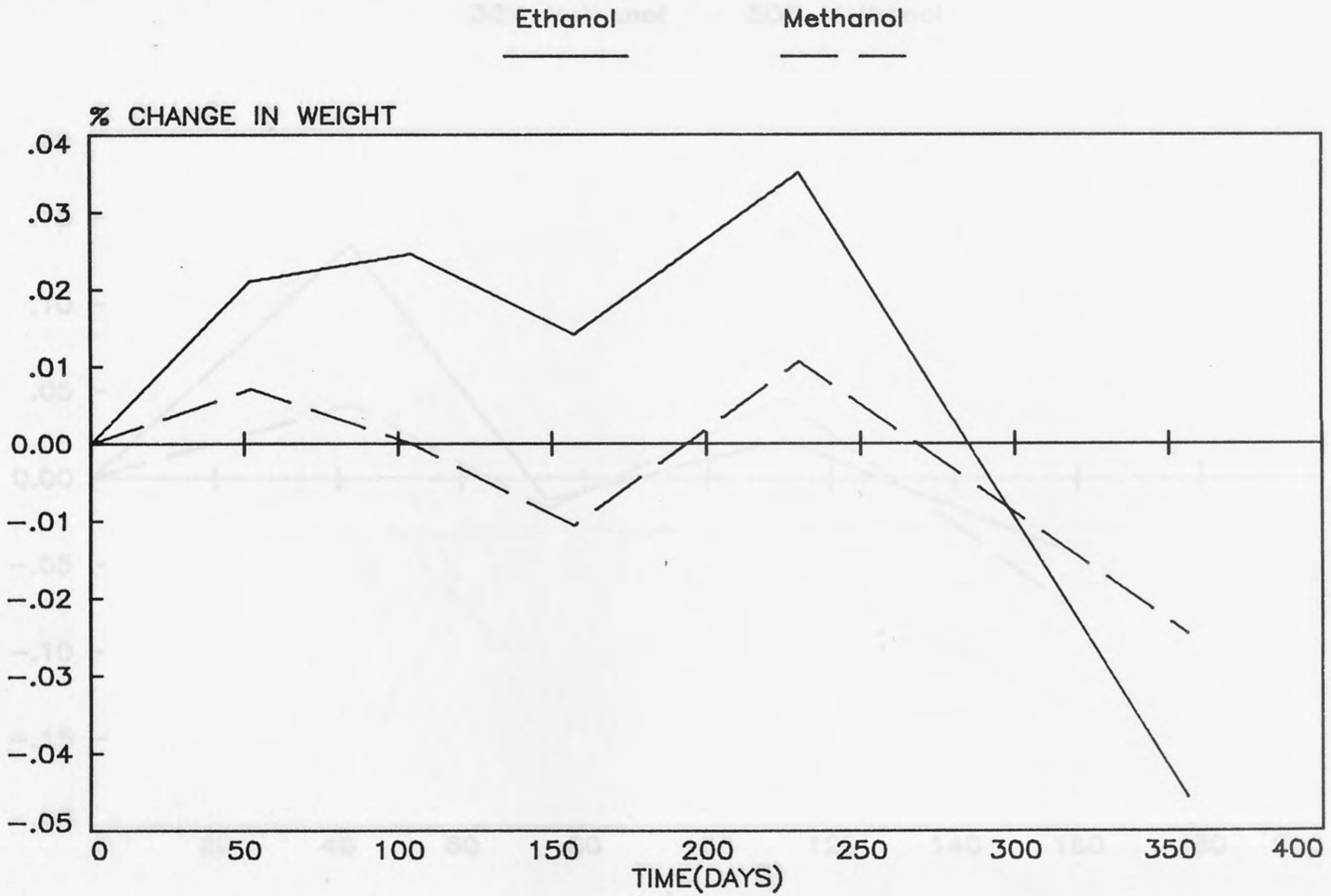

FIG: 4.4.9 THE OXIDATION AND CORROSION OF BRASS IN AERATED METHANOL/GASOLINE BLENDS

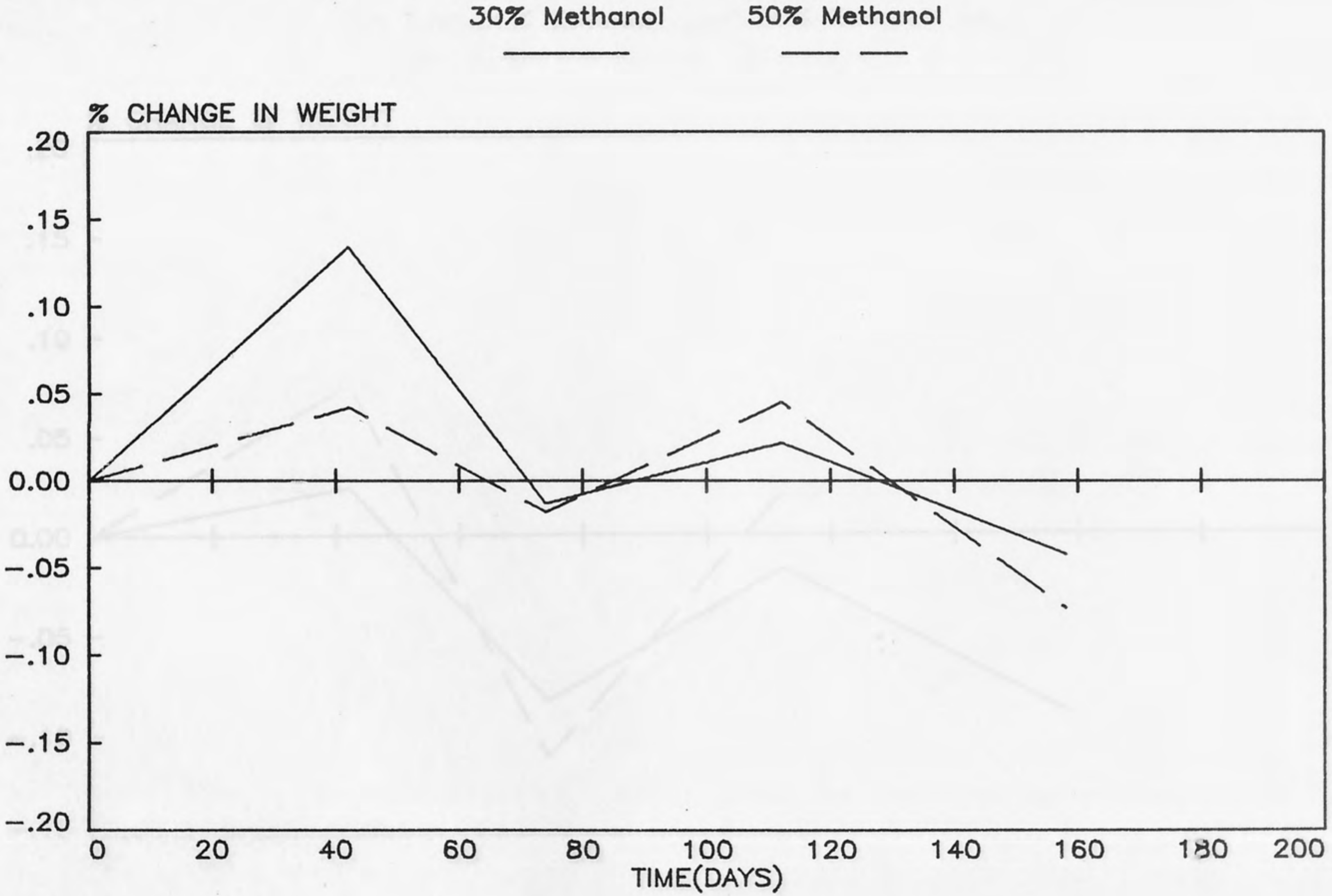

FIG: 4.4.10 THE OXIDATION AND CORROSION OF BRASS IN AERATED ETHANOL/GASOLINE BLENDS

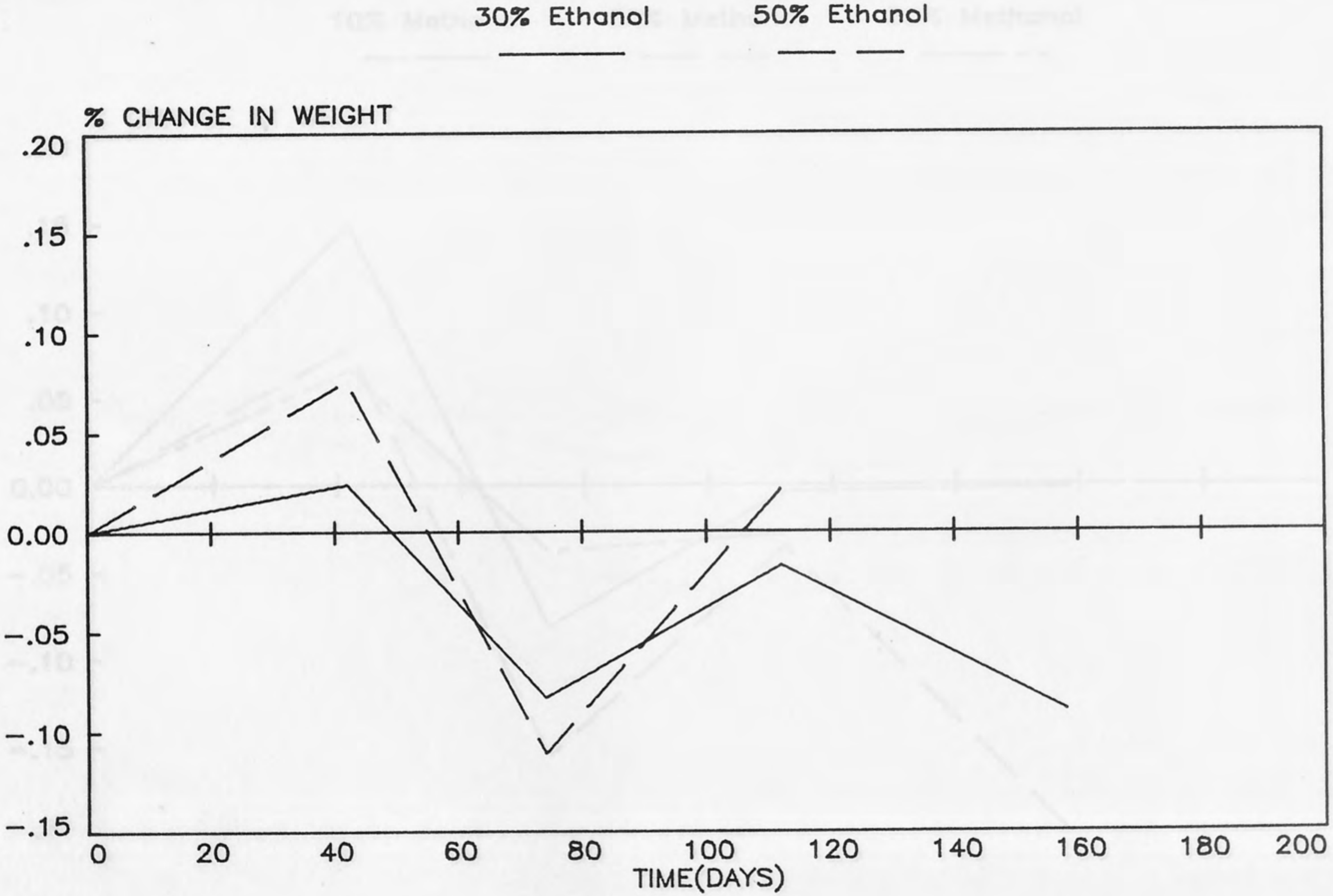

FIG: 4.4.11 THE OXIDATION AND CORROSION OF BRASS IN METHANOL/GASOLINE BLENDS AT 50 C

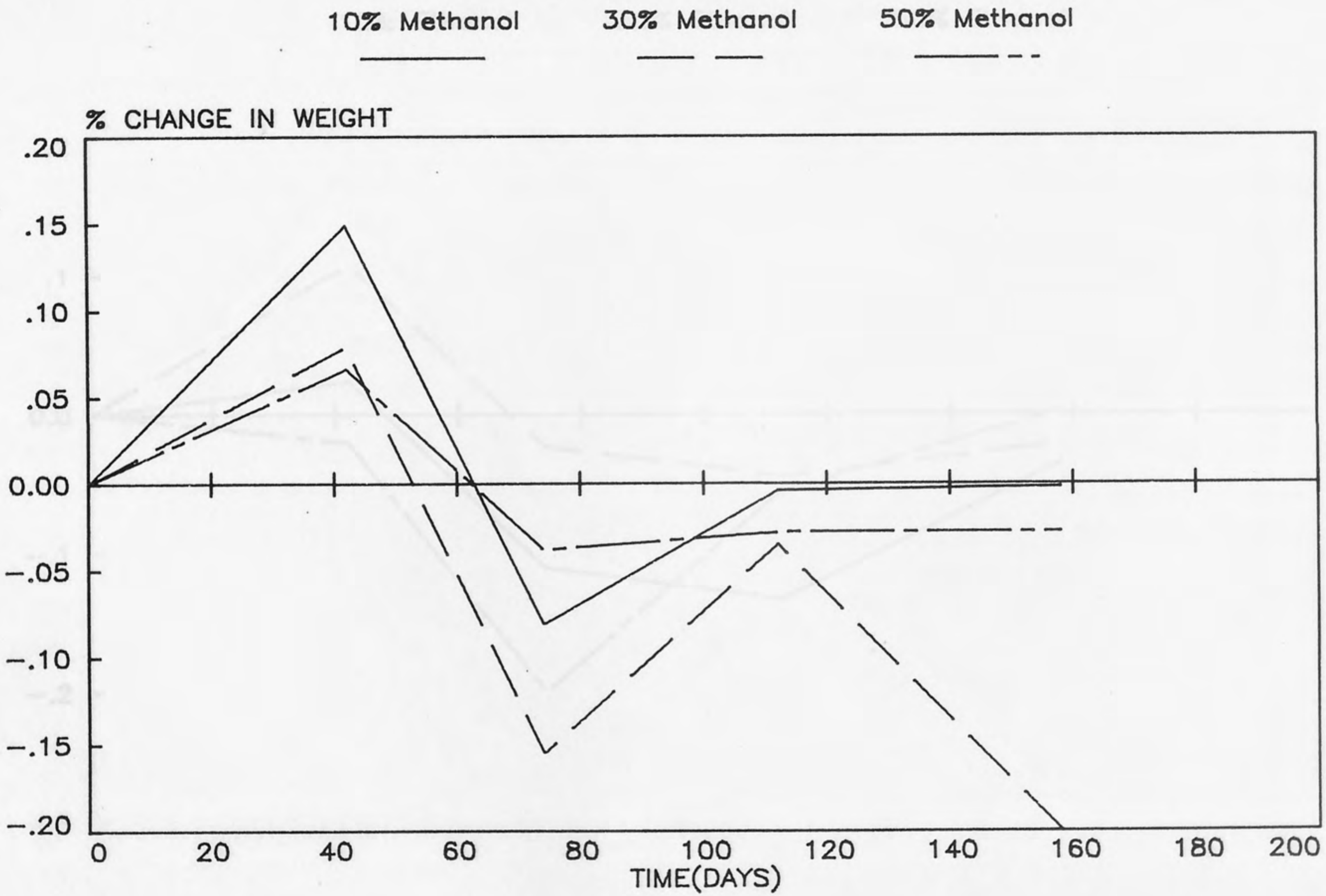

FIG: 4.4.12 THE OXIDATION AND CORROSION OF BRASS IN ETHANOL/GASOLINE BLENDS AT 50 C

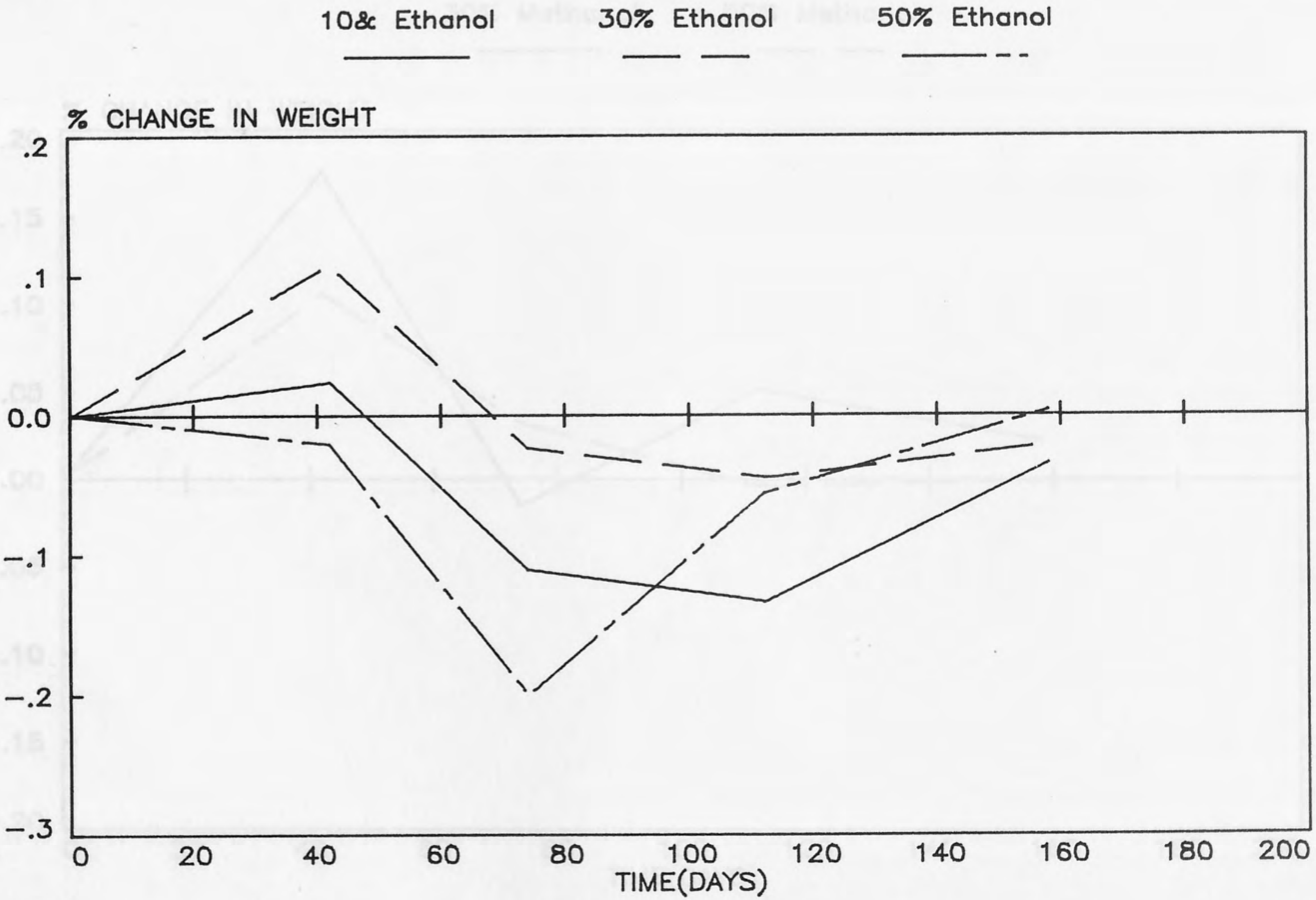

FIG: 4.4.13 THE OXIDATION AND CORROSION OF ZNIC IN AERATED METHANOL/GASOLINE BLENDS

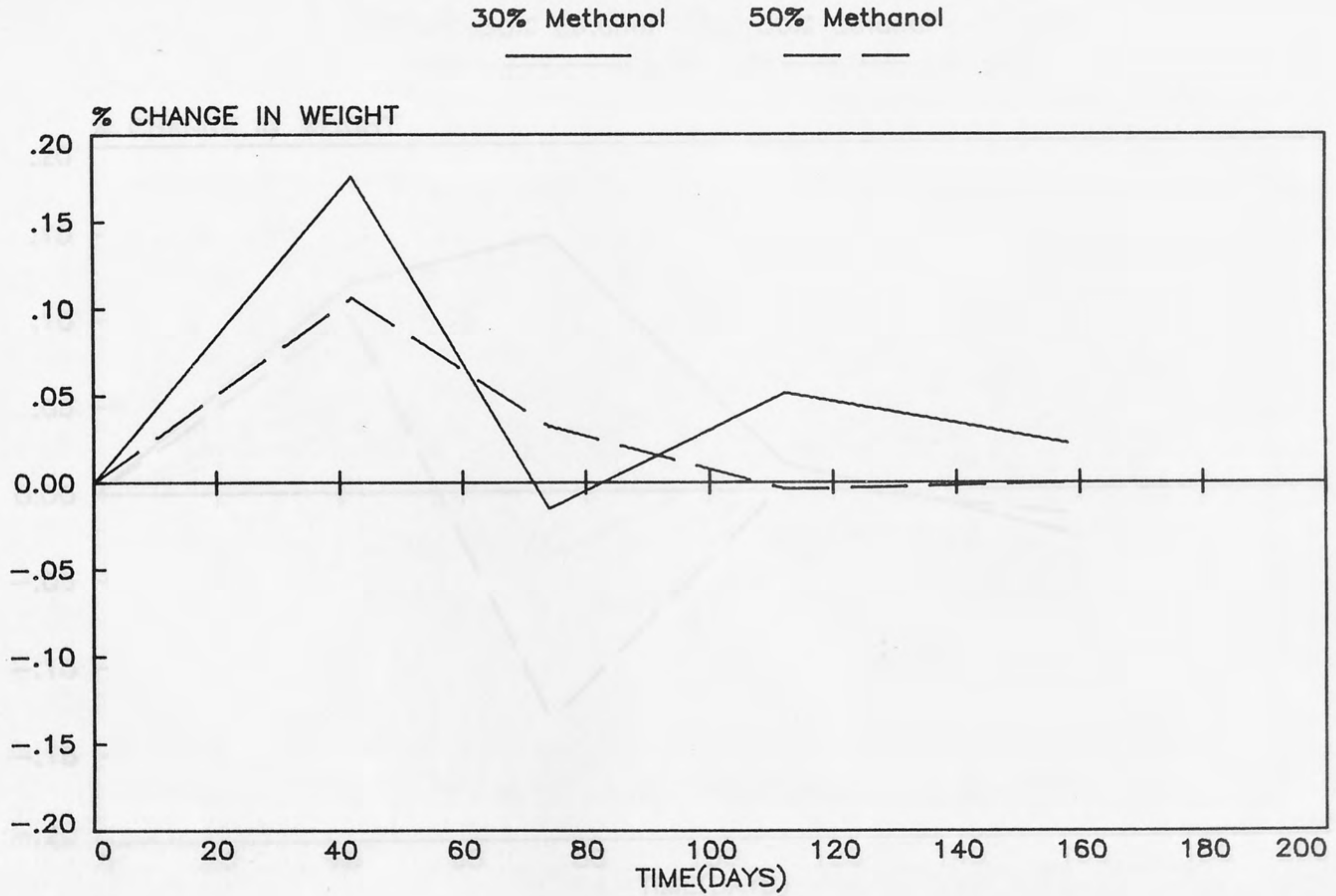

FIG: 4.4.14 THE OXIDATION AND CORROSION OF ZNIC IN AERATED ETHANOL/GASOLINE BLENDS

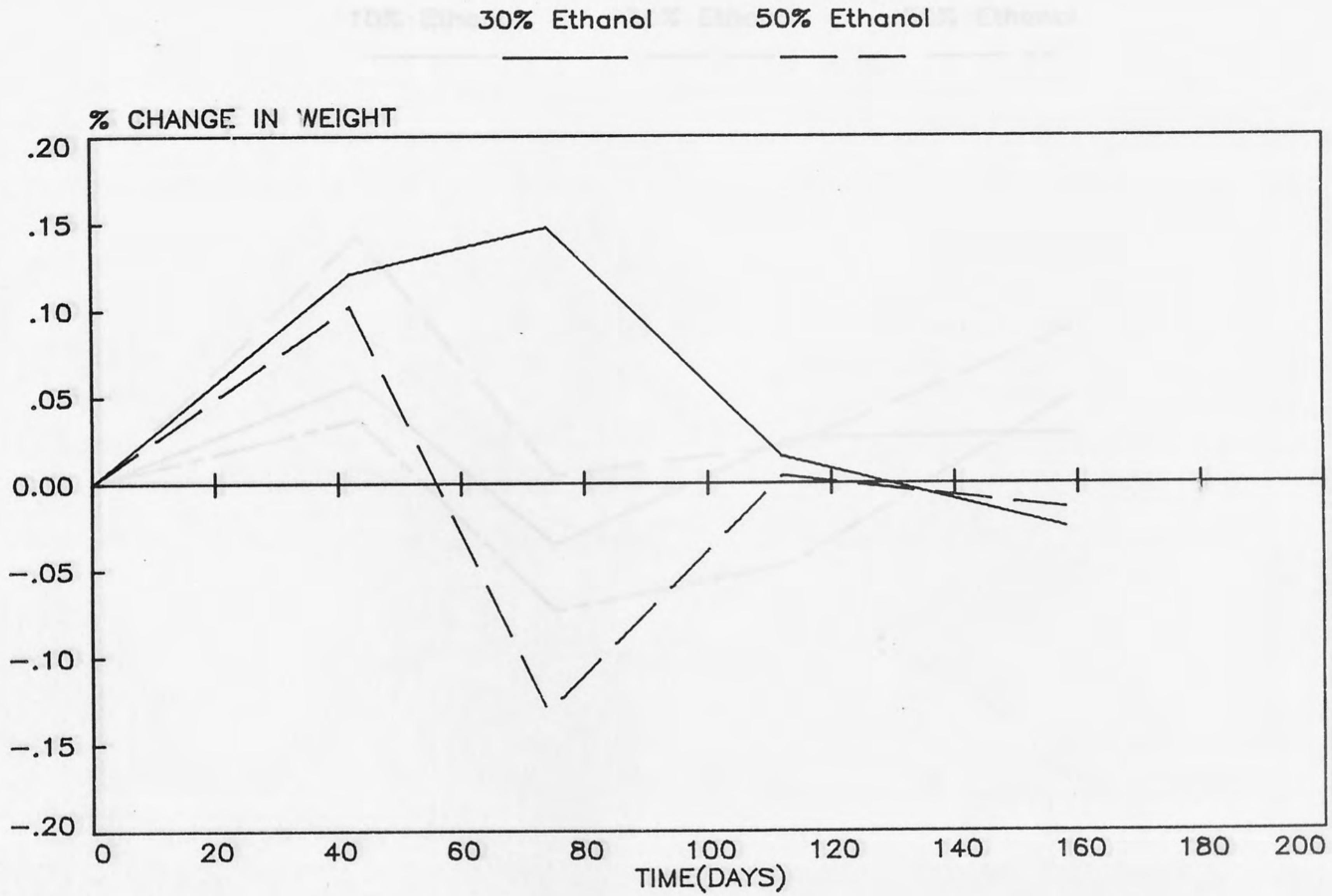

FIG: 4.4.15 THE OXIDATION AND CORROSION OF ZNIC IN ETHANOL/GASOLINE BLENDS AT 50 C

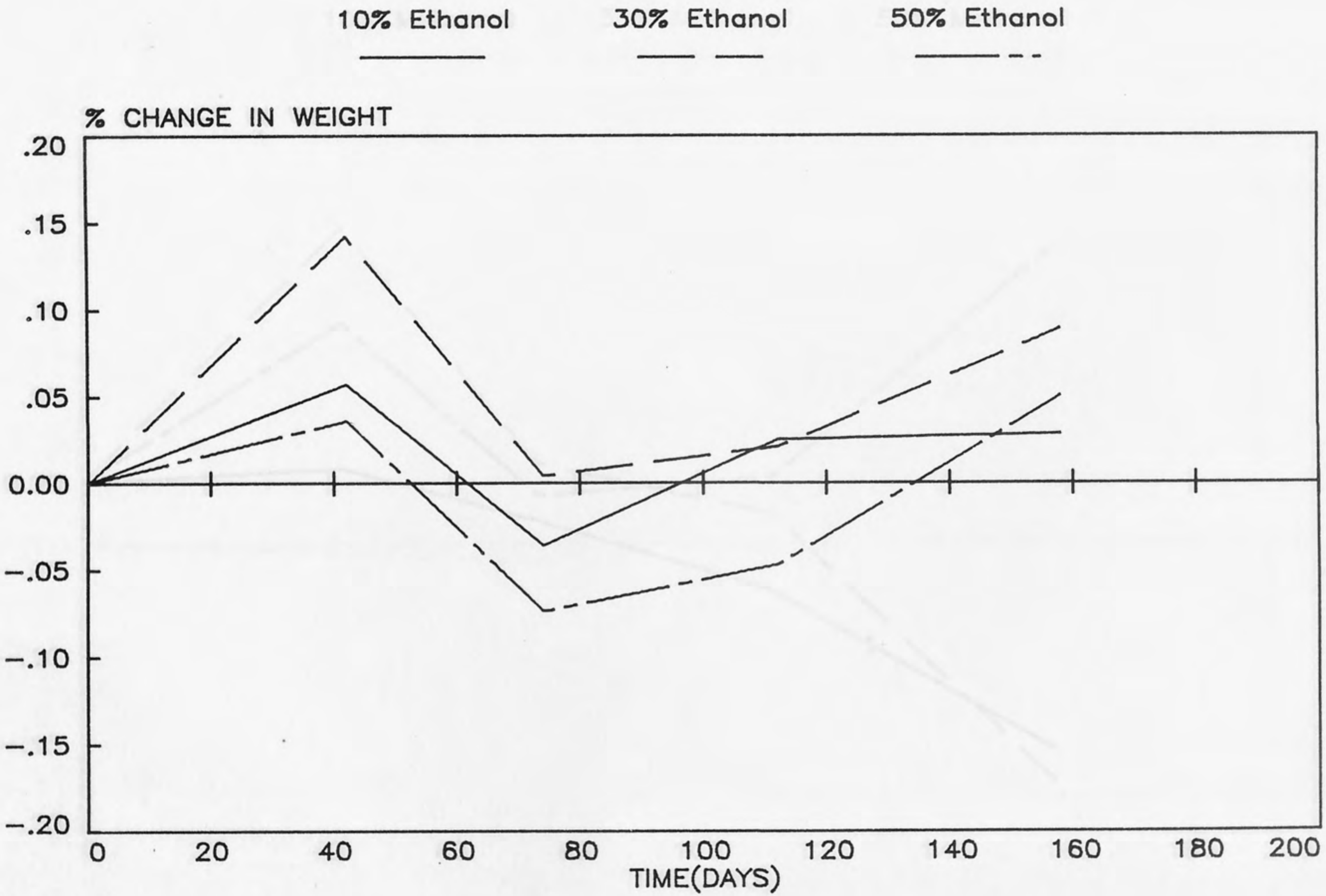

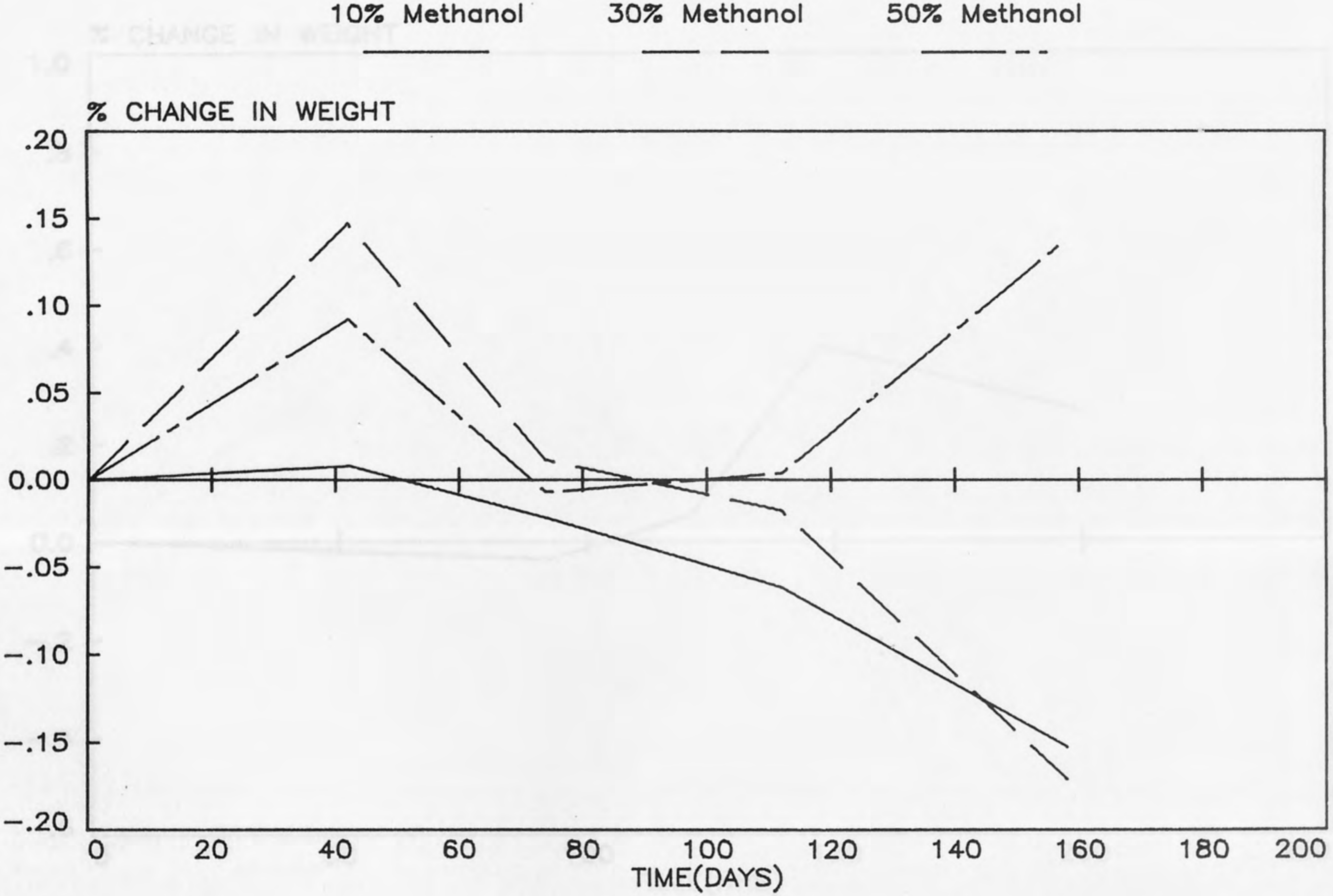

FIG: 4.4.16 THE OXIDATION AND CORROSION OF ZNIC IN METHANOL/GASOLINE BLENDS AT 50 C

FIG: 4.4.17 EFFECT OF HIGH TEMPERATURE ON OXIDATION AND CORROSION OF BRASS IN METHANOL (TEMP:80°C)

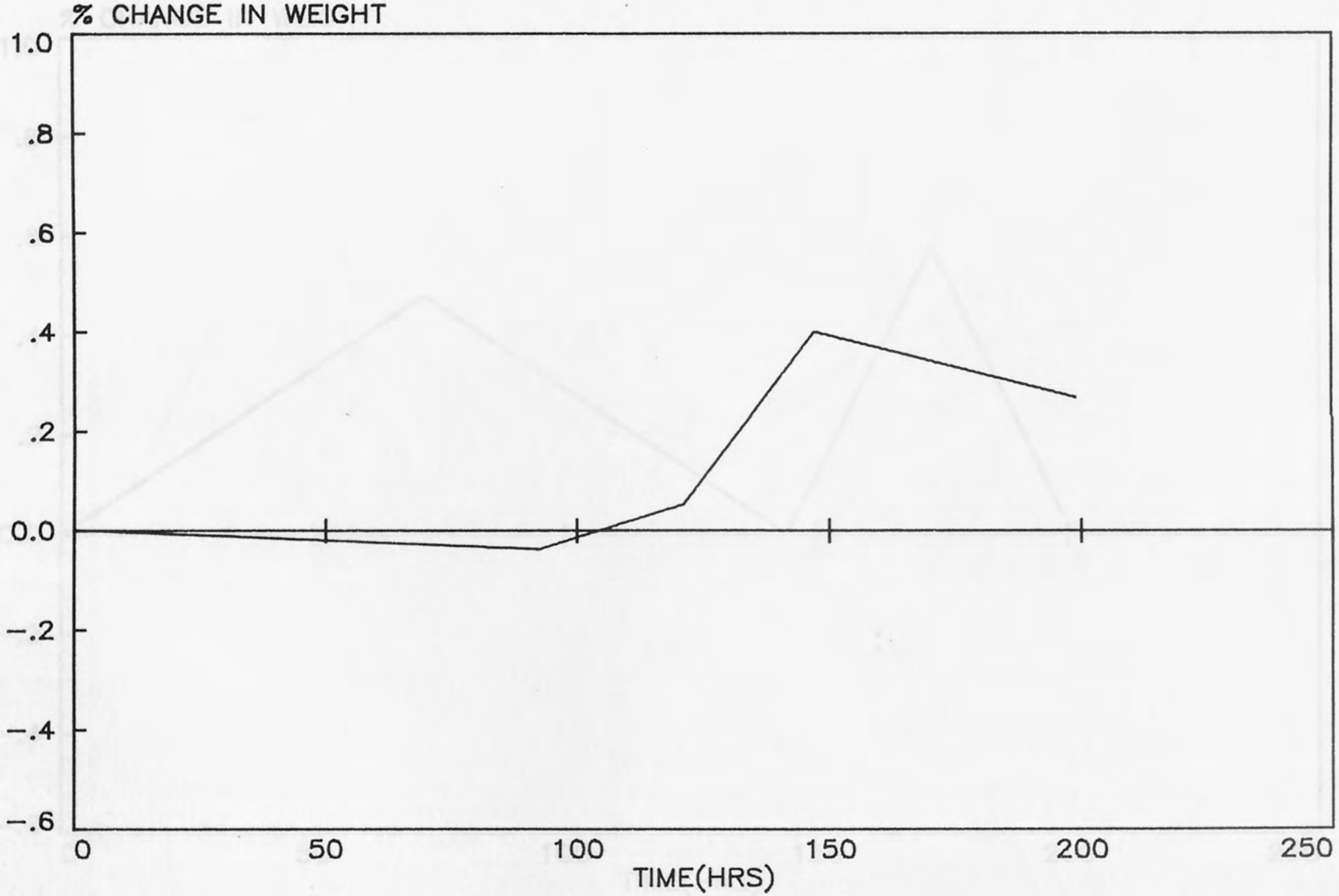

FIG: 4.4.18 EFFECT OF HIGH TEMPERATURE ON OXIDATION AND CORROSION OF BRASS IN ETHANOL (TEMP: 80°C)

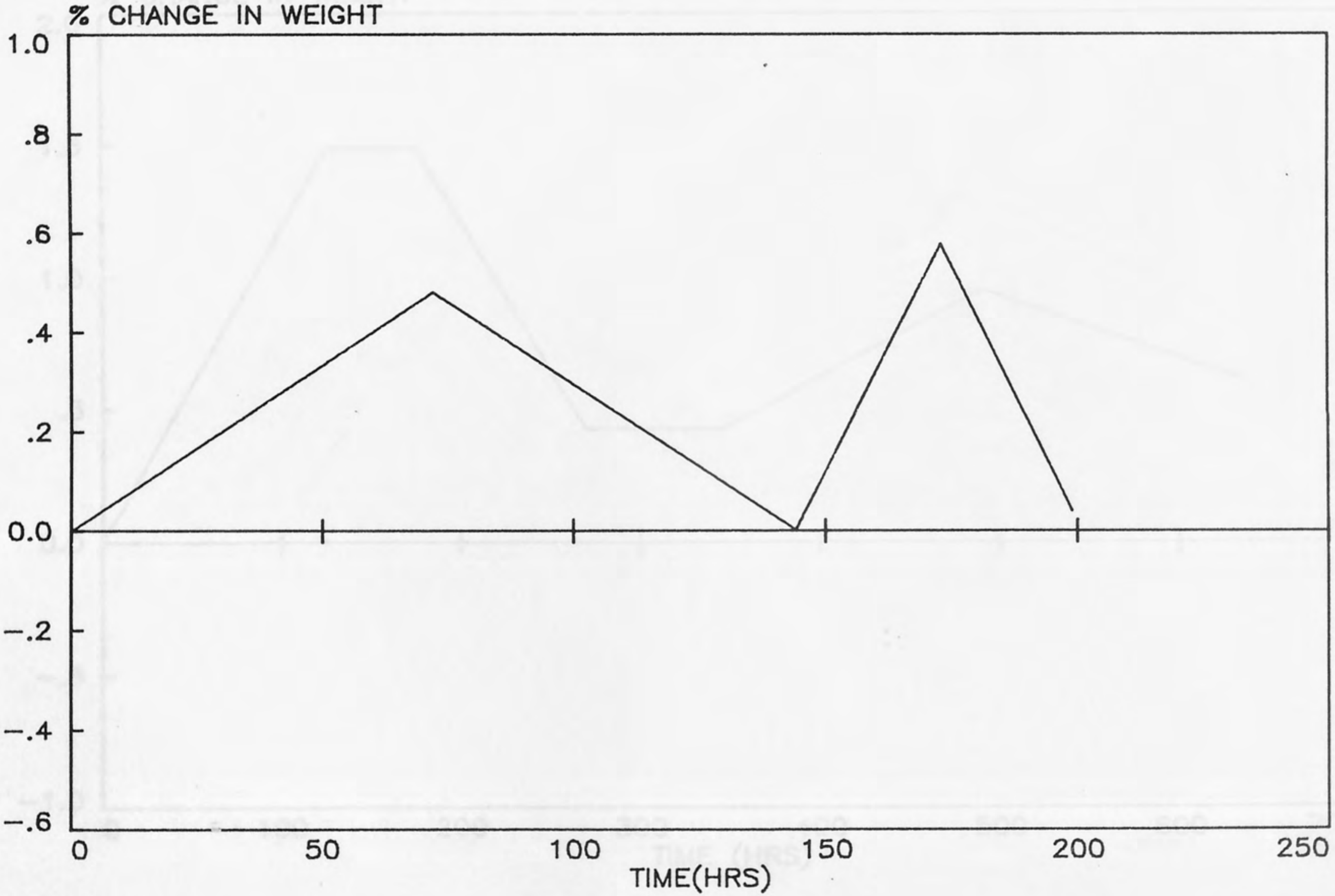

FIG: 4.4.19 EFFECT OF TEMPERATURE AND FORMIC ACID ON OXIDATION AND CORROSION OF ALUMINIUM

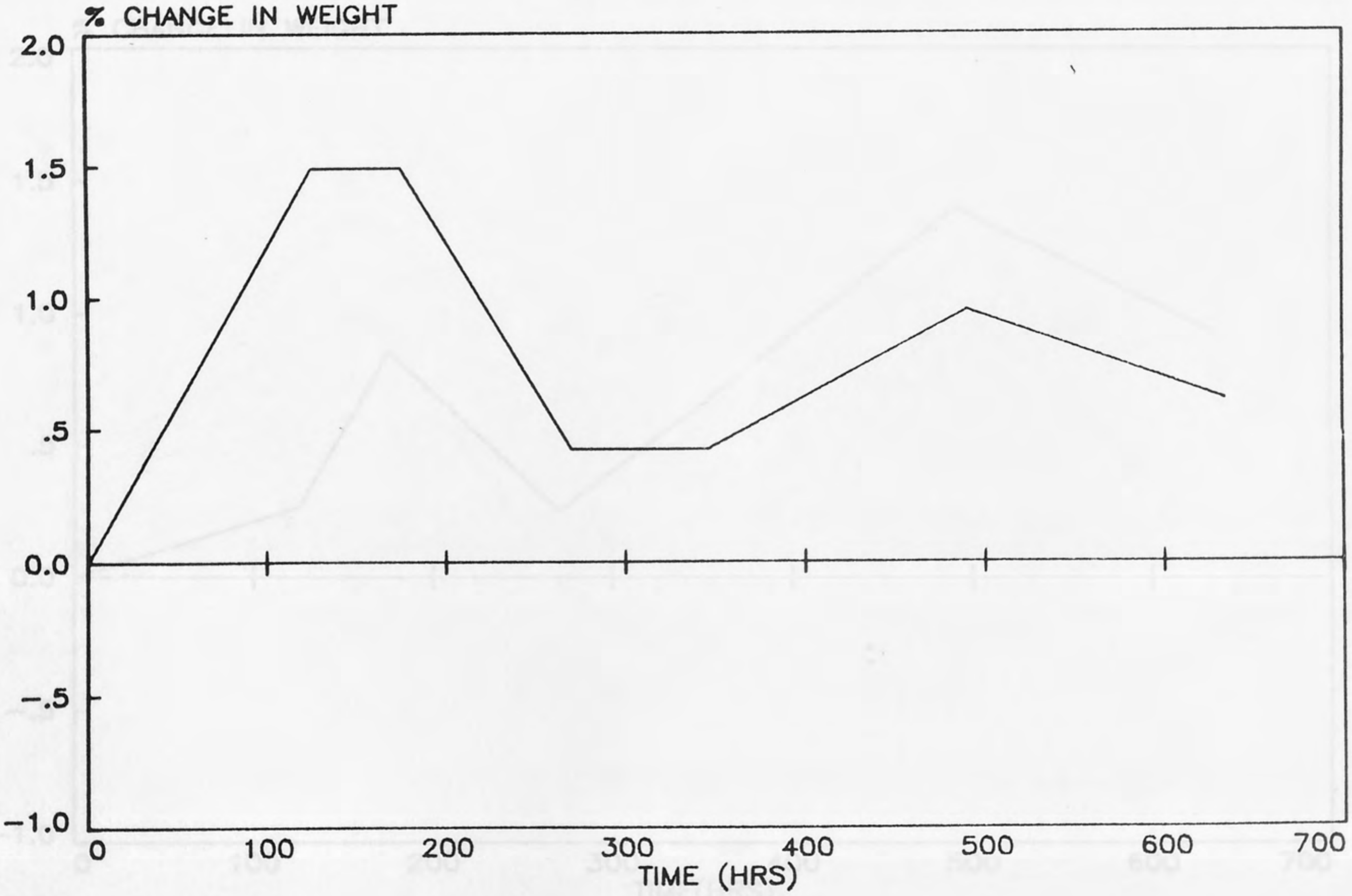

FIG: 4.4.20 EFFECT OF TEMPERATURE ON OXIDATION AND CORROSION OF ALIMINIUM IN METHANOL

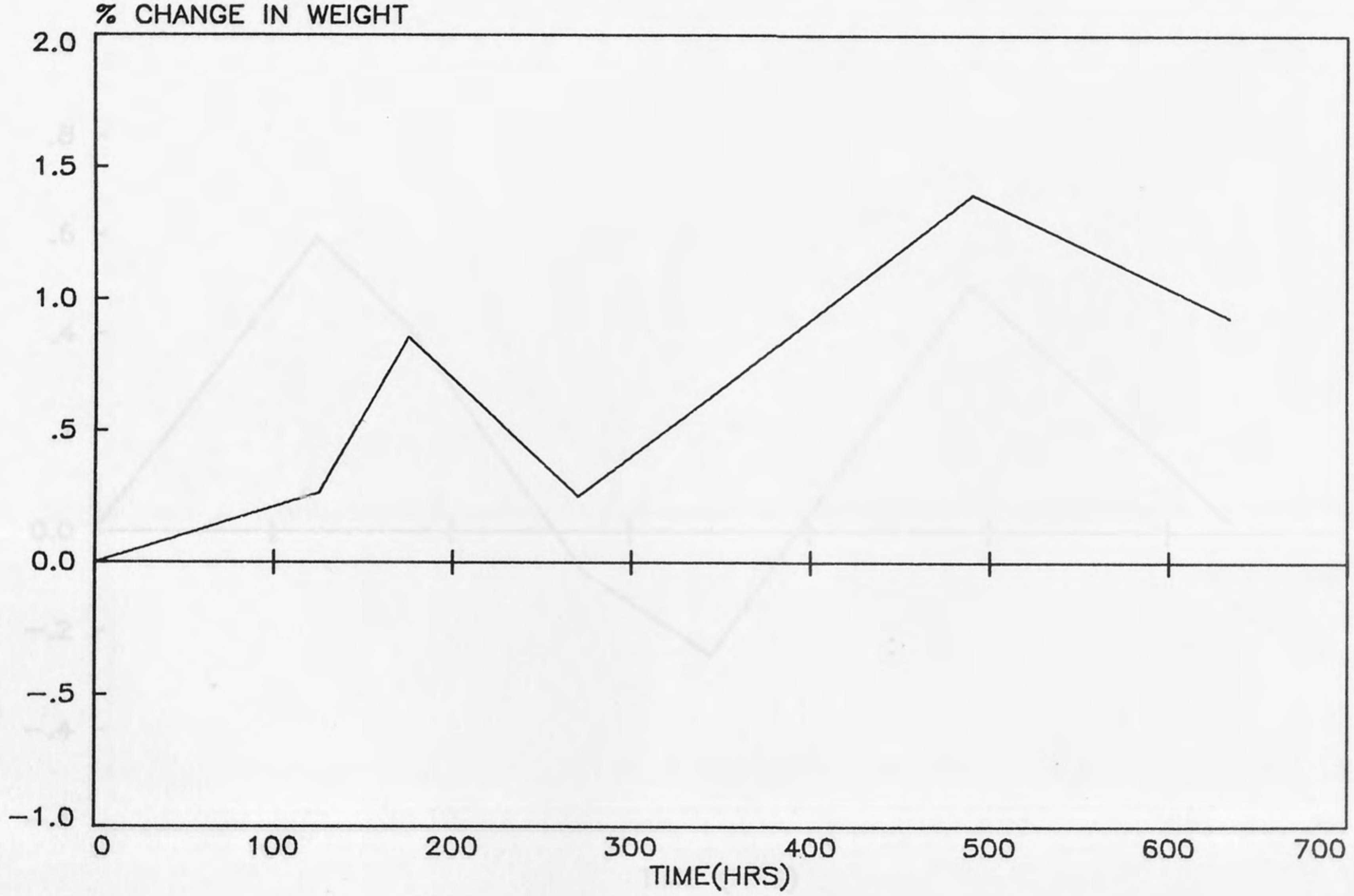

FIG: 4.4.21 EFFECT OF TEMPERATURE AND FORMIC ACID ON OXIDATION AND CORROSION OF COPPER IN METHANOL

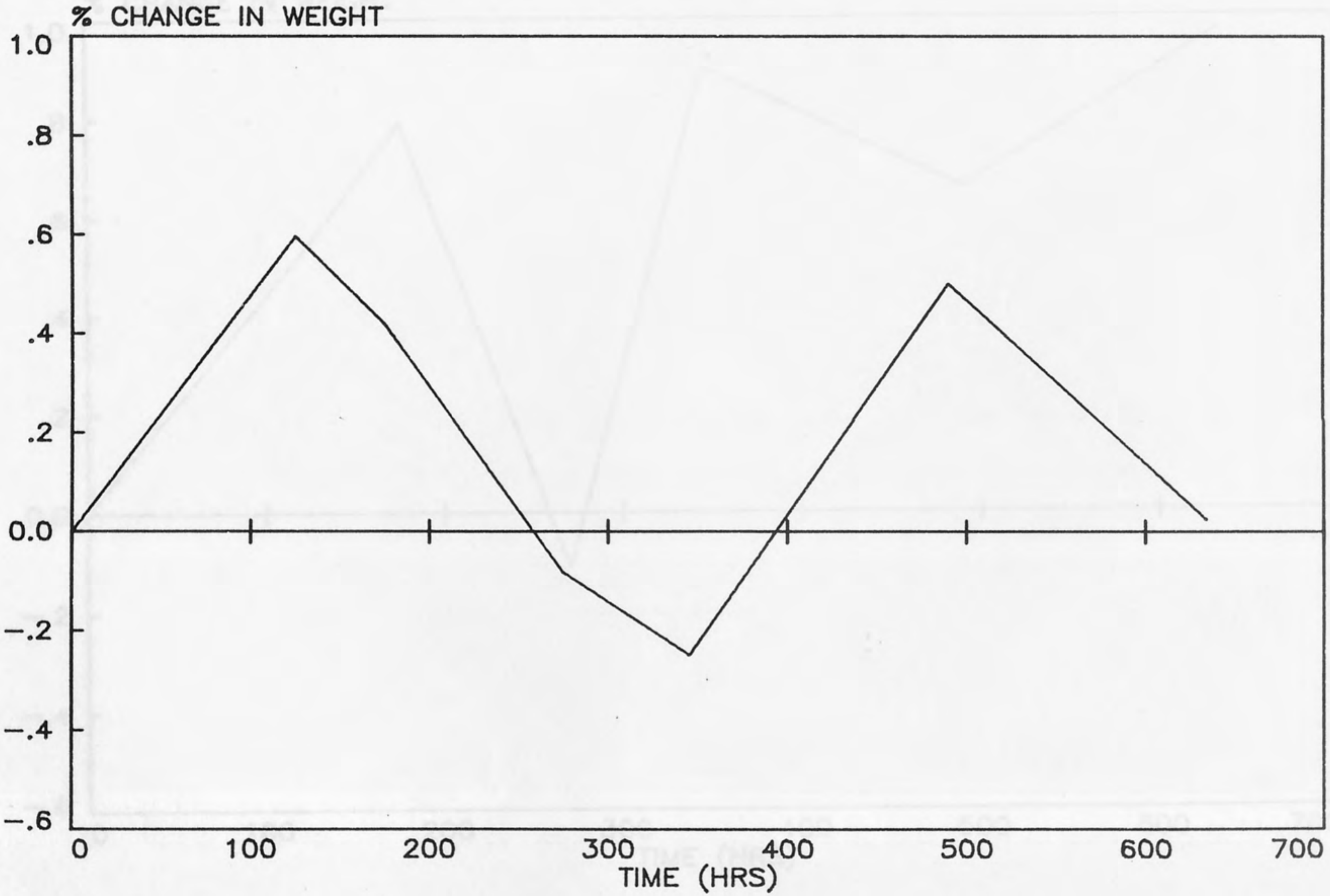

FIG: 4.4.22 EFFECT OF TEMPERATURE ON OXIDATION AND CORROSION OF COPPER IN METHANOL

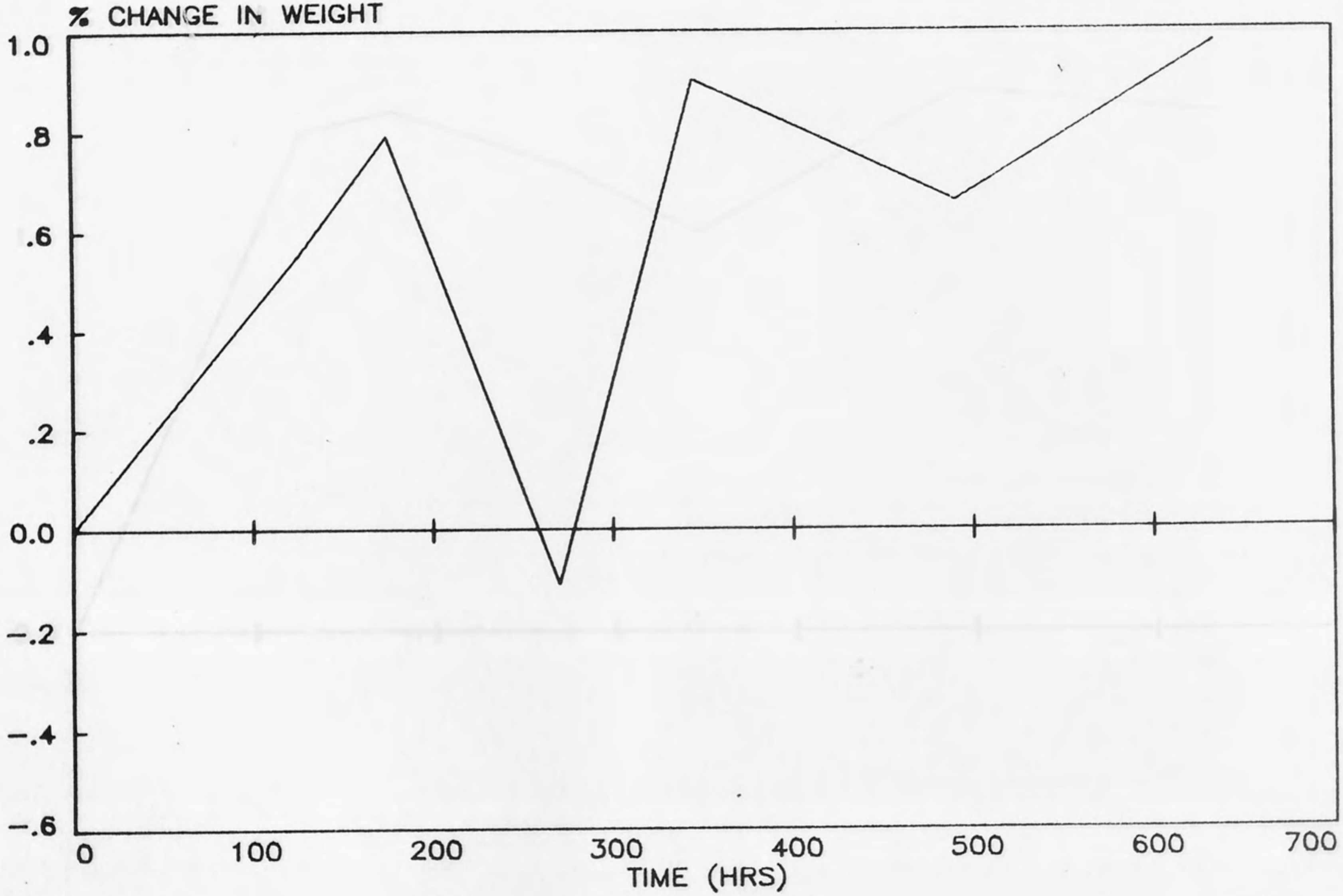

FIG. 4.4.23 EFFECT OF TEMPERATURE AND FORMIC ACID ON OXIDATION AND CORROSION OF STEEL IN METHANOL

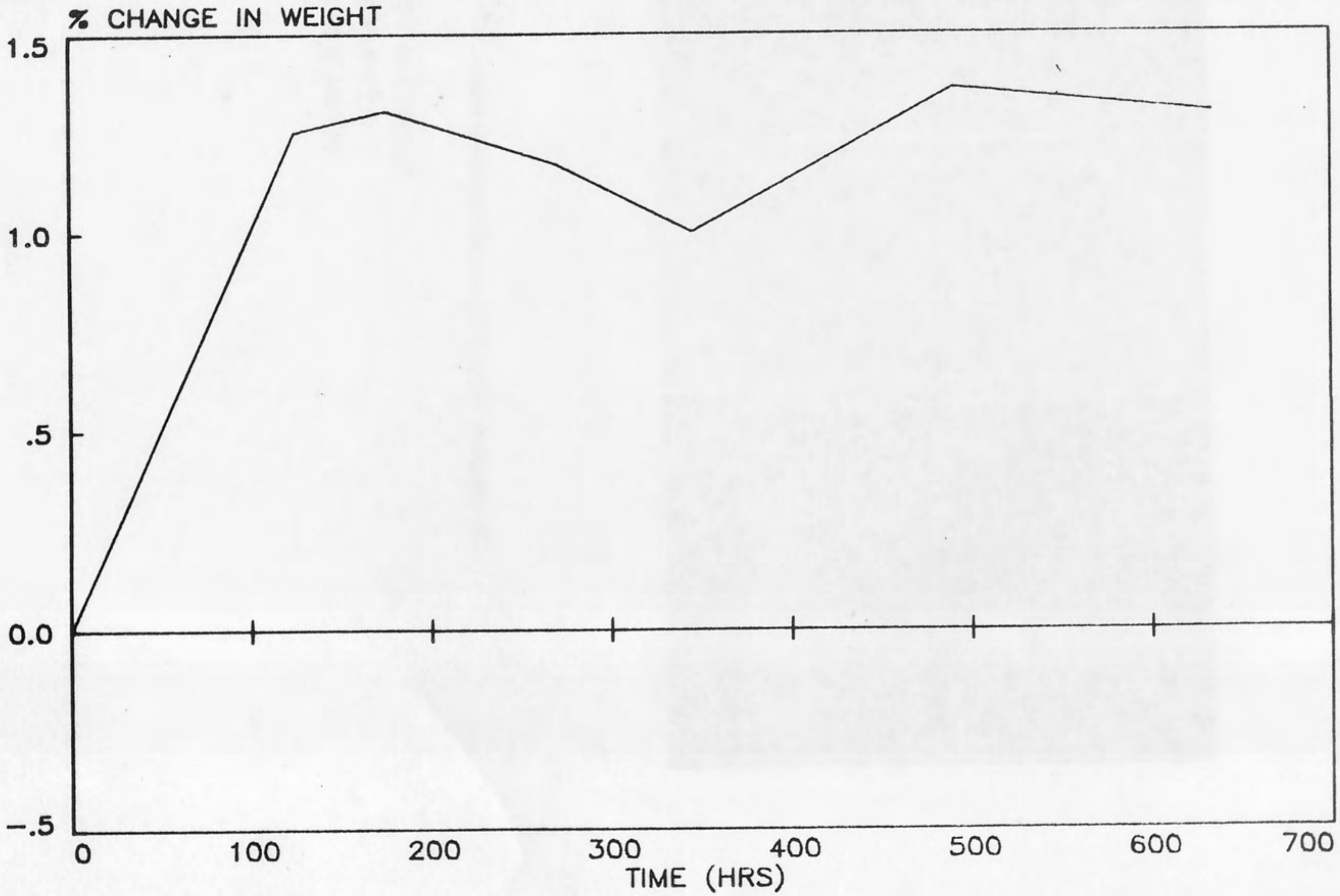

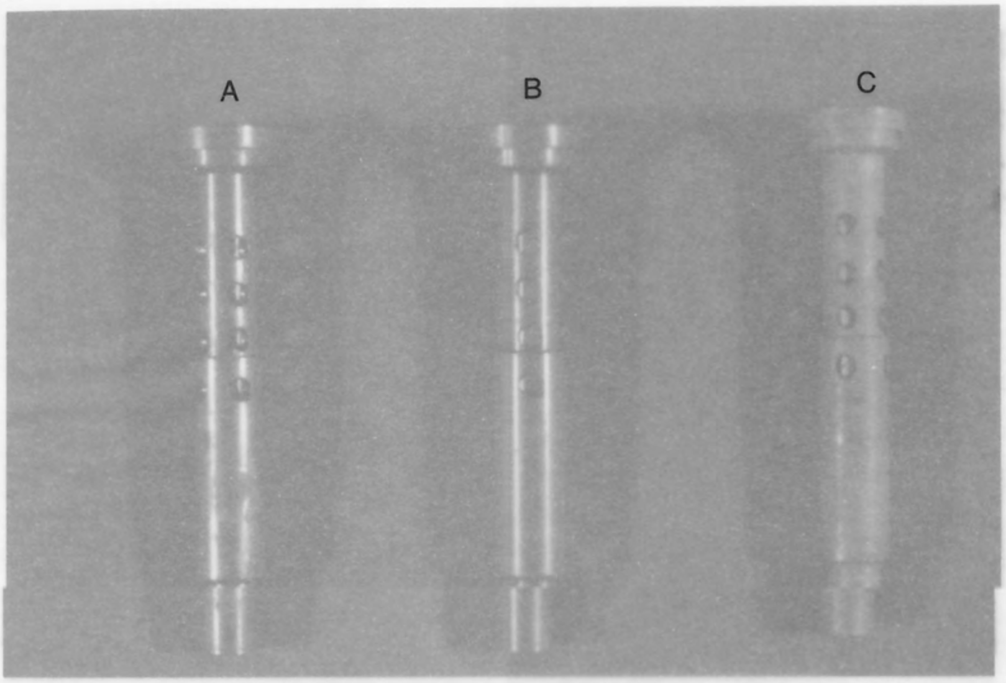

Plate 441: Brass in aerated solutions at room temperature

A - Brass in methanol
B - Brass in ethanol
C - Brass in gasoline

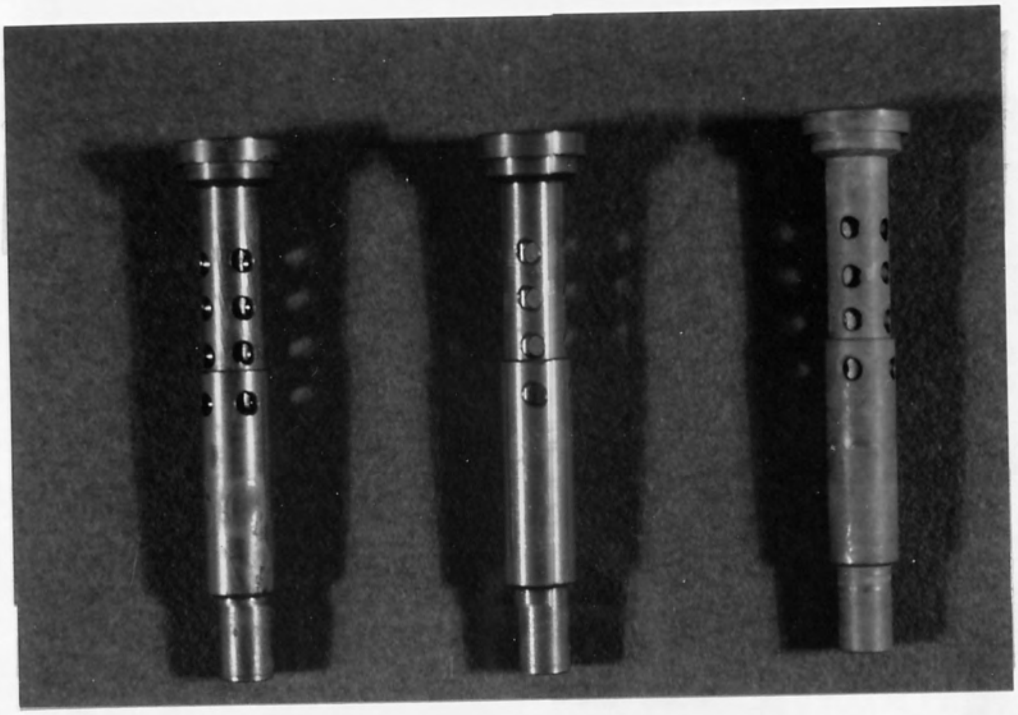

Plate 441: Brass in aerated solutions at room temperature

A - Brass in methanol
B - Brass in ethanol
C - Brass in gasoline

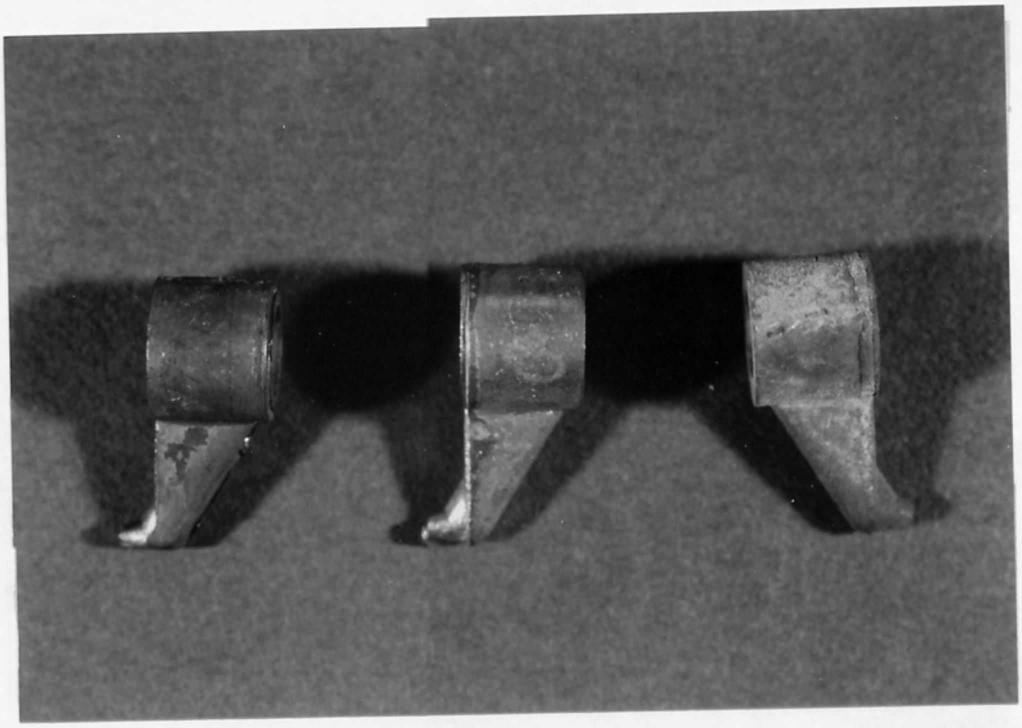

Plate 442: Zinc in aerated solutions at room temperature

A - Zinc in methanol
B - Zinc in ethanol
C - Zinc in gasoline

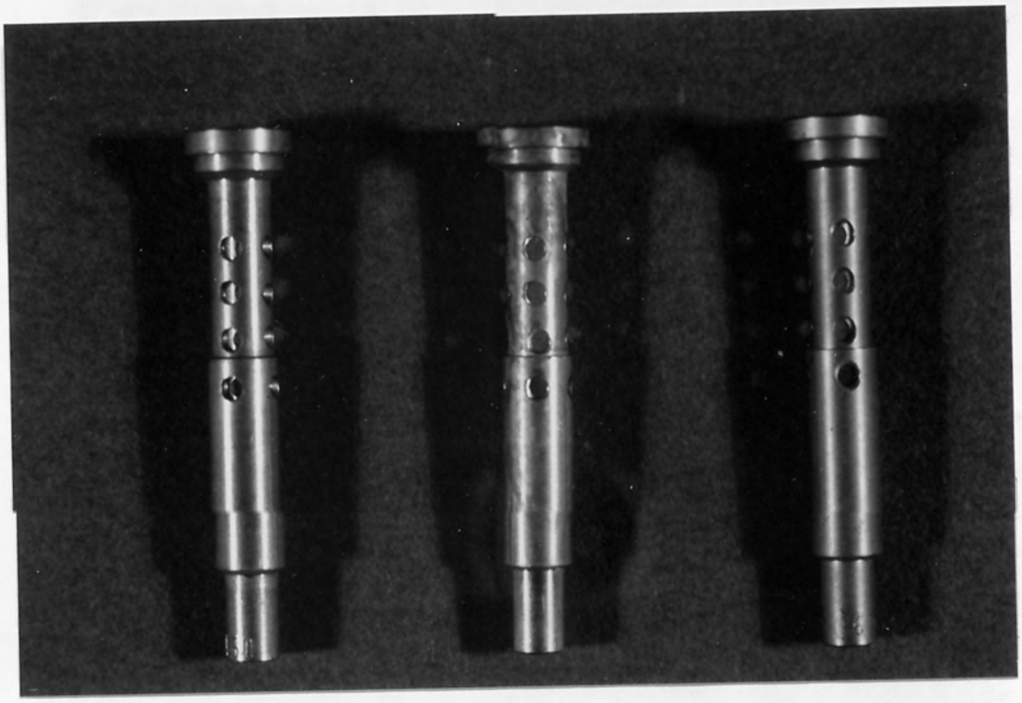

Plate 443: Brass in solutions at 50°C

A - Brass in methanol
B - Brass in ethanol
C - Brass in gasoline

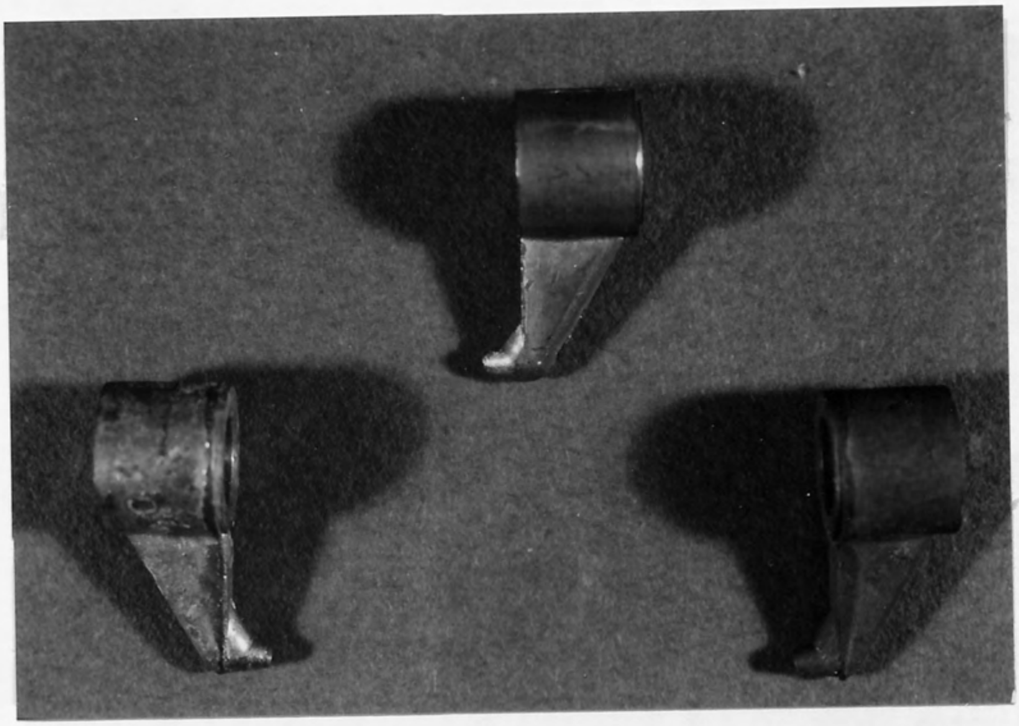

Plate 444: Zinc in solutions at 50^{o}C

A - Zinc in methanol
B - Zinc in ethanol
C - Zinc in gasoline

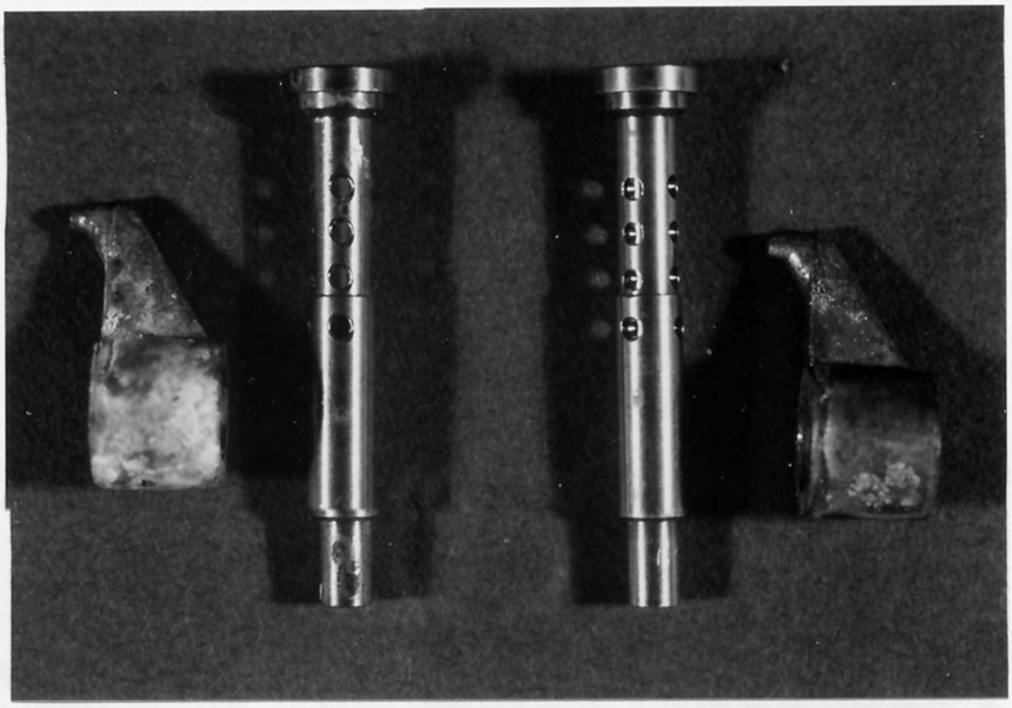

Plate 445: Brass and zinc in contact while suspended in aerated ethanol and methanol

A - Zinc in aerated ethanol
B - Brass in aerated ethanol
C - Brass in aerated methanol
D - Zinc in aerated methanol

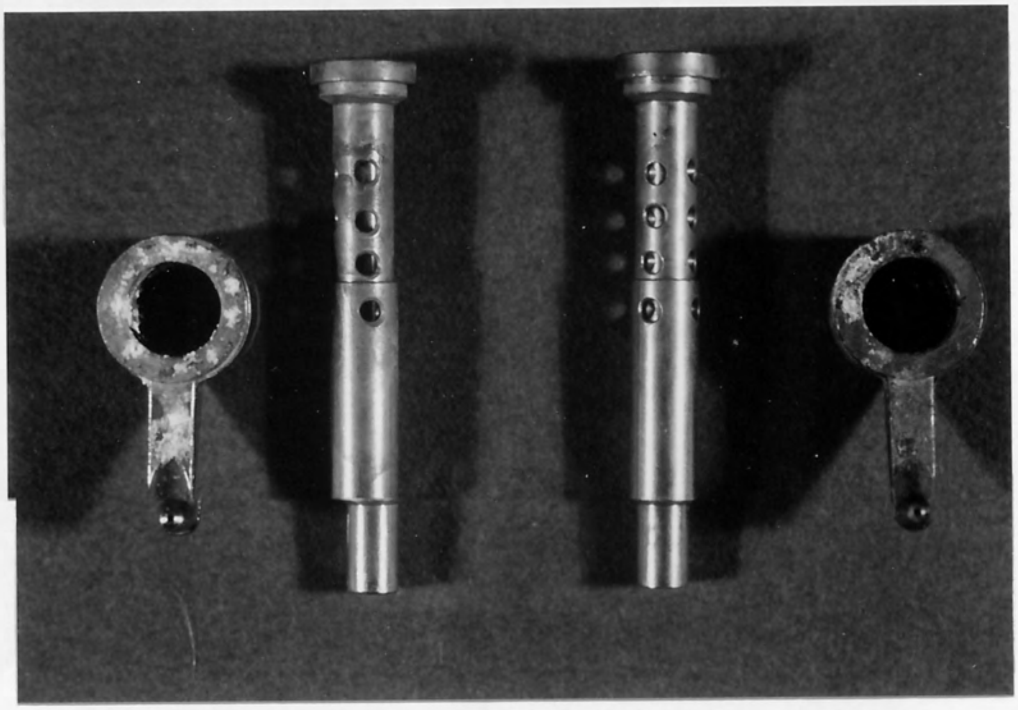

Plate 446: Brass and zinc in contact while suspended in ethanol and methanol at 50^{o}C

A - Zinc in ethanol
B - Brass in ethanol
C - Brass in methanol
D - Zinc in ethanol

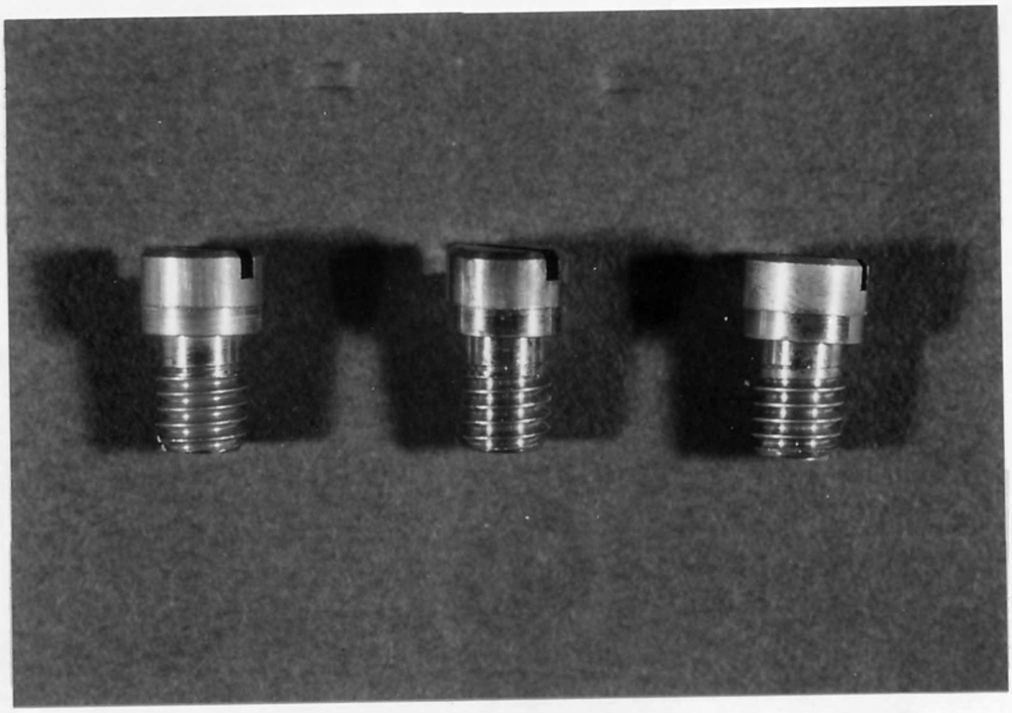

Plate 447: Brass in ethanol blends at 50^{o}C

A - Brass in 10% ethanol blend
B - Brass in 30% ethanol blend
C - Brass in 50% ethanol blend

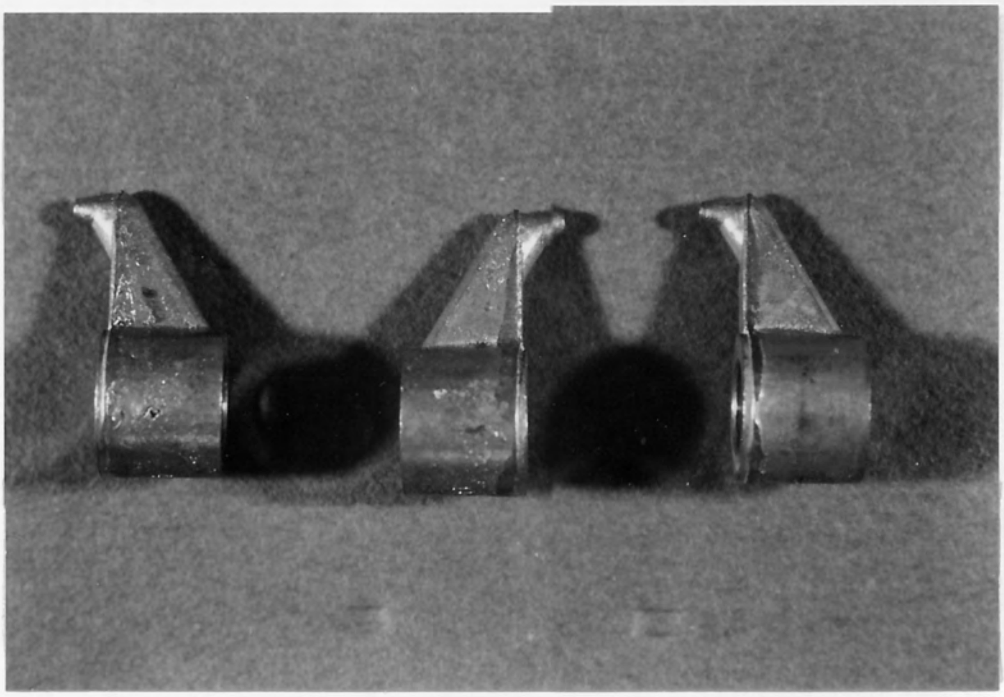

Plate 448: Zinc in ethanol blends at 50^{o}C

A - Zinc in 10% ethanol blend
B - Zinc in 30% ethanol blend
C - Zinc in 50% ethanol blend

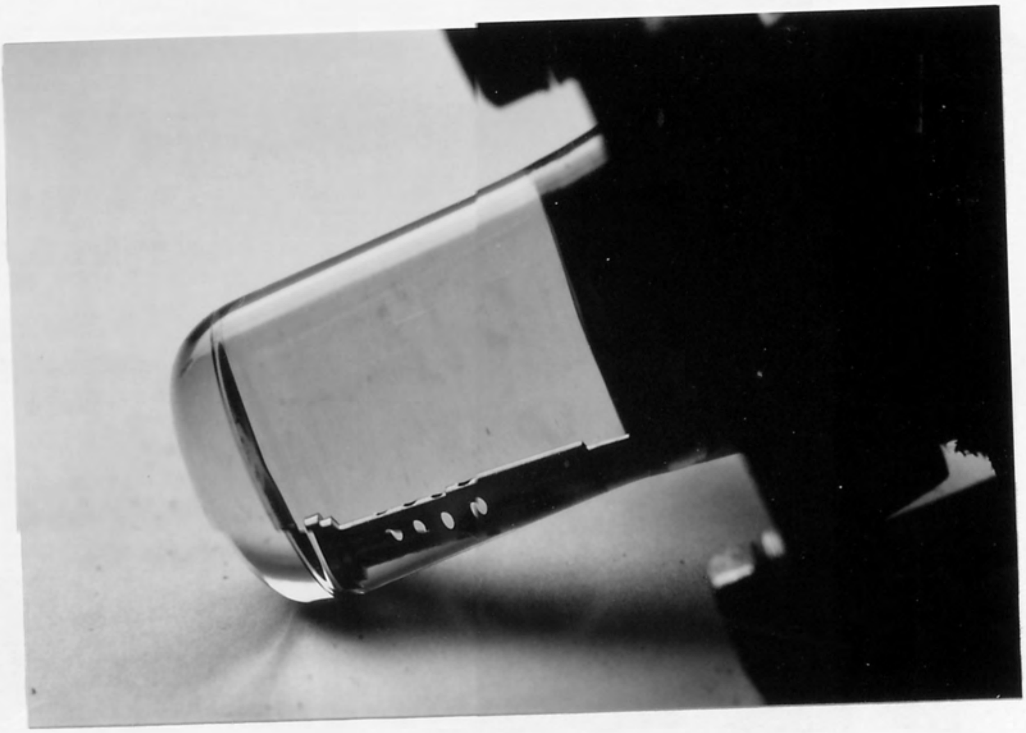

Plate 449: Brass in methanol at 90^{o}C

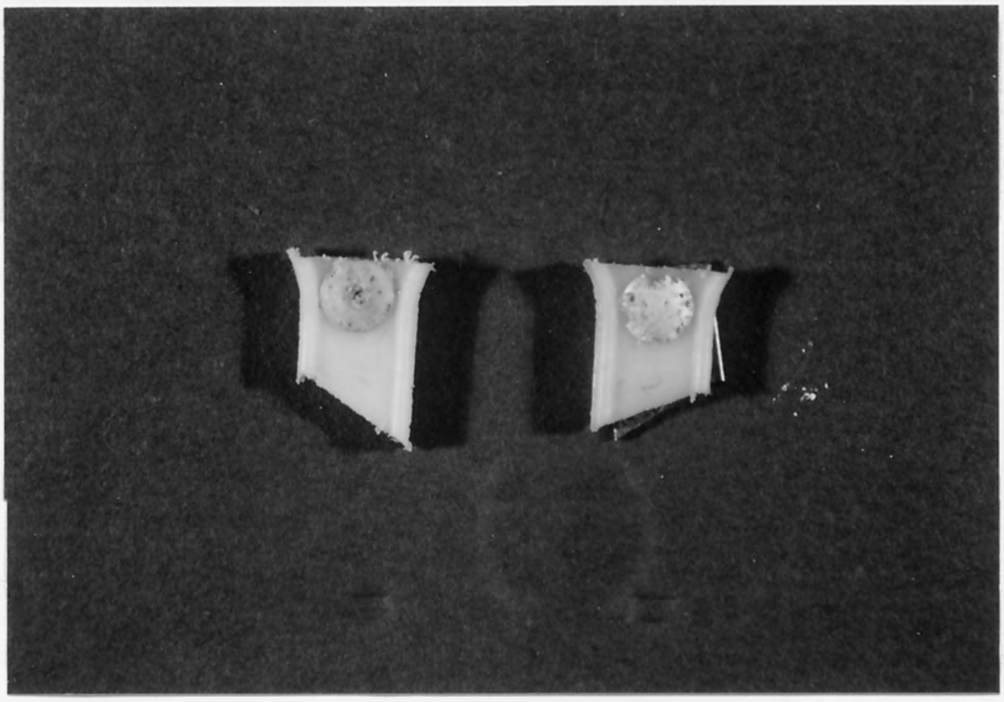

Plate 4410: Aluminium in methanol soluition at 65^oC

A - Aluminium in 95% v/v methanol and 5% v/v formic acid
B - Aluminium in methanol

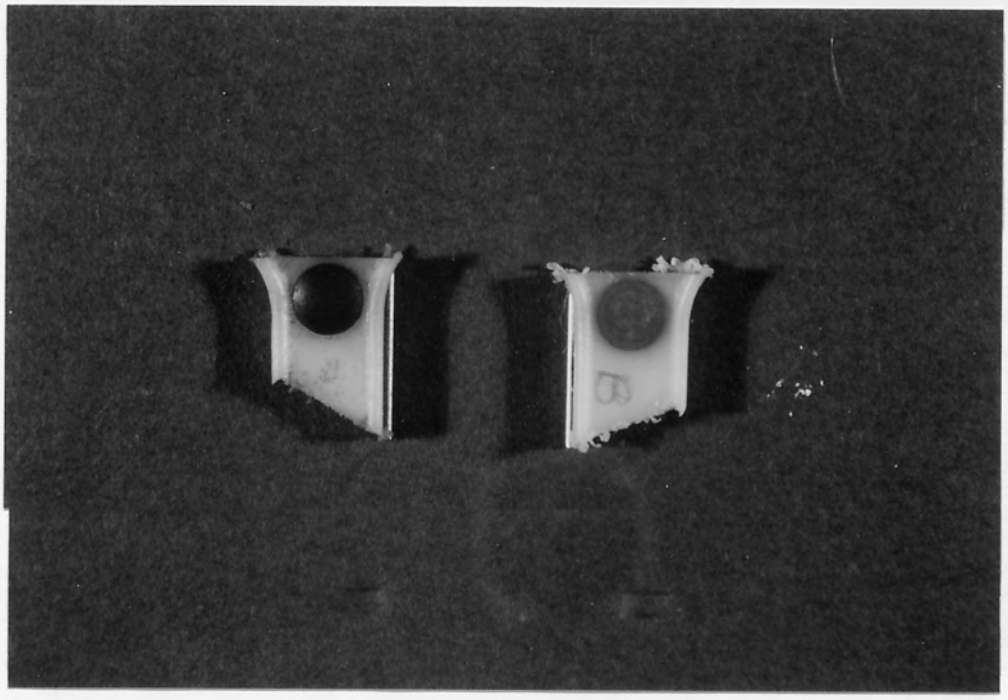

Plate 4411: Copper in methanol solutions at 65°C

A - Copper in 95% v/v methanol and 5% v/v formic acid
B - Copper in methanol

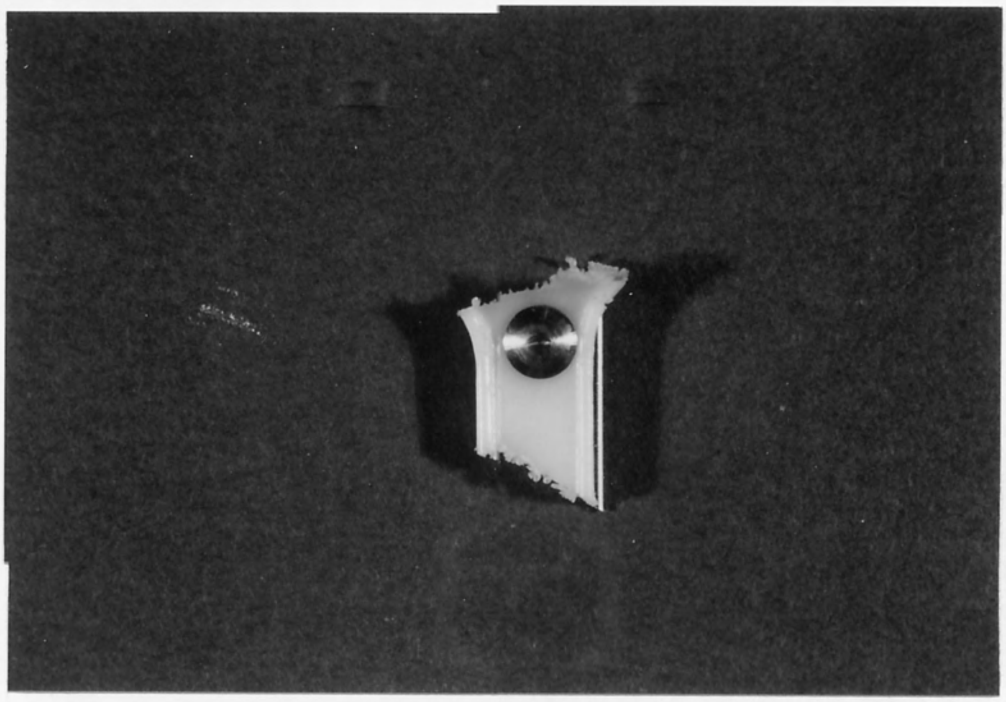

Plate 4412: Stainless steel in 95% v/v methanol and 5% v/v formic acid

Plate 4413: Section of carburettor after use with alcohols and alcohol/gasoline blended fuels

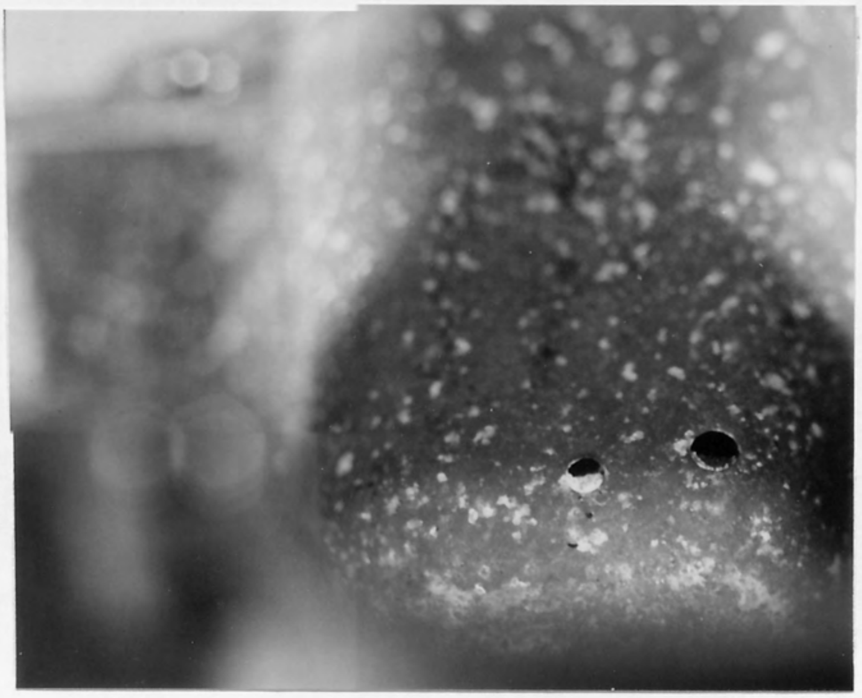

Plate 4414: Section of carburettor after use with alcohols and alcohol/gasoline blended fuels

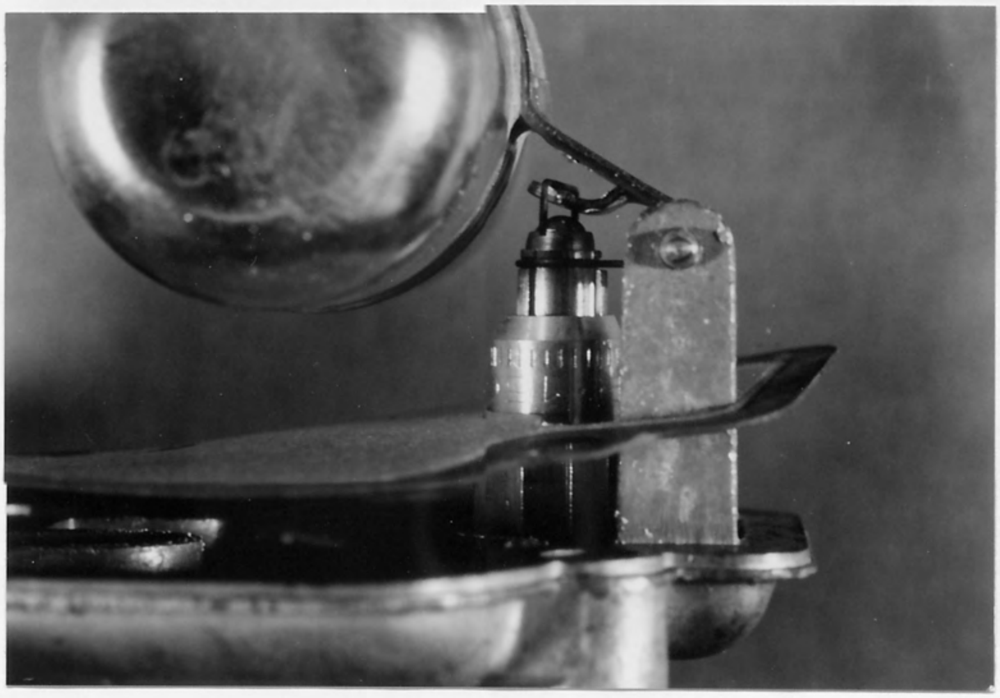

Plate 4415: Section of carburettor after use with alcohols and alcohol/gasoline blended fuels

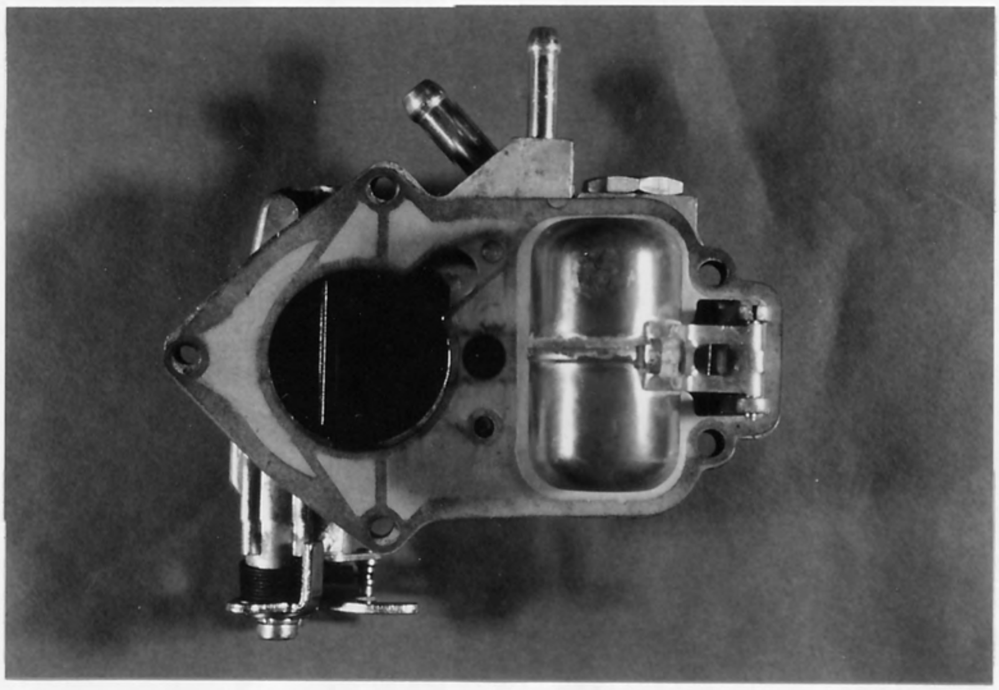

Plate 4416: Section of carburettor after use with alcohols and alcohol/gasoline blended fuels

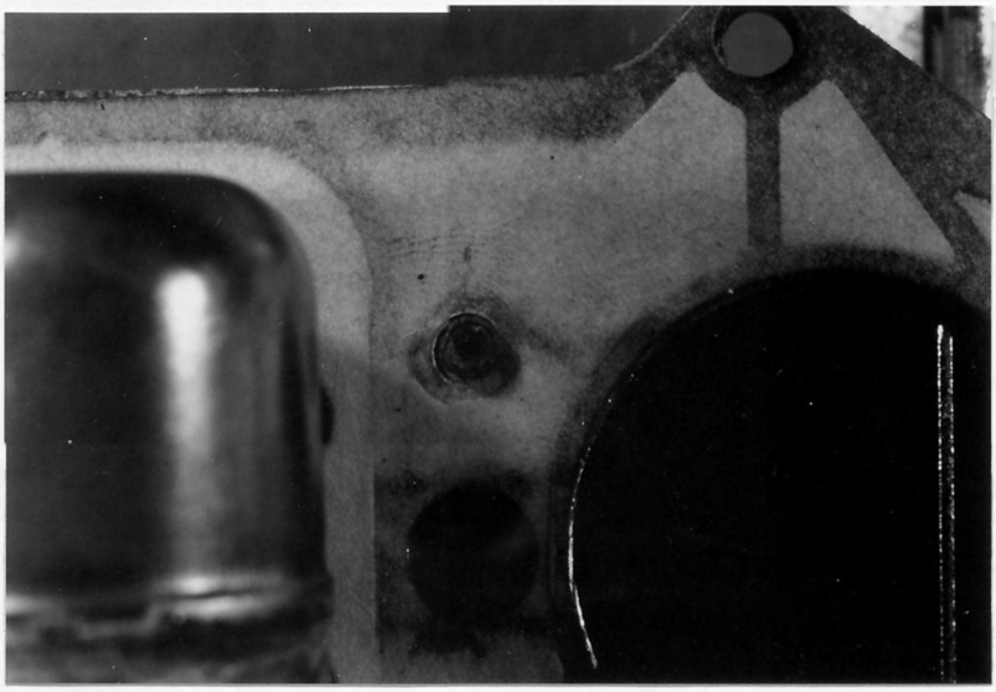

Plate 4417: Section of carburettor after use with alcohols and alcohol/gasoline blended fuels

Table 5.1 - Relation of F/A ratio to ratio of carbon, oxygen and nitrogen to hydrogen for methanol

F/A ratio	$l = \left(\frac{n_o}{n}\right)$	$k = \left(\frac{n_c}{n}\right)$	$m = \left(\frac{n_n}{n}\right)$
1:6	0.885	0.25	2.37
1:7	0.985	0.25	2.765
1:8	1.09	0.25	3.16
1:9	1.195	0.25	3.555
1:10	1.30	0.25	3.95
1:11	1.405	0.25	4.345

Table 5.2 - Relation of F/A ratio to ratio of carbon, oxygen and nitrogen to hydrogen for ethanol

F/A ratio	$l = \left(\frac{n_o}{n}\right)$	$k = \left(\frac{n_c}{n}\right)$	$m = \left(\frac{n_n}{n}\right)$
1:7	0.657	0.333	1.843
1:8	0.727	0.333	2.107
1:9	0.797	0.333	2.37
1:10	0.867	0.333	2.633
1:11	0.937	0.333	2.897
1:12	1.007	0.333	3.16
1:13	1.077	0.333	3.423

Table 5.3 - Relation of F/A ratio to combustion products

	% Combustion products									
F/A	CO	CO_2	O_2	H_2	H_2O	OH	H	O	NO	N_2
1/6	4.9313	7.8379	0.3591	2.23	22.726	0.7913	0.3748	0.0868	0.2742	60.389
1/7	2.9453	8.5159	1.8822	1.1399	21.1337	1.0293	0.2679	0.1581	0.4825	63.1391
1/8	1.9938	8.3299	2.4808	0.7179	18.23	1.1803	0.2126	0.2283	0.7544	64.8687
1/9	1.5167	7.8534	3.8106	0.5269	17.4956	1.2532	0.18221	0.2830	0.9126	66.1655
1/10	1.2373	7.3336	4.9928	0.42099	15.9984	1.2821	0.1621	0.3239	1.074	67.1736
1/11	1.0496	6.8453	6.044	0.3519	14.7184	1.2900	0.1489	0.3565	1.1745	68.0197

Fuel used: Methanol
Temperature: 2400°C

Table 5.4 - Relation of F/A ratio to combustion products

	% Combustion products									
F/A	CO	CO_2	O_2	H_2	H_2O	OH	H	O	NO	N_2
1/7	15.8947	2.9782	0.049	12.62	15.1609	0.2219	0.8916	0.010	0.0184	52.23
1/8	13.7117	3.8349	0.011	9.25	16.5809	0.2834	0.7633	0.015	0.0303	55.5134
1/9	11.57918	4.82	0.00025	8.57	17.566	0.3563	0.6434	0.022	0.0386	58.3694
1/10	9.4755	5.9214	0.00055	4.52	18.1102	0.4429	0.5336	0.034	0.0708	60.8357
1/11	7.4459	7.0424	0.12714	3.01	18.2529	0.5471	0.4353	0.0517	0.1306	62.9
1/12	5.6273	8.033	0.2896	1.97	18.03	0.6681	0.3523	0.0780	0.2591	64.6894
1/13	4.157	8.737	0.6278	1.3	17.517	0.7989	0.7861	0.1149	0.3841	66.077

Fuel used: Ethanol
Temperature: 2400°C

Appendix 2

Calculation of required jet diameters.

Let us consider for example a 60% v/v ethanol blend in gasoline.

From Table A1 we note that the calorific value of the fuel is 35662.2 Kj/Kg. Also from Table A1 we note that the percentage drop in calorific value is 24.87%.

It is thus necessary to increase the jet area by 24.87%.

For gasoline the jet diameter required is 1.35mm. The area of this jet is thus,

$$\text{area} \quad a = \frac{\pi D^2}{4} = \frac{\pi \times (1.35)^2}{4} = 1.431 \text{ mm}^2$$

Therefore an increase in jet area of 24.87% would yield an area of,

$$\frac{124.87}{100} \times 1.431 = 1.787 \text{ mm}^2$$

This area would hence give a diameter of $D^2 = \frac{1.787 \times 4}{\pi} = 2.275$

Therefore D = 1.508 mm.

This procedure was used for all the fuels and the resultant jet diameter requirements are given in Tables A1 and A2.

Table A1

JET DIAMETERS REQUIRED

% Ethanol	Latent heat of Vap (KJ/Kg)	Calorific value KJ/Kg	% drop from 4 star	Area of jet required (mm^2)	Diameter required (mm^2)
100	902	29772.8	49.45	2.133	1.647
90	829.8	31245.2	42.4	2.038	1.611
80	757.6	32717.5	36.0	1.946	1.574
70	685.0	34189.9	30.15	1.863	1.540
60	613.2	35662.2	24.87	1.787	1.51
50	541.0	37134.6	19.83	1.715	1.47
40	468.8	38606.9	15.25	1.649	1.45
30	396.6	40079.3	11.02	1.589	1.42
20	324.4	41551.7	7.08	1.532	1.40
10	252.2		3.42	1.480	1.373
0	180.0		0	1.431	1.35

Table A2

% Methanol	Latent heat of vap KJ/Kg	Calorific value (KJ/Kg)	% drop from 4 star (mm^2)	Area of jet required (mm^2)	Diameter required
100	1105	23864.8	87.0	2.676	1.85
90	1012.5	25927.9	71.62	2.456	1.77
80	920	27991.1	58.97	2.275	1.70
70	827.5	30054.2	48.06	2.119	1.64
60	735	32117.4	38.55	1.983	1.59
50	642.5	34180.6	30.18	1.863	1.54
40	550	36243.7	22.77	1.757	1.50
30	457.5	38306.9	16.16	1.662	1.46
20	365	40370.1	10.22	1.577	1.42
10	272	42433.2	4.86	1.501	1.38
0	180		0	1.431	1.35

Table A3

% Alcohol	Stoichiometric F/A ratio	
	Methanol	Ethanol
0	0.0689	0.0689
10	0.07754	0.07332
20	0.0862	0.0778
30	0.0948	0.0822
40	0.1035	0.0866
50	0.1121	0.0910
60	0.1207	0.0955
70	0.1294	0.0999
80	0.1380	0.1043
90	0.1467	0.1087
100	0.1553	0.1131

Appendix 3

Equations used

Torque T = multiplication factor x Mv (Nm)

Multiplication factor is determined by the calibration of the load cell.

Brake power (Bhp) $= \frac{2 \times \pi \times N \times T \times 10^{-3}}{60} = 1.047 \times 10^{-4}\ NT$ Kw

Indicated power (Ihp) = $\text{Imep} \times \frac{l}{12} \times \frac{\pi d^2}{4} \times \frac{N}{2} \times n \times 0.748$ Kw

Indicated mean effective pressure (Imep) $= 1296 \times \frac{(C_v)}{(A/F)} \times \eta_T \times \eta_V$

Thermal efficiency η_T $\frac{\text{Ihp} \times 10^3}{C_v \times w_f}$

Mechanical efficiency $\eta_M = \frac{\text{Bhp}}{\text{Ihp}}$

Nomenclature

Mv = milivolts on multiroll readout
N = revolutions per minute (RPM)
T = torque
C_v = calorific value of fuel Kj/Kg
w_f = weight of fuel g/s
L = length of stroke
d = diameter of bore
n = number of cylinders
A/F = air-fuel ratio

Appendix 4

1	Type (100GL.000)	4-stroke; OHV, push-rod operated; light alloy head
2	Cooling system	Water pump, radiator ($0.5kg/cm^3$) thermostat (85°/89°C)
3	Number of cylinders	4
4	Firing order	1-3-4-2
5	Idling speed	850 rpm
6	Bore	65mm
7	Stroke	68mm
8	Cubic capacity	$903cm^3$
9	Compression ratio	9:1
10	Break horse-power (DIN)	45 at 5600 rpm
11	Torque (DIN)	6.5 kg.m at 3000 rpm
12	Valve timing	17° BT - 44°AB - 57° BB - 3°AT
13	Needle valve	1.5mm
14	Float level (vertical)	6mm ± 0.25

Appendix 5

Engine Configuration

The engine is the Ricardo E6 single cylinder four-stroke cycle carburetted spark ignition engine with the following dimenions:

Piston area	cm^2	45.365
Cylinder head area	cm^2	45.365
Conn-rod length	cm	23.785
Stroke	cm	11.1
Bore	cm	7.6
Cylinder capacity	cm^3	507
Crankangle at inlet valve closure	deg	220
Crankangle at exhaust valve opening	deg	500
Compression ratio		Variable

```
 0 REM FLAME GAS COMPOSITIONS
 1 REM K1--K6 ARE EQUILIBRIUM CONSTANTS
 2 REM L=NUMBER OF"O"ATOMS/NUMBER OF"H"ATOMS
 3 REM M=NUMBER OF "N"ATOMS/NUMBER OF "H"ATOMS
 4 REM K=NUMBER OF "C"ATOMS/NUMBER OF "H"ATOMS
 5 REM A,B,C,D,E,F,G,H,I,J ARE PARTIAL PRESSURES
 0 DATA 0.0377,0.00588,0.0052,0.0251,0.0145,0.059,1.09,3.16,0.25
 0 READ K1,K2,K3,K4,K5,K6,L,M,K
 5 D=.001         :X1=.00001
 0 X=K2*(2*L+2*M+1)+((K2*K3/SQR(D))*(L+M+1))+(K2^2*K5/D)
 5 A1=K1*D*(2*K+2*L+2*M+1)+2*K2*D*(L+M+1)+K1*K3*SQR(D)*(K+L+M+1)
 7 B1=K2*K4*SQR(D)*(L+M+2)+K1*K2*K5-2*K2
 0 Y=A1+B1
 0 Z=2*K1*D^2*(K+L+M+1)+K1*K4*D*SQR(D)*(K+L+M+2)-2*K1*D
 0 E=(-Y+SQR(Y^2-4*X*Z))/(2*X)
 0 C=(E*K2/D)^2
 0 F=E*K3/SQR(D)
00 G=K4*SQR(D)
10 N=2*D+2*E+F+G
20 H=K5*SQR(C)
30 B=K*N/(1+K1/SQR(C))
40 A=K*N-B
50 I=L*N-A-2*B-2*C-E-F-H
60 J=1-A-B-C-D-E-F-G-H-I
70 Y1=K6*SQR(J)*SQR(C)
80 P=A+B+C+D+E+F+G+H+I+J
90 Z1=(Y1+1000!)/(I+1000!)
200 PRINT "Z1=";Z1
206 PRINT "p=";P
208 PRINT"d=":D
210 IF Z1>1.000005 THEN D=D+X1 :GOTO 40
220 IF Z1<.999999 THEN D=D-X1 :GOTO 40
240 PRINT "TEMPERATURE T=2400K"
242 PRINT "FUEL USED IS METHANOL"
243 PRINT "FUEL:AIR =8:1"
245 PRINT "PARTIAL PRESSURES ARE"
250 PRINT "CO=";A
260 PRINT "CO2=":B
270 PRINT "O2=";C
275 PRINT "H2=";D
280 PRINT "H2O=":E
290 PRINT "OH=":F
300 PRINT "H=";G
310 PRINT "O=";H
320 PRINT "NO=";I
330 PRINT "N2=";J
400 END
```